Control of biofilm formation in *Bacillus subtilis*

Dissertation

for the award of the degree

"Doctor rerum naturalium"

of the Georg-August-Universität Göttingen

within the doctoral program *Microbiology & Biochemistry*

of the Georg-August University School of Science (GAUSS)

submitted by

Jan Gerwig

from Hannover

Göttingen 2014

Reviewers

Prof. Dr. Jörg Stülke (supervisor and 1st reviewer)

Dr. Fabian Commichau (2nd reviewer)

Additional members of the examination board

Prof. Dr. Christiane Gatz (3rd thesis committee member)

Prof. Dr. Ivo Feussner

Prof. Dr. Carsten Lüder

Prof. Dr. Stefanie Pöggeler

Date of oral examination: 20.01.2015

I hereby declare that the doctoral thesis entitled, “Control of biofilm formation in *Bacillus subtilis*” has been written independently and with no other sources and aids than quoted.

Jan Gerwig

Danksagung

Wenn ich auf die vergangenen drei Jahre zurückblicke, dann sehe ich eine spannende, manchmal fast zu aufregende Zeit in der Erforschung von grundlegenden Mechanismen zur Steuerung der Biofilmbildung in „meinem Bakterium“ *Bacillus subtilis*. Ich möchte allen Menschen danken, die mich während dieser Zeit unterstützt haben und für mich da waren.

Ein herzliches Dankeschön geht an meinen Doktorvater Jörg Stülke, der mich für die mikrobiologische Forschung begeistert hat und mich während meiner Doktorarbeit tatkräftig mit Ideen unterstützt hat. Zudem bin ich dankbar für die Möglichkeit, meinen mikrobiologisch geprägten Horizont in der beschaulichen „Weltstadt der Proteomics“ Greifswald zu erweitern, auch wenn diese Forschungsreise nicht durch die Identifizierung eines Phosphorylierungsziels der Tyrosinkinase EpsB abgeschlossen werden konnte. In diesem Zusammenhang möchte ich Prof. Dr. Dörte Becher für die Möglichkeit zur Durchführung von Phosphoproteome-Analysen in ihrer Arbeitsgruppe danken und Dr. Katrin Bäsell und Sabryna Junker für die praktische Hilfe. Außerdem habe ich es sehr genossen, meine Forschungsergebnisse auf einigen nationalen und internationalen Tagungen zu präsentieren. Danke dafür!

Für die praktische Unterstützung und die gute Zusammenarbeit während der letzten beiden Jahre möchte ich Julia Busse danken. Außerdem danke ich meiner Praktikantin und Master-Studentin Kerstin Kruse für ihren Beitrag zu meiner Doktorarbeit, insbesondere bei der Isolierung und Charakterisierung der ersten *ymdB* Suppressor-Mutanten. Meiner Praktikantin Sumana Sharma und meinen beiden Bachelor-Studenten Cedric Blötz und Alexander Lockhorn danke ich für die engagierte und neugierige Arbeit an ihren Projekten. Dadurch hat mir meine „Betreuungsarbeit“ viel Freude bereitet. Des Weiteren danke ich Christina Herzberg für ihr Interesse an der Biofilm-Forschung und für ihre hilfreichen Tipps.

Ein weiterer Dank geht an die gesamte Abteilung Allgemeine Mikrobiologie und insbesondere an die Arbeitsgruppen Stülke und Commichau. Ich habe hier eine sehr kollegiale und warme Arbeitsatmosphäre erlebt und habe mich deshalb sehr wohl gefühlt.

Meinen aktuellen und ehemaligen „Thesis Committee“ Mitgliedern Prof. Dr. Christiane Gatz, Dr. Fabian Commichau und Dr. Böris Görke danke ich für hilfreiche Ratschläge. Meinen Gutachtern und Prüfern danke ich für ihre Bereitschaft zur Beurteilung meiner Doktorarbeit.

Nicola Stanley-Wall und ihrer Arbeitsgruppe möchte ich für die gute Zusammenarbeit danken. Für die Durchführung von Genomsequenzierungen zur Identifizierung von Suppressormutationen und für die „RNA Sequenzierung“ geht mein Dank an das Team des „Göttingen Genomics Laboratory“. Zu dem möchte ich meinem Nachfolger auf dem YmdB-Projekt Jan Kampf für die Hilfe bei der Nachbearbeitung der Genomsequenzierungen danken und wünsche ihm viel Erfolg bei der Weiterführung des Projekts.

Thank you a lot! Danke euch Allen!

Table of contents

List of publications ..... **III**

List of abbreviations ..... **IV**

1. Summary **1**

2. Introduction **2**

2.1. Biofilm formation in *B. subtilis* **2**

2.2. Regulation of cell differentiation and biofilm formation in *B. subtilis* **4**

2.3. Regulation of cell differentiation by the second messenger c-di-GMP **8**

2.4. The YmdB protein **11**

2.5. Tyrosine phosphorylation **13**

2.6. Objectives **18**

3. Materials and methods **19**

3.1. Bacterial strains and plasmids **19**

3.2. Media **19**

3.3. Methods **21**

3.3.1. General methods 21

3.3.2. Cultivation of bacteria 22

3.3.3. Transformation of *E. coli* 22

3.3.4. Transformation of *B. subtilis* 24

3.3.5. SPP1 phage transduction 24

3.3.6. Preparation and detection of DNA 26

3.3.7. Isolation of Δ*ymdB* suppressor mutants 31

3.3.8. Biofilm methods 32

3.3.9. Precipitation and staining of exopolysaccharides 33

3.3.10. Work with proteins 34

3.3.11. Work with RNA 44

3.3.12. Fluorescence microscopy 50

3.3.13. Preparations for quantification of cyclic nucleotide monophosphates in *B. subtilis* 51

4. Results **53**

4.1. The protein tyrosine kinases EpsB and PtkA differentially affect biofilm formation **53**

4.1.1. *In vivo* interaction between EpsA and EpsB 53

4.1.2. Cellular localization of the tyrosine kinase EpsB and its modulator protein EpsA 55

4.1.3. The role of tyrosine protein kinases and their modulators in complex colony and pellicle formation....56

4.1.4. Tyrosine kinases influence extracellular polysaccharide production....59

4.2. The YmdB protein as a regulator for biofilm formation 61

4.2.1. Deletion of the *ymdB* gene increases SinR protein levels....61

4.2.2. Suppressor mutations in the *ymdB* mutant restore biofilm gene expression 63

4.2.3. Overexpression of RNase Y in the *ymdB* deletion mutant does not restore complex colony structure 69

4.2.4. YmdB is a RNA-binding protein 70

4.2.5. Global and high-resolution analysis of the transcriptome in the *ymdB* deletion mutant by RNA sequencing....74

4.2.6. C-di-GMP and its influence on biofilm formation in *B. subtilis* 76

5. Discussion 79

5.1. The story behind the biofilm and cell differentiation defect of the *ymdB* mutant....79

5.2. Suppressor mutations – a bacterial way to evolve 87

5.3. Tyrosine kinases control cell differentiation....93

5.4. Outlook 97

6. References 100

7. Appendix....116

7.1. Materials....116

7.1.1. Chemicals 116

7.1.2. Utilities 117

7.1.3. Equipment 117

7.1.4. Commercial systems....118

7.1.5. Antibodies and enzymes 118

7.2. Bacterial strains 119

7.3. Oligonucleotids....125

7.4. Plasmids 138

7.5. Internet programs and software....141

7.6. Supplementary data 142

List of publications

Within this PhD thesis

Gerwig, J., Kiley, T.B., Gunka, K., Stanley-Wall, N., and Stülke, J. (2014) The protein tyrosine kinases EpsB and PtkA differentially affect biofilm formation in *Bacillus subtilis*. *Microbiol (United Kingdom)* **160**: 682–691.

Gerwig, J., and Stülke, J. (2014) Caught in the act: RNA-Seq provides novel insights into mRNA degradation. *Mol Microbiol* **94**: 5–8.

Gerwig, J., and Stülke, J. (2014) Far from being well understood: Multiple protein phosphorylation events control cell differentiation in *Bacillus subtilis* at different levels. *Front Microbiol* **5**: 704.doi:10.3389/fmicb.2014.00704.

Before this PhD thesis

Gunka, K., Tholen, S., **Gerwig, J.**, Herzberg, C., Stülke, J., and Commichau, F.M. (2012) A high-frequency mutation in *Bacillus subtilis*: requirements for the decryptification of the gudB glutamate dehydrogenase gene. *J Bacteriol* **194**: 1036–1044

Meyer, F.M., **Gerwig, J.**, Hammer, E., Herzberg, C., Commichau, F.M., Völker, U., and Stülke, J. (2011) Physical interactions between tricarboxylic acid cycle enzymes in *Bacillus subtilis*: evidence for a metabolon. *Metab Eng* **13**: 18–27.

List of abbreviations

% (vol/vol)	% (volume/volume)
% (wt/vol)	% (weight/volume)
Amp	ampicillin
AP	alkaline phospatase
ATP	adenosine triphosphate
B.	*Bacillus*
BACTH	bacterial two-hybrid system
c-di-GMP	cyclic diguanylate monophosphate
cat	chloramphenicol
CCR	combined chain reaction
CDP*	disodium 2-chloro-5-(4-methoxyspiro{1,2-dioxetane-3,2'-(5'chloro) tricyclo[3.3.1.13,7]decan}-4-yl)phenyl phosphate
CFP	cyan fluorescent protein
CHAPS	(3-[(3-Cholamidopropyl)dimethylammonio]-1-propanesulfonate
DNA	deoxyribonucleic acid
NTP	ribonucleoside triphosphate
dNTP	desoxyribonucleoside triphosphate
E.	*Escherichia*
EDTA	ethylenediaminetetraacetic acid
Ery	erythromycin
et al.	*et alia*
FA	formaldehyde
PFA	paraformaldehyde
Fig.	figure
fwd	forward
Glc	glucose
kan	kanamycin
LB	Luria Bertani (medium)
LFH-PCR	Long Flanking Homology PCR
linco	Lincomycin
mRNA	messenger RNA
NAD^+	nicotinamide adenine dinucleotide (oxidized)
NADH	nicotinamide adenine dinucleotide (reduced)
OD_x	optical density, measured at the wavelength λ = x nm
ori	origin of replication
P	promoter
PAGE	polyacrylamide gel electrophoresis
PCR	polymerase chain reaction
pH	power of hydrogen
PVDF	polyvinylidene difluoride
qRT-PCR	reverse transcription quantitative real-time PCR

RBS	ribosome binding site
rev	reverse
RNA	ribonucleic acid
RNase	ribonuclease
RT	room temperature
S	succinate
SDS	sodium dodecyl sulfate
SP	sporulation medium
spc	spectinomycin
SPINE	*Strep*-protein interaction experiment
Tab.	table
Tris	tris(hydroxymethyl)aminomethane
U	units
WT	wild type
YFP	yellow fluorescent protein

Units

A	ampere
bp	base pairs
°C	degree Celsius
Da	Dalton
g	gram
h	hour
l	liter
m	meter
M	molar (mol/l)
min	minute
sec	second
rpm	rotations per minute
V	Volt
W	Watt

Prefixes

k	kilo	10^{3}
m	mili	10^{-3}
µ	micro	10^{-6}
n	nano	10^{-9}

Nucleotids

A	Adenine
C	Cytosine
G	Guanine
T	Thymine
U	Uracil

Amino acid nomenclature (IUPAC-IUB notation, 1969)

A	Ala	Alanine	M	Met	Methionine
C	Cys	Cysteine	N	Asn	Asparagine
D	Asp	Aspartatic acid	P	Pro	Proline
E	Glu	Glutamatic acid	Q	Gln	Glutamine
F	Phe	Phenylalanine	R	Arg	Arginine
G	Gly	Glycine	S	Ser	Serine
H	His	Histidine	T	Thr	Threonine
I	Ile	Isoleucine	T	Tyr	Tyrosine
K	Lys	Lysine	V	Val	Valine
L	Leu	Leucine	W	Trp	Tryptophan

1. Summary

Biofilms can be considered as one main lifestyle of many bacteria in their natural environment. A bacterial biofilm is a cell community that is surrounded by a self-produced extracellular matrix. This matrix usually consists of polysaccharides, protein, lipids and extracellular DNA. Within this matrix the cells are protected from harmful components in the environment such as antibiotics or from predators and phages. Furthermore, the biofilm matrix enables the cells to float on liquid surfaces as a community or to cover solid surfaces such as plant roots, human tissue or even medical devices. Thus, the formation of biofilms by pathogenic bacteria can also serve as a virulence factor and needs to be considered as a threat to human health. The Gram-positive model organism *Bacillus subtilis* also forms biofilms in its natural environment. In the laboratory environment it forms wrinkled colonies on agar plates and structured floating biofilms, so-called pellicles, on the top of liquid medium. The regulation of matrix gene expression is highly complex and was subject of many studies. The main protein components of the matrix are encoded in the *tapA-sipW-tasA* operon and the *bslA* gene, whereas the machinery for exopolysaccharide synthesis and export is encoded within the *epsA-O* operon. One aim of this work was to study the function of the first two genes of the *epsA-O* operon, namely *epsA* and *epsB* that encode a tyrosine kinase modulator and the cognate kinase in the regulation of exopolysaccharide production. In this work, it was shown that the EpsB kinase and its modulator directly interact with each other and that deletion of the two genes reduces the biofilm structure suggesting a defect in exopolysaccharide production. Simultaneous deletion of the genes for EpsB and the only other known tyrosine kinase PtkA led to a complete loss of complex colony formation due to impaired exopolysaccharide production. The same was observed in the absence of both modulator proteins demonstrating that tyrosine kinases are essential for the formation of biofilms in *B. subtilis*. The expression of biofilm matrix and motility genes is mutually exclusive in *B. subtilis*. In the absence of the YmdB protein biofilm matrix gene expression is inhibited and instead all cells express motility genes. Thus, the *ymdB* mutant does not form complex colonies and pellicles anymore. This phenotype is due to the phosphodiesterase activity of the YmdB protein. In this work, it was demonstrated that impaired biofilm formation is due increased amounts of the master regulator of biofilm formation SinR. Interestingly, the formation of spontaneous suppressor mutations within the *sinR* gene restored biofilm matrix gene expression and enabled the cells to switch between sessile and motile life styles. However, the target of the YmdB phosphodiesterase remains unclear but the interplay with the major endoribonuclease RNase Y seems to be important. RNA sequencing of the *ymdB* mutant revealed potential processing targets for further research.

2. Introduction

The statement „biofilms are everywhere and the predominant life form of microbes in their natural environment" summarizes the main message of a review by Costerton *et al.* that was published in the year 1995. This publication was one of the first statements that pointed out the importance of biofilm research.

A microbial biofilm is a community of cells embedded in a self-produced extracellular matrix that allows them to attach to each other and often to surfaces. This matrix, usually composed of extracellular polysaccharides, proteins, nucleic acids and lipids (Flemming & Wingender, 2010), allows the attachment to surfaces and protects the cells form harmful environmental influences as antibiotics and predators (Costerton *et al*., 1995, Hall-Stoodley *et al*., 2004). Although bacterial biofilms are associated with e. g. chronic wound infections (Percival *et al*., 2012) and the colonization of the lung of patients that suffer from the genetic disorder cystic fibrosis (Costerton *et al*., 1999), basic research on bacterial biofilms has been neglected for quite some time. Researchers relied on cells cultivated in shaking flasks and tubes filled with rich medium under laboratory conditions. Under these conditions bacteria usually are present as single cells and "happily" consume the provided nutrients. These singular planktonic cells were used to understand basic mechanisms of gene expression and for cell biology. Without any doubt, early experiments with planktonic cells provided important insight into regulatory mechanism as for instance in a process that was called "diauxie" by Monod (1949) describing the preferred uptake of a carbon source that provide more energy to the cells and the switch to less preferred ones. However, biofilms show great phenotypical differences to planktonic cells and therefore are worth being studied to get a better understanding of all different bacterial life styles.

2.1. Biofilm formation in *Bacillus subtilis*

As an important model organism for Gram-positive bacteria, regulation of cell differentiation processes like sporulation has been studied intensively in *Bacillus subtilis* (e. g. Piggot & Hilbert, 2004). First studies addressing biofilm formation in *B. subtilis* at the genetic level were published at the beginning of the 21th century (Branda *et al*., 2001; Hamon & Lazazzera, 2001). Since then, unraveling the complexity of *B. subtilis* biofilms has become a flourishing research field.

The biofilm matrix

B. subtilis forms structured macro-colonies (considered as simple biofilms) on special agar plates and floating biofilms on the top of a liquid surface, so called pellicles (see Fig. 2.1; Branda *et al*., 2001). Within these biofilms the cells are embedded in a self-produced extracellular matrix. This matrix is

mainly composed of extracellular polysaccharides, proteins, nucleic acids and probably lipids (Marvasi *et al*., 2010; Cairns *et al*., 2014a). The machinery for synthesis and export of exopolysaccharides is encoded within the 15 gene *epsA-O* (*eps*) operon. Deletion of this operon leads to a loss of complex colony and pellicle formation (compare Fig. 4.3; López *et al*., 2010). However, with a few exceptions the protein products of the single genes have not been studied in detail. For example the *epsE* gene encodes a bifunctional protein that functions as a "molecular clutch" to inhibit flagella movement and as a glycosyltransferase for exopolysaccharide synthesis (Blair *et al*., 2008; Guttenplan *et al*., 2010). In addition, a regulatory RNA element was identified upstream of the *epsC* gene that might be important to ensure expression of the whole *eps* operon by processive antitermination (Irnov & Winkler, 2010). Before the start of this work, the first two genes of the *eps* operon, *epsA* and *epsB*, were only annotated as a tyrosine kinase modulator and the respective kinase due to homology. Also, the actual composition of the matrix exopolysaccharides is not known in detail, but seems to depend highly on substrate availability (Cairns *et al*., 2014a).

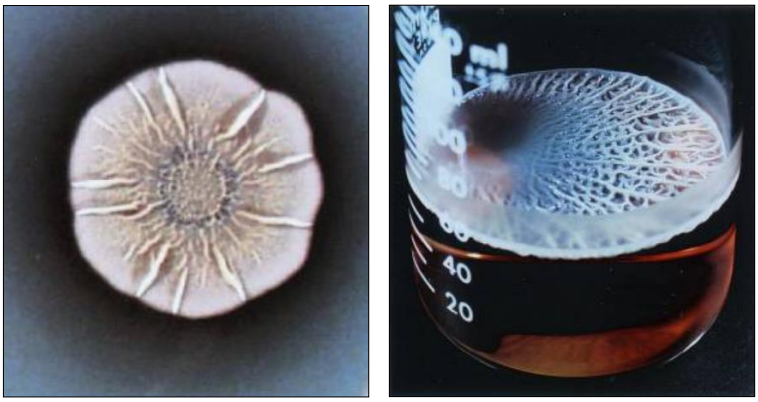

complex colony **floating biofilm (pellicle)**

Figure 2.1. Complex colony and pellicle formation of *B. subtilis*. The undomesticated *B. subtilis* wild type strain NCIB3610 forms structured colonies on biofilm-inducing MSgg medium and structured biofilms on the top of liquid MSgg medium. These floating biofilms are called pellicles (Branda *et al*., 2001).

The main protein components of the matrix are encoded in the *tapA-sipW-tasA* (*tapA*) operon. Deletion of the respective genes also leads to reduced colony structure and pellicle formation but the effects are milder as for the deletion of the whole *eps* operon. The *tasA* gene encodes a protein that builds up amyloid-like structures that confer, in association with the exopolysaccharides, structure and stability to the matrix (Branda *et al*., 2006; Romero *et al*., 2010). TasA proteins interact with TapA proteins that functions as membrane anchors for the amyloid-like fibers and are required for fiber polymerization (Romero *et al*., 2011 and 2014). The third gene of the operon, *sipW*, encodes a signal peptidase that is required for processing TasA and TapA proteins and for their proper secretion (Stöver & Driks, 1999a, b). Another protein component of the biofilm matrix is the BslA protein. This protein is a hydrophobin that covers the surface of a biofilm and prevents wetting of the matrix (Kobayashi & Iwano, 2012; Hobley *et al*., 2013). Loss of the BslA protein reduces the wrinkled appearance of *B. subtilis* colonies on biofilm-inducing agar plates. Most likely this effect is due to a synergistic effect with the polysaccharide components of the matrix. At least the localization of BslA

to the surface of the biofilm depends on the exopolysaccharides (Ostrowski *et al*., 2011; Kobayashi & Iwano, 2012).

2.2. Regulation of cell differentiation and biofilm formation in *B. subtilis*

The Spo0A protein and the phosphorelay

A central question of biofilm research is which external signals trigger the expression of factors required for the formation of complex and organized communities. An important system for sensing external signals in *B. subtilis* is the highly complex, two-component system-like "phosphorelay" (Burbulys *et al*., 1991). An initial step of the phosphorelay is the autophosphorylation of one of the five sensor kinases (KinA-E) on a histidine residue in response to external stimuli. Once autophosphorylated the sensor kinases phosphorylate the phosphocarrier protein Spo0F, which transfers the phosphate group to a histidine residue of a second protein called Spo0B. The function of Spo0B is the phosphorylation of the Spo0A protein which is the actual aspartate response regulator of the phosphorelay. The Spo0A protein binds to DNA and can function as a transcriptional activator or repressor. In principle, the stochastic phosphorylation state of the Spo0A protein determines if cells differentiate into a spore or become a matrix producer. High levels of phosphorylated Spo0A induce spore development, whereas medium levels lead to matrix production (Fujita & Losick, 2005; Fujita *et al*., 2005). In addition to the action of the kinases, several phosphatases directly or indirectly control the phosphorylation state of the Spo0A regulator. Several aspartyl phosphatases of the Rap protein family dephosphorylate the phosphocarrier protein Spo0F and thereby inhibit Spo0A phosphorylation or directly dephosphorylate Spo0A as shown for the Spo0E phosphatase (Perego & Hoch, 1991; Pottathil & Lazazzera, 2003; Ohlsen *et al*., 1994). Activity of histidine sensor kinases is controlled by several different signals such as the respiratory state of the cell sensed by KinA/ KinB (Kolodkin-Gal *et al*., 2013), the potassium concentration sensed by KinC (López *et al*., 2009) and sensing of the plant polysaccharides availability by interplay of KinC and KinD (Beauregard *et al*., 2013).

The KinD kinase seems to play a unique role among the kinases of the Kin group. As proposed by Aguilar *et al.* (2010) the protein is a check point that couples biofilm formation and sporulation. The authors observed that a lack in matrix production (e.g. in an *eps* mutant) delays sporulation and this seems to be due to low levels of phosphorylated Spo0A. Interestingly, deletion of the gene for KinD suppressed the sporulation defect in a matrix mutant. In contrast, overexpression of the *kinD* gene delayed sporulation. This observation was explained by dual activity as a kinase and phosphatase. In this case the respective activity should be determined by the availability of the matrix. The idea was that KinD keeps Spo0A-P levels low until the matrix can be sensed that is required for sporulation. However, this model has never been proven and requires further studies.

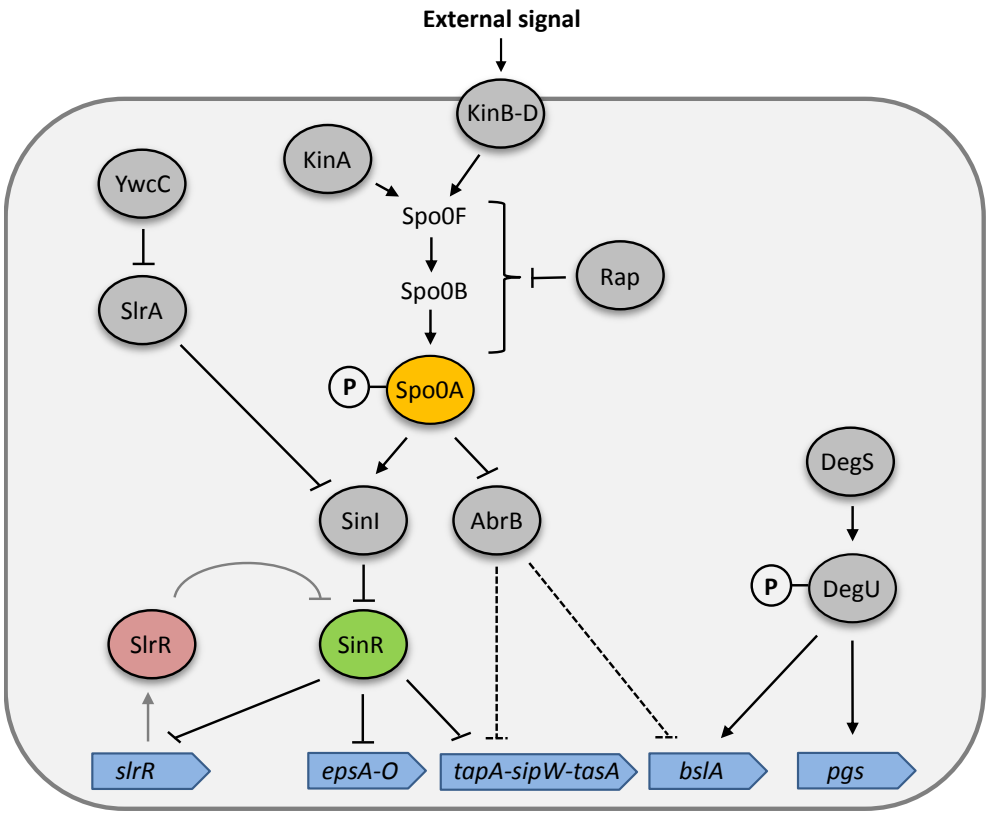

Figure 2.2. Simplified schematic overview of the regulation of biofilm formation in *B. subtilis.* Expression of the biofilm matrix genes for extracellular polysaccharide (*epsA-O*), protein components (*tapA-sipW-tasA*, *bslA*) and poly-DL-γ-glutamic acid (*pgs*) production are highly regulated by different pathways. Arrows indicate activating effects; repressive effects (or dephosphorylation events in case of the Rap phosphatases) are shown with T-bars. Dashed lines show indirect effects. P = phosphoryl group (modified from Vlamakis *et al*., 2013).

In addition to the complex activation of the Kin kinases, each of the Rap phosphatases is specifically inactivated by a cognate peptide (e.g. RapA by the PhrA-derived pentapeptide), that can also function as a quorum-sensing signal (Pottathil & Lazazzera, 2003). This highly complex regulatory network to control the phosphorylation state of the central regulator of cell differentiation Spo0A allows the integration of many different signals into the phosphorelay and underpins the importance of proper Spo0A phosphorylation (Bischofs *et al*., 2009).

The SinR protein and its antagonists

The central regulator of biofilm gene expression and of the switch between a sessile life style and motility is the SinR protein. Originally, the respective gene was studied due to a flagella-less and non-motile phenotype of the mutant and lack of autolysin expression (Fein, 1979; Pooley & Karamata, 1984; Sekiguchi *et al*., 1990). Later on the SinR protein was studied in more detail and termed the "master regulator for biofilm formation" (Kearns *et al*., 2005). In the same study the authors demonstrated that the *eps* operon for exopolysaccharide production is under negative control of the SinR protein and that, as stated before, the protein controls transition between a sessile and a motile

life style. Moreover, it was shown that mutations within the gene encoding the SinR protein can restore wild type like biofilm formation and cell chaining to mutants of the *sinI*, *ylbF* and *ymcA* genes that usually show a strong defect. At this time only the function of the *sinI* product was known. Once its expression is activated via the Spo0A-P regulator (compare Fig. 2.2), the SinI protein acts as an antagonist of the SinR protein and facilitates the switch between sessile and motile life style by interacting with SinR (compare Fig. 2.3). Later on the other two protein products were implicated in the control of the phosphorelay for Spo0A phosphorylation (Carabetta *et al*., 2013).

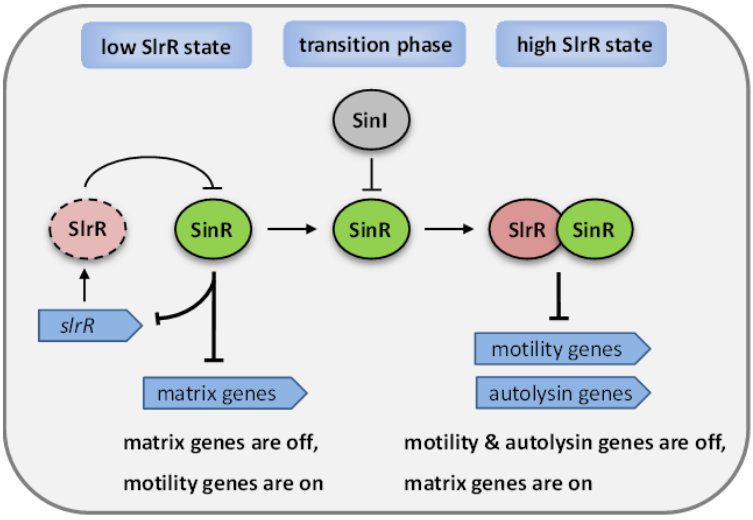

Figure 2.3. A bistable switch of the SinR and its antagonists controls cell differentiation. Inhibition of SinR by SinI shifts the system from the low SlrR state to the high SlrR state and allows expression of biofilm genes. During this state motility and autolysin genes are repressed by the SinR-SlrR hetero-complex. Arrows indicate activating effects; T-bars repressive effects (modified from Vlamakis *et al*., 2013).

Further experiments also revealed the *tapA-sipW-tasA* operon encoding the main protein components of the biofilm matrix as a target of the SinR regulator. By studying gene expression by microarray experiments with cells grown in LB medium until exponential growth phase the genes *spoVG*, *rapG*, *yvfV*, *yvfW*, *yvgN* and *ywbD* were identified as further targets of SinR. Consequently also SinR binding motifs upstream of the genes were described (Chu *et al*., 2006). In 2013, Winkelman *et al*. showed that the RemA protein is required as an activator for the expression of the *eps* operon and *tapA* operon but is excluded (in case of the *eps* operon) from the DNA by the SinR regulator due to overlapping binding motifs. Therefore, the SinR protein functions as a repressor and anti-activator of biofilm matrix gene expression. Besides the SinR antagonist SinI, several other proteins that counteract the SinR regulator have been described. A well-studied example is the SlrR protein. The respective gene itself is under negative control of SinR (Chu *et al*., 2008). Thus, inactivation of SinR by interaction with the SinI protein is required to induce higher SlrR protein levels. However, when SlrR is more abundant it also interacts with the SinR regulator and inhibits its DNA binding ability to the operator regions upstream of e. g. biofilm matrix genes (Chai *et al*., 2010b). The structural and thermodynamic details of the interaction of SinR with its antagonist were studied by Lewis *et al*. (1998), Colledge *et al*. (2011) and Newman *et al.* (2013). The authors showed that the SinR protein forms a tetramer and this tetramer is required for DNA binding. Once SinI is

bound to SinR the protein is present as a heterodimer and cannot bind its operator sequences on the DNA. SlrR seems to interact with SinR via the same domain as SinI ($SinR^{75-111}$) and both proteins most likely form a hetero-dimer (Newman *et al*., 2013). Interestingly, the SinR-SlrR complex also harbors DNA binding ability but now the SlrR part binds the DNA and the complex shows affinity to operator sequences of motility and autolysin genes. Hence, SinR functions as a co-repressor for SlrR in this case (Chai *et al*., 2010b). This way the interaction between SinR and SlrR controls the switch between motile and sessile life styles. To put it simple, high levels of SlrR protein facilitate biofilm gene expression and repress motility and autolysin genes, whereas low levels lead to motility and inhibit biofilm formation (Vlamakis *et al*., 2013; Chai *et al*., 2010b; compare Fig. 2.3). In this context it is important to note that certain cell differentiation processes like biofilm formation and motility are mutually exclusive states (only one process at once) and that the described decision-making happens on single cell level. Within a community under laboratory conditions or a covered surface in the environment only a subgroup of cells express matrix genes, not all cells are motile, competent, or exoprotease producers (López & Kolter, 2010).

A striking characteristic of the SlrR protein is its intrinsic instability. It contains a LexA-like autocleavage motif that makes it intrinsically instable. Furthermore, the ClpCP protease was implicated in degradation of the SlrR protein (Chai *et al*., 2010a). An alternative explanation for SlrR instability is the formation of SlrR aggregates that lead to degradation (Newman & Lewis, 2013). In general, instability of SlrR explains how cells can switch back from a sessile to a motile life style.

As mentioned before, only a subgroup of cells of a community expresses matrix genes. This was explained by the observation that only medium levels of phosphorylated Spo0A lead to the expression of sufficient amounts of SinI protein that in turn inhibits enough SinR protein to allow expression of the second antagonist SlrR. This distinct situation seems to be present only in a subset of cells (Chai *et al*., 2008). The switch between sessile and motile state regulated by SinR and its antagonist SlrR and SinI was studied intensively using a so-called mother machine (Wang *et al*., 2010) that allows visualizing the growth and division of single cells under constant conditions over time. Due to the constant conditions, influences on cell differentiation by external signals could be excluded. Interestingly, the motile state showed no memory, whereas the sessile state was time limited (Norman *et al*., 2013).

Another protein that was characterized as an antagonist of SinR is the SlrA protein. It is a paralog of the SinI protein and can also bind to the SinR repressor in order to inhibit it. Expression of the *slrA* gene is repressed by the YwcC protein. Under laboratory conditions this repression is relatively tight so that SlrA does not have a major impact on complex colony structure and pellicle formation (Kobayashi, 2008; Chai *et al*., 2009). In addition, several other proteins were implicated in the regulation of biofilm formation and the switch between motility and biofilm formation via SinR (compare e. g. Vlamakis *et al*., 2013).

Additionally regulatory pathways and mechanism

Another pathway for the control of biofilm matrix component synthesis is a two-component system consisting of the histidine sensor kinase DegS and the aspartate response regulator DegU (Murray *et al*., 2009). DegS-DegU controls the expression of poly-γ-DL-glutamic acid that is required for the formation of submerged biofilms (Stanley & Lazazzera, 2005) and the hydrophobin BslA (Kobayashi & Iwano, 2012; Hobley *et al*., 2013). Interestingly, the DegQ protein is involved in the phosphate transfer from the sensor kinase to the response regulator. In the laboratory wild type 168 the respective gene carriers a promoter down mutation explaining the deficiency of this strain to express the machinery for poly-γ-DL-glutamic acid synthesis (Stanley & Lazazzera, 2005; McLoon *et al*., 2011). Moreover, the DegS-DegU system is involved in controlling several other processes like swimming and swarming motility, exoprotease production and even sporulation (Cairns *et al*., 2014a).

The AbrB protein is beside the SinR protein the second prominent repressor of biofilm matrix and transition phase genes. Deletion of the *abrB* gene affects the expression of 39 genes, including several biofilm matrix genes like the *eps* operon. The sole number of affected genes demonstrates the global relevance of the regulator (Hamon *et al*., 2004). In order to activate the expression of genes repressed by AbrB, the Spo0A regulator represses the expression of the *abrB* gene itself (Strauch *et al*., 1990; Fujita *et al*., 2005).

2.3. Regulation of cell differentiation by the second messenger c-di-GMP

Second messengers like the intensively studied cyclic adenosine monophosphate (cAMP) are a distinct form of signaling molecules that are involved in a variety of cellular processes. They can be found in eukaryotes as well as in prokaryotic organisms. A well-known example from the eukaryotic kingdom is cell-cell communication via cAMP in the social amoeba *Dictyostelium discoideum*. Upon starvation the cells secrete cAMP which in turn is sensed by other cell to coordinate the formation of multicellular communities (Konijn *et al*., 1967; Loomis, 2014). In prokaryotes, cAMP is, for instance, involved in the regulation of carbon catabolite repression (Görke & Stülke, 2008). In this case the absence of a preferred carbon source induces the production of cAMP which binds to the cAMP receptor protein. Upon cAMP-binding, this protein activates the expression of genes for the utilization of alternative, less preferred carbon sources.

Another second messenger that was studied intensively during the last decades is cyclic dimeric guanosine monophosphate (c-di-GMP). This molecule was identified for the first time in 1987 by Ross *et al.* as a factor involved in regulation of cellulose synthesis in the Gram-negative acetic acid bacterium *Acetobacter xylinum*. Since its discovery in bacterial cells, c-di-GMP was implicated mainly in the regulation of motility and biofilm formation, but also of cell cycle and virulence (Sondermann *et al.*, 2012). The cellular homeostasis of c-di-GMP is regulated or maintained by interplay of c-di-GMP synthesizing and degrading enzymes, called diguanylate cyclases (DGC) and phosphodiesterases

(PDE), respectively. Synthesizing enzymes are usually characterized by a GGDEF domain and degrading enzymes contain EAL or HD-GYP domains (Fig. 2.4), but there are also cases in which one protein contains more than one of these domains. Several DGCs and PDEs contain sensing domains in addition to their enzymatically active domain. This way sensing of external signals and transfer of the signal by affecting c-di-GMP homeostasis by production (or degradation) of the second messenger are directly coupled. The actual signal that is sensed by the cells, or more specific by the sensory enzymes, can be of different origin. For example, *Klebsiella pneunomiae* senses blue light *via* a sensory domain of the phosphodiesterase BlrP1. Upon photon absorption the EAL phosphodiesterase domain is activated via a conformational change of the protein (Barends *et al.*, 2009; Winkler *et al.*, 2014). In addition, gas sensing c-di-GMP homeostasis proteins were described. Examples are the DosC and DosP cyclase/phosphodiesterase couple from *E. coli* which can sense oxygen availability (Tuckerman *et al.*, 2009).

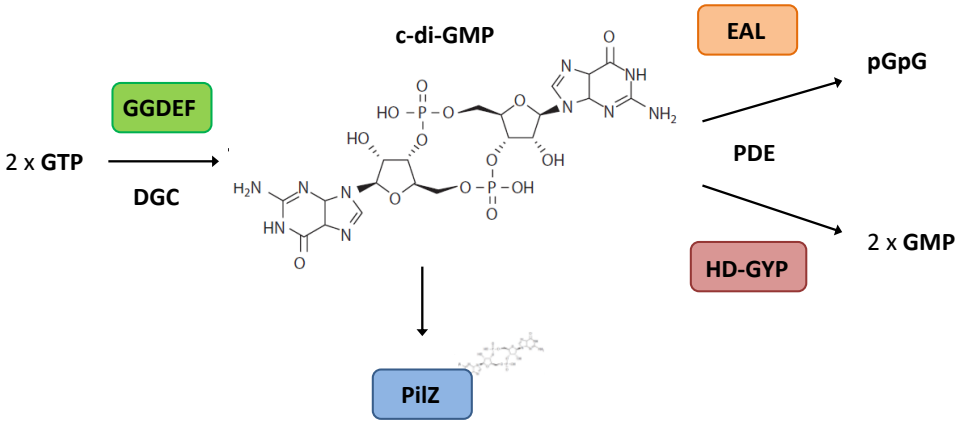

Figure 2.4. Control of c-di-GMP homeostasis. The second messenger c-di-GMP is synthesized by diguanylate cyclases (DGC) that contain a characteristic GGDEF domain, whereas phosphodiesterases (PDE) degrade c-di-GMP. These enzymes are characterized by EAL or HD-GYP domains. C-di-GMP binding proteins frequently contain a PilZ domain or non-functional EAL or HD-GYP domains (modified from Boyd & O'Toole, 2012)

In *Pseudomonas aeruginosa* the exopolysaccharide PsI activates the DGCs SadC and SiaD. This represents a positive feedback loop that enhances exopolysaccharide production because c-di-GMP activates exopolysaccharide production. However, the sensing mechanism is not understood so far (Irie *et al.*, 2012).

A common way how c-di-GMP regulates cellular processes is on post-translational level by binding to receptor proteins. This binding influences e. g. protein-protein interaction abilities or the enzymatic activity of the enzyme itself. Receptor proteins usually harbor a so called PilZ motif but also degenerated GGDEF domains can serve as a c-di-GMP receptor motif (see Fig. 2.4; Sondermann *et al.*, 2012). A well-studied example for a PilZ domain containing receptor protein and post-translational regulation by c-di-GMP is the YcgR protein from *E. coli*. This protein can interact with

the flagella motor upon binding of c-di-GMP and thereby influences swimming motility (Paul *et al*., 2010, Boehm *et al*., 2010).

Besides post-translational control *via* c-di-GMP, there are also several examples for control on transcriptional or translational level. For instance, c-di-GMP can bind to the FleQ regulator protein from *P. aeruginosa* to impair its DNA binding. Thereby c-di-GMP activates flagella gene expression and inhibits extracellular polysaccharide expression (Hickman & Harwood, 2008; Sondermann *et al*., 2012). Moreover, c-di-GMP can bind to regulatory element on the RNA (riboswitches) and thereby controls gene expression (Sudarsan *et al*., 2008).

Due to its discovery in Gram-negative bacteria research initially focused on the function of c-di-GMP in members of this bacterial phylum, but c-di-GMP is also present in Gram-positive bacteria and recently several publications shed light on the related signaling processes. Recent studies on the role of c-di-GMP in the human pathogen *Listeria monocytogenes* (Chen *et al*., 2014) and the actinobacterium *Streptomyces venezuelae* (Tschowri *et al*., 2014) are of special interest to get further inside into c-di-GMP signaling in Gram-positives. Chen *et al*. (2014) proposed that in *L. monocytogenes* elevated amounts of c-di-GMP induce the production of a novel exopolysaccharide that does not account greatly to biofilm formation but inhibits motility probably due to clumping of the cells. On the molecular level, increased exopolysaccharide production was explained by activating binding of c-di-GMP to a receptor protein involved in exopolysaccharide production. In the actinobacterium *S. venezuelae* that naturally exists in two different forms, vegetative hyphae and aerial sporulation hyphae, c-di-GMP controls differentiation between the two cell forms. As shown by Tschowri *et al.* (2014) this regulation is controlled via the novel c-di-GMP binding transcription factor BldD. On the phenotypical level, overexpression of PDE induced formation of sporulation hyphae, whereas overexpression of DGC impaired sporulation. This could be explained by c-di-GMP promoted dimerization of BldD via its C-terminal end. Only as a dimer the BldD protein shows a DNA-binding ability and inhibits the expression of sporulation genes. Interestingly, a tetramer of c-di-GMP is required to stabilize the BldD protein dimer. In comparison, three molecules of the closely related signaling factor c-di-AMP are required to stabilize formation of a DarA (c-di-AMP binding protein) trimere in *B. subtilis* (Sureka *et al*., 2014, Gundlach *et al*., 2014).

In *B. subtilis* the function of c-di-GMP is still only barely understood. In 2012, Chen *et al*. made a first attempt to elucidate its role for biofilm formation and motility in the less domesticated wild type strain NCIB3610. Although c-di-GMP regulates the switch between sessile and motile life style in Gram-negatives, the authors could not show any effect for the simultaneous deletion of several DGCs or PDEs on biofilm formation, respectively. However, they observed that deletion of the phosphodiesterase encoding gene *yuxH* decreases swarming motility compared to the wild type. In addition, they identified the PilZ domain containing protein YpfA as a potential c-di-GMP binding protein that might sense elevated c-di-GMP amounts, e.g. in a *yuxH* deletion mutant, and thereby

inhibits motility similar to the YcgR protein from *E. coli* (Paul *et al*., 2010, Boehm *et al.*, 2010). Recently these observations and enzymatic activities of the protein involved in *B. subtilis* c-di-GMP homeostasis were further analyzed by Gao *et al*. (2013). Initially the authors were not able to detect c-di-GMP in the NCIB3610 wild type but deletion of the gene for the phosphodiesterase YuxH (new name PdeH) or overexpression of the potential DGCs YdaK, YtrP (DgcP), YhcK (DgcK), and YkoW (DgcW) in *B. subtilis* enabled the authors to detect c-di-GMP in case of the last three enzymes. In contrast, overexpression of YdaK did not lead to detectable c-di-GMP amounts but *in vitro* data and the presence of a degenerated GGDEF supports a function as a c-di-GMP receptor protein (Gao *et al*., 2013). Also, *in vitro* studies with the three purified DGCs and the PDE confirmed the proposed enzymatic functions. Additionally, c-di-GMP binding assays with putative receptor protein YpfA (DgrA) and motility assays further supported its role as a c-di-GMP dependent regulator of motility in *B. subtilis*.

2.4. The YmdB protein

Initially, the protein aroused interest because the respective gene is located downstream and in the same operon with the gene encoding the major endoribonuclease RNase Y of *B. subtilis* (Lehnik-Habrink *et al*., 2011a, b; Shahbabian *et al*., 2009). Strikingly, the *ymdB* deletion mutant showed a strong overexpression of a certain protein in an SDS-PAGE analysis of cell extracts. This overexpressed protein could be identified as Hag, the flagellin protein (Diethmaier *et al*., 2011). In addition, deleting the *ymdB* gene resulted in a strong biofilm defect. Colonies formed on biofilm-inducing MSgg agar plates appeared smooth and shiny compared to the rough colonies of the wild type strain (see Fig. 2.5).

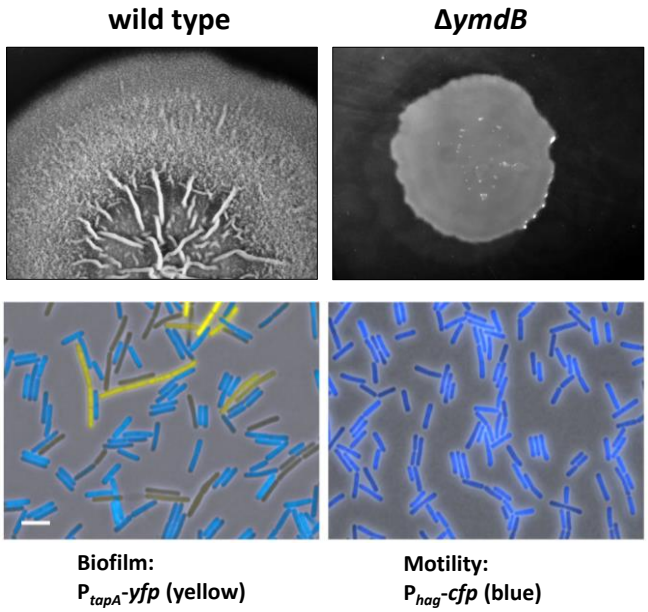

Figure 2.5 Phenotype of the Δ*ymdB* mutant strain. Loss of the YmdB phosphodiesterase leads to a drastically reduces colony structure on biofilm inducing MSgg agar plates. Single cell fluorescent microscopy revealed that the deletion of the *ymdB* gene inhibits bistable gene expression of motility (blue cells) and biofilm genes (yellow cells). In contrast to the wild type strain, all cells of the *ymdB* mutant express motility genes (Diethmaier *et al*., 2011, 2014).

These initial observations could also be confirmed on transcriptional level. As revealed by qRT-PCR, expression of *sigD* controlled motility genes, including the *hag* gene, was increased in the *ymdB*

deletion background, whereas the expression of biofilm matrix genes was decreased (Diethmaier *et al*., 2011). Moreover, these observations were also verified by microarray analysis (Diethmaier *et al*., 2014). Global transcriptome and qRT-PCR analyses are a well-suited way to obtain general changes in gene expression for a large amount of cultivated cells, but they struggle to answer what is going on at single cell level. Therefore, Diethmaier *et al*. (2011) constructed biofilm matrix gene (P_{tapA}-*yfp*) and motility gene (P_{hag}-*cfp*) reporter fusion to visualize expression of these genes as an example for their regulons at single cell level. Strikingly, in the *ymdB* deletion mutant all cells expressed motility genes and no cell chains but single and relatively short cells were visible (Fig. 2.5).In contrast, the isogenic wild type strain (168 background) showed several different cell types. Most obviously, elongated cells that arranged in chains and expressed biofilm matrix genes were visible. Moreover, shorter single cells expressing motility genes could be observed. A third cell type was characterized by no expression of any of the two reporter fusion and relatively short cells. These observations explained the transcriptome data on single cell level and suggest that the YmdB protein is involved in the regulation of switching between biofilm and motility genes expression. This expression is bistable, meaning that a single cell can only expression one gene set at the same time (Vlamakis *et al*., 2013; Dubnau & Losick, 2006).

Expression of biofilm matrix and motility genes is mainly controlled by the master regulator of biofilm formation SinR and the interaction with its antagonists, e.g. the proteins SinI and SlrR (compare 2.3.). Since transcription analyses revealed that the *slrR* is strongly repressed in the *ymdB* deletion mutant, Diethmaier *et al*. (2011) hypothesized that this might be the reason for the observed phenotypes and that overexpression of *slrR* could restore wild type phenotypes. Indeed, *slrR* overexpression restored complex colony formation to the *ymdB* mutant. In this context, a similar effect could also be observed for the deletion of the gene for the SinR protein in the *ymdB* deletion background, but in general it remained unclear how the YmdB protein influences the decision making between biofilm and motility gene expression. Novel insights were expected from studying suppressor mutants that appeared spontaneously and repaired the biofilm defect on the *ymdB* deletion mutant. Kruse (2013) was able to isolate several suppressor mutants and identified the origin for repaired colony structure within the *sinR* gene. Detailed analysis of the suppressor mutants showed that different point mutations within the *sinR* gene, but also deletion of the whole *sinR* gene and its genetic surrounding can restore biofilm matrix gene expression. The identified *sinR* mutations either lead to decreased SinR protein amounts or most likely affected the DNA binding or protein-protein interaction properties of the SinR protein. Also, suppressor mutants with less obvious mutations were identified that required further research (e. g. SinR: Trp104Leu and a SinR: Pro42Pro silent mutation).

In an attempt to identify the molecular function of the YmdB protein Diethmaier *et al*. (2014) characterized the protein structurally and enzymatically. The YmdB protein shares 44% sequence

identity with the 2', 3'-cyclic AMP phosphodiesterase DR1281 from *Deinococcus radiodurans* that is a member of the calcineurin-like metallophosphoesterase family (Shin *et al*., 2008). Therefore it seemed likely that YmdB also acts as a phosphodiesterase. *In vitro* experiments demonstrated that YmdB cuts the test substrate bis-*p*-nitrophenyl phosphate but showed no phosphatase activity as also shown for some other members of the calcineurin-like protein group.

To further understand the function of the YmdB protein the crystal structure was solved. As predicted, the obtained structure resembled the fold of a calcineurin-like metallophosphoesterase (phosphodiesterase) and consequently contains a dimetal cluster in its active site (probably Fe^{2+} and Fe^{3+}). Size exclusion chromatography and the crystal structure itself further suggest that YmdB naturally occurs as a tetramer built up by two YmdB dimers. The crystal structure suggested that an oxygen atom of the carboxyl-group of the glutamate (E) residue 39 is required for the stabilization of the metal ions in the active center. To test this assumption the glutamate residue was exchanged against the isosteric glutamine (Q) residue. As hypothesized, the E39Q within the YmdB protein drastically reduced phosphodiesterase activity *in vitro* and also inhibited, once introduced into wild type *B. subtilis* cell, complex colony and pellicle formation. This suggested that the enzymatically active YmdB protein is essential for biofilm formation (Diethmaier *et al*., 2014). In addition to processing of bis-*p*-nitrophenyl phosphate, YmdB can also process 2', 3'-cyclic AMP (as shown for DR1281 from *D. radiodurans*) and 3', 5'-cyclic AMP but has no activity against c-di-GMP. However, the enzymatic constants of these reaction compared to values from the literature suggest that cyclic nucleotides are not the main target of the YmdB phosphodiesterase.

2.5. Tyrosine phosphorylation

A major task for living beings is to adapt to changing conditions and the stresses in their environment. This can be managed on the level of gene expression but also on post-translational level which is in many cases the fastest way. One prominent example for a post-translational modification is protein phosphorylation which can be found in all domains of life and often controls the enzyme activity or DNA binding ability of a protein (Pawson & Scott, 2005; Grangeasse *et al*., 2007). A distinct kind of protein phosphorylation which is especially well-studied in eukaryotes is tyrosine phosphorylation. However, it can also be found in archaea and bacteria (Pawson & Scott, 2005; Chao *et al*., 2014; Kennelly, 2014). Examples from eukaryotes are receptor tyrosine kinases which belong to the family of cell surface receptor protein and sense signals *via* their external ligand binding site. In response to the signal they transfer phosphate to the hydroxyl group of tyrosines of target proteins. This way receptor tyrosine kinases are involved in the regulation of many important processes like cell cycle, cell proliferation and cell differentiation (Schlessinger, 2000). Moreover, a deviant form of tyrosine kinases activity is characteristic for several human oncogenes, including the

chimeric *BCR-ABL* gene product that is involved a particular kind of chronic leukemia (Pawson & Scott, 2005).

Bacterial tyrosine kinases in *B. subtilis*

Bacterial tyrosine kinases make up an own protein class that can only be found in prokaryotes and lacks the typical Hanks-type motif of their eukaryotic counterparts (Chao *et al*, 2014; Cousin *et al*., 2013). The structure of BY kinases is characterized by an N-terminal transmembrane loop (flanked by two transmembrane α-helixes) which is thought to have a sensory role and a cytosolic C-terminal domain which contains the catalytic sites. These sites usually include a Walker A, Walker A' and a Walker B motif which are required for nucleotide binding and a C-terminal tyrosine cluster which is important for (auto-) phosphorylation (Grangeasse *et al*., 2010; Grangeasse *et al*., 2012). An important difference regarding the organization of tyrosine kinases in Gram-negative and Gram-positive bacteria is that the transmembrane domain and the cytosolic membrane form a single protein in Gram-negatives, whereas in Gram-positive bacteria the two domains are present as separate proteins (Grangeasse *et al*., 2010). Although separate proteins, there are several examples from Firmicutes that the transmembrane domain affects kinase activity suggestion a modulator function (Mijakovic *et al*., 2003; Morona *et al*., 2003; Soulat *et al*., 2006; Elsholz *et al*., 2014). The genome of *B. subtilis* contains two genes encoding a BY kinase, namely *ptkA* and *epsB*. The PtkA and EpsB proteins also contain the characteristic Walker A, A', B motifs and a C-terminal tyrosine cluster, respectively. Moreover, PtkA contains three tyrosine residues (Tyr-225, 227, 228) and EpsB contains two tyrosine residues (Tyr-225, 227) at the C-terminal end. In general, amino acid sequence comparisons show that EpsB is slightly truncated at the C-terminal end compared to PtkA (see Fig. 2.6). Initial studies on the function of the protein products, revealed that PtkA autophosphorylates on a tyrosine residue *in vitro* but failed to show this for EpsB. Only when purified from *E. coli*, the EpsB protein could be detected using anti-P-Tyr antibodies. The authors suggested that the lack in ability to autophoshorylate *in vitro* might be due to previous autophosphorylation or phosphorylation by *E. coli* tyrosine kinase during the purification process. This would block *in vitro* phosphorylation with radioactive ATP later on (Mijakovic *et al*., 2003). However, EpsB was not studied afterwards for a decade (Gerwig *et al*., 2014; Elsholz *et al*., 2014).

Since the PtkA tyrosine kinase autophosphorylates *in vitro*, Mijakovic *et al.* (2003) wondered which residues were important for autophosphorylation. Using mutational analyses they were able to show that the Asp-81 und Asp-83 residues of the Walker A' motif are essential for autophoshorylation and that the tyrosine residues in the C-terminal tyrosine cluster are required for effective autophosphorylation. Besides the autophosphorylation ability of PtkA, they also identified the UDP-glucose dehydrogenase Ugd and TuaD as targets of the PtkA protein. Later on, tyrosine 70 residue of the Ugd protein was identified as the phosphorylated amino acid (Petranovic *et al*., 2009).

Supporting the view that the transmembrane domain and the cytosolic domain of tyrosine kinases from Gram-positives, although separate proteins, are functionally connected, it was shown that the cytosolic PtkA kinase requires its cognate transmembrane protein TkmA to phosphorylate the Ugd protein. Interestingly the phosphatase PtpZ, also encoded in the *tkmA-ptkA-ptpZ-ugd* operon, desphophorylates the Ugd protein and thereby inactivates it (Mijakovic *et al.*, 2003). This demonstrated that the *tkmA-ptkA-ugd-ptpZ* operon forms a functional unit.

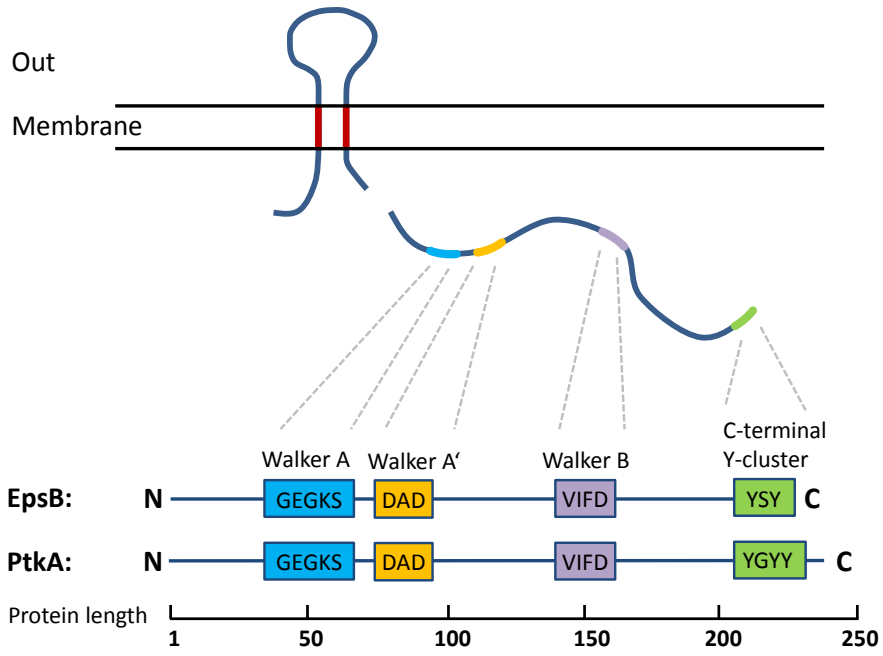

Figure 2.6. Structure of the tyrosine kinases PtkA and EpsB as examples for Gram-positive bacteria. Tyrosine kinases from Gram-positive bacteria usually consist of a transmembrane modulator protein and a cytosolic protein that contains the active sites. The active sights of the PtkA kinase and its homolog EpsB are highly conserved, but the C-terminal tyrosine cluster of EpsB is truncated (adapted from Grangeasse *et al.*, 2007).

Other phosphorylation targets of the PtkA kinase are the single-stranded DNA-binding proteins SsbA and SsbB (Mijakovic *et al.*, 2006; Petranovic *et al.*, 2007). Tyrosine phosphorylation of the two proteins was shown to effect DNA replication and the bacterial cell cycle. Consequently, *ptkA* and *ptpZ* mutants showed a severe growth defect. Strikingly, Kiley & Stanley-Wall (2010) could not reproduce this growth defect and no difference in nucleoid localization in a *ptkA* or *ptpZ* mutant in the NCIB3610 background. Thus, the authors suggest that this discrepancy might be due to different cultivation conditions or due to use of different genetic backgrounds. However, the role of PtkA in DNA replication is unclear and remains to be further studied. A novel and attractive facet of tyrosine phosphorylation by the PtkA kinase was proposed by Jers *et al.* in 2010. The authors could show that tyrosine phosphorylation can influence the activity of several proteins, but also demonstrated an effect on the cellular localization of the target proteins, including the glycolytic enzyme enolase, the flagellar filament assembly protein YvyG, the apartate semialdehyde dehydrogenase Asd and several

other protein (InfA, Ldh, OppA, YjoA, YnfE, YorK). Recently, the FatR protein was identified as an interaction partner of PtkAs cognate transmembrane modulator TkmA. Further experiments demonstrated that phosphorylation of FatR, a regulator of polyunsaturated fatty acid synthesis, on the Tyr-45 residue decreases its DNA-binding ability (Derouiche *et al*., 2013). This presents an example how tyrosine phosphorylation regulates metabolism. Very recently, also the glycosyltransferase and motility inhibitor EpsE could be identified as the first known target of the tyrosine kinase EpsB (Elsholz *et al*., 2014).

Functional relevance of bacterial tyrosine kinases in extracellular/ capsular polysaccharide synthesis and biofilm formation

From the current state of research it is hard to propose "the" specific function BY kinases fulfill in bacterial cells and also the actual mechanism of their action need to be clarified. However, studies for several BY kinases show that these proteins are involved in capsular and extracellular polysaccharide production and thereby influence virulence and biofilm formation. Fitting perfectly to this assumption, tyrosine kinase genes often cluster with genes required for synthesis and export of capsule and extracellular polysaccharides as shown for the BY kinase encoding genes *wzc* from *E. coli*, *capB2* from *Staphylococcus aureus*, and *cpsD* from *Streptococcus pneunomiae* (Wugeditsch *et al*., 2001; Soulat *et al*., 2007; Morona *et al*., 2000). Moreover, there are several examples that directly connect tyrosine phosphorylation and extracellular and capsular polysaccharide production. For the Etk protein that is expressed in a subset of different pathogenic *E. coli* strains, Ilan *et al*. (1999) could demonstrate *in vitro* tyrosine kinase activity and proposed that protein tyrosine kinases of pathogenic *E. coli* are important for virulence and exopolysaccharide production. An example from Gram-positive bacteria is the protein tyrosine kinase CpsD from *S. pneumoniae*. In this case, autophosphorylation of CpsD negatively effects capsular polysaccharide production and the cognate CpsC protein is required for this effect (Morona *et al*., 2000).

As shown for the BY kinase Wzc from *E. coli,* tyrosine kinases are part of a big complex for synthesis and export of extracellular polysaccharides but the Wzc protein is only required for assembly of capsular polysaccharides but not directly involved in synthesis (Wugeditsch *et al*., 2001; Whitfield, 2006). One possibility function within this complex might be that of a scaffold protein that forms a membrane anchor for other subunits and controls the conformation of the whole complex depending on the own phosphorylation state (Whitfield, 2006; Olivares-Ilana *et al*., 2008; Grangeasse *et al*., 2012). In Gram-positive bacteria an octameric complex of the transmembrane modulator protein component might built up a transmembrane channel that serves for the export of polysaccharides. In Gram-negatives, like *E. coli*, where kinase and transmembrane domain form one single protein a second protein is required. This protein, called Wza forms an octameric channel that spans the inner and outer membrane and interacts with the BY kinase Wzc (Collins *et al*., 2007).

Besides known interactions of BY kinases with putative polysaccharide channels it is striking that they are structurally similar to polysaccharide co-polymerases (Morona *et al*., 2009). This further supports the hypothesis that at least some BY kinase determine polysaccharide length as co-polymerases and thereby influence polysaccharide production (Bechet *et al*., 2010; Whitfield, 2006).

A first hint that tyrosine phosphorylation could affect biofilm formation in *B. subtilis* presented the regulation of the UDP-glucose dehydrogenase Ugd *in vitro* (Mijakovic *et al*., 2003; Petranovic *et al*., 2009), because UDP-glucose is considered as a precursor molecule for exopolysaccharide synthesis (Chai *et al*., 2012). In 2010, Kiley & Stanley-Wall addressed the relevance of tyrosine phosphorylation and especially of the proteins encoded within the *tkmA-ptkA-ptpZ-ugd* operon in more detail. In their study they demonstrated that the deletion of the *ptkA* gene in the undomesticated NCIB3610 affects biofilm formation and that the kinase PtkA is required for effective sporulation under biofilm-forming conditions. In agreement with previous work, mutation of the Walker A' motif (D81A, D83A) of PtkA resulted in the same biofilm and sporulation defect as deletion of the whole gene. Surprisingly, mutation of conserved residues in the C-terminal tyrosine cluster (Y255A, Y227A and Y228A) did not affect colony and pellicle structure, suggesting a minor role of these residues for biofilm formation (compare Fig. 2.6). This observation challenges the *in vivo* relevance of the *in vitro* results obtained by Mijakovic *et al.* (2003) showing that the mutated PtkA protein does not autophosphorylate. Kiley & Stanley-Wall (2010) also studied the other genes of the *tkmA-ptkA-ptpZ-ugd* operon. They showed that the kinase modulator protein TkmA is also required for biofilm formation but the phenotype of a deletion mutant is different from a *ptkA* deletion mutant. The authors explain this with a potential interaction of TkmA with other proteins, e. g. the EpsB kinase. Moreover, they demonstrated that the deletion of phosphatase encoding *ptpZ* leads to the same phenotype as a *ptkA* deletion mutant. In this case further studies are needed to understand the underlying mechanism. In an attempt to identify the biofilm-related phosphorylation target of PtkA, the authors deleted the genes for the several tyrosine phosphorylated proteins, including the ones for the PtkA targets Ugd and TuaD, but failed to show a connection to biofilm formation. Therefore, the mechanism how the PtkA kinase affects biofilm formation and its potential phosphorylation targets remains to be identified (compare 5.3).

Mechanistic insights how the second known *B. subtilis* tyrosine kinase EpsB influences biofilm formation or more precise extracellular polysaccharide (EPS) production was published recently (Elsholz *et al*., 2014). The authors propose that EPS production is subject to a self-enforcing feedback regulation involving the EpsB kinase and its modulator protein EpsA. The EpsA protein seems to sense EPS via its extracellular domain and stimulates autophosphorylation of the EpsB kinase in the absence of EPS. This autophosphorylation inactivates the kinase activity of EpsB. If EPS is present EpsB does not get autophosphorylated but instead transfers the phosphate residue to the glycosyltransferase EpsE which is involved in the synthesis of EPS and thereby activates the protein.

Inducing point mutations into EpsB the authors could confirm the results of Kiley & Stanley-Wall (2010) for the homologous PtkA kinase that the amino acids Asp-81 and Asp83 are important for biofilm formation and kinase activity. Exchanging the aspartate residues against alanines lead to the same less structure colonies and pellicles as observed for the *epsB* deletion mutant. Furthermore, mutating the residues Tyr-225 and Tyr-227 to a phenylalanine (blocking of phosphorylation) induced complex colony structure, whereas mimicking a phosphorylation by exchanging the two residues by a glutamate reduced complex colony structure similar to the deletion mutant (compare Fig. 2.6 and chapters 5.3 and 5.4).

2.6. Objectives

Biofilm formation and the differentiation into different cell types are of great importance for the well-being of the model bacterium *B. subtilis.* Therefore, the switch between e.g. motile and sessile life styles is highly regulated. One main objective of this work was to study the function of the putative tyrosine kinase EpsB and its cognate modulator EpsA in the regulation of biofilm formation and extracellular polysaccharide production. Since *B. subtilis* contains a second homologous tyrosine kinase modulator couple, the proteins PtkA and TkmA, which had been implicated in the regulation of biofilm formation and sporulation before (Kiley & Stanley-Wall, 2010), this works also aimed to elucidate if the two systems have overlapping function or can replace each other. For this purpose the respective tyrosine kinase and modulator genes were deleted on its own and in parallel to study phenotypical effects of a loss of the protein.

The second main objective was to further elucidate the molecular mechanism by which the YmdB phosphodiesterase influences biofilm formation and cell differentiation. To identify the initial cause for reduced expression of the SinR antagonist and repression target SlrR, SinR protein amounts were determined in the *ymdB* mutant in comparison to the wild type. Furthermore, spontaneous suppressor mutants were isolated and characterized to gain novel insights into the mechanism of YmdB action. Since the YmdB protein was characterized as a phosphodiesterase before, YmdB might also act as an RNase. To address this hypothesis, RNA binding experiments with the YmdB protein and RNA sequencing were performed.

Finally, it was tested if changes in c-di-GMP concentration influence biofilm formation in *B. subtilis*. In Gram-negative bacteria, this second messenger has been implicated in switching between sessile and motile life styles.

3. Materials and methods

Materials: chemicals, aids, … and oligonucleotides are listed in the appendix.

3.1. Bacterial strains and plasmids

Bacterial strains and plasmids are listed in the appendix.

3.2. Media

Buffers, solutions and media were prepared with deionized water and autoclaved (20 min at 121°C and 2 bar). Thermolabile substances were dissolved and sterilized by filtration. Solutions are related to water, other solvents are indicated.

Bacterial growth media and optional additives

B. subtilis was grown in C-minimal, MSgg, YT or LB medium, supplemented with specific additives as indicated. CSE-Glc minimal medium was supplemented with 0.5% (w/v) glucose (Glc), sodium succinate (S) (final concentration 8 g/l) and potassium glutamate (E) (final concentration 6 g/l). Further variations of carbon sources are indicated. Basic media were supplemented with 1.7% (w/v) agar for solidification. MSgg minimal medium was solidified with 1.5% (w/v) Bacto (BD) agar (adapted from Pietack, 2010).

5x C salts (1 l)	KH_2PO_4	20 g
	K_2HPO_4 x 3 H_2O	80 g
	$(NH_4)_2SO4$	16.5 g
III` salts (1 l)	$MnSO_4$ x 3 H_2O	0.232 g
	$MgSO_4$ x 7 H_2O	12.3 g
10 x MN medium	K_2HPO_4 x 3 H_2O	136 g
	KH_2PO_4	60 g
	Sodium citrate x 2 H_2O	10 g

1x C minimal medium	5x C salts	20 ml
(100 ml)	Tryptophan (5 mg ml^{-1})	1 ml
	Ammonium iron citrate (2.2 mg ml^{-1})	1 ml
	III` salts	1 ml
	H_2O_{deion}	ad 100 ml
1x CSE medium	5x C salts	20 ml
(100 ml)	Tryptophan (5 mg ml^{-1})	1 ml
	Ammonium iron citrate (2.2 mg ml^{-1})	1 ml
	III` salts	1 ml
	Potassium glutamate (40%)	2 ml
	Sodium succinate (30%)	2 ml
	H_2O_{deion}	ad 100 ml
SP medium	Nutrient Broth	0.8 g
(1 l)	$MgSO_4$ x 7 H_2O	0.25 g
	KCl	1.0 g
	H_2O_{deion}	ad 1 l
	autoclave, after cooling addition of:	
	$CaCl_2$ (0.5 M)	1 ml
	$MnCl_2$ (10 mM)	1 ml
	Ammonium iron citrate (2.2 mg ml^{-1})	2 ml
MNGE medium	1x MN medium	8.77 ml
(10 ml)	Glucose (20%)	1 ml
	Potassium glutamate (40%)	50 µl
	Ammonium iron citrate (2.2 mg ml^{-1})	50 µl
	Tryptophan (5 mg ml^{-1})	100 µl
	$MgSO_4$ x 7 H_2O (1 M)	30 µl
	+/- CAA (10%)	100 µl
LB medium	Tryptone	10 g
(1 l)	Yeast extract	5 g
	Sodium chloride	10g
YT medium	compare phage transduction (chapter 3.3.5.)	

MSgg medium compare biofilm methods (chapter 3.3.8.)

Antibiotics

Antibiotics were prepared as 1000-fold concentrated stock solutions. Ampicillin, spectinomycin, lincomycin and kanamycin were dissolved in deionized water, chloramphenicol, erythromycin and tetracyclin in 70% ethanol. All solutions were sterile filtrated and stored at -20°C. Autoclaved medium was cooled down to approximately 50°C. Then the antibiotics were added to their final concentration.

Selection concentration for *E. coli*

Ampicillin	100 µg ml^{-1}
Kanamycin	50 µg ml^{-1}
Streptomycin	100 µg ml^{-1}

Selection concentration for *B. subtilis*

Chloramphenicol	5 µg ml^{-1}
Erythromycin[1]	2 µg ml^{-1}
Kanamycin	10 µg ml^{-1}
Lincomycin[1]	25 µg ml^{-1}
Spectinomycin	150 µg ml^{-1}
Tetracycline	12.5 µg ml^{-1}

[1]For selection on *ermC* a mixture of erythromycin and lincomycin was used in their respective concentration, see above.

3.3. Methods

3.3.1. General methods

An overview of general methods that are described in the literature and were used for this work is presented in **Tab. 3.1**. on the next page.

Table 3.1. General methods

Method	Reference
Absorption measurement	Sambrook *et al.*, 1989
Ethidium bromide staining of DNA	Sambrook *et al.*, 1989
Precipitation of nucleic acids	Sambrook *et al.*, 1989
Gel electrophoresis of DNA	Sambrook *et al.*, 1989
Gel electrophoresis of proteins (denaturing)	Laemmli, 1970
Ligation of DNA fragments	Sambrook *et al.*, 1989
Determination of protein amounts	Bradford, 1976
Plasmid preparation from *E. coli*	Sambrook *et al.*, 1989
Sequencing according to the chain termination method	Sanger *et al*., 1977

3.3.2. Cultivation of bacteria

Unless otherwise stated, *E. coli* was grown in LB medium at 37°C and 200 rpm in tubes and flasks. *B. subtilis* was grown in LB medium, CSE-Glc and MNGE medium at 37°C or 28°C in tubes and Erlenmeyer flasks. Fresh colonies from plates or glycerol cultures were used for inoculation. Furthermore, overnight liquid cultures were used. Growth was measured at a wavelength of 600 nm (adapted from Pietack, 2010).

Storage of bacteria

E. coli was kept on LB medium agar plates up to 4 weeks at 4°C. For long-term storage glycerol cultures were used. *B. subtilis* was cultured on YT and LB medium agar plates not longer than 3 days. SP agar plates and tubes were used for the long-term storage of *B. subtilis*. For the storage of bacteria in glycerol, 800 µl of a fresh overnight culture was gently mixed with 350 µl of 50% glycerol. Stocks were frozen and stored at -70°C (adapted from Pietack, 2010).

3.3.3. Transformation of *E. coli*

Preparation of competent *E. coli* DH5α and XL1 blue cells (Inoue *et al*., 1990)

At first, 250 ml SOB medium within a 1 l flask was inoculated with a colony of *E. coli* DH5*α* or XL1 blue and incubated at room temperature and 200 rpm for at least 36 hours until an OD_{600} of about 0.6 was reached. Then the cells were incubated on ice for 10 minutes and centrifuged for 10 minutes at 2,500 g and 4°C. The pellet was resuspended in 80 ml transformation buffer (TB). Again the cell

suspension was centrifuged as described before and resuspended in 20 ml TB. While pivoting the cell suspension, DMSO was added to a final concentration of 7% and the suspension was incubation on ice for further 10 minutes. Subsequently, the cells were frozen in liquid nitrogen as aliquots of 200 µl. The long-term storage of the competent cells was performed at -70°C (adapted from Pietack, 2010).

SOB medium	20 g tryptone
(1 l)	5 g yeast extract
	0.584 g NaCl
	0.188 g KCl
	2.032 g $MgCl_2$
	2.064 g $MgSO_4$
TB (1 l)	3.04 g PIPES
	2.2 g $CaCl_2$ x H_2O
	18.64 g KCl
	10.84 g $MnCl_2$ x H_2O

Preparation of competent *E. coli* BL21 cells using the $CaCl_2$ method (Lederberg & Cohen, 1974)

To prepare competent *E. coli* cells, 4 ml LB medium were inoculated with a single colony or with a cryoculture of *E. coli* BL21 and the culture was incubated with agitation over night at 37°C. In the morning, 100 ml LB medium (1 l flask) was inoculated to an OD_{600} of 0.05–0.1 and the culture was grown at 37°C until the culture had reached an optical density of about 0.3. Then the cells were transferred into two 15 ml falcon tubes and the cells were harvested by centrifugation for 6 min at 5,000 rpm and 4°C. Afterwards, the supernatant was discarded and the cells were resuspended in 5 ml of ice-cold $CaCl_2$ solution. Subsequently, the cells were incubated for 30 min on ice and collected again by centrifugation as described before. Next, the cell pellet was resuspended in 1 ml of ice-cold $CaCl_2$ (50 mM) solution. Now the cells were competent and ready for transformation (adapted from Rothe, 2012).

Transformation of competent cells

Competent cells were defrosted on ice if required, and 10–100 ng DNA was added to 200 µl cells. The suspension was mixed and incubated on ice for 30 minutes. The heat shock was performed at 42°C for 90 seconds. Afterwards, the samples were incubated for 5 minutes on ice. After addition of 600 µl LB medium, the samples were incubated for 60 minutes at 37°C (with shaking). 100 µl and the concentrated rest of the cells were plated on LB selection plates with ampicillin (adapted from Pietack, 2010).

3.3.4. Transformation of *B. subtilis* (Kunst & Rapoport, 1995)

Preparation of competent cells

Ten milliliters of MNGE medium containing 1% CAA were inoculated with an overnight culture of *B. subtilis* to an optical density of OD_{600} = 0.1. This culture was grown at 37°C with aeration until an OD_{600} of 1.3 was reached. Then the culture was diluted with 10 ml MNGE medium without CAA and incubated again for one hour. After the incubation step, the cells were directly used for transformation or harvested by centrifugation (5 min; 5,000 rpm; RT). In case of centrifugation, the supernatant was retained in a sterile falcon tube. The pellet was resuspended in 1/8 of the supernatant and supplemented with glycerol to a final concentration of 10%. Aliquots of 300 µl were frozen in liquid nitrogen and stored at -70°C (adapted from Pietack, 2010).

Transformation of the competent cells

The 300 µl cell aliquots were defrosted at 37°C and the following solution was added:

1.7 ml	1 x MN
43 µl	20% glucose
34 µl	1 M $MgSO_4$

To 400 µl of this cell suspension 0.1 µg–1 µg was added and incubated for 30 minutes at 37°C (with shaking). Then 100 µl expression solution [500 µl yeast extract (5%), 250 µl CAA (10%), 250 µl deion. water and 50 µl tryptophan (5 mg/ ml)] was added and incubated for further 60 minutes at 37°C. Afterwards the cells were plated on selective medium (adapted from Pietack, 2010).

3.3.5. SPP1 phage transduction (Kearns *et al*., 2005; Yasbin & Young, 1974)

In contrast to the domesticated *B.s.* 168 strain, the less domesticated NCIB3610 strain does not take up foreign DNA by natural competence. Therefore, transfer of foreign DNA was mediated by SPP1 phage transduction.

Preparation of phage lysates

To prepare a SPP1 phage lysate for transduction of NCIB3610 strains 10 ml YT medium (supplemented with antibiotics if needed) were inoculated with a fresh colony of the cells that carry the gene deletion (resistance marker) that is supposed to be transferred. The cells were cultivated at 37°C and 200 rpm to an OD_{600} of 0.4–0.8. Then, a dilution series of the SPP1 phage (*B. subtilis* 168) was prepared in YT medium (10^{-1}–10^{-9}). For the infection with the phages 0.1 ml of the dilutions 10^{4}-10^{-9} (e. g.) were mixed with 0.9 ml of the cultivated cells (use 15 ml falcon tubes) and the mixture was incubated for 15 min at 37°C without shaking. Next, 3 ml of pre-warmed/fluid (microwave) YT

soft agar was added and everything was mixed by vortexing. Then the soft agar mixture was poored on selective (with one or more antibiotics) YT plates and the plates were dried for 20 min followed by an over night incubation at 37°C. On the next day, a plate that showed clear lysis halos but no complete lysis of the cells (Fig. 3.1) was chosen and the phage-containing soft agar was removed by adding 3 ml of liquid YT medium and scratching with a pipette tip. The soft agar and the liquid medium were conveyed to a conic 50 ml falcon tube and vortexed to release the phages. Next, the mixture was centrifuged for 10 min at 5,000 rpm and the phage-containing supernatant was transferred to a new falcon tube.

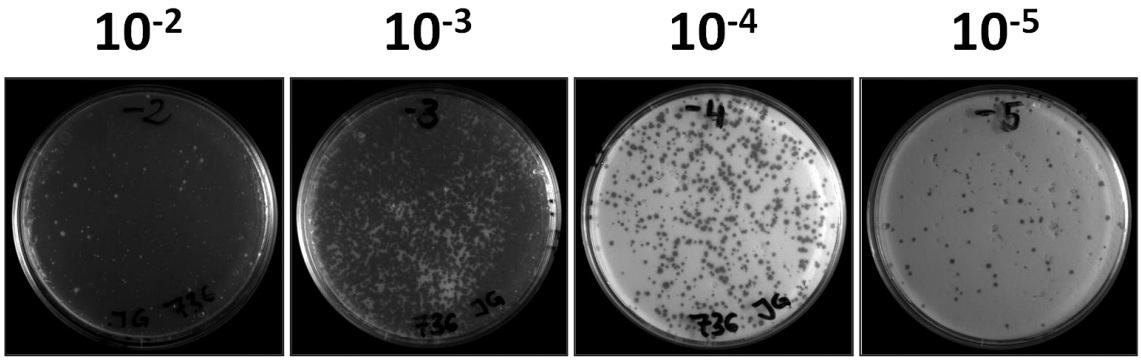

Figure 3.1. Overview of the agar plates for the preparation of phage lysate. In this example the dilution step 10^{-3} was chosen for the preparation of phage lysate. This plate shows some remaing cells but clear lysis. In contrast, the lysis on the plate of the dilution step 10^{-2} is complete and only some (propably phage resistant) cells are growing. Also, the plate with the dilution step 10^{-4} should not be used for the preparation of phage lysate because the extent of cell lysis might be too small.

To digest free DNA, 10 µl DNase I (25 µg/ ml) was added and the mixture was incubated for 10 min at RT. The digested supernatant was sterile filtrated (0.2 µm filter) and the phage lysate was stored at 4°C. All phage work was performed under the laminar flow cabinet which was sterilized with 70% ethanol and by UV light irridation subsequent to the experiments (adapted from Diethmaier, 2011).

Transduction of the recipient strain

For transduction 10 ml YT medium was inoculated with a fresh colony of the NCIB3610 (derivative) recipient strain and incubated at 37°C and 200 rpm until the culture reached an OD_{600} of 0.4 to 0.8. For the infection 0.9 ml of the recipient strain was mixed with 0.1 ml of the phage lysate (10^{-1}–10^{-2} dilutions). Then, 9 ml liquid YT medium was added and the mixture was incubated for 30 min at 37°C without shaking. As a control the phages were incubated without the recipient strain and *vice versa*. After the incubation the mixture was centrifuged for 10 min at 5,000 rpm, the supernatant was discarded, and the cells were resuspended in the remaining volume. Next, the cell suspension was plated on selective YT medium plates containing sodium citrate and incubated over night at 37°C. On the next days, single antibiotic resistant colonies appeared on the selective plates. These cells were

streaked out several times on selective plates (sodium citrate containing YT medium and then on SP) to separate them from the phages. Once a single phage-free colony could be obtained, it was cultivated and chromosomal DNA was isolated to perform a check-PCR for the presence of the transferred DNA fragment.

Please note: For some transductions, especially if a spectinomycin resistance marker was transferred, a cell plaque appeared on the selective plates on the next morning. This made it difficult to isolate transductants. Therefore, CSE-Glc 0.5% plates containing $MgSO_4$ (1 M), $MnSO_4$ (0.1 M), and sodium citrate (1 M) were used to suppress plaque growth (adapted from Ferrari *et al*., 1978).

YT (1 l) 10 g tryptone
5 g yeast extract
5 g NaCl
ad 1000 ml
autoclave, after cooling addition of:
10 ml $MgSO_4$ (1 M)
1 ml $MnSO_4$ (0.1 M)
only for selective plates:
10 ml sodium citrate (1 M)

Components that were added to the medium after sterilization were autoclaved as well. For the preparation of plates 1.5% (w/v) agar was added to the medium, for the preparation of soft agar 0.5% (w/v) was used. Sodium citrate was only added to the plates for the selection of transductants to avoid hyperinfection of the phages. For transduction of tetracycline resistance markers no sodium citrate was added to the selective plates. To prepare CSE-Glc agar plates for phage transduction out of 500 ml medium 7.5 g Bacto agar was dissolved in 300 ml deion. water and autoclaved. After cooling the remaining sterile components, including $MgSO_4$, $MnSO_4$, sodium citrate, and enough water to fill up to 500 ml were added.

3.3.6. Preparation and detection of DNA

Preparation of plasmid DNA from *E. coli*

Plasmid DNA was prepared from *E. coli* carrying the desired plasmid. An overnight culture (4 ml) with cells carrying the desired plasmid was harvested (2 min; 13,000 rpm). The plasmid DNA was isolated using the Mini Prep Kit (Macherey-Nagel, Düren, Germany) according to the manufacturer's instructions. HPLC water was used for elution of the DNA from the columns. All steps were performed at room temperature (adapted from Pietack, 2010).

Isolation of genomic DNA of *B. subtilis*

Genomic DNA of *B. subtilis* was isolated using the DNeasy Tissue Kit (Qiagen, Hilden, Germany). *B. subtilis* was grown overnight in LB medium and cells from 1.5 ml culture volume were harvested (2 min; 13,000 rpm; RT). The pellet was resuspended in 180 µl lysis buffer and incubated at 37°C for 60 min. The further steps for the isolation of the genomic DNA were performed according to the manufacturer's instructions (adapted from Pietack, 2010).

Agarose gel electrophoresis

For analytical separation of DNA fragments agarose gels containing 1 to 2% (w/v) agarose (according to the expected fragment size) were prepared in TAE buffer. The DNA samples were mixed with 5x DNA loading dye to facilitate loading and to indicate the migration of the samples in the gel. A voltage of about 120 V was applied until the color marker reached the last third of the gel. DNA fragments migrate towards the anode with a velocity that is proportional to the negative logarithm of their length. After electrophoresis, gels were incubated in ethidium bromide solution for 15 min and briefly rinsed with H_2O_{deion}. Fluorescence of ethidium bromide bound to DNA was detected by excitation with UV light (λ = 254 nm) using a GelDoc Imager (BioRad, USA). For the estimation of the size of the DNA fragments, the GeneRuler™ DNA Ladder Mix and λ-DNA marker were used (adapted from Pietack, 2010).

Sequencing of DNA

Sequencing was performed based on the chain termination method (Sanger) with fluorescence labelled dideoxynucleotides. The sequencing reactions were conducted by SeqLab (Göttingen), LGC Genomics (Berlin) and the "Göttingen Genomics Laboratory" (G2L) of the Georg-August-University Göttingen. Whole genome sequence and assembly of the sequencing data to the NCIB3610 reference genome (accession number CM000488) was performed with a shotgun Illumina approach by the G2L.

Digestion of DNA

The digestion of DNA with endonucleases was performed with buffers recommended by the manufacturer. Reaction buffers, concentration of enzymes and DNA as well as incubation temperatures were chosen according to the manufacturer's instructions. The digestion was allowed to proceed for up to 1 h and was, if possible, followed by heat inactivation of the restriction endonucleases. The DNA was purified using the PCR Purification Kit (Qiagen, Hilden, Germany) following the manufacturer's instructions (adapted from Pietack, 2010).

Dephosphorylation of DNA

To avoid re-circularization of a previously digested DNA vector, the 5' phosphate groups of the linearized vectors were removed prior to the ligation reaction. The dephosphorylation of the 5' prime end of DNA fragments was performed with the FastAP (alkaline phosphatase) (Thermo Scientific, Lithuania) with buffers supplied by the manufacturer. Approximately 10–20 ng/ µl DNA were mixed with 1 µl FastAP (1 U/ µl) and incubated at 37°C for 15 min. The FastAP was inactivated at 75°C for 10 min (adapted from Pietack, 2010).

Ligation of DNA

DNA fragments were ligated using T4-DNA ligase (Thermo Scientific, Lithuania) with buffers supplied by the manufacturer. The ligation reaction contained 20–200 ng of vector DNA and an excess of the DNA fragment (insert to vector molar ratio of 3:1 to 5:1). The reaction was started by adding 5 U T4-DNA ligase to a final volume of 20 µl. The ligation occurred for 2 h at RT or overnight at 16°C (adapted from Pietack, 2010).

Polymerase chain reaction (PCR)

The polymerase chain reaction was performed with chromosomal DNA or plasmid DNA as a template.

<u>Reaction mix for the *Phusion* polymerase (50 µl):</u>

1 µl primer 1 (20 pmol)
1 µl primer 2 (20 pmol)
1 µl template DNA (about 50 ng)
10 µl 5 x *Phusion* HF buffer
0.5 µl *Phusion* polymerase (2 U μl^{-1})
1 µl dNTPs (12.5 µmol ml^{-1})
35.5 µl deion. water

<u>Reaction mix for the *Taq* polymerase (50 µl):</u>

2 µl primer 1 (20 pmol)
2 µl primer 2 (20 pmol)
2 µl template DNA (about 100 ng)
5 µl 10 x *Taq* polymerase buffer
1 µl *Taq* polymerase (5 U μl^{-1})
2 µl dNTPs (12.5 µmol ml^{-1})
36 µl deion. water

The reaction mix was briefly vortexed, spun down, and then the reaction was performed in a Thermocycler with one of the following programs:

Taq polymerase:

Number of cycles	Reaction	Temperature	Duration/ cycle
	initial denaturation	96°C	5 min
	denaturation	96°C	1 min
30 {	annealing	50–60°C	1 min
	elongation	72°C	0.5–4 min
1	final elongation	72°C	10 min

After the end of the program the reaction mix was cooled to 12°C.

Phusion polymerase:

Number of cycles	Reaction	Temperature	Duration/ cycle
1	initial denaturation	98°C	20 sec
	denaturation	98°C	10 sec
30 {	annealing	50–60°C	30 sec
	elongation	72°C	0.5–3 min
1	final elongation	72°C	10 min

After the end of the program the reaction mix was cooled to 12°C.

Purification of PCR products

PCR products were purified with the PCR-Purification Kit (Qiagen, Hilden, Germany).

Solutions for working with DNA

Agarose gel 1%	1% (w/v) agarose in 1x TAE
For gel electrophoresis of DNA	

DNA color marker 5x	5 ml glycerol (100%)
For gel electrophoresis of DNA	4.5 ml deion. water
	200 µl TAE (50x)
	0.01 g bromophenol blue
	0.01 g xylene cyanol

TAE buffer 50x	2 M Tris
For gel electrophoresis of DNA	57.1 ml acetic acid (100%)
	100 ml EDTA (0.5 M, pH 8.0)
TE buffer pH 8.0	10 mM Tris-HCl pH 8.0
	1 mM EDTA
RNase A	20 mg/ml in deion. water,
	inactivation of DNases by heating
	for 20 minutes at 85°C (Roche)
Lysis buffer	50 mg lysozyme
For isolation of chromosomal	50 µl Tris-HCl pH 8.0 (1 M)
DNA from *B. subtilis*	10 µl EDTA pH 8.0 (0.5 M)
	2.5 ml deion. water

Long flanking homology PCR (LFH-PCR)

Deletion of a gene in *B. subtilis* was performed with the long flanking homology PCR (LFH-PCR) technique (Wach, 1996) that was adapted for use in *B. subtilis*. For this purpose, genes that mediate resistance against chloramphenicol, kanamycin, erythromycin, and spectinomycin were amplified from the plasmids pGEM-cat, pDG780, pDG1513 and pDG1726, respectively (Guerout-Fleury *et al*., 1995). DNA fragments of about 1,000 bp flanking the target gene at its 5' and 3' ends were amplified. The 3' end of the upstream fragment as well as the 5' end of the downstream fragment extended into the target gene in a way that all expression signals of genes up- and downstream of the gene remained intact (usually about 150 bp). The joining of the two fragments to the resistance cassette was performed in a second PCR. Joining was allowed by complementary sequences of 25 bp that were attached to the single fragments by the respective primers. Thus, the 3` end of the upstream fragment was linked with the 5` end of the resistance cassette and the 3` end of the resistance with the 5` end of the downstream fragment. For the LFH joining reaction, about 150 ng of the up- and downstream fragments and 150 ng of the resistance cassette were used. The fused fragment was amplified by PCR using the forward primer of the upstream fragment and the reverse primer of the downstream fragment. *B. subtilis* was transformed with the PCR products and transformants were selected on plates. Clones were examined by check PCR for the integrity of the resistance cassette. The DNA sequence of the flanking regions was verified by sequencing (adapted from Tholen, 2009; Pietack, 2010).

Reaction mix for the LFH-PCR with *Phusion* polymerase (50 µl):

4 µl primer 1 (20 pmol)

4 µl primer 2 (20 pmol)

3 µl upstream flanking region (about 150 ng)

3 µl downstream flanking region (about 150 ng)

3 µl resistance cassette (about 150 ng)

10 µl 5x *Phusion* HF buffer

0.5 µl *Phusion* polymerase (2 U μl^{-1})

1 µl dNTPs (12.5 µmol ml^{-1})

21.5 µl deion. water

Program for the LFH-PCR with *Phusion* polymerase:

Number of cycles	Reaction	Temperature	Duration cycle
1	initial denaturation	98°C	1 min
	denaturation	98°C	10 sec
10 {	annealing	50–60°C	30 sec
	elongation	72°C	1–2 min
1	pause	12°C	∞
	denaturation	98°C	10 sec
30 {	annealing	50–60°C	30 sec
	elongation	72°C	1–2 min[1]
1	final elongation	72°C	5 min

After the end of the program the reaction mix was cooled to 12°C. The primers were added during the pause, after the first ten cycles. [1]Time for elongation increased 5 sec per cycle.

3.3.7. Isolation of Δ*ymdB* suppressor mutants

To get spontaneous mutants that suppress the Δ*ymdB* phenotype, the *ymdB* deletion strain GP1574 was grown in 10 ml LB medium (with respective antibiotics) in a 100 ml flask shaking at 200 rpm and 37°C. 100 µl of the culture were transferred into fresh 10 ml LB medium every morning and evening for about 2.5 days. The suspension was then plated on MSgg agar plates in dilutions of 10^{-4} to 10^{-6} and incubated at 30°C over night and then at RT until biofilm forming papillae were visible. For a few day old cells, suppressor mutants could be identified by fluorescence microscopy using the SteREO Lumar.V12 stereo microscope (Carl Zeiss Microscopy). Suppressor mutants were streaked out repeatedly on MSgg or on SP plates containing appropriate antibiotics until all colonies had the same phenotype. In addition, suppressor mutants were isolated from several weeks old SP plates that

showed papillae growth on top of the origin strain. These papillae were separated from the origin strain as described before (adapted from Kruse, 2013).

3.3.8. Biofilm methods

Complex colony formation on agar plates

To monitor complex colony formation a fresh single colony of *B. subtilis* was used to inoculate 4 ml of LB medium supplemented with the appropriate antibiotics and the cells were cultivated at 37°C and 200 rpm until they reached an OD_{600} between 0.5 and 1.0 (mid-exponential growth phase). Then 10 µl of the cells were dropped carefully on top of an MSgg medium agar plate. To ensure that the agar plates are nicely dried, the plates were placed under the laminar flow cabinet for 3 to 5 hours (while cells were growing). Next, the plate was incubated at 30°C for one day and at room temperature for another day. Complex colony structure was documented using a stereo fluorescence microscope (Carl Zeiss Microscopy, Göttingen) equipped with an AxioCam MRc digital camera. Images were taken at 9.6 fold magnification and processed with ZEN 2012 (blue edition) software (Carl Zeiss Microscopy).

Biofilm assay in liquid medium (pellicle formation)

Pellicle formation was analyzed in liquid MSgg medium. For this purpose, the cells were cultivated as described for the complex colony formation assay. When the cells reached mid-exponential growth phase, 8 µl of the cells were used to inoculate 8 ml of liquid MSgg medium within a well of a 6-well plate. Then, the plate was placed on black paperboard and incubated for 3 to 4 days at room temperature until the wild type strain showed a thick and structured (NCIB3610) pellicle. Finally, pellicle formation was documented by taking pictures with a Canon Powershot SX200 IS digital camera.

Preparation of MSgg medium (Branda *et al*., 2001)

Since it is not possible to autoclave a mixture of the different components of the MSgg medium, single components were sterilized first and mixed afterwards. For the preparation of plates 1.5% (w/v) Bacto agar for minimal medium (BD, Heidelberg) was added to the medium. For the preparation of 500 ml medium, deion. water was added to 7.5 g agar to a total volume of 300 ml and the mixture was autoclaved. Next, the salts and the other components (preheated) were added to the warm agar to obtain a final volume of 500 ml. The single components are listed in Tab. 3.2. To avoid precipitation of the salts, the agar was mixed continuously prior to pouring the plates. To ensure reproducible colony phenotypes, exactly 25 ml medium were used for every plate. The plates were stored in the refrigerator at 4°C.

Table 3.2. Components of MSgg minimal medium

Component	Concentration (stock)	Volume (ml)	Final concentration	Remarks
potassium phosphate buffer pH 7.0	1 M	2.5	5 mM	
MOPS pH 7.0	1 M	50	100 mM	autoclaved, stored in the dark at 4°C
glycerol	50%	5	0.5%	
thiamine (vitamine B1)	20 mM	0.05	2 µM	sterile filtrated, stored in the dark at -20°C
potassium glutamate	40%	6.25	0.5 %	
L-Trp/L-Phe	10 mg/ml per component	2.5	50 µg/ml per component	sterile filtrated, stored at 4°C
$MgCl_2$	1 M	1	2 mM	
$CaCl_2$	700 mM	0.5	700 µM	
$MnCl_2$	50 mM	0.5	50 µM	
$FeCl_3$ x 6 H_20	50 mM	0.5	50 µM	prepared freshly in a 15 ml tube, not sterilized
$ZnCl_2$	1 mM	0.5	1 µM	
H_2O_{bidest}		ad to a total volume of 500 ml		

3.3.9. Precipitation and staining of exopolysaccharides

To analyse the formation of extracellular polysaccharides, precipitation and staining of polymers present in the culture supernatant was performed as described by Guttenplan *et al.* (2010). We used the *sinR tasA* mutant to enhance the production of extracellular polysaccharides and facilitate release from the cell. Initially, 10 ml YT medium (supplemented with 10 mM $MgSO_4$ and 100 µM $MnSO_4$ after autoclaving) were inoculated with a fresh colony and grown for 24 h at 37°C and 200 rpm. Then cells were harvested by centrifugation at 8,500 rpm for 5 min. The supernatant of the cells (and for some strains none-pelleted slime) was transferred to a new falcon tube and put on ice. In a next step, 500 µl vortexed supernatant was mixed with 1.5 ml ice-cold ethanol (100%) in a 2 ml tube to precipitate exopolysaccharides within the supernatant. This mixture was centrifuged for 5 min at 13,000 rpm and the supernatant was discarded. The precipitate was dried at room temperature until no liquid was visible anymore. Subsequently, the pellet was resuspended in 100 µl 1x SDS sample

buffer and 10 µl were loaded on a 12% SDS gel (extra-long stacking gel) and run for 30 min at 200 V. To stain exopolysaccharides with the Stains-All dye the stacking and resolving gel was fixed for 24 h in fixing solution and stained in 100 ml staining solution over night (light-tight box). Before the staining solution was applied to the gel, half of the resolving gel was cut off and the gel was rinsed in 25% (v/v) isopropanol several times (3x 10 sec and 3x 10 min) to remove SDS and acetic acid. Please note that Stains-all precipitates in contact to SDS. Furthermore, it is light sensitive and the staining fades away when exposed to light! The stained gel was documented with a Canon CanoScan 8800F scanner.

To precipitate EPS in a 24-well plate, 500 µl of the supernatant was mixed with 1.5 ml ethanol (100%). For a better visualization of the precipitate, glycerol was added to a final concentration of up to 17% (v/v). Pictures were taken with Zeiss SteREO Lumar.V12 Stereomicroscope (connected with AxioCam Mrc). The result can be improved by the use of 6-well or 12-well plates and higher sample volumes.

Solutions for precipitation and staining of exopolysaccharides

Fixing solution	25% (v/v) isopropanol 3% (v/v) acetic acid
Staining solution	5 ml of 1 mg/ml Stains-All [AppliChem] in formamide 50 µl β-mercaptoethanol 95 ml Stains-All base solution *store at 4°C in the dark*
Stains-All base solution	16.6% (v/v) isopropanol 5.5% (v/v) formamide 1% 1.5 M Tris-HCl pH 8.8
Washing solution	25% (v/v) isopropanol

3.3.10. Work with proteins

Western blot

The blotting of proteins on PVDF membranes (BioRad, USA) was carried out with semi dry blotting equipment. After the electrophoresis, the gels were equilibrated in transfer buffer for 30 sec. The PVDF membrane was activated in methanol (100%) for a short time and subsequently incubated in transfer buffer for 5 minutes. Then the transfer of the protein was performed for one hour at

0.8 mA/ cm^2. In order to block unspecific binding sites the membrane was incubated in skim milk blocking solution (Blotto) for 1–3 hours. In a next step, polyclonal antibodies against the protein of interest were applied onto the membrane. The antibodies against the FLAG-tag, the SinR and the HPr proteins were used as dilutions of 1:10,000 in Blotto (over night). After three washing steps of 30 minutes each, the membrane was incubated with the second antibody (anti-rabbit IgG, coupled to an alkaline phosphatase) which was diluted 1:100,000 in Blotto. Then the membrane was washed twice for 20 min in Blotto and rinsed with deion. water. Before applying the substrate CDP* (Roche, Mannheim, Germany) on the membrane, the membrane was incubated in puffer III for 5 minutes to increase the pH value. The signal of the chemiluminescent substrate CDP* was detected with a ChemoCam imager (Intas, Göttingen, Germany) (adapted from Pietack, 2010).

Quantitative Western blots for the determination of SinR amounts

To determine SinR protein amounts quantitative Western blotting was applied. For this purpose, 4 ml LB medium was inoculated with a fresh colony and grown over day at 28 or 37°C and 200 rpm. This culture was used to inoculate another 4 ml LB medium culture for overnight growth at 28°C and 200 rpm so that the cells had reached the late exponential (early stationary) growth phase in the morning. With this culture 15 ml LB medium supplemented with the appropriate antibiotics was inoculated to an OD_{600} of 0.1. The cells were cultivated at 37°C and 200 rpm until they reached an OD_{600} of about 2.5. Then, 2 ml aliquots of this culture were harvested by centrifugation at 13,000 rpm for 2 min. Cell pellets were stored at -20°C or directly disrupted with lysozyme. For this purpose, cell pellets were resuspended in 50 µl lysis buffer (100 µl LD/ DNase mix and 4 ml ZAP buffer) and incubated for 30 min at 37°C with occasional vortexing. Subsequently, samples were centrifuged for 10 min at 13,000 rpm and 4°C to separate cell debris from the soluble cell contents. Supernatants were transferred to new reaction tubes and the protein content was determined as described by Bradford *et al.* (1976) (adapted from Kruse, 2013). Protein extracts (15 or 20 µg) were mixed with 5x PAP, heated for 15 min at 95°C and applied to 15% SDS-PAGE. Detection of the SinR proteins was performed with a specific antibody (gift of D. Kearns and Y. Chai). As a control the HPr protein was detected in aliquots from the same extraction that were applied to a separate gel for subsequent blotting with an HPr-specific antibody (laboratory collection).

Determination of relative SinR protein amounts using ImageJ

Quantification of the density (intensity) of Western blot signals was performed with the image processing program ImageJ (Schneider *et al.*, 2012; http://imagej.nih.gov/ij/) as described at http://www.lukemiller.org/ImageJ_gel_analysis.pdf. In brief, a Western blot image derived from detection with a SinR-specific antibody was imported into ImageJ and the rectangular selection tool was used to measure signal intensity of each Western blot lane. For this purpose, the number “1” on

the keyboard was press to mark the first selection, by pressing “2” the rectangular selection field for every further lane was dublicated and by pressing “3” the profile plots for each lane where shown. Then, the straight line selection tool was used to separate the highest peak (main signal) from the background noise by creating a closed area. Next, the so-called wand tool was used to select the area of interest of every single signal by clicking into the closed area. Finally, the intensity values for every area appeared in a new window and were used for further calculations. The same procedure was performed for the Western blot signals with the HPr-specific antibodies. To normalize the resulting intensity values for SinR protein of a certain cultivation, they were divided by the respective values for HPr protein. Then, the mean of the normalized values of three biological replicates was calculated and the value for the reference strain was set to 1 by dividing all values by the value for the reference. Now changes in SinR intensity (protein amounts) of the strains of interest could be visualized in a bar chart.

Overexpression of recombinant proteins in *E. coli*

An overnight culture of *E. coli* BL21, carrying the relevant plasmid, was used to inoculate 500 ml of LB medium to an OD_{600} of 0.1. Cultures were grown at 37°C and 200 rpm until they had reached an optical density of 0.6 to 0.8. Expression of recombinant proteins was induced by the addition of isopropyl-β-D-thio-galactopyranoside (IPTG, final concentration: 1 mM) (Carl Roth, Karlsruhe). The cultures were cultivated for further three hours. To test the expression, small aliquots (sample [µl] = $100/OD_{600}$) were taken before (t_0) and every hour after induction (t_1 to t_3). The samples were boiled in SDS loading dye for 15 min and analyzed by SDS-PAGE. The main culture was harvested by centrifugation (10 min; 5,000 rpm; 4°C). After removing the supernatant the cells were washed in cold buffer W, transferred to a falcon tube and centrifuged again (5 min at 8,500 rpm and 4°C). Then the pellets were stored at -20°C (adapted from Pietack, 2010).

Purification of proteins via a *Strep*-Tactin-Sepharose® column

For the purification on proteins with a *Strep*-tagII sequence a *Strep*-Tactin-Sepharose® column (IBA, Göttingen) with a matrix volume of 0.5 ml was used for 500 ml culture. This matrix specifically binds a sequence of eight amino acids (WSHPQFEK). Furthermore, this binding can be reversed by applying D-desthiobiotin which displaces the *Strep* peptide. The specific binding of the peptide to the matrix allows the purification of tagged proteins out of a protein mixture. At first, the column was equilibrated with 10 ml buffer W. Then the whole crude extract was applied onto the column. The washing of the column was performed by applying 5 ml buffer W in fractions of 1.25 ml (W1 – W4). Subsequently, the bound protein was eluted with 1.75 ml buffer E in fractions of 250 µl (E1) and 500 µl (E2 – E4). Then the protein content of the single fractions was determined as described by Bradford *et al.* (1976) (adapted from Pietack, 2010).

Cell disruption with the French press

The precooled bomb was filled with the cell suspension and the remaining air was squeezed out before the bomb was locked. After closing the release valve the bomb was placed in the French press and set under pressure. The disruption took place with a pressure of 18,000 psi and was performed three times (adapted from Pietack, 2010).

***In vivo* detection of protein-protein interactions**

The *Strep*-Protein Interaction Experiment (SPINE) was performed according to Herzberg *et al*. (2007). This experiment was used to identify potential interaction partners of recombinant *B. subtilis* proteins *in vivo*. This method combines the purification of recombinant proteins via their *Strep*-tagII and a cross-linking of adjacent proteins (~2 Å) by addition of formaldehyde. A treatment with formaldehyde leads to the reversible cross-linking of proteins via methylene bridges. These bridges can be reversed after purification by heating.

For the experiment a preculture of *B. subtilis* harboring the overexpression plasmid (pGP380 and pGP382 derivatives) of the *Strep*-tagged protein of interest was cultivated for about 10 hours at 37°C in LB medium containing the appropriate antibiotics. This culture was used to inoculate 100 ml CSE medium (0.5% glucose) and was grown overnight at 28°C. One liter of the same medium was then inoculated with the second preculture to an OD_{600} of 0.1. When this culture had reached an OD_{600} of 1.0 to 1.2, 500 ml were supplemented with formaldehyde (4% (w/v) in PBS pH 6.5) to a final concentration of 0.6%. This culture was incubated for additional 20 minutes. The cells of the untreated half of the culture and the formaldehyde treated cells were harvested by centrifugation (10 min; 5,000 rpm; 4°C) (Sorvall RC 6+, F9S 4x1000Y rotor). Then the cells were washed in 15 ml buffer W and harvested again. The cell pellets were stored at -20°C. For the preparation of the crude extract, the pellet was thawn and resuspended in 15 ml buffer W. Cell disruption was carried out using a French press. Subsequently, the cell extract was purified via a *Strep*-Tactin-Sepharose® column (IBA, Göttingen). Proteins that were cross-linked to the recombinant protein were coeluted during the purification. The resulting fractions were analyzed by denaturing gel electrophoresis. By heating the samples prior to electrophoresis cross-linking of the proteins was reversed. After electrophoresis, proteins were transferred to a PVDF membrane and potential interaction partners could be identified with specific antibodies (adapted from Meyer, 2009; Pietack, 2010).

Separation of membrane and cytosolic proteins by ultracentrifugation

Before the actual separation of membrane and cytosolic proteins, the *B. subtilis* strains of interest were grown in LB medium at 37°C and 200 rpm. When the cells reached an OD_{600} of 1.0 they were harvested by centrifugation and washed with ice-cold membrane buffer M. The cell pellets can be stored at -20°C or directly be used for the experiment. For protein separation cells were resuspended

in ice-cold membrane buffer M again and disrupted by using a French press (3x 18,000 psi). Next, the disrupted cells were centrifuged in a 50 ml falcon tube for 15 min at 8,500 rpm, the supernatant was transferred to a 15 ml falcon tube, and centrifuged again for 30 min at 8,500 rpm to get rid of cell debris. Then a sample of this supernatant was taken as crude extract (CE) sample and the remaining volume was transferred to a 35 ml ultracentrifugation tube. Ultracentrifugation was performed at 100,000 x g and 4°C for 1 h. Afterwards a sample of the supernatant was taken and regarded as the cytosolic fraction. The rest of the supernatant was discarded and the pellet was dissolved with 500 µl membrane buffer M. Then the ultracentrifuge tube was refilled with ice cold membrane buffer M and a second ultracentrifugation step was performed at 100,000 x g and 4°C for 30 min. Again, the supernatant was discarded (but a sample was kept as a washing step in order to prove that all cytosolic proteins were removed) and the procedure was repeated. If applicable, another ultracentrifugation step was performed. Finally, the pellet was dissolved with 500 µl membrane buffer M containing 5% CHAPS. This sample was regarded as the membrane fraction.

The protein amount in the CE, cytosolic and membrane fractions was determined as described by Bradford *et al*., (1976). For further analysis SDS-PAGE and Western blotting using an antibody for the detection of the target protein was performed. For the detection with α-FLAG antibodies 15 µg CE were loaded on the gels, for RNase Y detection 5 µg, and for CggR detection 10 µg were used. For the cytosolic and the membrane fraction 28 µl were used. In addition a second SDS-PAGE analysis was performed to analyze different protein patterns of cytosolic and membrane fractions. To verify the Western blot result for the protein of interest, it was important to use controls. For this, additional detections with α-CggR antibodies (control for the isolation of the cytosolic fraction; 1:10,000 in blotto) and α-RNase Y antibodies (control for the isolation of the membrane fraction; 1:50,000 in blotto) were performed. After blotting the membrane was cut into 3 parts and each part was incubated with the respective antibody (adapted from Mehne *et al*., 2013).

Buffers for the separation of membrane and cytosolic proteins

Buffer M	50 mM NaH_2PO_4
	50 mM Na_2HPO_4 pH 6.8
	if needed 5% (w/v) CHAPS was added

Bacterial two-hybrid assay

For the detection of primary protein-protein interactions the bacterial two-hybrid system (B2H) was used (see Fig. 3.2). Therefore, the genes for proteins of interest were fused to the C- and N-terminal domain of the adenylate cyclase from *Bordetalla pertussis*, respectively. For cloning four different

vectors were used. The high-copy vectors pUT18 and pUT18C allow the expression of proteins fused to the T18 domain of the *B. pertussis* adenylate cyclase, whereas the low-copy vectors p25-N and pKT25 allow the expression of proteins fused to the T25 domain. Furthermore, the vectors pUT18 and p25-N are constructed for the expression of N-terminal fusions to the protein of interest and the vectors pUT18C and pKT25 allow the expression of C-terminal fusion proteins (Karimova *et al*., 1998, Claessen *et al*., 2008). DNA fragments for the genes of the proteins of interest were obtained by PCR. The PCR products were digested with *Kpn*I and *Xba*I and cloned into the vectors of the two-hybrid system that had been linearized with the same enzymes. The resulting plasmids were used for cotransformations of *E. coli* BTH101 and the protein-protein interactions were then analyzed by placing 4 µl drops of the cells on LB plates containing ampicillin (100 µg/ml), kanamycin (50 µg/ml), X-Gal (80 µg/ml) (5-bromo-4-chloro-3-indolyl-ß-D-galactopyranoside) and IPTG (0.5 mM) (isopropyl-ß-D-thiogalactopyranoside), respectively. The plates were incubated for a maximum of 48 h at 30°C. Then, the plates were documented with a Canon CanoScan 8800F scanner. Interacting proteins were identified through cleavage of X-Gal and the resulting blue-colored cells. As a positive control the plasmids pKT25-zip and pUT18C-zip were also cotransformed. They encode subunits of a leucin zipper protein and show a strong interaction (adapted from Meyer, 2009; Lehnik-Habrink, 2011).

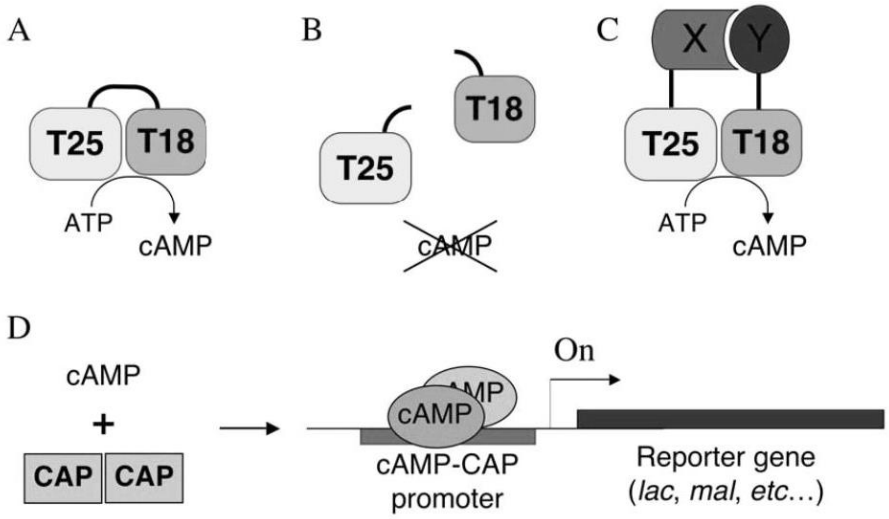

Figure 3.2. Principle of the bacterial two-hybrid system. (A) The catalytic domain of the adenylate cyclase from *B. pertussis* constists out of two complementary fragments, T25 and T18, and is responsible for the synthesis of cAMP. (B) If the two fragments are separated the enzyme is inactive. (C) Fusion of the two fragments to interacting proteins X and Y allows reconstitution of the fragments and synthesis of cAMP. (D) Synthesis of cAMP allows transcription of reporter genes (e.g. *lacZ*). Interaction between hybrid proteins results in high β-galactosidase activity (adapted from Meyer, 2009).

Denaturing gel electrophoresis of proteins (SDS-PAGE)

Denaturing protein gels were prepared as described by Laemmli *et al*. (1970) and Garfin (2009). The gels consist of a stacking and a separating gel, which were poured to a thickness of 1 mm. Before applying the samples on the gel they were mixed with SDS sample buffer (5x) and heated for 15 min at 95°C. The separation of the proteins was performed at 120 to 150 V.

Coomassie staining of polyacrylamide gels

Protein gels were stained with Coomassie Brilliant Blue. For this purpose, the gels were incubated in coomassie staining solution (fixation of proteins in parallel) for about 10-15 minutes and the gels were destained until an optimal contrast between protein bands and background was reached. This step was usually performed over night at room temperature (adapted from Pietack, 2010).

Solutions for coomassie staining of proteins

Staining solution	0.5% (w/v) Coomassie brilliant blue
	10% (v/v) acetic acid
	45% (v/v) methanol
Destaining solution	5% (v/v) acetic acid
	20% (v/v) ethanol

Silver staining of polyacrylamide gels

The silver staining is a very sensitive method for staining polyacrylamide gels. Silver stainings are widely used to check the purity of protein extracts and to identify protein-protein interactions. One advantage is the high sensitivity with a detection limit of about 5 ng protein per band. A disadvantage of the silver staining is the pour reproducibility and the lack of quantification. This is linked to the physics of the accumulation of silver particles (Butcher & Tomkins, 1985). During the staining, silver ions build up complexes with the glutamate, aspartate and cysteine amino acid residues of the proteins and thereby get reduced to metallic silver. Therefore, the intensity of the silver staining depends on the amino acid sequence of the respective proteins and can vary considerably. The protein bands were stained according to method of Nesterenko (1994). For that purpose, the polyacrylamide gels were incubated on a shaker with the following reagents and in the stated order (adapted from Meyer, 2009). An overview of all steps is shown on the next page.

Step	Reagent	Duration
Fixing	Fixer	1 to 24 h
Washing	ethanol 50%	3 x 20 min
Reduction	Thiosulfate solution	1 min 30 sec
Washing	deion. water	3 x 20 sec
Staining	Impregnating	25 min
Washing	deion. water	2 x 20 sec
Development	Developer	until suffiently stained
Washing	deion. water	20 sec
Stoping	Stop solution	5 min

Solutions for working with proteins

Blotto		1 x TBS
for Western blotting	2.5%	skim milk powder
	0.1%	Tween 20
Developer (100 ml)	6 g	Na_2CO_3
for silver staining	2 ml	thiosulfate solution
	50 µl	formaldehyde
	ad 100 ml	H_2O_{deion}
Fixer (100 ml)	50 ml	methanol (100%)
for silver staining	12 ml	acetic acid (100%)
	100 µl	formaldehyde (37%)
	ad 100 ml	H_2O_{deion}
4% Formaldehyde solution	40 g	paraformaldehyde
(for SPINE)	ad 1 l	1x PBS pH 6.5

Impregnator (100 ml)	0.2 g	$AgNO_3$
for silver staining	37 µl	formaldehyde (37%)
	ad 100 ml	H_2O_{deion}
10 x PBS	80 g	NaCl
	17.8 g	Na_2HPO_4 x $2H_2O$
	2.4 g	KH_2PO_4
		pH 6.5 adjusted with HCl
	ad 1 l	H_2O_{deion}
Buffer III	0.1 M	Tris
for Western blotting	0.1 M	NaCl
		pH 9.5 adjusted with HCl
Buffer E	100 mM	Tris-HCl pH 8
for SPINE	150 mM	NaCl
	1 mM	EDTA
	2.5 mM	Desthiobiotin
Buffer W	100 mM	Tris-HCl pH 8
for SPINE	150 mM	NaCl
	1 mM	EDTA
Stacking gel	1.3 ml	Acrylamide-Bisacrylamide (30%)
for denaturing gel	1 ml	Tris-HCl pH 6.8
electrophoresis of proteins	5.5 ml	H_2O_{deion}
	80 µl	SDS (10%)

	80 µl	APS (10%)
	8 µl	TEMED
5x SDS sample buffer	1.4 ml	1 M Tris-HCl pH 7
for denaturing gel electrophoresis of proteins	3 ml	Glycerol (100%)
	2 ml	SDS (20%)
	1.6 ml	β-mercaptoethanol (100%)
	0.01 g	Bromophenol blue
	2 ml	H_2O_{deion}
Stop solution (100 ml)	1.86 g	EDTA
for silver staining	ad 100 ml	H_2O
10x TBS	60 g	Tris
	90 g	NaCl
		pH 7.6 adjusted with HCl
	ad 1 l	H_2O_{deion}
Thiosulfate solution	20 mg	$Na_2S_2O_3$ x 5 H_2O
(100 ml)	ad 100ml	H_2O
for silver staining		
Transfer buffer	15.2 g	Tris
for Western blotting on PVDF membranes	72.1 g	glycerol
	750 ml	methanol (100%)
	ad 5 l	H_2O_{deion}

Separating gel (12%)	4 ml	acrylamide-bisacrylamide (30%)
for denaturing gel electrophoresis of proteins	2.5 ml	Tris-HCl pH 8.8
	3.3 ml	H_2O_{deion}
	100 µl	SDS (10%)
	100 µl	APS (10%)
	4 µl	TEMED

Separating gel (15%)	5 ml	acrylamide-bisacrylamide (30%)
for denaturing gel electrophoresis of proteins	2.5 ml	Tris-HCl pH 8.8
	2.3 ml	H_2O_{deion}
	100 µl	SDS (10%)
	100 µl	APS (10%)
	4 µl	TEMED

LD/ DNase mix (10 ml)	100 mg lysozyme solved in 10 ml $H_2O_{deion.}$
	10 mg DNase I
	the solution was stored as 500 µl aliquots at -20°C
1x ZAP buffer	50 mM Tris-HCl pH 7.5
	200 mM NaCl

3.3.11. Work with RNA

***In vitro* transcription**

To detect certain RNAs within the elution fraction of protein purifications by dot blot, DIG labelled RNA probes were synthesized by *in vitro* transcription using Digoxygenin (DIG) labelled RNA probes. The probes are *in vitro* transcribed *anti-sense* RNAs with a length of about 200 bp that consist of labelled nucleotides which can be recognized by specific antibodies. A DNA template of the first 200 bp of the transcript of interest was amplified by PCR using Phusion™ polymerase (Thermo Scientific). The fragment contained a T7 RNA polymerase promoter (underlined) and an overhang for better polymerase binding at the 5´end of the non-coding strand that was added by the reverse primer:

5´- ATATATCTAATACGACTCACTATAGGGAG-primer-3´

The DNA fragment was purified with the QIAquick PCR Purification Kit (Qiagen) and used as a template for *in vitro* transcription by T7 RNA polymerase. For *in vitro* transcription the following reaction was prepared:

Reaction mixture for *in vitro* transcription (100 µl):

DNA template with T7 promotor	15 µl
NTP mix (25mM each)	20 µl
10x transcription buffer	10 µl
RNase inhibitor (40 U)	1 µl
1 M DTT	2 µl
T7 RNA polymerase (80 U)	4 µl
RNase-free water	48 µl

T7 transcription buffer, RNA polymerase, DIG RNA labelling mix and RNase inhibitor were purchased from Roche Applied Science. The reaction was incubated at 37°C for 2 h and then stopped by the addition of 1 µl 0.5 M EDTA (pH 8.0). RNA was precipitated by the addition of 12.5 µl 4 M LiCl and 350 µl ice-cold ethanol (96%) and by overnight incubation at -80°C. RNA was sedimented by centrifugation (30 min; 13,000 rpm and 4°C), the pellet washed with 70% ice-cold ethanol and then dried at 60°C for 10 min or 30 min at RT to remove traces of ethanol. Then, RNA was eluted in 50 µl DEPC treated water containing 1 µl RNase inhibitor and stored at -80°C. To control the quality of the RNA probe, dilution series (in steps of 10^{-1}) were prepared, 1 µl of each dilution step spotted onto a nylon membrane and luminescence was tested as described for dot blot experiments (adapted from Eilers, 2010).

The amplification of RNA samples for electrophoretic mobility shift assays was conducted basically as described before but unlabeled nucleotides were used (Roche Applied Science). Furthermore, primers for the amplification of the DNA template for *in vitro* transcription contained the T7 RNA polymerase promoter at the 5’ end of the forward primer to produce no *anti-sense* RNA later on.

Electrophoretic mobility shift assay (EMSA)

To analyze RNA-protein interactions *in vitro* an Electrophoretic Mobility Shift Assay (EMSA) was applied. For this purpose a protein was incubated with the 5’ region of a certain RNA (potential regulatory region) and afterwards loaded onto a polyacrylamide gel to perform a gel electrophoresis

run. As free RNA runs faster than protein-bound RNA, the formation of a RNA-protein complex can be detected by a retardation of the RNA ("shift").

For the electrophoresis a 10% native Tris/acetate gel was prepared. To avoid contamination with RNases, the glass plates for the gels and all the components of the gel chamber were washed with 70% ethanol wearing gloves. After polymerization of the gel all components of the gel chamber were assembled and filled with the cold 1x running buffer (25 mM Tris/acetate buffer). Before starting with the actual shift assay a pre-run (1 h, 90 V) was performed. For the shift assay the gels was loaded with the samples and electrophoresis was performed for 3 h at 100 V. The pre-run and the shift assay were carried out in the cold room at 4°C. After the run, the gel was stained in an ethidium bromide solution (freshly prepared) for 5 min and incubated in a water bath for another 5 min. The picture was taken with a Gel-doc (Bio-Rad-Laboratories, USA) (adapted from Schilling *et al*., 2006).

Preparation of the samples for the shift assay:

RNA (50 pmol)	x µl
10x Tris-acetate buffer	2 µl
NaCl (5 M)	1 µl
RNase-free water	ad 20 µl

1.) incubation at 95°C for 2 min

2.) incubation on ice for 5 min

protein (10–50 pmol)	x µl
glycerol (50%)	4 µl

In addition, samples that contained only RNA or protein solution were prepared simultaneously. This way it is possible to discriminate between RNA and RNA-protein complexes and to test if the protein solution is free of RNA, respectively. To ensure equal volumes for all samples RNase-free water was added.

Buffers and solution for the gel shift

10% native Tris/acetate gel	4 ml 30% polyacrylamide
for 2 gels	1.2 ml 250 mM Tris-acetate pH 5.5
	6.8 ml H_2O
	200 µl 10% (w/v) ammonium persulfate (APS)
	10 µl TEMED

3 M sodium acetate	pH 5.2 adjusted with acetic acid, autoclaved
10x Tris/acetate electrophoresis buffer	250 mM Tris-acetate pH 5.5 adjusted with acetic acid, autoclaved

Co-elution experiments for the analysis of protein-RNA interaction

The *Strep*-tag proteins were purified by affinity chromatography as described in 3.3.10. But in contrast to the SPINE experiment, only the samples cross-linked with formaldehyde were used. The isolation of RNA out of the elution fraction (E2) was performed by chloroform: isoamyl alcohol (24:1)/ phenol precipitation. For the isolation of RNA out of the elution fraction 2 (E2), 450 µl were mixed with 450 µl of a phenol/chloroform/isoamyl alcohol mixture (Roti-P/C/I; Carl Roth, Karlsruhe) and were strongly shaken for 1 minute. To avoid shearing of nucleic acids the samples were not vortexed. Then the samples were centrifuged for 15 minutes at room temperature to separate the phases. After the centrifugation the aqueous phase (400 µl) was removed and precipitated by addition of lithium chloride (4 M). Afterwards the RNA was resolved in 50 µl RNase-free water (Roth, Karlsruhe, Germany) for 10 minutes at 65°C and the concentrations were determined photometrically by using a NanoDrop® (PeqLab, Erlangen, Germany). For the analysis of the RNA from the elution fraction by dot blot, 20 µl of the RNA were applied to a nylon membrane and crosslinked by UV light for 90 sec using the GelcDoc Imager (adapted from Göpel *et al*., 2013; Gerwig, 2011).

Lithium chloride precipitation

To 400 µl of the elution fraction, 40 µl 4 M lithium chloride and 1200 µl ice-cold ethanol (96%) were added. Then the samples were incubated over night at -20°C. Next, the samples were centrifuged for 15 minutes at 0°C. Afterwards the liquid was removed and the pellet (visible) was washed with ethanol (70%) once and dried for 30 minutes at room temperature under the laminar flow cabinet (pellet not visible anymore). Then the RNA pellet was solved in RNase-free water as described above.

DNase I digestion

For the DNase I digestion the DNase I (RNase-free) from Roche (Thermo Scientific, Lithuania) was used. The reaction mix was prepared in accordance to the manufacturers' instructions. The incubation time was extended to 60 min.

Reverse transcription quantitative real-time PCR (qRT-PCR)

The iScript™ One-Step RT-PCR Kit with SYBR® Green (Bio-Rad, Hercules, USA) was used for the RT-PCR analysis. The reactions were performed with the following reaction protocol in 20 µl set ups in an iCycler (Bio-Rad) as specified by the manufacturer (Diethmaier *et al*., 2011).

Reaction set up:

2x SYBR Green RT-PCR reaction mix	10 µl
Primer forward	1.2 µl
Primer reverse	1.2 µl
Nuclease-free H_2O	x µl
RNA template	x µl
iScript reverse transcriptase	0.4 µl
Total volume	20 µl

Reaction Protocol:

cDNA synthesis	10 min at 50°C
iScript reverse Transcriptase inactivation	5 min at 95°C
PCR cycling and detection (30 to 45 cycles)	10 sec at 95°C
	10 sec at 60°C
Melt curve analysis (optional)	1 min at 95°C
	1 min at 55°C
	10 sec at 55°C
	(80 cycles, increasing each by 0.5°C each cycle)

Calculation of fold changes:

Fold changes = $2^{-\Delta\Delta ct}$

$\Delta\Delta Ct = (Ct\text{-}Ct_{const})RNA^2 – (Ct – Ct_{const.})RNA^1$

Ct= Ct value of the respective gene

$Ct_{const.}$ = Mean of the Ct values of the internal control genes *rpsE* und *rpsJ*

RNA^1 = RNA of the respective reference strain (e.g. wild type)

RNA^2 = RNA of the mutant strains of interest

Dot blot for RNA detection

The nylon membrane with the cross-linked RNA (compare protein-RNA co-purification experiments) was incubated with 20 ml pre-hybridisation buffer at 68°C in a hybridisation oven for 1 h. Then the pre-hybridisation buffer was replaced with hybridisation buffer (25 µl DIG-labelled RNA probe solved in 15 ml hybridisation buffer) and incubated overnight at 68°C in the hybridisation oven. The next

day, the hybridisation buffer was transferred into a falcon tube and stored at -20°C until further usage. The membrane was washed twice for 15 min with 50 ml washing solution 0.1x SSC and twice with 50 ml washing solution 2x SSC, each at room temperature, to get rid of unbound RNA probes. Detection of RNA-RNA hybrids on the membrane followed directly after the hybridization step. All steps were performed at room temperature and with gentle shaking. The membrane was incubated with buffer DIG-P1 for 5 min and for 30 min with buffer DIG-P2. Then, anti-DIG antibodies (Roche Applied Science) coupled with alkaline phosphatase dissolved in buffer DIG-P2 (1:10,000) were added onto the membrane and incubated for 30 min. After this, the membrane was washed and equilibrated three times for 5 min with buffer III. For visualisation of RNA-RNA hybrids, the membrane was put between clear plastic foil and incubated with 2.5 µl CDP* (diluted in 500 ml buffer III) for 5 min. CDP* (Roche Applied Science) is a substrate of the alkaline phosphatase coupled to the anti-DIG antibody, resulting in chemo-luminescence as a coproduct of the reaction which can be visualized and quantified. Depending on the intensity of the chemo-luminescence, the membrane was exposed for 5 to 45 min in a ChemoCam imager (INTAS, Göttingen) (adapted from Eilers, 2010).

Buffer and solutions for working with RNA

Blocking solution	10% (w/v) blocking reagent in buffer Dig-P1 autoclaved
Killing buffer	20 mM Tris/HCl pH 7.5 5 mM $MgCl_2$ autoclaved, then addition of 20 mM NaN_3
10x MOPS-Puffer	200 mM MOPS 50 mM sodium acetate 10 mM EDTA adjusted to pH 7.0 with NaOH sterile filtrated
Sodium lauroyl sarcosinate 10%	10% sodium lauroyl sarcosinate in H_2O_{deion} autoclaved

5x buffer Dig-P1	1 M malic acid 1.5 M NaCl adjusted to pH 7.5 with NaOH, autoclaved
Buffer Dig-P2	1% blocking reagent in 1x buffer Dig-P1
Buffer III	0.1 M Tris/HCl 0.1 M NaCl pH 9.5, adjusted with HCl
SSC (20x)	3 M NaCl 0.3 M sodium citrate adjusted to pH 7.0 with HCl, autoclaved
Prehybridization solution (500 ml)	200 ml 100% formamide 100 ml 20 x SSC 8g blocking solution 4 ml 10% sodium lauroyl sarcosinate 28 g SDS ad 500 ml with water, warm up to dissolve the compounds and store at -20°C
Washing solution 0.1 x SSC	0.1 x SSC 0.1% SDS
Washing solution 2 x SSC	2 x SSC 0.1% SDS

3.3.12. Fluorescence microscopy

The microscopy was performed as described by Diethmaier *et al*. (2011). An over-night culture of 4 ml LB medium (with the appropriate antibiotics) was inoculated from a glycerol culture or a fresh single colony. In the morning, 10 ml LB medium in a 100 ml flask without a baffle were inoculated to an OD_{600} of 0.05. Then the cells were cultivated in the dark at 37°C and 200 rpm and harvested in the exponential (0.7–1.0) or late exponential (about 1.5) growth phase. To harvest the cells, 1 ml of the culture was centrifuged in a 1.5 ml reaction tube impermeable to light for 1 min at 13,000 rpm. Afterwards, the supernatant was discarded and the cells were resuspended in PBS buffer pH 7.5 (in a

volume that was 1/10 of the OD_{600} of the culture). The resuspended cells were kept on ice until microscopy. In the dark one drop of cell suspension (about 6 µl) was placed on a microscope slide covered with agarose (1% in water). This way, the cells were immobilized in order to prevent movement of the cells during microscopy. Fluorescence images were obtained with an Axioskop 40 FL fluorescence microscope, equipped with an AxioCam MRm digital camera and the AxioVision Rel 4.8.2 software was used for image processing (Carl Zeiss, Göttingen, Germany). For fluorescence microscopy the YFP HC filter set (BP 500/24, FT 520, LP 542/27; AHF Analysetechnik, Tübingen) and the Filterset 47 (BP 436/25, FT 455, BP 480/40; Carl Zeiss) were used for YFP and CFP detection, respectively. Images were taken at 2.0 sec exposure time (adapted from Diethmaier, 2011; Kruse, 2013).

3.3.13. Preparations for quantification of cyclic nucleotide monophosphates in *B. subtilis* (Sprangler *et al.*, 2010)

For measurement of c-di-GMP levels in *B. subtilis* cell extract, cultures were grown in MSgg or CSE-Glc medium to an OD_{600} of 1. Two times 10 ml of these cultures were centrifuged for 20 min at 4°C and 2.55 × g. Pellets were resuspended in 800 µl extraction mix and 700 µg glass beads (0.1 mm) were added. Samples were immediately frozen in liquid nitrogen and then heated at 95°C for 10 min. Cells were disrupted mechanically in the Qiagen TissueLyserII for 7.5 min at 30 Hz. The suspension was centrifuged for 5 min at 4°C and 13,000 rpm. The supernatant was transferred into a fresh tube and stored on ice. The remaining pellet was dissolved in 600 µl extraction mix and incubated on ice for 15 min. Cell disruption and centrifugation was repeated. The remaining pellet was again mixed with 400 µl extraction mix and kept on ice for 15 min. After another centrifugation, all three supernatants were mixed and stored at -20°C over night. The next day, samples were centrifuged for 10 min at 4°C and 13,000 rpm. Supernatants were transferred into a new reaction tube and steamed down to pellets using a Speed-Vac at 40°C. HPLC-MS/MS measurements to analyze c-di-GMP contents of the prepared samples were carried out at the mass spectrometry laboratory for low-molecular weight bacterial and eukaryotic metabolites of the Hannover Medical School (adapted from Bötz & Kruse, 2013). To normalize the results, protein contents of 1 ml of the original cell cultures were determined. For this, 1 ml samples were taken simultaneously to the 10 ml samples. Cells were pelleted by centrifugation and then dissolved in 800 µl 0.1 N NaOH. Samples were boiled at 95°C for 15 min and then centrifuged for 5 min a 13,000 rpm. Protein amounts of the supernatants were determined as described by Bradford *et al.* (1976). The resulting values were used to estimate the protein content of the samples used for HPLC-MS/MS.

Solution for preparations of cNMP measurements

Extraction mix	8 ml	acetonitrile
	8 ml	methanol
	4 ml	deion. water

4. Results

4.1. The protein tyrosine kinases EpsB and PtkA differentially affect biofilm formation

Protein phosphorylation is a versatile mechanism to control the activity of proteins. In *B. subtilis* protein phosphorylation on different amino acid residues controls important cell differentiation processes, like sporulation, competence development, motility, and biofilm formation (Macek *et al*., 2007; Vlamakis *et al*., 2013). Recently, the tyrosine kinase PtkA and its cognate transmembrane modulator TkmA were implicated in controlling biofilm formation and sporulation but the role of the homologous tyrosine kinase EpsB and its transmembrane modulator EpsA remained unstudied (Kiley & Stanley-Wall, 2010). Therefore, we addressed the role of the putative tyrosine kinase EpsB and its modulator EpsA for biofilm formation in this work.

4.1.1. *In vivo* interaction between EpsA and EpsB

Co-purification experiments

The EpsA and EpsB proteins are similar to the TkmA transmembrane kinase modulator and the PtkA protein tyrosine kinase of *B. subtilis*, respectively. It is well established that modulator proteins stimulate the activity of their cognate protein kinases by protein-protein interaction. To address whether this is also the case for EpsA and EpsB, we analyzed the potential interaction between these two proteins.

For this pupose, the strain GP1589 carrying plasmid pGP2126 was used. In this strain, EpsA carries a C-terminal FLAG-tag and pGP2126 allows overexpression of EpsB fused to an N-terminal *Strep*-tag. Additionally, the gene for the anti-activator (and master regulator of biofilm formation) SinR was deleted to ensure a high expression level of EpsA. The isolation of protein complexes from *B. subtilis* cells was performed by using the SPINE technology (Herzberg *et al.*, 2007; compare 3.3.10.).

If the EpsA and EpsB proteins interacted with each other, one would expect that the FLAG-tag epitope bound to EpsA is detectable in the elution fractions containing *Strep*-EpsB. As EpsA contains two transmembrane domains and is likely to be a membrane protein, the possible interaction between EpsA and EpsB was fixed using formaldehyde as cross-linker. *Strep*-EpsB with its bound interaction partners was purified by its binding to *Strep*-Tactin columns. Both the cell extract and the elution fractions were analyzed by SDS-PAGE and subjected to Western blot analysis. As shown in Fig. 4.1A, EpsA-FLAG was present in the crude extract. Importantly, EpsA-FLAG co-eluted with EpsB in a protein preparation obtained with cross-linking. To ascertain the specificity of the binding of EpsA to EpsB, it was tested whether CggR, a cytoplasmic transcription factor, also co-purified with EpsB. As shown in Fig. 4.1B, CggR was expressed under the tested conditions. However, CggR did not co-elute with EpsB. Additionally, an empty vector control was used to ensure that EpsA-FLAG does not bind to

the *Strep*-Tactin columns unspecifically. In this case, EpsA-FLAG could also not be detected in the elution fractions. Therefore, the elution of EpsA is caused by a specific interaction with EpsB. These results demonstrate an interaction between the membrane protein EpsA and the putative protein kinase EpsB.

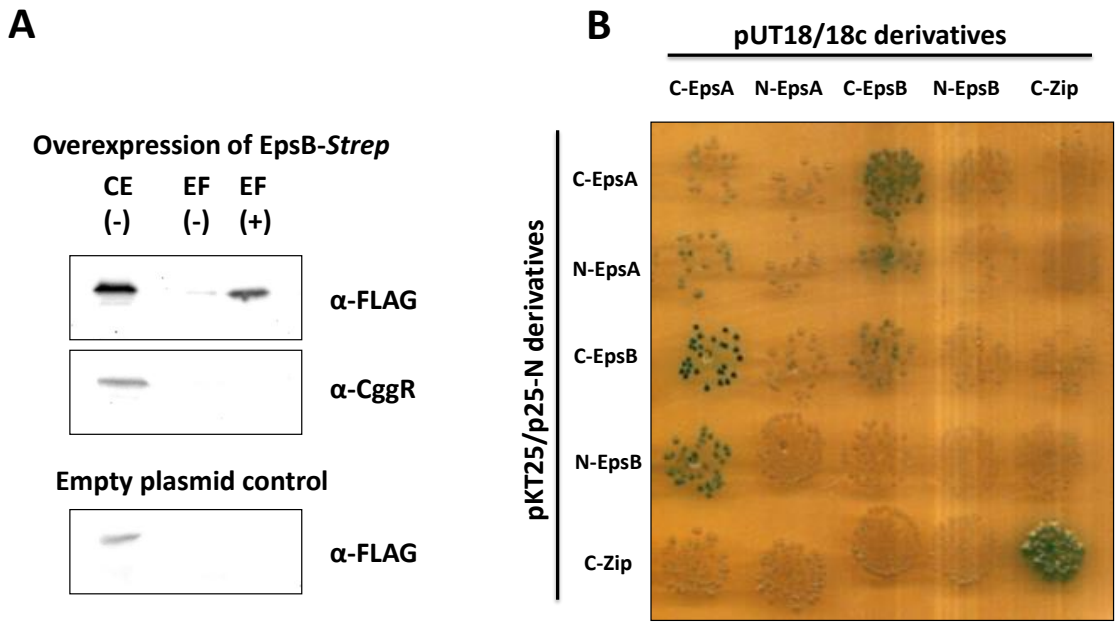

Figure 4.1. The tyrosine kinase EpsB and its cognate modulator protein EpsA interact physically. (A) EpsA-FLAG co-purifies with EpsB-*Strep*. To ensure high expression of EpsA-FLAG the gene for the anti-activator SinR was deleted in this strain. EpsB-*Strep* was purified in the absence (-) or presence (+) of the cross-linker formaldehyde. The different proteins were detected by Western blotting with specific antibodies. CE = crude extract, EF = elution fraction. (B) EpsA and EpsB interact in the bacterial two-hybrid system. The genes encoding EpsA and EpsB were cloned in vectors that allow the expression of EpsA and EpsB fused to the N- or C-terminus of the T18 or T25 domains of the *B. pertussis* adenylate cyclase, respectively. The *E. coli* transformants harboring both vectors were incubated on X-Gal containing plates. Degradation of X-Gal and the resulting blue color of the cells indicate interaction due to the presence of a functional adenylate cyclase.

Bacterial two-hybrid studies

Since the results from the co-purification experiments did not allow concluding whether the interaction between EpsA and EpsB is direct or indirect. To address this question, the interaction was studied using the bacterial two-hybrid (B2H) system. The B2H system is based on the interaction-mediated reconstruction of adenylate cyclase (CyaA) activity from *Bordetella pertussis* in *E. coli* (Karimova *et al.*, 1998). Proteins suspected to interact physically were fused with separated domains of the adenylate cyclase as described in chapter 3.3.10. As shown in Fig. 4.1B, EpsA and EpsB clearly interacted with each other in this heterologous *E. coli* system, whereas neither of the two proteins exhibited an interaction with the control protein (leucine zipper of yeast Gcn4p). Thus, EpsA and EpsB are capable of interacting specifically and directly with each other.

4.1.2. Cellular localization of the tyrosine kinase EpsB and its modulator protein EpsA

Since the transmembrane domain (modulator) and the enzymatically active domain of tyrosine kinases consist of two separate proteins in Gram-positive bacteria, an interaction between these two proteins is important in order to phosphorylate their target proteins (Mijakovic *et al.*, 2003; Grangeasse *et al.*, 2012). The interaction between the transmembrane protein EpsA and EpsB was shown in the chapter before. The question addressed here is whether the predicted transmembrane localization of the so far unstudied tyrosine kinase modulator protein EpsA can be demonstrated *in vivo*. Furthermore, a possible co-localization of the EpsB kinase with its modulator EpsA at the membrane was analyzed. Interestingly, it was proposed that localization of EpsB might be dynamic so that EpsB co-localizes with potential cytosolic target protein. Thus, identification of EpsB within the cytosol could further support this assumption (Jers *et al*., 2010).

To confirm the predicted localization of the modulator EpsA in the membrane, the strain GP1589 (compare 4.1.1.) containing an *epsA*-FLAG fusion within the chromosome was used. The cellular localization of the proteins was determined by ultra-centrifugation and Western blotting as described in 3.3.10. The results of this experiment are presented in Fig. 4.2.

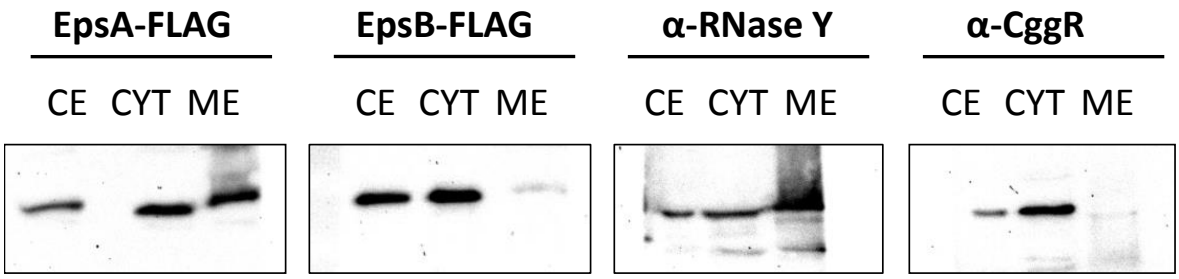

Figure 4.2. The kinase modulator EpsA is a membrane-bound protein, whereas the EpsB kinase is located in the cytosol. Separation of cytosolic (CYT) and membrane (ME) proteins form cell extracts (CE) of strains expressing EpsA-FLAG (GP1589) and EpsB-FLAG (GP1547) by ultracentrifugation. The experiments were performed in a *sinR* deletion background to ensure high expression of the *eps* operon. The different proteins were detected with respective antibodies. As prove of principle, the detection of RNase Y and CggR is only shown for strain GP1589.

As controls, antibodies against the membrane-bound protein RNase Y and the cytosolic protein CggR were used to detect the proteins within the three different fractions of the cultivations of the *epsA*-FLAG and *epsB*-FLAG strains, respectively. In accordance to previous work (Lehnik-Habrink *et al*., 2011a; Mehne *et al*., 2013) RNase Y was mainly detected within the membrane fraction (contaminations in the cytosolic fraction) and the repressor protein of the glycolytic *gap* operon CggR was located within the cytosol. This supports the reliability of the applied ultracentrifugation method.

In the crude extract a signal at the size for EpsA-FLAG could be detected. This shows that EpsA-FLAG is expressed under the chosen conditions. Also, a clear signal in the membrane fraction but not in the cytosolic fraction could be obtained. Therefore, the predicted localization of EpsA within the membrane could be confirmed.

Next, it was analyzed if the respective kinase EpsB also localizes to the membrane fraction as shown for its modulator. If this is the case it would support a model of a stable complex of EpsA and EpsB at membrane rather than a dynamic interplay between the two proteins. To address this question the *epsB*-FLAG containing strain GP1547 was used. Strikingly, EpsB-FLAG was detected within the cytosolic fraction but not in the membrane fraction (very weak signal, but also in control strain). This indicates that the interaction between the EpsB tyrosine kinase and its modulator EpsA is not stable enough to "survive" separation by ultracentrifugation. Therefore, it is tempting to speculate that the interaction between the modulator EpsA and the kinase EpsB is rather dynamic than stable and that EpsB co-localizes with its potential targets as suggested for the homologous tyrosine kinase PtkA by Jers *et al*. (2010).

4.1.3. The role of tyrosine protein kinases and their modulators in complex colony and pellicle formation

It is well established that BY-kinases are implicated in extracellular polysaccharide synthesis in many species (Grangeasse *et al*., 2012). The location of the *epsA* and *epsB* genes in the *eps* operon encoding the functions for extracellular polysaccharide formation in *B. subtilis* biofilms was highly suggestive of a role for these proteins in biofilm formation. To address the role of the putative BY-kinase EpsB and its transmembrane modulator EpsA in biofilm formation, the respective genes were deleted in the undomesticated NCIB3610 wild type strain. Furthermore, a *ptkA* deletion mutant (NRS2544) was received from Nicola Stanley-Wall and the gene for the respective transmembrane modulator TkmA was deleted to study possible overlapping or additive functions of the homologous modulators and kinases. To demonstrate that the EpsB kinase and its cognate modulator EpsA work together in one functional process a double mutant was studied.

In the laboratory strain, *B. subtilis* 168, the *epsC* gene carries a point mutation and encodes an inactive protein (McLoon *et al*., 2011). Any genetic transfer of constructed *epsA* and *epsB* alleles is likely to co-transfer this *epsC* mutation. Therefore we constructed the strains GP1540, GP1535 and GP1528 that carry a single deletion of *epsA* and *epsB* or a simultaneous deletion of *epsAB* in the background of the strain AM373, respectively. This strain carries the *epsC* wild type (*epsC*$^{+}$) allele (McLoon *et al*., 2011) and is naturally competent. This allows the construction of mutants by transformation with LFH-PCR products (compare 3.3.6.).

Initially, the role of the BY-kinase EpsB in biofilm formation was addressed. For this purpose, complex colony formation of the *epsB* mutant strain GP1575 was compared with the respective control strains. In agreement with previous reports (Branda *et al*., 2001), the wild type strain formed well-structured colonies (Fig. 4.3A) and thick and wrinkled pellicles (Fig. 4.3B). The isogenic *epsB* mutant GP1575 also formed structured colonies; however, the wrinkles resulting from exopolysaccharide accumulation were completely lost (Fig. 4.3A). Similarly, the pellicle formed by the *epsB* mutant strain was less structured than observed for the wild type (Fig. 4.3B).

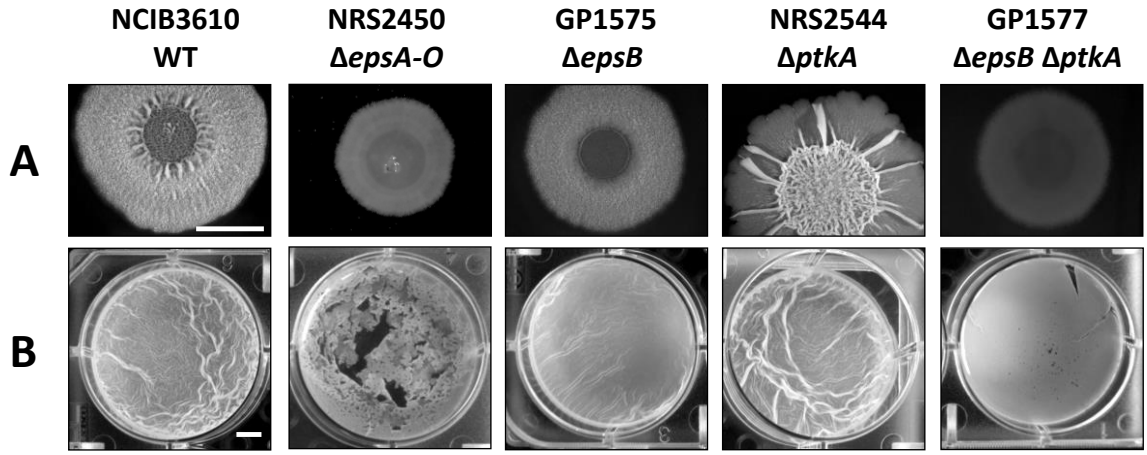

Figure 4.3. The deletion of tyrosine kinase genes in the wild type strain NCIB3610 leads to less structured colonies and pellicles. (A) Complex colony formation on MSgg agar plates. (B) Pellicle formation on top of liquid MSgg medium. Bars, 5 mm.

The *epsB* deletion did, however, not have an impact as significant as the deletion of the entire *epsA-O* operon; thus suggesting that exopolysaccharide biosynthesis was reduced but not completely lost in the *epsB* mutant. To rule out the possibility that the replacement of the *epsB* gene by an *aphA3* resistance cassette might have a polar effect on the expression of the downstream genes of the *eps* operon a resistance cassette lacking a transcription terminator downstream of the *aphA3* gene was used. Moreover, the expression of the downstream *epsC* gene in the wild type strain 168 and the *epsB* mutant GP1518 was compared by qRT-PCR. The *epsC* expression was not abolished by the *epsB* deletion.

To support the hypothesis that the transmembrane modulator EpsA is required for the function of the cognate EpsB protein, the *epsA* gene was deleted in the undomesticated NCIB3610 wild type strain resulting in the strain GP1600. As shown for the *epsB* mutant, the *epsA* mutant strain formed structured colonies but the wrinkles were lost (Fig. 4.4A). Also, the pellicle of the *epsA* mutant strain looked similar to pellicles formed by the *epsB* mutant (Fig. 4.4B). The observation that an *epsA* mutant has the same phenotype as an *epsB* mutant suggests that EpsA and EpsB act in one pathway of biofilm formation and supports the idea that the EpsA modulator is required for the function of

the EpsB protein. To further study the idea that EpsA and EpsB act in one pathway of biofilm formation the *epsAB* mutant GP1637 was constructed and its biofilm phenotype was analyzed. As expected, the *epsAB* double mutant showed the same phenotype as *epsA* and *epsB* single mutants supporting the initial idea that both proteins act in one pathway.

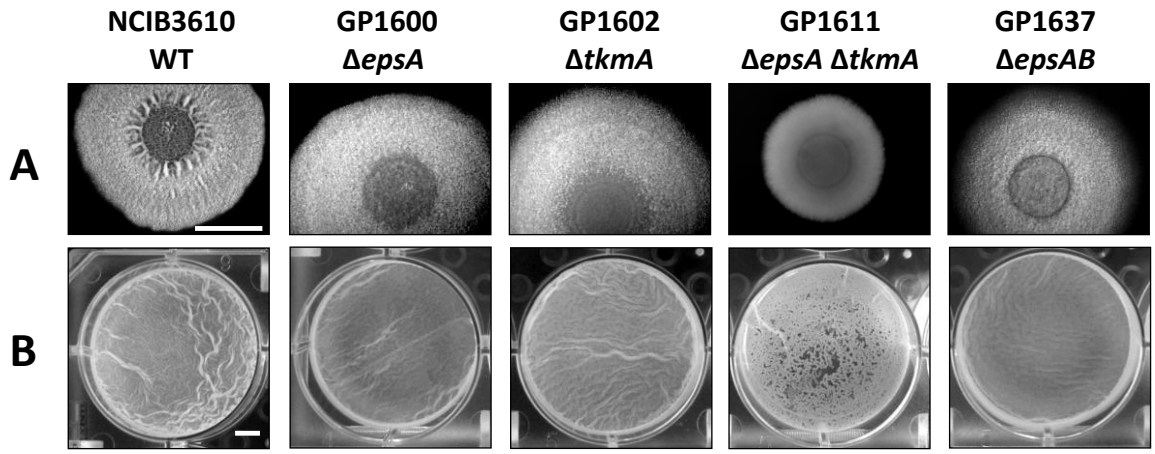

Figure 4.4. The deletion of tyrosine kinase modulator genes in the wild type strain NCIB3610 leads to less structured colonies and pellicles. (A) Complex colony formation on MSgg agar plates. (B) Pellicle formation on top of liquid MSgg medium. Bars, 5 mm.

Since EpsB and PtkA are the only BY-kinases in *B. subtilis* the question was addressed if both proteins have complementary function for biofilm formation. For this purpose, the effect of the inactivation of *epsB* to that of a *ptkA* mutation was compared and the phenotype resulting from a loss of both BY-kinases was studied. As observed previously (Kiley & Stanley-Wall, 2010), the *ptkA* mutant NRS2544 formed structured and strongly wrinkled colonies; however, these colonies lacked a rough outer region that is usually the area of sporulation and fruiting body formation (see Fig. 4.3A). The pellicles formed by the *ptkA* mutant were similar to those of the isogenic wild type strain (see Fig. 4.3B). The most severe phenotype was observed for the *epsB ptkA* double mutant GP1577. This strain was unable to form structured colonies, and was thus very similar to *epsA-O* or *ymdB* mutants (see Fig. 4.3, Diethmaier *et al.*, 2011).

Additionally, a complementation assay with the *epsB ptkA* mutant strains GP1634 was performed. This strain contained a functional copy of the *epsB* gene under the control of a xylose-induced promoter in the non-essential *xkdE* locus. Expression of the ectopic *epsB* gene upon addition of xylose to the biofilm medium restored the formation of a thick and structured pellicle (Fig. 4.5). In conclusion, the data support the idea of a role for the BY-kinases in biofilm formation. Interestingly, the simultaneous deletion of the genes coding for the two kinase modulators EpsA and TkmA in the NCIB3610 strain (GP1611) leads to the same phenotype as the deletion of both BY-kinases (see Fig. 4.4). As shown for the *epsB ptkA* mutant, the ectopic expression of *epsA* in the *epsA*

tkmA mutant (GP1636) also restored the formation of a thick and wrinkled pellicle (compare Fig. 4.6). Once again, this supports the idea that the two modulator proteins EpsA and TkmA are required for the function of their cognate BY-kinases, EpsB and PtkA, respectively.

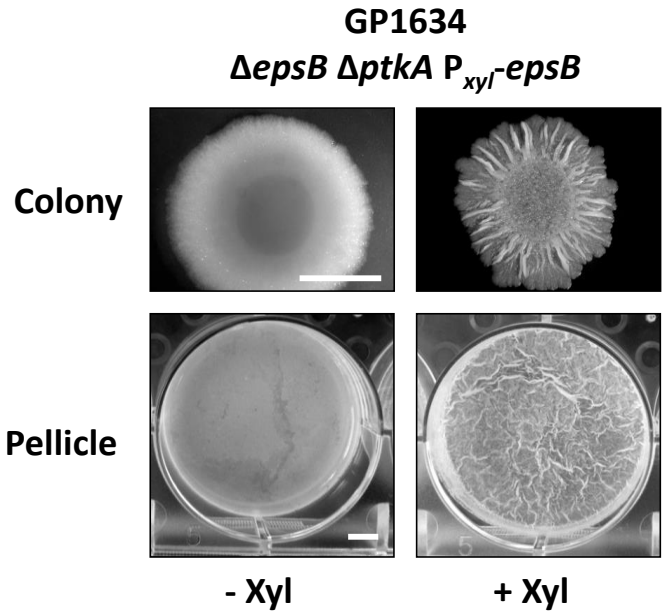

Figure 4.5. Ectopic expression of *epsB* complements the phenotype of the *epsB ptkA* double mutant. Complex colony and pellicle formation on MSgg agar plates and on top of liquid MSgg medium. The expression of *epsB* was induced by addition of xylose to the medium. Bars, 5 mm.

In summary, the results reported above clearly demonstrate the implication of EpsB and PtkA in biofilm formation and suggest distinct roles for the two enzymes in this process. As reported previously, PtkA seems to be required for the biofilm-associated sporulation whereas EpsB is mainly responsible for exopolysaccharide biosynthesis.

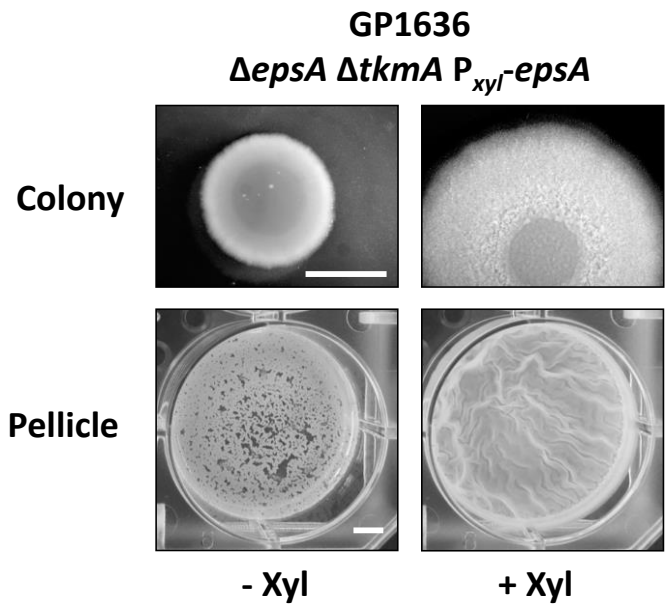

Figure 4.6. Ectopic expression of *epsA* complements the phenotype of the *epsA tkmA* double mutant. Complex colony and pellicle formation on MSgg agar plates and on top of liquid MSgg medium. The expression of *epsB* was induced by addition of xylose to the medium. Bars, 5 mm.

4.1.4. Tyrosine kinases influence extracellular polysaccharide production

Exopolysaccharides (EPS) are a major component of the biofilm matrix (Branda *et al.*, 2001). The proteins for the synthesis and export of the EPS are encoded within the *epsA-O* operon. As shown in

Fig. 4.3, the deletion of the putative BY-kinase EpsB leads to a loss of the wrinkled colony and pellicle structure, which might indicate a loss of EPS production. The location of the *epsB* gene in the *epsA-O* operon supports this idea. To test our assumption that EpsB is involved in the production of EPS, we made use of a strain with deletions of the *sinR* and *tasA* genes to enhance the production and release of EPS from the cells. The resulting cells were cultivated and the EPS within the supernatant of the culture medium were precipitated by ethanol. As a positive control the *sinR tasA* deletion strain GP1622 was used and as a negative control an *epsA-O* deletion was introduced resulting in strain GP1629. As expected, EPS could be precipitated within the supernatant of strain GP1662, whereas the *epsA-O* deletion strain totally lacked EPS production. Surprisingly, no major effect on the amount of EPS was observed in the *epsB* deletion strain (Fig. 4.7).

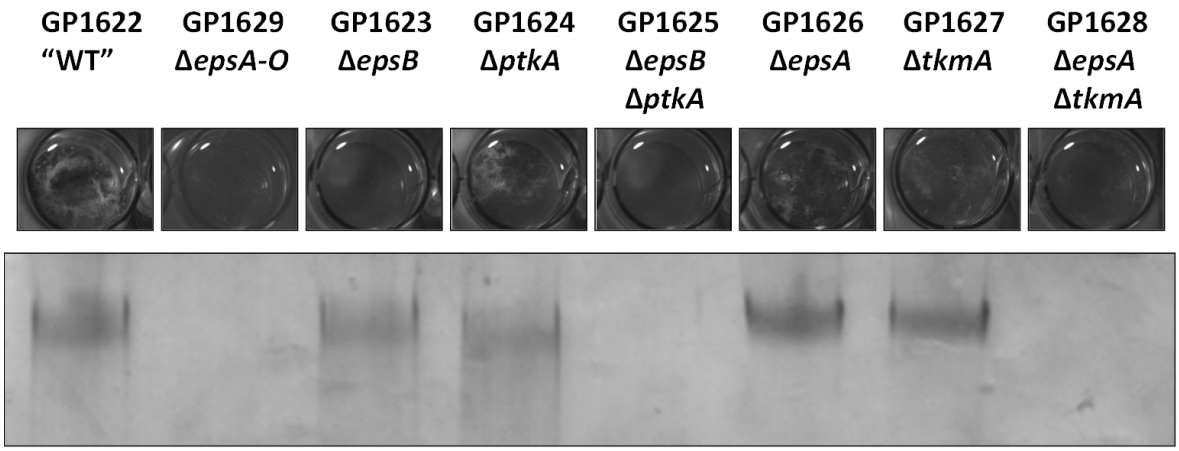

Figure 4.7. The deletion of tyrosine kinases affects exopolysaccharide production. All strains contain a Δ*sinR-tasA* deletion to facilitate the release of exopolysaccharides into the culture medium. (A) Ethanol-precipitated supernatant from the indicated strains in the chambers of a 24-well plate. (B) Ethanol-precipitates resolved in the stacker of a SDS-PAGE gel stained with Stains-all dye.

This finding suggests that the putative kinase activity of EpsB is dispensable for EPS production or that EpsB can be functionally replaced by the second BY-kinase, PtkA. However, in a recent publication using a more exact quantitative EPS assay, EPS amounts were reduced in *epsB* deletion mutant but not totally absent (Elsholz *et al*., 2014). Next, the implication of the second BY-kinase PtkA in EPS production was addressed. In agreement with the wrinkled colony and pellicle structure of the *ptkA* mutant, similar amounts of EPS as in the wild type were observed. Thus, PtkA is not directly involved in the regulation of EPS synthesis by the proteins encoded within the *epsA-O* operon. Interestingly, no EPS was detectable in the *epsB ptkA* double mutant. This observation is in perfect agreement with the complete lack of biofilm formation in the *epsB ptkA* double mutant and suggests that PtkA does also affect EPS production, at least in the absence of EpsB. Furthermore, production of the *epsA* and *tkmA* modulator single mutants and the *epsA tkmA* double mutant was

monitored. As shown for the respective BY-kinase mutants, the modulator single mutants are able to produce EPS, whereas the *epsA tkmA* mutant shows no EPS production (Fig. 4.7). This supports the requirement of EpsB and PtkA for their modulator proteins.

4.2. The YmdB protein as a regulator for biofilm formation

Biofilm formation in *B. subtilis* is highly regulated for instance by tyrosine kinases as shown in the previous chapter. Another protein involved in regulation is the phosphodiesterase YmdB. The deletion of the respective gene leads to highly reduced biofilm formation (Fig. 4.8A) and influences the expression of about 800 genes. Especially, transcripts for the main components of the biofilm matrix are less abundant, whereas expression of motility genes is induced (Diethmaier *et al*., 2011, 2014). Although the deletion of the *ymdB* gene has a strong effect on cell differentiation it is not clear how the YmdB phosphodiesterase acts mechanistically to control biofilm formation and cell differentiation in general. Therefore, the aim of this work was to further understand how the YmdB protein acts as a regulator for biofilm formation.

4.2.1. Deletion of the *ymdB* gene increases SinR protein levels

Biofilm formation and motility are mutually exclusive processes in *B. subtilis* (Blair *et al*., 2008; Vlamakis *et al*., 2013). The switch between these two states is controlled by the SinR protein and its antagonists SinI and SlrR. The SinR protein is expressed constitutively (Gaur *et al*., 1988; Nicolas *et al*., 2012) and represses expression of biofilm genes and the gene for its antagonist SlrR. Repression of biofilm genes by SinR is relieved by binding of the antagonist SinI. When SinI is bound to SinR, SlrR protein is produced and can also bind SinR proteins. Upon binding of SlrR to SinR the repression of biofilm gene expression is prevented and SlrR inhibits, in complex with its co-repressor SinR, the expression of motility and autolysis genes (Chai *et al*., 2010b). This way it is ensured that a cell can only be a matrix producer or motile at the same time. Diethmaier *et al*. (2011) argued that reduced expression of the *slrR* gene is responsible for the biofilm defect of the *ymdB* mutant. At first sight, lack of the SinR antagonist SlrR can explain reduced biofilm formation, but it is not in line with the observation that SinR protein amounts are increased in the *ymdB* mutant (Wicht, 2010, this work). The SinR protein represses transcription of the *slrR* gene, whereas SlrR inhibits SinR-mediated repression by interacting with SinR. Therefore, elevated SinR amounts are the initial cause that explains decreased expression of the *slrR* gene resulting in a biofilm defect of *ymdB* mutant and changes in cell differentiation. Since the *sinR* gene is transcribed constitutively and transcript levels are not affected by the deletion of the *ymdB* gene, it is likely that YmdB controls SinR protein amounts on post-transcriptional or translational level.

To study the initial observation by Wicht (2010) in more detail, the SinR protein amounts in the undomesticated wild type NCIB3610 and the isogenic *ymdB* mutant strain GP921 (Diethmaier *et al*., 2011) were determined by Western blot analysis. As shown in Fig. 4.8B, SinR proteins were barely detectable in the wild type strain. In contrast, the *ymdB* mutant strain showed a clear signal for SinR. Elevated SinR protein amounts could also be observed in the *ymdB* mutant in the background of the *B. subtilis* strain 168 and in the enzymatically inactive *ymdB* point mutant GP969 (Diethmaier *et al*., 2014; compare Fig.7.1).

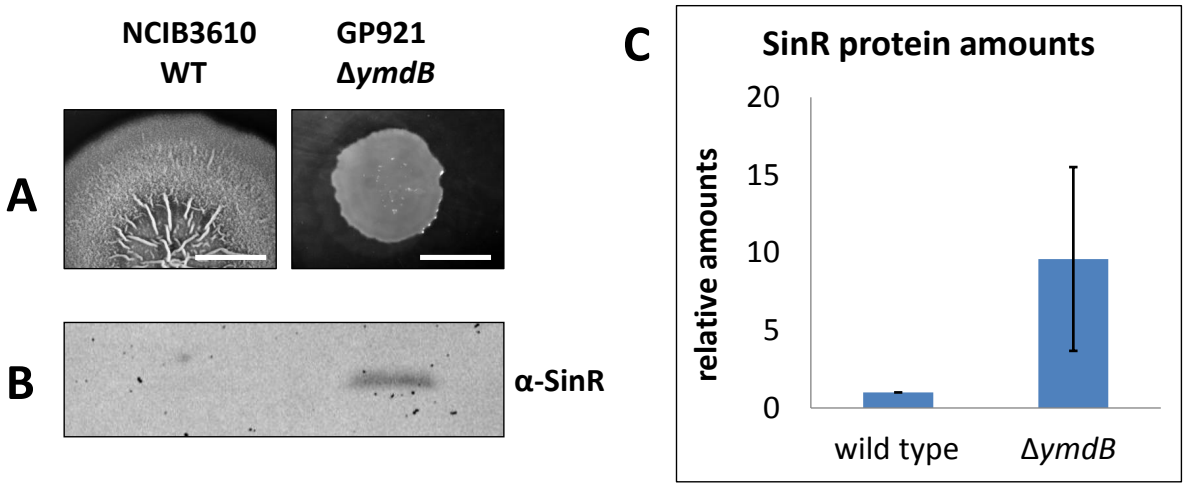

Figure 4.8. SinR protein amounts are increased in the *ymdB* deletion mutant. (A) Complex colony formation of the NCIB3610 wild type and the *ymdB* deletion mutant GP921 on MSgg agar plates. Bars, 5 mm. (B) Detection of the SinR protein with a specific antibody within the NCIB3610 and GP921 strains by Western blot analysis. (C) Quantitative analysis of SinR protein amounts in the *ymdB* mutant GP1574 compared to the wild type GP1561 by Western blot. The SinR signals were normalized with the signals for HPr protein which was used as a loading control. Bars represent the relative mean (wild type set to 1) of the values for SinR protein determined by Image J. Error bars indicate standard deviations of 3 biological replicates.

To further support these observations, the *ymdB* mutant strain GP1574 and the isogenic wild type strain GP1561 (compare chapter 4.2.2.) were used for densitometry experiments. For this purpose, the cells were cultivated as for the previous experiments and SinR protein amounts were analyzed by Western blotting. In parallel, HPr protein amounts were determined and used to normalize SinR amounts. As shown in Fig. 4.8C SinR protein amounts were about 10 times higher in the *ymdB* mutant than in the wild type strain supporting previous observations. Consequently, elevated protein amounts of the master regulator of biofilm formation in the *ymdB* mutant explain its biofilm defect. However, it remains to be elucidated if this effect is a direct or indirect effect of *ymdB* gene deletion.

4.2.2. Suppressor mutations in the *ymdB* mutant restore biofilm gene expression

Generation of *ymdB* suppressor mutants and identification of their genetic variations

In accordance to the observation of Diethmaier *et al*. (2011) that deletion of the *sinR* gene in the *ymdB* mutant restores complex colony structure, we observed that the *ymdB* mutant forms suppressor mutants in which biofilm matrix gene expression is restored (Kruse, 2013). The responsible suppressor mutations could be identified within the *sinR* gene. Interestingly, mutations at different positions led to amino acid exchange in the SinR protein affecting SinR protein properties (interaction with antagonist/ itself and DNA-binding ability) and protein stability. Unfortunately, these suppressor mutants were isolated from several different genetic backgrounds.

To establish a versatile screening strain as a uniform background for the identification of further suppressor mutations, the Δ*ymdB* mutant strain GP1574 was constructed. This strain harbors an YFP reporter fusion for the expression of biofilm genes (P_{tapA}-*yfp*) and a CFP reporter fusion for the expression of motility genes (*hag-cfp*). This way restored biofilm and bistable gene expression of potential suppressor mutants could be studied by using fluorescence microscopy. As controls, the isogenic wild type strain GP1561 and the Δ*ymdB* Δ*sinR* mutant strain GP1818 were constructed. By using these strains, the effects of suppressor mutants could be monitored in comparison to the wild type situation or to a strain lacking the SinR protein.

Isolation of suppressor mutants of the *ymdB* deletion strain GP1574 was performed in different ways. An overview of the isolated suppressors and the generation procedure is shown in Tab. 4.1. After isolation of a suppressor mutant with an altered phenotype the *sinR* gene was sequenced to identify mutations. Interestingly, several different suppressors with a mutated *sinR* gene could be identified but also suppressor mutants with (partially) restored biofilm formation that carried a non-mutated *sinR* gene were identified. To identify the mutation of the suppressor mutants GP1638, GP1639 and GP1646 that carried an intact *sinR* gene, chromosomal DNA was isolated and whole genome sequencing was performed in cooperation with the “Göttingen Genomics Laboratory” (G2L). This way a mutation in the SinR operator motif upstream of the *epsA* gene (and also upstream of the neighboring *slrR* gene) could be identified in the strain GP1638 (compare Fig. 4.9A). This mutation most likely inhibits binding of the SinR anti-activator to the operator and allows expression of the *eps* operon. In addition, this mutation seems to enable expression of the *slrR* gene because the *tapA-sipW-tasA* operon is also relieved from repression as shown in Fig. 2.3 (Chu *et al*., 2006; Newman *et al*., 2013). Presence of all mutations was confirmed by Sanger sequencing (for primer compare Tab. 7.3).

Furthermore, a mutation within the type III polyketide synthase encoding gene *bpsA* was identified. This gene was not implicated in biofilm formation so far and deletion of the gene did not affect sensitivity to cell-wall antibiotics and heat resistance (Nakano *et al*., 2009). In addition, it is mainly

expressed during sporulation (Nicolas *et al*., 2012). However, non-ribosomally synthesized peptides, as e. g. surfactin or spore killing factors, were shown to control cell differentiation processes (Marvasi *et al*., 2010; González-Pastor, 2011). Moreover, it was proposed that the Kin kinases respond to so far unknown signals to regulate differentiation of the inner and outer region of a colony (McLoon *et al*., 2011). Thus, the implication of the *bpsA* gene in biofilm formation appears worth studying.

Table 4.1. Overview of the isolated suppressor mutants of the *ymdB* deletion strain GP1574.

Strain	Similar strains	Mutation	Isolation method
GP1638		SinR operator between the *epsA* and *slrR* genes (T→C)	Cells were cultivation in LB medium for 1 day and dilution series were plated on MSgg agar plates to obtain single colonies. After incubation at 30°C for 1 day the plates were stored at RT for several days until suppressors appeared.
GP1639		BpsA (BcsA): Val257Leu (GTG → CTG) type III polyketide synthase	
GP1646	GP1647, GP1648	not in the *sinR* gene (location unknown)	Cells were streaked out on SP plates and stored at RT for several weeks. From this plate single papillae (suppressors) were isolated.
GP1649		SinR: Trp104Arg (TGG→ AGG) (homo/hetero-dimerization domain)	compare GP1638, but cultivation for 60 h and every morning and every evening 100 µl of the growing culture was transferred to fresh 10 ml LB medium before plating the cells on MSgg plates.
GP1650	GP1801-GP1804, GP1806-GP1808	SinR: Ala85Thr (GCG → ACG) (homo/hetero-dimerization domain)	Separation streak out on SP plates (containing kanamycin, spectinomycin and chloramphenicol) and storage for several weeks. Separately grown papillae were streaked out repeatedly until all single colonies appeared homogeneous.
GP1805	GP1809	SinR: Leu99Ser (TTA → TCA) (unstable protein)	

Due to the mucoid appearance of the strain GP1646 it was hypothesized that the cells contain a mutated variant of the master regulator for cell differentiation Spo0A that induces poly-DL-γ-glutamic acid production. Therefore, the *spo0A* gene was sequenced but unfortunately no mutation could be identified within the gene. In a next attempt to identify mutations that partially restored biofilm gene expression in the Δ*ymdB* background, whole genome sequencing was performed as described before. However, sequencing of the strain GP1646 was not successful and needs to be repeated.

Characterization of the suppressor mutants of the *ymdB* deletion strain GP1574

To characterize the different suppressor mutations in detail, pellicle and complex colony formation was tested. Moreover, expression of biofilm and motility reporter genes was visualized on colony

level and on single cell level. To assess if the SinR mutations in the different suppressor influence protein stability or if the other mutations indirectly affect SinR protein amounts Western blot analyses were performed. As references for the characterization, the wild type GP1561 and the *ymdB* mutant strain GP1574 were used. As described for the NCIB3610 strain in chapter 4.1.2., the wild type strain **GP1561** formed thick and wrinkled pellicles on liquid MSgg biofilm medium and wrinkled colonies on agar plates (see Fig. 4.9A). Observation of the colony with a fluorescence stereo microscope revealed a strong expression of the biofilm reporter fusion (P_{tap}-*yfp*) and a weak expression of the motility reporter fusion (*hag-cfp*) that was only slightly more intense than the fluorescence observed for a wild type strain without a *cfp*-reporter fusion (results not shown). This suggests high levels of CFP auto-fluorescence on colony level. On single cell level, the wild type strain showed bistable expression of biofilm and motility genes. Chains of elongated cells expressed matrix genes, whereas shorter single cells expressed motility genes. In contrast, the *ymdB* deletion strain **GP1574** did not form a pellicle on top of liquid MSgg medium and also the colonies appeared smooth and unstructured. On colony level, no expression of biofilm genes was visible but a strong expression of motility genes could be observed. Supporting previous results (Diethmaier *et al*., 2011) also no expression of biofilm genes was detected using single cell fluorescence microscopy. All cells expressed motility genes and were relatively short. Moreover, no cell chains appeared as it was described for the wild type strain, indicating expression of autolysis genes in the *ymdB* mutant.

The suppressor mutant **GP1649** carrying a mutation that leads to a SinR Trp104Arg protein variant, showed a similar phenotype as the wild type strain. The suppressor mutant also forms stable pellicle and structured colonies with a rough surface. However, the characteristic wrinkles of the wild type colony were not visible. Furthermore, colonies showed strong expression of biofilm and weak expression of motility genes. On single cell level, bistable expression of biofilm and motility genes could be observed, which is characteristic for the wild type strain. The SinR protein amounts in this suppressor mutant were comparable to the *ymdB* mutant strain, indicating that the Tyr104Arg mutation influences only the properties of the SinR protein and thereby restores expression of biofilm genes in the *ymdB* mutant. However, the further role of this specific amino acid needs to be further studied. Colledge *et al.* (2011) propose that amino acid 104 is part of SinR's SinI binding domain, but in the structural data of Newman *et al*. (2013) this specific residue is not required for SinR-SinI interaction. Interestingly, this suppressor mutation was isolated quite frequently by Kruse (2013) from different *ymdB* deletion strains. Another mutation in SinR that was identified frequently led to an exchange of alanine 85 to threonine. As an example for a suppressor mutant that harbors this kind of mutation, strain **GP1650** was studied in detail (see Fig. 4.9B). As shown for strain GP1649, the Ala85Thr mutation restored stable pellicle and complex colony formation in the *ymdB* mutant GP1574. Furthermore, fluorescence microscopy revealed expression of biofilm and motility genes as described for the wild type strain.

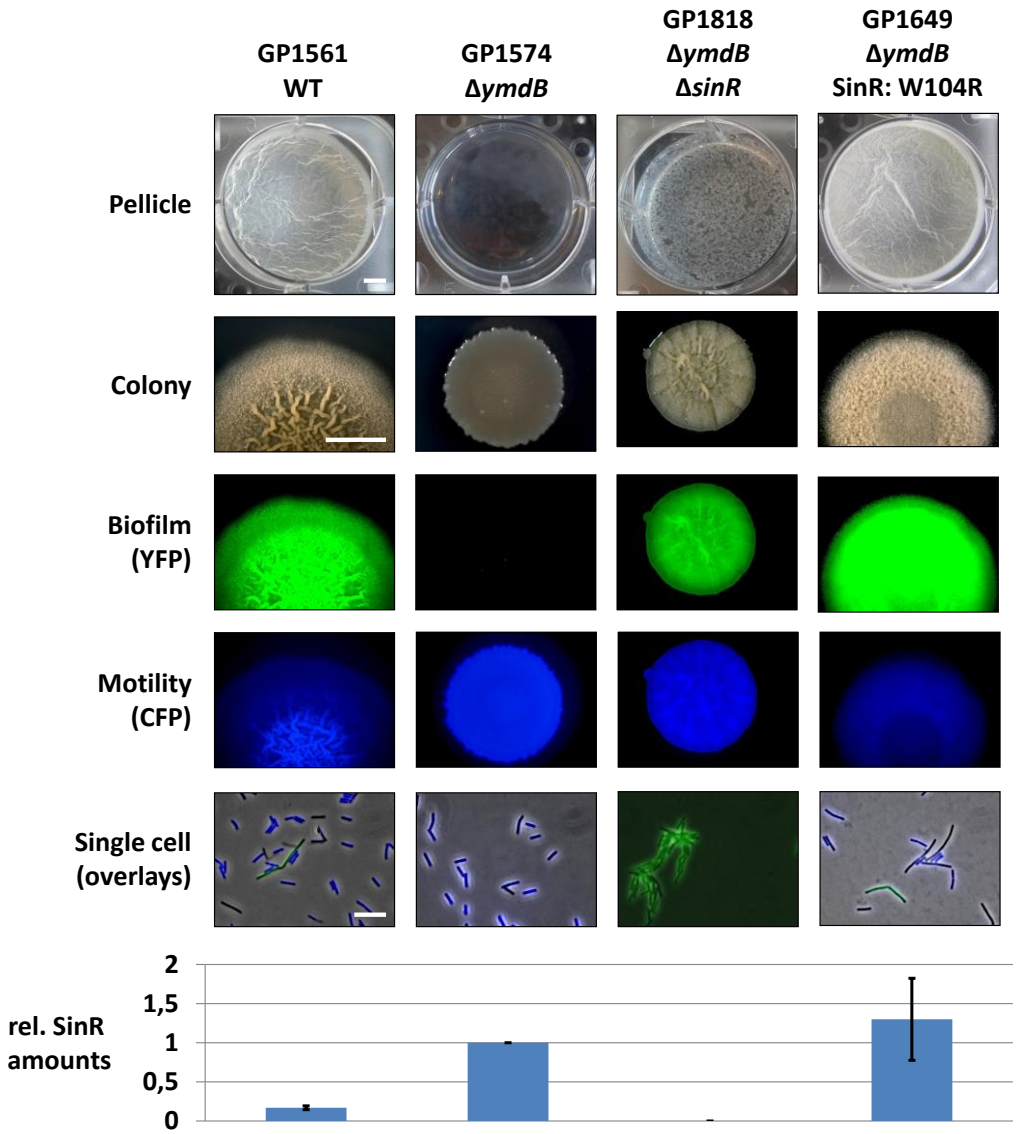

Figure 4.9(A). Characterization of *ymdB* suppressor mutants. All strains harbor P_{tapA}-*yfp* biofilm (green) and *hag-cfp* motility (blue) fluorescence reporter fusion. The suppressor mutant GP1649 was derived from the parental strain GP1574. Complex colony and pellicle formation was monitor on MSgg agar plates or with liquid MSgg medium. Fluorescence signals of the complex colonies were detected with an exposure time of 1.5 sec with the respective filter set. For the YFP signal of the strain GP1818 the exposure time was reduced (auto exposure) due to a very strong signal. Bars, 5 mm. The single cell images are overlays of the images for transmitted light (grey) and the images for the reporter fusions. Cells were cultivated in LB medium until mid-exponential growth phase and images were taken with an exposure time of 1.5 sec. Bars, 10 µm. The bar chart shows the densitometry ratios of the SinR protein amounts (divided by HPr). The values were normalized so that the strain GP1574 had a value of 1. Error bars represent the standard deviation of three replicate Western blots.

Looking at single level, several elongated cells building up chains but also some smaller cells were visible. Some of the elongated cells showed expression of biofilm genes, while the shorter cells expressed motility genes.

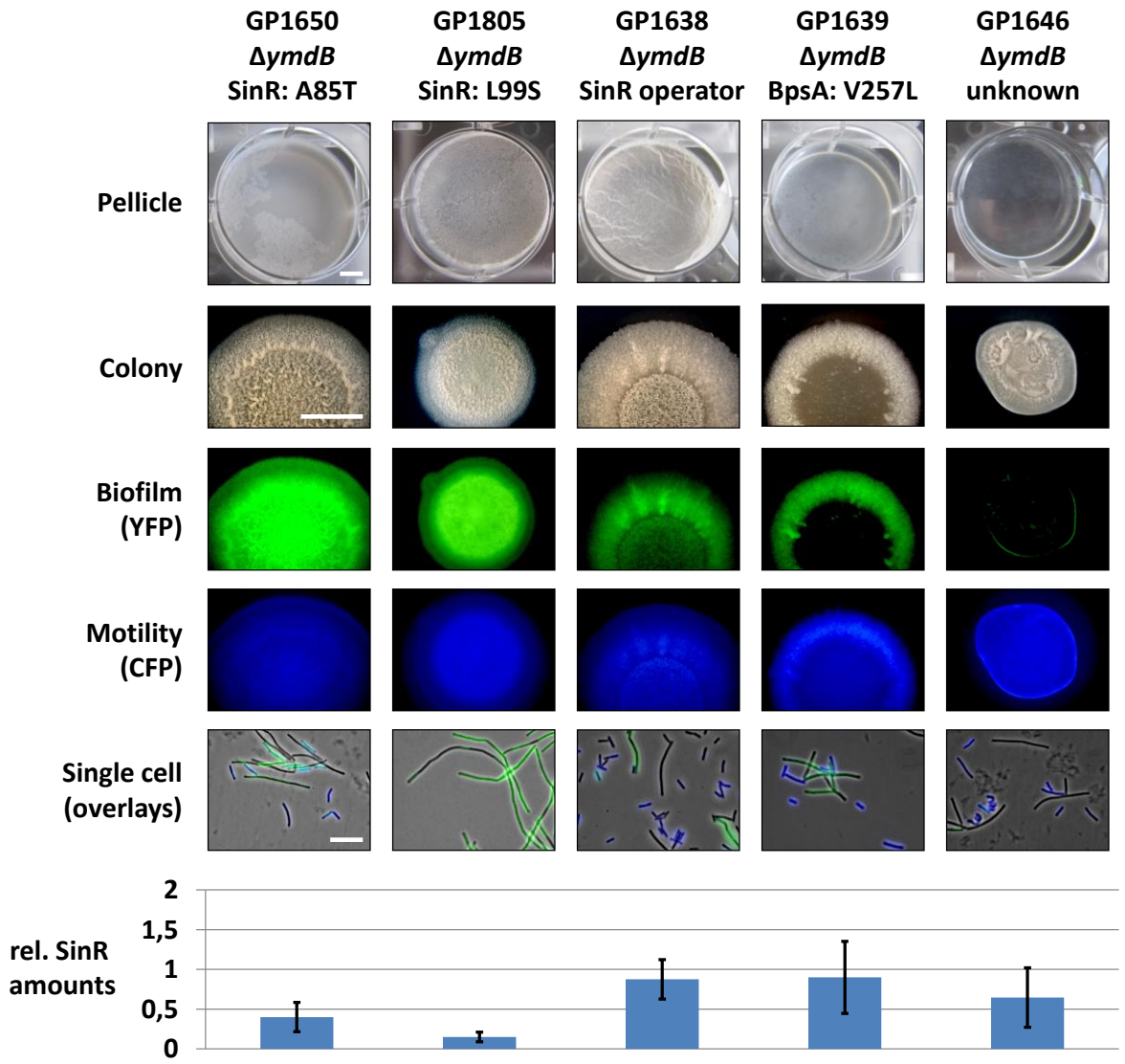

Figure 4.9(B). Characterization of *ymdB* suppressor mutants. All strains harbor P_{tapA}-*yfp* biofilm (green) and *hag-cfp* motility (blue) fluorescence reporter fusion. The suppressor mutants GP1638, GP1639, GP1646 and GP1650 were derived from the parental strain GP1574. For the YFP signal of the strain GP1805 the exposure time was reduced (auto exposure) due to a very strong signal. Compare Fig. 4.8(A) for a detailed description.

This indicates that the Ala85Thr mutation of the SinR affects bistable gene expression. However, SinR protein amounts were similar to the one in the *ymdB* mutant and higher than in the wild type strain. Therefore, it is likely that Ala85Thr mutation in the multimerization domain of SinR affect SinR-tetramer formation or interaction with its antagonist as also concluded by Chai *et al*. (2010b).

A third type of *ymdB* suppressor with a mutated SinR protein is the strain **GP1805** that carries a Leu99Ser amino acid exchange. This strain shows slightly smaller colony as shown for the Δ*ymdB* and the Δ*ymdB* Δ*sinR* mutant but the colonies exhibited a rough and structured surface. Also, this mutation restored pellicle formation in the *ymdB* deletion background. Moreover, the strain showed a very high expression of biofilm genes on colony level (shorter exposure time used to avoid overexposed pictures) and only a weak signal for the CFP motility reporter gene. In addition, single

cell fluorescence microscopy revealed that the cells are highly elongated, build up cell chains and strongly express biofilm genes but no motility genes. This nicely fits the phenotype of the Δ*ymdB* Δ*sinR* mutant strain GP1818, except that the cells of the suppressor mutant GP1805 are longer. In accordance, SinR densitometry also revealed that SinR protein amounts are decreased in the strain GP1805, indicating that the Leu99Ser mutation in SinR affects protein stability.

Besides the Δ*ymdB* suppressor mutants that carry mutations in the *sinR* gene, three different types of suppressor mutants with (partially) restored biofilm biofilm matrix gene and bistabile expression of biofilm and motility genes could be identified. The suppressor mutant **GP1638** (mutation in the SinR operator between the *epsA* and *slrR* genes, compare Fig. 4.10) and **GP1639** (BpsA: Val257Leu) showed a very similar phenotype.

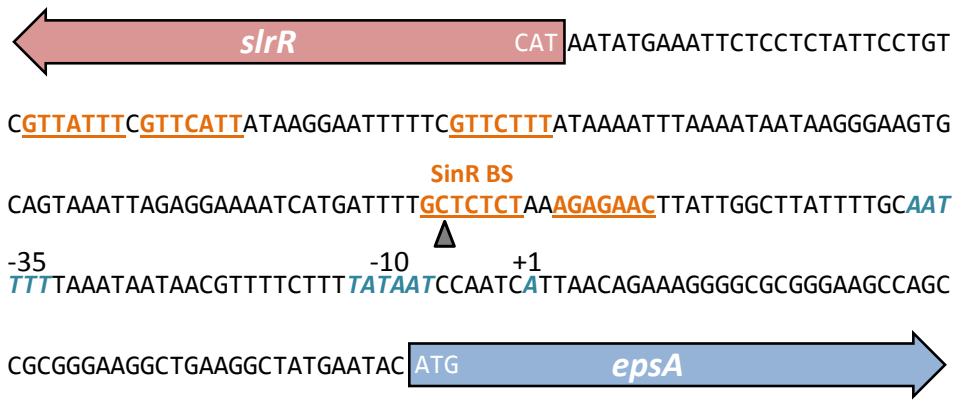

Figure 4.10. Mutation in the SinR binding sequence between the *slrR* and *epsA* genes restores biofilm gene expression in the Δ*ymdB* suppressor mutant GP1638. The location of the mutations (T→C) is marked with a triangle. The binding sequences of the SinR proteins are underlined. The promoter sequence and the transcription start of the *epsA* gene are in italics.

Both suppressors formed stable pellicles and structured colonies on agar plates but lacked the strongly wrinkled inner region of the colony. However, the pellicles of strain GP1639 appear thinner than the ones of GP1638 and the inner part of GP1639 colonies appeared rather shiny as the surface of the Δ*ymdB* mutant than rough as the respective part of GP1639 colonies. This observation was also reflected by the expression of the YFP biofilm gene reporter fusion on colony level. The whole colony of strain GP1638 expressed biofilm genes, whereas colonies of strain GP1639 only expressed biofilm genes in the outer region of the colony. In addition, both strains showed weak expression of the motility reporter fusion. On single cell level, both strains showed restored expression of biofilm genes compared to the *ymdB* mutant strain. In addition, small motility gene expressing cells and elongated biofilm gene expressing cells could be obtained. Furthermore, SinR protein amounts in both suppressors were not affected. Compared with all other suppressor mutants, the strain **GP1646** is very unique. Cells of this strain form no pellicle as it is typical for the Δ*ymdB* mutant but colonies appear more structured than Δ*ymdB* mutant colonies and the colony surface appears rather mucoid

than rough. Biofilm gene expression on colony level is only visible on the very edge, while motility genes seem to be weakly expressed all over the colony. On single cell level short and elongated cells are visible. Some of the short cells express motility genes as it was observed for the wild type strain. However, biofilm gene expression is hardly detectable because only very few cells show fluorescence when excited with light of the respective wavelength for YFP. As shown for the suppressors GP1638 and GP1639, SinR protein amounts are comparable to amounts in the *ymdB* mutant strain GP1574. Unfortunately, it remains unclear which mutation is responsible for the observed phenotype.

4.2.3. Overexpression of RNase Y in the *ymdB* deletion mutant does not restore complex colony structure

The gene for the YmdB protein is located in one operon downstream of the *rny* gene which encodes the major *B. subtilis* endoribonuclease RNase Y. Furthermore, it was shown that RNase Y co-purifies with the YmdB protein suggesting a direct or indirect interaction and supporting the idea of a functional connection between the two proteins (Diethmaier, 2011). Interestingly, depletion of the expression of RNase Y stabilizes several transcripts including the one for the master regulator of biofilm formation SinR (Lehnik-Habrink *et al*., 2011b).

To test that the effect of RNase Y on *sinR* transcript stability influences biofilm formation, the authors overexpressed RNase Y from the plasmid pGP1201 and monitored complex colony formation in the background of the 168 wild type strain. Indeed, overexpression of RNase Y led to more wrinkled colonies supporting a role of RNase Y in control of biofilm formation (Fig. 4.11).

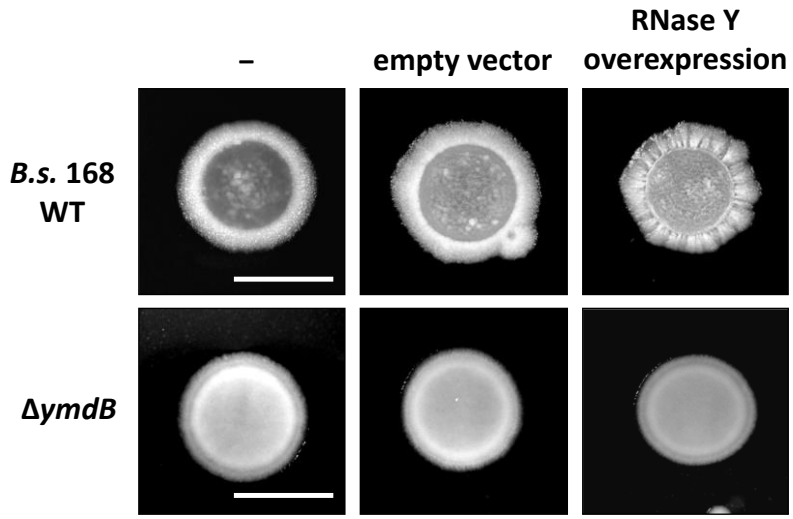

Figure 4.11. Overexpression of RNase Y does not induce complex colony structure in the *ymdB* mutant in contrast to the wild type strain. Complex colony formation of the *ymdB* mutant GP583 and the *B. subtilis* wild type 168 without a plasmid, containing the empty vector pBQ200 or the plasmid pGP1201 for RNase Y overexpression, respectively. Bars, 5 mm.

Assuming a functional connection between RNase Y and the YmdB protein in regulating biofilm formation, the effect of the overexpression of RNase Y should be different in the *ymdB* deletion mutant. To test this assumption, the *ymdB* deletion strain GP583 was transformed with the RNase Y overexpression plasmid pGP1201 and complex colony structure on erythromycin and lincomycin containing MSgg plates was analyzed. As a positive control the same procedure was performed for the 168 wild type strain in parallel. Indeed, overexpression of RNase Y did not induce complex colony formation in the *ymdB* deletion mutant, whereas the outer region of the wild type colony appeared more wrinkled upon RNase Y overexpression. This demonstrated that induced biofilm formation by RNase Y overexpression depends on the presence of the YmdB protein and suggests that both proteins have connected functions in controlling biofilm formation. To exclude that the presence of the overexpression plasmid had an effect on colony complexity the wild type and the Δ*ymdB* mutant strain were transformed with the empty plasmid pBQ200. Presence of the empty plasmid did not change the colony phenotype on biofilm agar plates (see Fig. 4.11).

4.2.4. YmdB is a RNA-binding protein

Regulation on post-transcriptional or translational level is a common mechanism to regulate protein amounts, for example by RNA-binding proteins that inhibit translation of the bound mRNA (Babitzke *et al*., 2009). As shown in chapter 4.2.1, the biofilm defect of the *ymdB* mutant is due to elevated SinR protein amounts compared to the wild type strain. Strikingly, microarray analysis revealed no difference in *sinR* mRNA levels between the two strains (Diethmaier *et al*., 2014). An attractive explanation for this observation is that SinR protein amounts are controlled on translational level. For instance, one could imagine that the YmdB protein binds the 5’ region of the *sinR* mRNA and thereby inhibits translation by blocking the Shine-Dalgarno sequence or serves as a road block for the ribosome. To test YmdB binding ability to *sinR* mRNA *in vitro* electrophoretic mobility shift assays (EMSAs) were performed. For this purpose, *E. coli* BL21 was transformed with the *Strep*-YmdB expression plasmid pGP1917. Cells were cultivated in LB medium and expression of the recombinant protein in the heterologous host was induced by addition of IPTG (for further information compare Lockhorn, 2014). The YmdB protein was then purified from the cell extract via its *Strep*-tag as described in chapter 3.3.10. In parallel, the first 200 ribonucleotides of the *sinR* transcript were amplified by *in vitro* transcription. A rather short fragment was chosen to ensure optimal shifting ability that can be impaired when using longer fragments. For the EMSA purified YmdB protein was mixed with *sinR* mRNA and loaded on a native polyacrylamide gel. After electrophoresis, RNA was detected by staining with ethidium bromide. If the YmdB protein binds to *sinR* mRNA, the RNA runs slower through the gel and a second band that runs higher (corresponding to the YmdB-*sinR* RNA complex) can be detected in the gel.

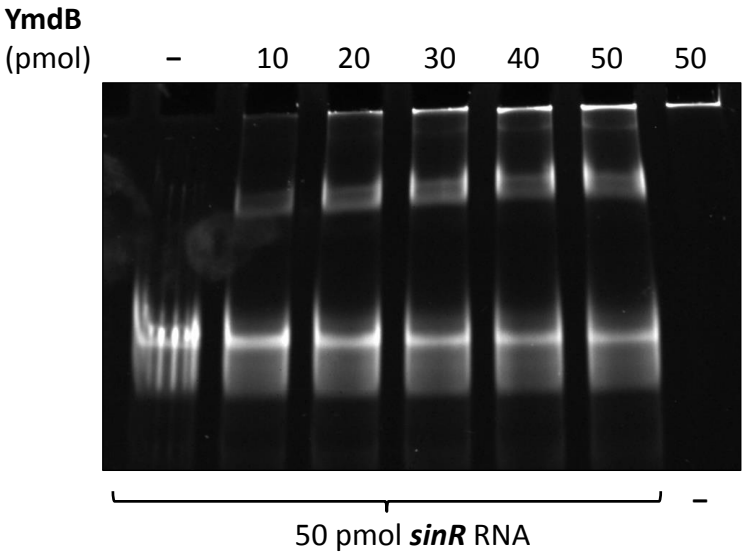

Figure 4.12. *Strep*-YmdB binds *sinR* RNA *in vitro*. Electrophoretic mobility shift assay to determine the RNA-binding ability of the YmdB protein to *sinR* RNA. The first 200 bp of the *sinR* transcript were produced by *in vitro* transcription and incubated with increasing concentrations of *Strep*-YmdB purified from *E. coli* BL21.

As shown in Fig. 4.12, incubation of the *sinR* RNA with purified YmdB protein led to the formation of a second band that ran slower through the polyacrylamide gel, whereas the *sinR* RNA without the protein showed only the lower RNA-specific band. This suggested that the YmdB protein can bind to the first 200 ribonucleotides of the *sinR* transcript. To exclude that the purified YmdB protein contains any RNA contamination the protein was applied on the gel without RNA. In the respective lane no RNA was detectable.

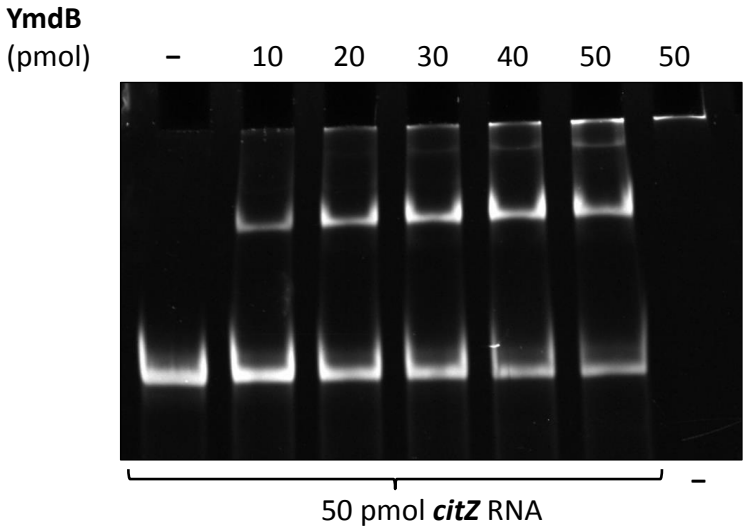

Figure 4.13. *Strep*-YmdB binds *citZ* RNA *in vitro*. Electrophoretic mobility shift assay to determine the RNA-binding ability of the YmdB protein to *citZ* RNA as a negative control. The first 200 bp of the *citZ* transcript (5' UTR) were produced by *in vitro* transcription and incubated with increasing concentrations of *Strep*-YmdB purified from *E. coli* BL21.

To test if the binding of the YmdB protein to the *sinR* transcript is specific, the first 200 ribonucleotides of the *citZ* transcript were amplified and incubated with the YmdB protein as described before (Pechter *et al*., 2013). Incubation of the *citZ* RNA with the YmdB protein also retarded the migration of the RNA trough the gel (see Fig. 4.13).

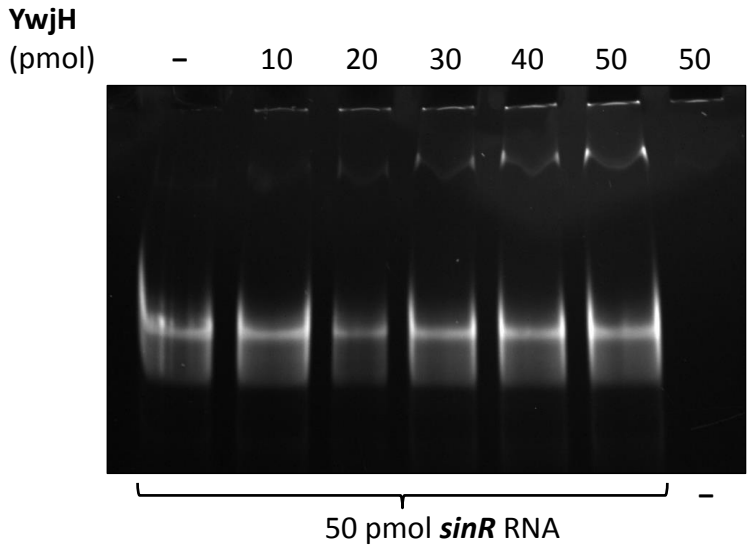

Figure 4.14. *Strep*-YwjH does not bind *sinR* RNA *in vitro*. Electrophoretic mobility shift assay with *sinR* RNA and YwjH as a control protein to determine the specificity of the YmdB binding to *sinR* RNA. The first 200 bp of the *sinR* transcript were produced by *in vitro* transcription and incubated with increasing concentrations of *Strep*-YwjH purified from *E. coli* BL21.

This indicates that the YmdB protein binds RNA unspecifically. Furthermore, the *Strep*-tagged transaldolase YwjH was expressed in BL21 from the plasmid pGP819. The purified protein served as a control that *sinR* RNA does not interact with proteins in general or the *Strep*-tag used for protein purification. The results of the EMSA with YwjH and the *sinR* transcript are depicted in Fig. 4.14.
In this case, addition of the *Strep*-YwjH to the *sinR* RNA did not lead to retardation of the *sinR* RNA. This further supports the idea that YmdB is a RNA binding protein and shows that the *sinR* RNA does not bind to proteins unspecifically.

***In vivo* co-purification experiments**

The EMSAs could show that the YmdB protein binds RNA *in vitro*. However, no specificity towards a particular RNA was visible. Therefore, we wondered if this is different *in vivo*. To search for specific YmdB-RNA interactions the *ymdB* deletion strain GP583 was transformed with the plasmid pGP1920. This plasmid allows overexpression of *Strep*-tagged YmdB protein that carries an E39Q amino acid exchange within the active center. The YmdB E39Q protein variant is enzymatically inactive (Diethmaier *et al.*, 2014) but still binds RNA *in vitro* (results not shown). Using this protein for RNA co-purification experiments ensured that bound RNA is not subject to any degradation by YmdB. The *ymdB* deletion strain GP583 harboring the overexpression plasmid was cultivated in CSE-Glc medium as described for the SPINE method in chapter 3.3.10. To detect transient YmdB-RNA interactions formaldehyde was used to cross-link interactions. After purification of *Strep*-YmdB from the cell extract, the RNA in the elution fraction (E2) was isolated. Then, drops of the total RNA in solution were placed on a nylon membrane. Subsequently, particular RNAs were detected by hybridizing with specific DIG-labelled RNA probes and detection with DIG-antibodies (Roche).

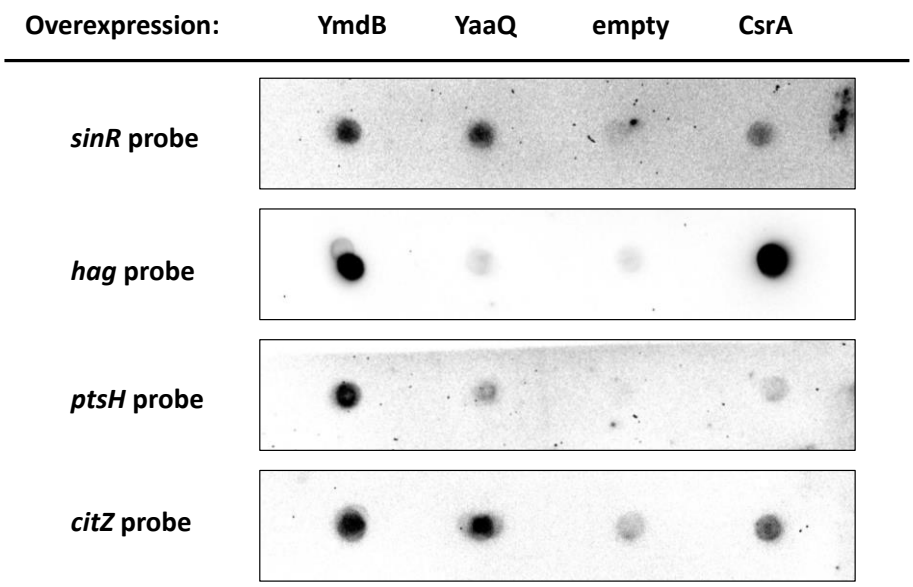

Figure 4.15. YmdB-RNA co-purification experiments. Dot blot analysis of RNA precipitated from the elution fractions of the purifications of *Strep*-tagged YmdB, YaaQ and CsrA variants from *B. subtilis*. The c-di-AMP binding protein YaaQ served as a negative control, the *hag* RNA-binding protein CsrA was used as a positive control. In addition, an empty vector control was used to test unspecific binding to the *Strep*-tactin matrix. Each dot represents 20 µl of RNA solution isolated from the respective purification dropped on a nylon membrane in 2 µl steps.

As a control the *csrA* deletion strain GP469 harboring the *Strep*-CsrA overexpression plasmid pGP381 was employed. The CsrA protein regulates flagellin synthesis on translational level by binding to the flagellin encoding *hag* mRNA. Therefore, CsrA is an excellent positive control because it specifically binds *hag* mRNA. Moreover, it can easily be used as a negative control to exclude unspecific binding of certain RNAs, in this case *sinR* mRNA. Experimentally, *sinR* and *hag* probes were applied to detect the respective RNAs within the elution fractions of the two purifications. To exclude the unspecific binding of unrelated RNAs probes for the detection of the first 200 bp of the highly expressed *ptsH* and *citZ* transcripts were used. In addition, RNA from the *ymdB* deletion strain GP583 containing the empty plasmid pGP380 and the *yaaQ* (*darA*) deletion strain GP1712 overexpressing a *Strep*-tagged YaaQ protein (pGP2603) was detected with the same probes. As shown in Fig. 4.15, the *hag* transcript was enriched within the total RNA of the elution fraction from the CsrA overexpression indicating that the method allows identification of specific RNA-protein interactions. Moreover, the *hag*, *sinR*, *citZ* and *ptsH* transcripts were not enriched in the RNA from the elution fraction of the empty vector control. Next, the elution fraction from the YmdB purification was tested for the presence of the four transcripts. Strikingly, the *sinR* transcript as well as the three control transcripts could be detected with about the same intensity within the total RNA from the elution fraction. In agreement to the *in vitro* experiments (EMSAs), this shows that YmdB binds RNA unspecifically.

However, the *sinR* and the *citZ* transcripts were also detectable within the total RNA isolated from the elution fraction of the purification of the c-di-AMP binding protein YaaQ. This protein most likely does not bind RNA. Therefore, the method comprises the unspecific co-purification of RNA probably due to cross-linking with formaldehyde during cultivation. To further study if YmdB binds the e. g. *sinR* RNA specifically *in vivo* it would be useful to repeat the experiments without cross-linking.

4.2.5. Global and high-resolution analysis of the transcriptome in the *ymdB* deletion mutant by RNA sequencing

RNA sequencing is a powerful tool to globally study changes in gene expression on transcript level. In addition, this method enables the identification of RNA turnover intermediates and minor RNA processing events at the 5' or 3' end of an mRNA. For example, by applying RNA sequencing Liu *et al*. (2014) identified the *cggR* transcript as a target for 3'-5' processing by the polynucleotide phosphorylase PNPase. As hypothesized before (see 4.2.4.), the YmdB phosphodiesterase might be involved in processing of the *sinR* mRNA on a level that is not detectable by qRT-PCR or microarray analysis because only few ribonucleotides, e.g. containing the ribosome binding site, are cleaved off. This would inhibit translation of the mRNA and explain elevated protein amounts of the master regulator for biofilm formation SinR in the *ymdB* deletion strain. Moreover, this could explain why the enzymatic function of the phosphodiesterase and putative RNase YmdB is required for expression of biofilm matrix genes and complex colony formation (Diethmaier *et al*., 2014).

To analyze the *sinR* transcript on single ribonucleotide level by RNA sequencing, the strain GP969 encoding an enzymatically inactive YmdB protein and, as a reference, the isogenic wild type strain GP966 were cultivated in LB medium until they reached an OD_{600} of 2.5. From these cells total RNA was isolated and the overexpression of the *hag* gene and decreased expression of *slrR* and the *tapA* gene was confirmed by qRT-PCR. Moreover, elevated SinR protein amount were confirmed within total protein extract via Western blotting as described in 4.2.1 (compare Fig. 7.1). The remaining RNA was sent for RNA sequencing to the "Göttingen Genomics Laboratory" (G2L).

The resulting data were analyzed with the TraV transcriptome browser (Dietrich *et al*., 2014). This browser allows visualizing the abundance of specific transcripts (cDNA reads) mapped to a reference genome. In Fig. 4.16 the abundance of the transcripts of the *sinI-sinR* region in the *ymdB* mutant strain GP969 and the wild type strain GP966 are compared. Interestingly, *sinI* transcript amounts are about 2-fold lower in the *ymdB* mutant than in the wild type strain. For the *sinR* transcript no difference in transcript abundance and length was detectable. This underlines that changes in *sinR* transcript abundance do not cause elevated SinR protein amounts in the *ymdB* mutant and is contradictory to our initial hypothesis that the YmdB protein performs minor 5' or 3' processing of the *sinR* mRNA. This suggests that YmdB influences SinR protein amounts indirectly, e. g. on the level of protein stability.

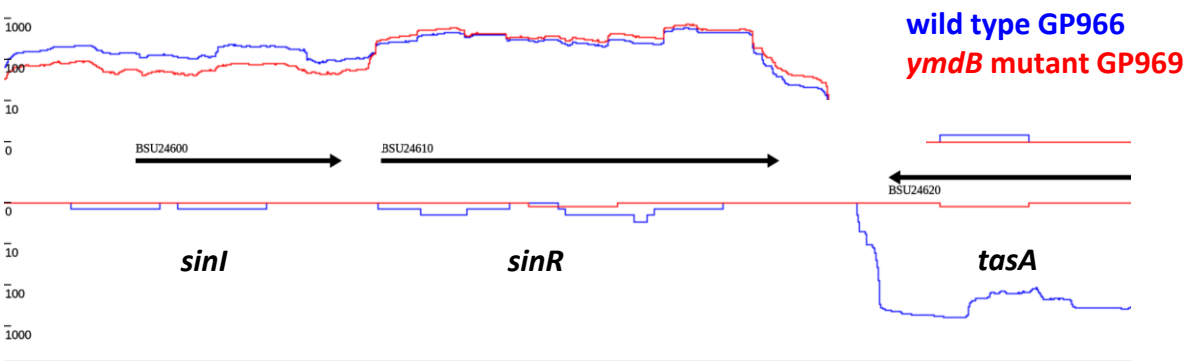

Figure 4.16. Strand-specific visualization of the RNA sequencing data of the *sinI-sinR* region with the TraV transcriptome browser. The blue line represents the transcript abundance (transcribed to cDNA) of wild type strain GP966 and the red line that for the *ymdB* mutant strain GP969 mapped to the genome of *B.s*. 168.

Thus, it was hyphotesizes that the YmdB protein indirectly influences SinR protein amounts by affecting the stability of transcripts encoding proteins involved in proteolysis. To test this assumption the abundance and length of transcripts for proteolysis proteins of the *ymdB* mutant GP969 and the wild type strain GP966 was compared in the TraV transcriptome browser. An overview of the addressed transcripts and their fold changes is shown in Tab. 7.8. Interestingly, the transcript for the ClpX protease subunit was slightly more abundant in the *ymdB* mutant than in the wild type strain. Furthermore, the 5' untranslated region of the *clpX* transcript was truncated in the *ymdB* mutant compared to the wild type (see Fig. 4.17).

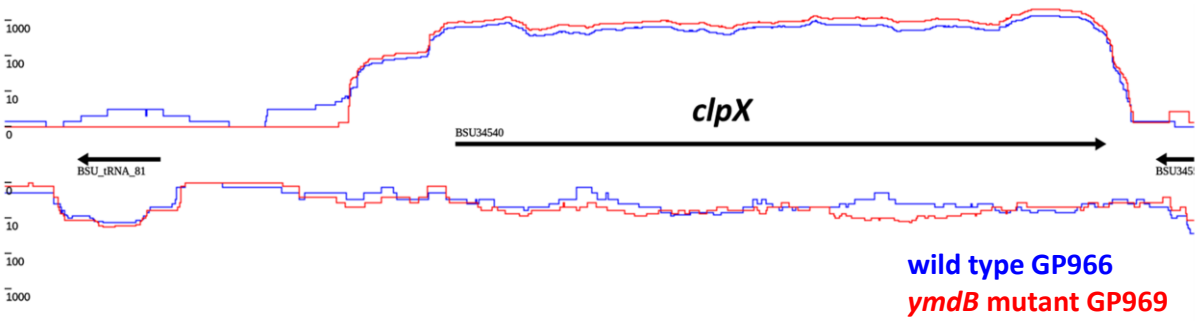

Figure 4.17. Strand-specific visualization of the RNA sequencing data of the *clpX* region with the TraV transcriptome browser. The blue line represents the transcript abundance (transcribed to cDNA) of wild type strain GP966 and the red line that for the *ymdB* mutant strain GP969 mapped to the genome of *B.s*. 168.

This indicates that processing of the 5' region in the *ymdB* protein is not functional and suggests a protective function of the YmdB protein or an indirect effect on transcriptional level due to

inactivation of YmdB. Since the 5' region of mRNAs is often required for the regulation of translation initiation (Soper *et al*., 2010; Lay *et al*., 2013), a processing event might affect the abundance of the ClpX protein. However, the RNA sequencing results have to be reproduced in order to draw reliable conclusions.

4.2.6. C-di-GMP and its influence on biofilm formation in *B. subtilis*

C-di-GMP is a well-known regulator of cell differentiation in many Gram-negative bacteria like *E. coli* and the facultative human pathogen *P. aeruginosa* where it is important for the regulation of biofilm formation and switching between motile and sessile life styles (Hengge *et al.*, 2009). The role of c-di-GMP in Gram-positive bacteria is far less studied. At the beginning of this study, there was only one study about the role of c-di-GMP in *B. subtilis* (Chen *et al*., 2012). The authors identified four putative diguanylate cyclases (DGCs) due their characteristic GGDEF motif (YdaK, YhcK, YtrP, YybT), the YkoW protein that might function as a diguanylate cyclases or as a phosphodiesterase due to a GGDEF and a EAL domain, and the two putative phosphodiesterases YkuI and YuxH containing a EAL domain. To test if c-di-GMP is involved in the control of biofilm formation and motility in *B. subtilis* the authors constructed deletion mutants of the respective genes.

Interestingly, they identified the PilZ domain containing protein YpfA as a c-di-GMP binding protein and proposed a c-di-GMP signaling pathway that controls motility but does not affect biofilm formation. However, the authors failed to delete the *ydaK* gene and hence no mutant lacking all known DGCs was tested for biofilm formation. Moreover, only the phenotype of the mutants was studied but c-di-GMP levels were not determined. Therefore, mutants lacking all putative DGCs (Δ*ydaK* Δ*ytrP* Δ*yybT* Δ*yhcK* Δ*ykoW*) and PDEs (Δ*yuxH* Δ*ykuI* Δ*ykoW*) were constructed and c-di-GMP levels in this mutant were determined by HPLC-MS/MS, respectively. Since the YkoW protein might function as a DGC or as a PDE the respective gene was deleted in both strains. In addition to the measurements, biofilm formation of the mutants was tested.

Moreover, previous experiments (Diethmaier, 2011) revealed decreased c-di-GMP concentrations in the Δ*ymdB* mutant strain. A possible explanation could be overexpression of the phosphodiesterases YuxH and the putative phosphodiesterase YkoW (contains DGC and PDE domain) in the *ymdB* mutant as microarray data suggest (Diethmaier *et al*., 2014). Therefore, we constructed a strain lacking all putative PDEs in the *ymdB* deletion background and monitored biofilm formation.

Loss of all diguanylate cyclases and phosphodiesterases affects c-di-GMP homeostasis

To determine c-di-GMP levels in the strain GP1598 lacking all DGCs and in the strain GP1599 lacking all known phosphodiesterases, the cells were cultivated in CSE-Glc minimal medium to mid-exponential growth phase. The construction of the used strains was described in detail by Blötz (2013). The isolation of c-di-GMP from cell extract was performed accordingly to 3.3.13. As shown in

Fig. 4.18, the deletion of all known DGCs in strain GP1598 (Δ*ydaK* Δ*ytrP* Δ*yybT* Δ*yhcK* Δ*ykoW*) totally abolished production of c-di-GMP suggesting that there are no further c-di-GMP producing enzymes in *B. subtilis* than the deleted ones. Moreover, the c-di-GMP concentration in the PDE deletion strain GP1599 (Δ*yuxH* Δ*ykuI* Δ*ykoW*) elevated c-di-GMP concentration compared to the wild type strain 168.

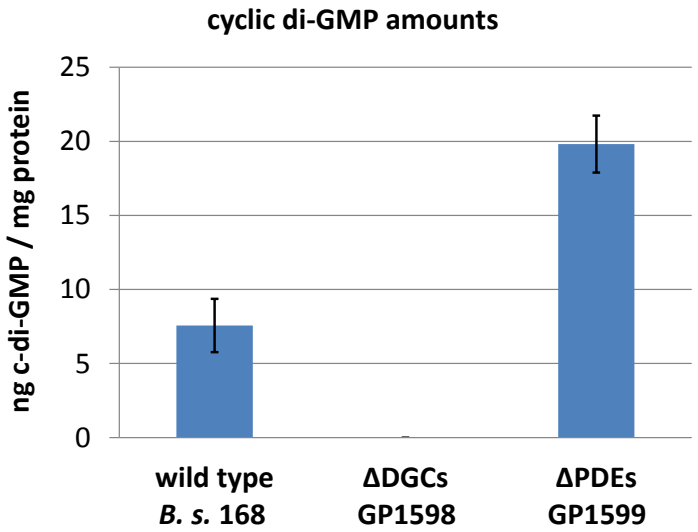

Figure 4.18. Deletions of diguanylate cyclases (DGCs) and phosphodiesterases (PDEs) affects cyclic di-GMP amounts. Bars show the mean of three biological replicates as c-di-GMP amounts in ng c-di-GMP normalized by the total protein content in mg. Error bars indicate the standard deviation.

In summary, simultaneous deletion of the known DGCs or PDEs can abolish or increase c-di-GMP concentration in *B. subtilis*, respectively. This supports the idea of a functional c-di-GMP signaling pathway proposed by Chen *et al*. (2012). Interestingly, Gao *et al.* (2013) were able to characterize the proteins YtrP, YhcK and YkoW as DGCs and YuxH as a PDE supporting our observation that deletion of the respective genes influences c-di-GMP homeostasis. Unfortunately, this work was published shortly after this project was totally completed.

Complex colony and pellicle formation

In contrast to the work of Chen *et al.* (2012) we were able to delete all putative DGCs in strain GP1598 and showed that this strain produces no c-di-GMP anymore. To test the hypothesis that changes in c-di-GMP levels influence biofilm formation in general and that elevated c-di-GMP levels in the Δ*ymdB* mutant can complement the biofilm defect of the mutant, biofilm tests were performed. Looking at colony and pellicle structure of the c-di-GMP defective mutant GP1598 and the overexpressing mutant GP1599, no changes in colony structure and stable pellicle formation could be observed compared to the wild type. All colonies showed a rough but unwrinkled surface as typical for the *B. subtilis* 168 laboratory strain and pellicles were stable but unstructured (Fig. 4.19A). Also, the simultaneous deletion of PDEs in the Δ*ymdB* mutant did not rescue the biofilm defect. The Δ*ymdB* mutant strain GP583 and the *ymdB* PDEs deletion strain GP1595 (Δ*ymdB* Δ*yuxH* Δ*ykuI* Δ*ykoW*), were both not able to form a pellicle and colonies appeared smooth and unstructured as typical for the Δ*ymdB* mutant (Fig. 4.19B).

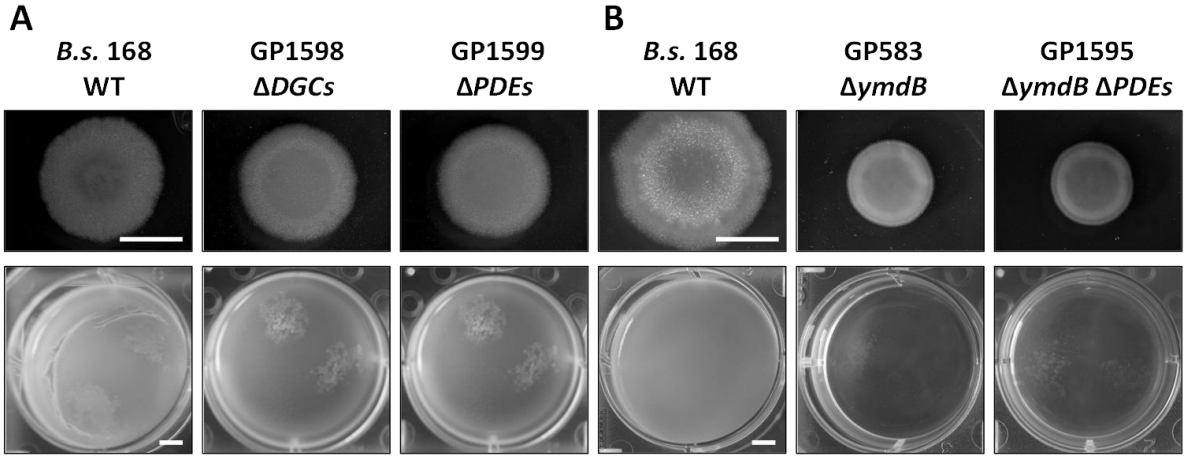

Figure 4.19. Simultaneous deletion of all diguanylate cyclase or phosphodiesterases has no effect on biofilm formation, respectively (A). Deletion of all phosphodiesterases in the Δ*ymdB* mutant does not restore biofilm formation (B). All strains used in this biofilm assays are derivatives of the *B. s.* laboratory wild type strain 168**.** Minor differences between the phenotypes of the wild type in A and B are due to different cultivation temperatures (room temperature). Bars, 5 mm.

This implies that decreased c-di-GMP levels in the Δ*ymdB* mutant and the biofilm defect are just a non-functional correlation. *In toto*, changes in c-di-GMP concentration do not affect biofilm formation in the Gram-positive model organism *B. subtilis* although this second messenger is important for regulation of biofilm formation in Gram-negative bacteria.

5. Discussion

Many bacteria depend on their ability to live together as multicellular communities in order to survive under harsh environmental conditions. In these communities, also referred to as biofilms, cells are embedded within a self-produced extracellular matrix that is mainly composed of polysaccharides and proteins (Hall-Stoodley *et al*., 2004). This matrix enables the cells to cover a solid surface or to float as a community and can protect them from harmful environmental substances such as antibiotics or from predators. Additionally, biofilm or matrix production can function as a virulence factor, as described for the genetic disorder cystic fibrosis that goes along with colonization of the lung by a *P. aeruginosa* biofilm (Costerton *et al*., 1999). In general, up to 80% of human bacterial infections are related to biofilm formation underlining the importance of research on biofilms (Römling & Balsalobre, 2012). In this work, the Gram-positive soil bacterium *B. subtilis* was chosen as a model system to study the control of biofilm formation and cell differentiation. During this work, it was demonstrated that tyrosine kinases are absolutely required for biofilm formation and exopolysaccharide production and that their activity depends on their cognate modulator proteins. Furthermore, elevated protein amounts of the SinR regulator protein in the biofilm-defective *ymdB* mutant were identified as the cause of the defect. Interestingly, this defect was repaired in spontaneously arising suppressor mutation within e.g. the *sinR* gene.

5.1. The story behind the biofilm and cell differentiation defect of the *ymdB* mutant

Despite intense investigation of the molecular function of the YmdB protein in controlling biofilm formation, the target of YmdB could not be identified. Since the phosphodiesterase activity of YmdB is essential for biofilm formation, the target needs to contain a phosphodiester bond as it can be found in several different molecules such as DNA, RNA, cyclic nucleotides, cyclic dinucleotides and in phospholipids. Therefore, searching for YmdB processing targets is a challenging task.

How does loss of YmdB increase SinR protein amounts?

Loss or inactivation of the YmdB phosphodiesterase drastically reduces biofilm matrix production and inhibits bistable expression of biofilm and motility genes as it is characteristic for *B. subtilis* wild type cells. To address this strong phenotype, e.g. transcriptome levels were studied on global scale to identify novel factors and gain insight how the YmdB phosphodiesterase controls cell differentiation mechanistically. However, the mechanism of YmdB action is still not fully understood (Diethmaier *et al.*, 2011 & 2014). This works adds another piece to the “puzzle of YmdB function” by demonstrating that elevated amounts of the master regulator of biofilm formation SinR explain the biofilm and cell differentiation defect. Therefore, the action of YmdB seems to be closely connected

to the production or stability of the SinR regulator. However, the target of the YmdB protein is still unknown and the final picture of the "puzzle of YmdB function" remains unclear.

Since there is no indication that *sinR* transcript amounts are affected by the loss of the YmdB protein, it appears very unlikely that YmdB is directly involved in the degradation of the *sinR* mRNA, e. g. in concert with the major endoribonuclease RNase Y that is encoded in the same operon. Thus, it was hypothesized that YmdB might process the 5' (or even the 3') end of the *sinR* mRNA and thereby inhibits translation and synthesis of SinR protein, respectively (compare Lockhorn, 2014).

Specific processing of the 5' end of an mRNA without affecting overall transcript amounts/ stability has been barely described in literature. Nevertheless, the RegB endoribonuclease from *E. coli* cuts, not exclusively, but with high specificity within the ribosome binding site of certain T4 bacteriophage mRNAs (Uzan *et al*., 1988; Sanson & Uzan, 1993). Thereby it destabilizes the mRNAs of early phage genes, by providing processing targets for other RNases like RNase E and G. In contrast, mRNAs of late stage phage genes are not fully degraded by RNases but translation initiation from the mRNAs is impaired due to non-functional ribosome binding sites (Durand *et al*., 2012b). Similar processes have not been described in *B. subtilis* before and YmdB shows no homology to the RegB protein or any other endoribonucleases. Moreover, RNA sequencing of the *ymdB* mutant strain revealed no processing or stabilization of the 5' and 3' of the *sinR* transcript compared to the wild type strain. This excludes no modification of the 5' or the 3' end of the *sinR* transcript but opposes the idea of impaired translation initiation by processing of the ribosome binding site. Endonucleolytic processing of mRNAs by RNase E in *E. coli* is more efficient when the target RNA exhibits a monophosphorylated 5' end for endonuclease binding and subsequent processing (Mackie, 1998). Since processing of an mRNA by RegB results in a 5' OH-group any further efficient degradation by RNase E or G is impaired. Thus, In *E. coli*, the 5' end of the RegB processing product is phosphorylated by an enzyme called polynucleotide kinase/phosphatase to ensure efficient degradation (Durand *et al.*, 2012b).

Monophosphorylated 5' ends are also required for efficient endo- and exoribonucleolytic processing of mRNAs by RNase Y and RNase J1 in *B. subtilis* (Shahbabian *et al*., 2009; Mathy *et al*., 2007). Since mRNAs usually contain a triphosphate at the 5' end, Diethmaier (2011) hypothesized that YmdB might process the triphosphate end of certain mRNAs and generates monophosphorylated mRNA for further processing as it was described for the enzyme RppH (Richards *et al.*, 2011). Although such a pre-processing would explain why overexpression of RNase Y does not induce biofilm formation in the absence of YmdB (compare 4.2.3) such interplay on *sinR* mRNA processing is not supported by the RNA sequencing result that showed no effect on *sinR* transcript length or stability. Furthermore, the activity of the RppH RNA pyrophosphohydrolase is nucleotide specific and prefers a guanosine residue in the second position of the mRNA which is not the case for the *sinR* mRNA (Gaur *et al*., 1988; Hsieh *et al.*, 2013; Piton *et al.*, 2013). Deletion of the *B. subtilis* gene for RppH did not totally abolish pyrophosphohydrolase activity suggesting the presence of a functional homolog (Hsieh *et al.*,

2013). Therefore, it is possible that the YmdB protein shows this activity on other targets and thereby indirectly affects SinR protein amounts. However, initial tests for a pyrophosphohydrolase acivity of YmdB were negative (Diethmaier, 2011). Hence, it needs to be studied if the YmdB protein and RNase Y work together in the processing of certain target RNAs.

Small regulatory RNAs as the target molecules of the YmdB protein?

Electrophoretic mobility shift assays and co-purification experiments with YmdB showed that YmdB is a RNA binding protein. It is well-known that RNA binding proteins like CsrA from *B. subtilis* or *E. coli* can inhibit translation initiation by blocking the ribosome binding sites of their target RNAs. Although, this binding can stimulate RNA turnover, the proteins are not directly involved in processing (Romeo *et al*., 2013). Since the enzyme activity of YmdB is required to fulfill its function in the cell and the inactive enzyme still binds RNA (results not shown), the YmdB protein does not act by simply blocking the ribosome binding site of the *sinR* or other mRNAs.

Alternative molecules that can inhibit translation initiation are small (regulatory) RNAs. Similar to the CsrA proteins, small RNAs can also bind to the ribosome binding site of mRNAs and thereby inhibit translation initiation (Lay *et al*., 2013). Less often, small regulatory RNAs can even activate translation as e. g. described for the translation of the mRNA for the *E. coli* stress sigma factor RpoS. Upon their binding, inhibitory secondary structures within the 5’ untranslated region of the mRNA are resolved and translation can proceed (Soper *et al*., 2010; Lay *et al*., 2013). In *E. coli*, base-pairing of the small RNAs with the sequence of the target mRNA usually requires the RNA chaperone Hfq (Lay *et al*., 2013). If YmdB is involved in processing of a small regulatory RNA that directly regulates *sinR* mRNA translation, this RNA must have an activating effect. Otherwise elevated SinR protein amounts in the absence of YmdB are not reasonable. Alternatively, a recent study in *E. coli* suggests that anti-adaptor RNAs can counteract the degradation of regulatory RNAs by blocking their binding to adaptor protein that subject them to degradation by RNase E (Göpel *et al*., 2013). Thus, YmdB could also be involved in the processing of such an anti-adaptor RNA. Consequently, elevated amounts of the anti-adaptor RNA in an *ymdB* mutant would lead to increased amounts of the activating regulatory RNA and induce SinR expression. Since binding of small regulatory RNAs to the 5’ untranslated region of their target mRNA frequently involves the RNA chaperone Hfq, loss of Hfq should influence biofilm formation assuming *sinR* translation initiation is controlled by a small regulatory RNA. Interestingly, transcriptome analysis with a *B. subtilis hfq* deletion mutant revealed an up-regulation of genes from the GerE and ComK regulons for sporulation and competence genes, respectively (Hämmerle *et al*., 2014). Although, regulation of biofilm formation is closely connected to competence and sporulation, control of *sinR* mRNA translation involving Hfq appears unlikely. In general, the authors suggest a rather minor impact of *B. subtilis* Hfq on post-transcriptional regulation compared to *E. coli*, because the stability of only 6 out of more than 100 predicted small

regulatory RNAs was affected in the *hfq* deletion strain (Hämmerle *et al*., 2014). This suggests that small regulatory RNA based regulation is acchieved mainly without Hfq in *B. subtilis*, as also described for highly specific binding events in *E. coli* (Soper *et al*., 2010). In summary, direct (or indirect) regulation of SinR protein amounts by small RNA processing/ degradation by YmdB is an attractive idea. To further elucidate RNase activity of YmdB *in vitro* assays could be a first step.

Does the YmdB protein indirectly control proteolysis?

Since SinR protein amounts are elevated in the *ymdB* mutant while mRNA levels remain constant it seems likely that SinR protein amounts are regulated on post-translation level. Therefore, it is an attractive idea that SinR protein amounts are kept constant by proteolysis in wild type cells but (specific) proteolysis is impaired in the *ymdB* mutant. In general, protein degradation needs to fulfill two distinct functions: getting rid of the bulk of truncated and miss-folded proteins and controlling the amounts of certain proteins for regulatory reasons (Kirstein *et al*., 2009). In eukaryotes, protein degradation is performed by the interplay of the proteasome and SCF (Skp1, Cullin, F-box containing) complexes that poly-ubiquitinate certain proteins and thereby mark them for degradation. In this case the target specificity is mediated by the F-box protein that guides the complex to the degradation target (Laney & Hochstrasser, 2004).

Protein degradation in prokaryotes has been mainly studied in the model organisms *E. coli*, *B. subtilis* and *Caulobacter crescentus* (Battesti & Gottesman, 2012). In these organisms protein degradation is mainly performed by complexes of energy-dependent proteases of the AAA+ family and Hsp100/Clp proteins. These proteases complexes can be involved in general and in regulatory protein degradation at the same time. For example, in *B. subtilis* the ClpXP protease complexes degrade truncated SsrA-peptide labelled proteins that resulted from ribosome stalling on the mRNA (Wiegert & Schumann, 2001). In a so called *trans*-translation mechanism a tmRNA that serves as a transfer and a messenger RNA at the same time removes the stalled ribosome from the mRNA. This is accomplished by an initial incorporating an alanine residue and by encoding a Stop codon containing peptide (SsrA) tag that labels the truncated protein for degradation (Kirstein *et al*., 2009). In contrast, degradation of specific targets is usually mediated by adaptor proteins that, comparable to the F-box proteins in eukaryotes, bind to the target proteins and guide them to the Clp proteases (Kirstein *et al*., 2009; Battesti & Gottesman, 2012).

Effects of regulatory proteolysis of specific target proteins can be illustrated on the example of the ComK transcription factor for the expression of competence genes in *B. subtilis*. The ComK protein is degraded by the ClpCP protease complex during logarithmic growth. Degradation is mediated by the adaptor protein MecA that allows the assembly of the ClpCP complex and guides ComK to the protease complex (Turgay *et al.*, 1998; Prepiak & Dubnau, 2007). Upon amino acid starvation and high cell density, quorum-sensing signals are produced that lead to the expression of the anti-

adaptor protein ComS (Magnuson *et al*., 1994; Solomon *et al*., 1996; Lazazzera *et al*., 1997). This protein binds to MecA instead of ComK and relieves ComK from proteolysis allowing transcription of competence genes (Prepiak & Dubnau, 2007).

Assuming that the SinR protein is a target of specific regulatory proteolysis the question arises which protease acts on SinR and which adaptor protein mediates proteolysis. So far proteolysis of SinR has not been considered, although the regulatory pathways it acts in are well studied. Therefore, it seems unlikely that SinR protein amounts are changed drastically by proteolysis but it sounds reasonable that regulated proteolysis keeps SinR protein amounts constant to prevent unwanted cell differentiation processes. For instance, regulated proteolysis of the RpoS sigma factor has been described as a mechanism to reduce the noisiness of stress response induction in addition to regulation by a negative feed-back loop on transcriptional level (El-Samad *et al*., 2006). If targeted proteolysis of the SinR aims to keep protein amounts constant, the loss of the YmdB protein could (indirectly) disrupt the mechanisms that balance SinR protein amounts and thereby induce a drastic phenotypic change.

In general, regulation of cell differentiation (apart from competence development) by directed proteolysis is a common mechanism and well-studied in *B. subtilis* (Konovalova *et al*., 2014), but without any experimental evidence, e. g. from global protein-protein interaction studies with SinR it is difficult to assess which adaptor proteins and proteases might be involved in SinR proteolysis. However, proteolysis of the SinR protein might involve the protease ClpP and its cognate ATPases ClpC or ClpX. Since the deletion of the ClpP protease affects competence, sporulation and motility, processes which are also affected in a *ymdB* mutant, a functional connection is an attractive idea. Moreover, loss of the ClpP protease does not show the same phenotype as a MecA mutant indicating that additional targets exist (Msadek *et al*., 1998; Gottesman, 1999). These additional targets might even be regulators of biofilm formation, because the affected processes are closely connected. Moreover, the MecA homolog YpbH does also influence sporulation but is not involved in degrading ComK or ComS, suggesting alternative targets (Persuh *et al*., 2002).

Proteolysis of SinR (or its putative cognate adaptor protein) by the ClpXP complex appears especially attractive because the RNA sequencing of the *ymdB* mutant and the wild type strain revealed that the long 5’ untranslated leader sequence (5’ UTR) of the *clpX* transcript (Irnov *et al.*, 2010) is processed in the *ymdB* mutant (compare Fig. 4.17). This might indicate a regulatory event on mRNA level that influences translation efficiency and ClpX protein amounts later on (compare Fig. 5.1). Despite this interesting correlation, the influence of the YmdB protein on *clpX* transcript length and a functional connection between transcript length and ClpX protein amounts needs to be further studied, especially because Diethmaier *et al.* (2014) observed reduced *clpX* transcript amounts in microarray experiments whereas the RNA sequencing results in this study rather support a stabilization of the *clpX* transcript apart from the 5’ UTR.

If the SinR protein is directly degraded it would be in company with the Spx transcription factor that is also degraded by the ClpXP complex. Degradation of Spx is initiated by the YjbH adaptor protein and most likely prevented by the anti-adaptor protein YirB (Kommineni *et al*., 2011). Spx controls the expression of genes for high temperature tolerance. Consequently, deletion of the *spx* gene leads to tolerance of higher temperatures upon increased Spx levels. Interestingly, ClpX protein was also implicated in proteolysis of the sigma factor H (Spo0H) that plays a key role in regulating *spo0A* transcription and deletion of the gene for Spo0H reduces biofilm complexity (Branda *et al*., 2001; Liu *et al*., 1999). Furthermore, effects on Spo0H proteolysis might explain drastic changes in sporulation gene expression in the *ymdB* mutant (Diethmaier *et al*., 2014). However, to judge the functional connection between YmdB and Spo0H, further studies are required.

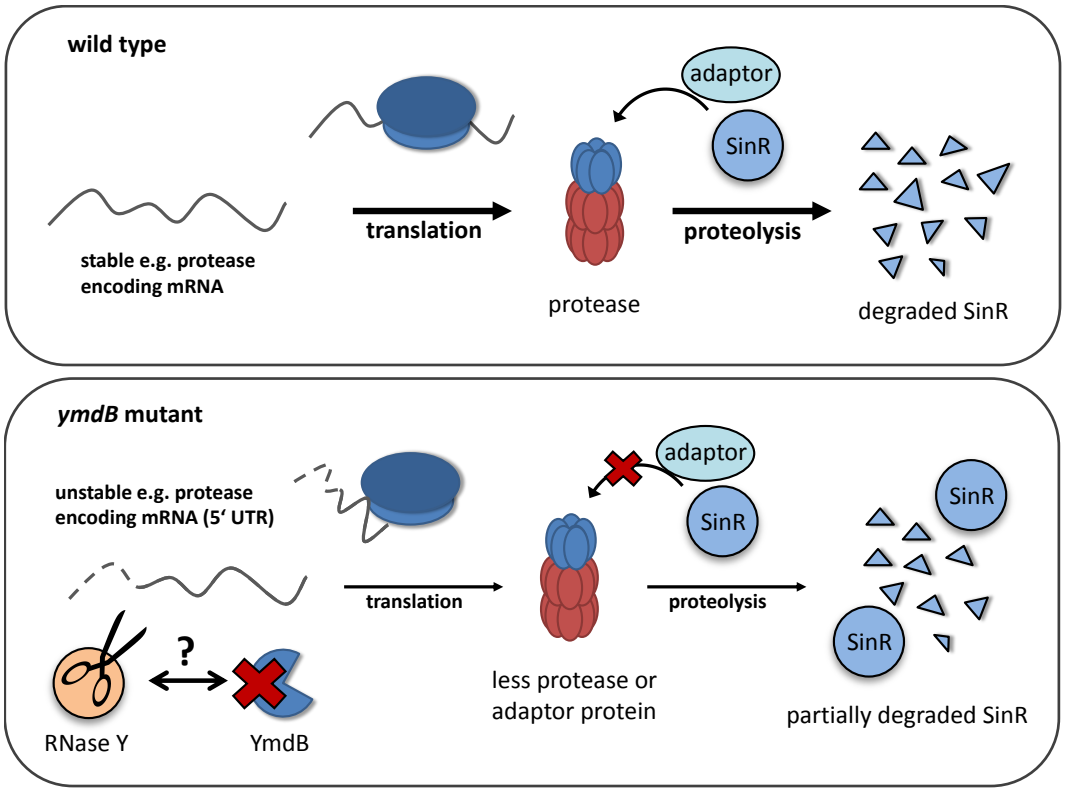

Figure 5.1. Model how the YmdB phosphodiesterase indirectly influences SinR protein amounts.

A further example for a putative control of biofilm formation and motility by proteolysis is the degradation of SinR antagonist SlrR by Clp proteases. Chai *et al*. (2010a) demonstrated that the SinR antagonist SlrR is stabilized upon deletion of the gene for ClpC protease component and Newman & Lewis (2013) proposed a model for SlrR instability that assumes SlrR self-interaction and aggregation leading to degradation by Clp proteases. Degradation of SlrR by the ClpCP protease would explain why motility is affected in the *clpP* mutant. However, it is tempting to speculate that the interplay between the two antagonists is also controlled by SinR proteolysis (e. g. by SlrR acting as an anti-adaptor protein for SinR).

Despite the unclear role of the Clp proteases in the regulation of biofilm formation, for the FtsH protease a clear connection has been proposed (Yepes *et al*., 2012). In contrast to the Clp proteases, FtsH combines the ATPase and peptidase activity within one protein and requires, besides its interaction partner SpoVM, no further adaptor proteins for directed degradation. However, the interplay between the FtsH protein and SpoVM is not totally understood (Prajapati *et al*., 2000; Kirstein *et al*., 2009).

FtsH seems to have a dual function in controlling biofilm formation. Activated by direct interaction with the flotillins FloT and FloA which are required for the formation of micro compartments (lipid rafts) it regulates the sensor kinase KinC that is at the starting point of the phosphorelay controlling biofilm formation and sporulation (Yepes *et al*., 2012). Moreover, FtsH can degrade the Spo0A phosphatase Spo0E and several Rap phosphatases that directly or indirectly decrease Spo0A phosphorylation and hence inhibit biofilm formation and sporulation (Le & Schumann, 2009; Mielich-Süss *et al.*, 2013). Although the biofilm defect of an *ftsH* mutant can be complemented by an additional deletion of the *sinR* gene (as shown for the *ymdB* mutant), the idea that SinR is a direct target of the FtsH protease is only partially in agreement with the published observation. Strikingly, even an *abrB* deletion complemented the *ftsH* deletion although this was only possible to a minor extent in the *ymdB* mutant.

The interplay between YmdB and RNase Y in *cggR-gapA* mRNA processing

Since the first experiments aiming to elucidate the cellular role of the YmdB protein, the idea of a functional connection between the YmdB protein and the major endoribonuclease RNase Y was present (compare 2.4). Due to the genetic organization of the respective genes in one operon and their direct or indirect interaction (Diethmaier, 2011) the idea of a functional connection is very promising and was discussed before (Diethmaier, 2011; Diethmaier *et al.*, 2014). Thus, this chapter aims to discuss the less considered impact on *cggR-gapA* mRNA degradation.

Regulating the abundance of the mRNA template for translation is an important factor to control protein amounts. The abundance of mRNAs can be controlled by varying transcription rates or by RNA degradation/ inactivation. Degradation is crucial to limit the half-life of mRNAs in order to allow fast adaptation to changing environmental conditions (Gerwig & Stülke, 2014a; Lehnik-Habrink *et al*., 2012). RNA degradation is performed by interplay of endo- and exoribonucleases. In *B. subtilis*, the initial endoribonucleolytic processing is conducted by the major endoribonuclease RNase Y (Shahbabian *et al*., 2009). Subsequently, different exoribonucleases can degrade the resulting RNA fragments in 5’-3’ (mainly RNase J1) and in 3’-5’ direction (mainly PNPase) (Lehnik-Habrink *et al*., 2012).

The polycistronic *cggR-gapA-pgk-tpi-pgm-eno* operon and especially the bicistronic *cggR-gapA* transcript, encoding the glycolytic enzymes and the cognate repressor CggR, represent a well-studied

model system for the concerted degradation of RNAs by different enzymes. Although located on one transcript, the mRNAs for the CggR and the GapA proteins are differently abundant. This is due to the combined action of RNase Y and PNPase in degrading the *cggR* transcript and due to the stabilization of the *gapA* transcript by its 5' and 3' secondary structures that prevent degradation (Ludwig *et al*., 2001). Once RNase Y has performed its initial endonucleolytic cut between *cggR* and *gapA* (Commichau *et al.*, 2009), PNPase degrades the *cggR* mRNA in 3'-5' direction. Consequently, the *cggR* transcript is stabilized in a mutant missing the gene encoding PNPase (Liu *et al*., 2014) and in strains in which the gene for RNase Y is depleted (by a factor of 2 to 2.5) (Lehnik-Habrink *et al*., 2011b; Laalami *et al*., 2013, Durand *et al*., 2012a). However, one draw-back of these studies is that the YmdB protein was neglected. Due to its location downstream of the gene for RNase Y and its lack of an own promoter, depletion (loss) of RNase Y also leads to depletion of YmdB. Hence, it is hard to distinguish between effects of RNase Y depletion and the ones connected to loss of the YmdB protein. Aware of this general problem, Lehnik-Habrink (2011) re-addressed the expression of several affected transcripts of microarrays with RNase Y depleted cells. For this purpose, the YmdB protein was expressed ectopically in cells lacking RNase Y and qRT-PCR was conducted to identify differences to the initial microarray data. Supporting the author's assumption that YmdB plays a minor role in RNA processing or degradation the abundance of several transcripts affected by RNase Y depletion, including the *tapA*, the *sunT* and the *trpEDCFBA* operons did not differ substantially when the YmdB protein was expressed ectopically. However, the transcriptome data of the *rny-ymdB* depletion experiment was not compared to the transcriptome data of an *ymdB* deletion strain in detail.

Strikingly, in *ymdB* deletion cells harvested from stationary growth phase, the *cggR* transcript is decreased by a factor of 5 compared to wild type cells (Diethmaier *et al.*, 2014). In contrast, depletion of RNase Y increases the abundance of the *cggR* transcript by a factor of about 2.5 (Lehnik-Habrink *et al.*, 2011b) and also Northern blot experiments support transcript stabilization (Lehnik-Habrink, 2011). This suggests that YmdB has a protective effect on the stability of the *cggR* transcript, whereas RNase Y has a negative effect. Taking the phosphodiesterase activity of the YmdB protein into account, YmdB might totally remove the triphosphate 5' end of *cggR-gapA* transcript so that it is less accessible for the RNase Y endoribonuclease. Thus, the lack of RNase Y on its own should result in a higher stabilization of the *cggR* transcript than initially thought. In conclusion, results of the global RNase Y depletion transcriptome experiments have to be analyzed carefully with respect to polar effects of the simultaneous *ymdB* depletion.

In summary, it remains unclear if the decreased *cggR* transcript abundance is related to changes in gene expression or due to increased degradation of the *cggR* transcript in the absence of the YmdB protein. However, it is striking that the abundance of the *gapA* transcript is not influenced in the *ymdB* mutant strain, although both genes are encoded in one operon. This supports the assumption

that RNA degradation causes decreased *cggR* transcript amounts. This observation can be a starting point to identify targets that are dually regulated by YmdB and RNase Y.

5.2. Suppressor mutations – a bacterial way to evolve

In biology, the term fitness describes how well an organism is adapted to its environment. When conditions frequently change, organisms that can quickly adapt have a higher fitness than other less flexible organisms. Certain abilities of an individual can by chance lead to better adaptation to changing conditions and higher fitness compared to the other members of the group. This allows e. g. survival and/or higher reproduction rates. One big advantage of sexual reproduction is the mixing of the genetically encoded characteristics of the parent generation. This results in new characteristics for the offspring and increases the variability within a group. However, in contrast to e. g. mammals, bacteria do not reproduce sexually but by cell division and hence descendants are clonal copies of the parent generation that possess the same characteristics. So how does genetic diversity arise within a bacterial community?

A well described example to gain new abilities is horizontal gene transfer that implies transfer of genes between organisms of the same species but also between distant lineages (Koonin *et al*., 2001; Popa & Dagan, 2011). Some bacteria like *B. subtilis* even developed machineries for the uptake of foreign DNA that can be expressed under stress conditions. During this competence state cells can integrate foreign DNA into their own chromosome via homologous recombination or use the DNA as a nutrient source (Hamoen *et al*., 2003). This way, bacteria can exchange and gain certain characteristics which might be useful in the future.

An alternative way to generate diversity within a bacterial community is the acqusition of mutations. During harmful conditions bacteria activate the SOS response and thereby induce the expression of alternative, so-called translesion polymerases. These special polymerases can cope with errors on the DNA and allow read-through but their replication fidelity is very low. Thus, errors are introduced into the genome and putative adaptive mutations are generated with a higher frequency. Although, mutations generate genetic diversity, they can also lead to genetic instability. Therefore, mutation frequency needs to be highly regulated (Denamur & Matic, 2006; Sale *et al*., 2012). However, even without induced mutation rates, not all replication errors or mutations caused by external influences are repaired and can thus by chance lead to new abilities. Early work by Luria & Delbrück (1943) supported the assumption that mutations arise independently from selection and by chance lead to advantageous abilities. Although this assumption is still prevailing, it has been discussed intensively. Initially, Cairns *et al*. (1988) pointed out a pitfall of the experiments by Luria & Delbrück (1943): in the respective experiments cells were pre-cultivated without any selective pressure and then a lethal selective pressure was applied to select for suppressor mutants that can survive. This method only detects mutations that were acquired randomly prior to selection but does not exclude that cells

induce mutagenesis in response to sublethal stresses. To further question the idea that mutations always appear randomly, the reversion of a frame-shift mutation in a gene for lactose metabolism was examined under selective conditions leading to the description of examples of so-called adaptive mutagenesis (Cairns *et al*., 1988; Cairns & Foster, 1991). However, the observed effects require special conditions (location of the mutated gene on a plasmid) and were RecA-dependent. Thus, a RecA-dependent amplification model in which the number of alleles determines the mutation frequency was proposed opposing the induction of mutation rates in response to selective pressure (Slechta *et al*., 2002, Roth *et al*., 2006). This gene amplification model was, for instance, applied to explain the evolution of antibiotic resistances which are a big threat for human health (Sandegren & Andersson, 2009; Andersson & Hughes, 2009). Especially, when sublethal doses of selective pressure/ antibiotic concentrations are applied antibiotic resistances can arise very quickly (under certain conditions even within 10 hours) and enable the resistant cells to cultivate new niches of higher selective pressure (Zhang *et al*., 2011).

Suppressor mutations restore biofilm formation in the *ymdB* mutant

As described above (compare 4.2.2), the biofilm-defective *ymdB* mutant acquires suppressor mutations that restore biofilm matrix gene expression. These mutations are mainly found within the gene for the master regulator of biofilm formation SinR. For the Δ*ymdB* suppressor mutations it has not been studied if these are a result of adaptive mutagenesis (and thus appear with higher frequency) or due to accidentally unrepaired replication errors that cause a phenotypical change in the *ymdB* deletion background. To answer the question if the observed mutations are advantageous for the cells and might even form with higher frequency as suggested by Cairns *et al*. (1988), it needs to be determined if there is a selective pressure that drives the *ymdB* mutant to restore biofilm matrix again. For instance, competition experiments between the *ymdB* mutant and wild type cells under the different conditions suppressor mutations were derived from could give answers.

In general, Δ*ymdB* suppressor mutants with restored biofilm formation could be isolated from varying cultivation conditions that most likely cause different selective pressure. Thus, it was easier to observe biofilm forming Δ*ymdB* suppressor mutants under some conditions. Several suppressor mutants were isolated after growth in rich medium for several days followed by plating on minimal biofilm-inducing agar plates. In this system, suppressor mutants were selected due to a wrinkled and rough colony phenotype that clearly distinguished them from the smooth and shiny colonies of the parental strain. Unfortunately, it remains unclear if the majority of suppressor mutations appeared during pre-cultivation or on the selective plates itself, because it is difficult to determine if a single colony started off as a matrix-producing suppressor or gained this ability during growth on the selective agar plate. However, it seems more likely that the suppressor mutations were generated on the agar plates because it usually required several days until wrinkled colonies became visible. In

addition, *ymdB* mutant cells show no growth defect (MSgg medium) or only a slight (LB) growth defect in liquid medium with agitation (results not shown). Thus, it is unlikely that Δ*ymdB* suppressor mutants out-compete *ymdB* mutant cells. However, long-term cultivation experiments (up to 60 days) with the undomesticated wild-type strain revealed that even this biofilm-forming strain acquires mutation in liquid cultures that increase matrix production when cultivated for more than a week. Hence, it was speculated that fine-tuning of matrix production might be of evolutionary advantage (Leiman *et al.*, 2014). In this context, restored matrix production in the *ymdB* mutant might be a big advantage leading to a more rapid formation of suppressors.

In further experiments, suppressor mutants were isolated (without any pre-cultivation) as papillae that appear after several weeks (or at least several days) and grew on top of a community of cells that were streaked out on an SP agar plate as it is frequently performed in the laboratory. In this case the mutations most likely appeared during growth on the agar plate because the papillae were not visible at the beginning. Moreover, on agar plates matrix formation might produce clear benefits because the matrix might prevent the cells from dehydration and is required for sporulation. Probably due to its lack in matrix production the *ymdB* mutant does not sporulate efficiently under biofilm-forming condition (results not shown; compare Aguilar *et al*., 2010). Therefore, restored matrix production also allows the cells to sporulate efficiently when nutrients get limiting. Mutations within the *sinR* gene might even be beneficial due to other regained abilities like restored motility. However, it has to be tested if these processes are affected in the Δ*ymdB* suppressor mutants.

Furthermore, it was also possible to isolate Δ*ymdB* suppressor mutants from agar plates that carried an intact *sinR* gene but have a mutation in a so far unknown gene leading to the formation of mucoid colonies (compare GP1646). Strikingly, it was also possible to isolate mucoid suppressor mutants from other biofilm defective *Bacillus* mutant strains (compare Lockhorn, 2014). Therefore, it might be a common trait that defects in matrix production are compensated by the production of alternative extracellular substances like poly-γ-DL-glutamatic acid.

A situation in which biofilm forming cells (suppressor mutants) seem to have a clear advantage compared to *ymdB* mutant cells is in non-agitated liquid medium. Under this condition (e. g. pellicle assay) *ymdB* mutant cells are not able to colonize the liquid surface and therefore show no growth, probably due to limited oxygen access. In contrast, Δ*ymdB* suppressor mutants colonize the air-liquid interface as observed for the wild type and thus have a clear growth advantage. In this context, the appearance of suppressor mutations that enable the *ymdB* mutant to form pellicles explains why the *ymdB* mutant seems to form pellicles after an (elongated) period of time (results not shown; Pozsgai *et al*., 2012).

Restored biofilm formation - you get what you select for

In a recent publication, van Ditmarsch *et al.* (2013) aimed to study evolutionary aspects behind the motility of the facultative human pathogen *P. aeruginosa*. For this purpose, they subjected the bacteria to repeated rounds of swarming (movement over semisolid surfaces that requires flagella) and isolated suppressor mutants with a hyper-swarming phenotype. Under normal conditions *P. aeruginosa* exhibits only one polar flagellum, but the mutants produced several flagella. According to previous observations (Dasgupta & Ramphal, 2001), the reason for the hyper-swarming and multi-flagellated phenotype could be mapped to mutations in the gene for the regulator of flagella synthesis FleN. Supporting the importance for FleN in controlling flagella synthesis, the same mutations were isolated from several independent experiments. The FleN protein is an anti-activator that interacts with the FleQ regulator (compare 2.3., binds c-di-GMP via Walker A motif) and thereby also control switching between sessile and motile state. Thus, competition experiments between the newly isolated hyper-swarmers and the original strain showed that the mutants are impaired in biofilm formation and not compatible with the wild type cells. Consequently, the authors interpreted their observations as an evolutionary trade-off between biofilm formation and motility. In a commentary by D. Kearns (2013) the interpretation of the results by van Ditmarsch *et al.* (2013) as experimental evolution was seriously questioned. In fact, the results would present a good example for classical forward genetics. For experimental evolution cells are cultivated for a long time and a rather low selective pressure is applied resulting in a diversity of acquired mutations, whereas selective pressure is rather strong in the case of forward genetics. This often leads to the isolation of one distinct mutation (Kearns, 2013). Obviously, this is the case for the work of van Ditmarsch *et al.* (2013).

One main aim of this project was to isolate Δ*ymdB* suppressor mutants that show restored biofilm formation by using forward genetics. Studying the observed suppressor mutants in detail should help to shed light on the molecular origins of the biofilm defect of the *ymdB* deletion mutant. For this purpose, the cells were cultivated for a longer period of time and potential suppressor mutants were directly screened for changes in colony morphology (biofilm formation). As often the case in forward genetics experiments, mutations in the most obvious target, in this case the *sinR* gene, were isolated with high frequency. However, additional suppressors with mutations in SinR operator sequences and in so far unknown genes could be identified (compare 4.2.2.). Consequently, the design of the suppressor mutant screening allows the identification of additional, less obvious mutations but in summary “we got what we selected for” (Kearns, 2013)!

SinR suppressor mutations – a common event

Interestingly, several other authors also observed independently that suppressor mutations in the *sinR* gene can restore complex colony formation to biofilm-defective mutants. Loss of SinI, one main

antagonist of the SinR regulator, leads to drastically reduced complex colony structure (Bai *et al*., 1993; Kearns *et al*., 2005). However, mutations within the *sinR* gene can restore complex colony structure to *sinI* deletion mutants. Similar observations were made for mutants of the *ylbF* and *ymcA* genes that also show a severe biofilm-defect similar to the one observed for a *ymdB* mutant (Kearns *et al*., 2005). These two genes encode proteins involved in the regulation of the phosphorelay for Spo0A phosphorylation and thereby also control SinI expression (compare 2.2) (Carabetta *et al*., 2013). Mutations led to amino acid exchanges in the DNA-binding domain of the SinR protein (*ylpF*: SinR-P42S, *ymcA*: SinR-V50A) and to truncated or elongated SinR protein variants due to stop codon insertions or duplications of regions at the end of the *sinR* gene (*sinI*: SinR-aa 100) (Kearns *et al*., 2005). In addition, Chai *et al*. (2010b) also isolated spontaneous Δ*ymcA* suppressor mutants within the *sinR* gene and studied these in detail. The authors isolated two different classes of suppressor mutations, several mutations concentrated in the DNA binding domain of the SinR protein (V26G, A27T) and others clustered in the interaction domain (D55Y, E67Y, E79K, D84G, D84N, A85T). In a next step, the mutations were transferred to the wild type background and effects on cell differentiation were studied on single cell level. Interestingly, the mutations induced matrix production and cell chaining.

In this work, suppressor mutants were isolated that restore biofilm matrix gene expression and (partially) bistable gene expression. As shown before, an Ala85Thr mutation in the multimerization domain of SinR can restore biofilm matrix gene expression to defective mutants (Chai *et al*., 2010b). However, the authors observed chains of elongated cells (probably) due to repression of autolysin genes and overexpression of matrix genes when the mutation was transferred to the wild type background. This means that the Ala85Thr mutation inhibits SinR tetramer formation (and thereby matrix and *slrR* gene repression) but still allows SinR-SlrR hetero-complex formation that represses autolysin and motility genes. The same suppressor mutation was also observed several times in the Δ*ymdB* background. However, in the *ymdB* mutant chains of elongated cells expressing matrix genes were visible as described before but also several short cells expressing motility genes were present. The simplest explanation is that this difference is due the absence of the YmdB protein. Most likely the SinR Ala85Thr still possess a residual ability to form a tetramer to repress the expression of its antagonist SlrR so that, due to elevated SinR protein amounts in the *ymdB* mutant, in some cells biofilm genes are still repressed and motility and autolysin genes are expressed.

The same explanation might also apply to the Trp104Arg mutation in the SinR gene that also restored matrix gene expression and bistable gene expression and was identified by Kruse (2013) several times (SinR: Trp104Leu). However, this mutation was not described in the literature before and effects were never studied in the wild type background. Thus, transfer of the mutation into the wild type strain might be useful to get a deeper understanding of the effects of the mutation. Moreover, the ability of the SinR protein with a mutated Trp104 to interact with its antagonists needs to be

further analyzed *in vitro* and *in vivo*, because it was suggested that this amino acid, in contradiction to previous results (Colledge *et al*., 2011), is not involved in the interaction with the antagonist (personal communication, R. Lewis). Supporting this assumption, SinR: Trp104Leu was still able to interact with SlrR, SinI and itself in bacterial two-hybrid experiments in *E. coli* (see Fig. 7.2). However, this system does not provide any information about the multimerization state of the complexes.

The SinR: Leu99Ser mutation was also not described before, but in contrast to the other SinR mutations, this mutation destabilizes the protein. Therefore, the phenotype of this mutant is very similar to that of the *ymdB sinR* mutant. However, it is difficult to explain why the cells do not express autolysin and motility genes at the same time although there is no SinR protein present. One possible explanation is that elevated SlrR levels (due to loss of SinR) repress motility and autolysin genes on its own. At least, the SlrR protein can bind to the operator upstream of *lytE* on its own but with a lower affinity than the SlrR-SinR complex and, moreover, deletion of the *slrR* gene increases expression of autolysin genes (Chai *et al*., 2010a). Strikingly, Kruse (2013) observed chains of not elongated cells in *ymdB sinR* mutant that expressed matrix and motility genes at the same time. Differences between the experiments might be due to different genetic backgrounds (NCIB3610 and 168, respectively) or due to additional mutations that e. g. impair motility gene expression in the NCIB3610 background. Another possibility is that residual SinR protein, in complex with its co-repressor SlrR still allows repression of motility and autolysin genes but SinR protein amounts are not sufficient to substantially repress expression of biofilm matrix genes and the gene for *slrR*.

Beside the formation of complex biofilm-like colonies and pellicles, *B. subtilis* can form surface adhered biofilms. For this surface adherence the SipW protein, encoded in one operon with genes for the TapA and TasA biofilm matrix proteins, is required. Consequently, deletion of the gene for SipW impairs surface adherence but mutations in the *sinR* gene restore ability to form surface-adhered biofilms to a *sipW* mutant. Interestingly, the well-studied signal peptidase activity (compare 2.1.) is not required for surface adherence but SipW seems to be a bifunctional protein that also controls expression of the *eps* and *tapA* operons when surface attached biofilms are formed. Thus, the authors speculate that e.g. direct inhibition of the SinR regulator by the SipW protein might explain this observation. The regulatory role of SipW on SinR is further supported by the fact that exopolysaccharides, as a direct target of SinR repression/ anti-activation, are required for the effect of SinR suppressor mutation (Terra *et al*., 2012). As already observed by Kearns *et al.* (2005) changes in an alanine stretch at the of the *sinR* gene led to a frame-shift and a truncated SinR protein. Since the *sipW* gene (operon) is down-regulated in the *ymdB* mutant it is reasonable to assume that the *ymdB* mutant is also impaired in surface adherence. Although not tested, *sinR* mutations would probably also restore surface adherence to the *ymdB* mutant strain. Hence, the system described by Terra *et al*. (2012) seems suitable for the isolation of further, maybe different, *sinR* suppressor mutations.

Another case, in which suppressor mutations in the *sinR* gene were described is a study with mutants defective in galactose catabolism (Chai *et al*., 2012). As known for some time, the deletion of the gene encoding the GalE UDP-galactose-4-epimerase catalyzing the reversible conversion of UDP-galactose to UDP-glucose is lethal in the presence of galactose (Krispin & Allmansberger, 1998). This is probably due to the accumulation of UDP-galactose that might be toxic for the cells. Chai *et al*. (2012) observed that mutations in the *sinR* gene (Trp78stop, Leu74Ser) that relieves the *eps* operon from repression and enhance exopolysaccharide production, allowed *galE* mutant cells to grow in the presence of galactose. This indicates that UDP-galactose can serve as a precursor for exopolysaccharide production and that enhanced EPS production can rescue *galE* mutant cells in the presence of galactose. However, mutations in the *sinR* gene could only be observed when a second copy of the *galT* gene encoding the UDP-galactose synthesizing protein was introduces into the chromosome. Otherwise, only mutations within the *galT* gene could be isolated. This indicates that mutations in *galT* are the most obvious ones and that the selection pressure for a *galE* mutant in the presence of galactose is too high to observe the formation of “minor” mutations within e. g. the *sinR* gene. As observed for the *ymdB sinR* suppressors the identified mutations cluster within the interaction domain but the locations differ from the ones identified in this work and Kruse (2013).

Strikingly, Leiman *et al*. (2014) observed that not only biofilm defective mutants acquire mutations in the *sinR* gene but also the biofilm forming NCIB3610 strain does so when cultivated for a long period of time (at least 6 day in liquid agitated medium). Again, mutations in the interaction domain of SinR (Gly89Arg, Ser107Pro) were identified but also a silent mutation in the codon for serine 57 was discovered. This silent mutation (also compare Kruse, 2013) suggests that certain codons influence ribosome processing and thereby control SinR protein amounts as already suggested by Subramaniam *et al.* (2013).

In summary, mutations in the gene for the master regulator SinR seem to be a common way to restore biofilm formation and surface attachment to biofilm-defective mutants. Since mutations in the *sinR* gene have severe effects on cell differentiation, especially the switch between sessile and motile life style, it appears unlikely that mutations within *sinR* are favorable under natural, frequently changing conditions.

5.3. Tyrosine kinases control cell differentiation

Novel regulatory tyrosine phosphorylation adds even more complexity to the regulatory network for cell differentiation

Recent studies in *B. subtilis* suggest that tyrosine phosphorylation plays an important role in the regulation of biofilm formation and cell differentiation, in addition to known mechanisms of transcriptional regulation and protein-protein interactions (compare 2.2; Vlamakis *et al*., 2013, Mielich-Süss & Lopez, 2014; Mhatre *et al*., 2014). In Gram-positive bacteria, tyrosine kinases consist

of a transmembrane modulator protein and a cytosolic kinase protein (Grangeasse *et al*., 2012). *B. subtilis* encodes two protein tyrosine kinase/ modulator couples, PtkA/ TkmA and EpsB/ EpsA. Interestingly, the simultaneous deletion of either both kinase or modulator genes totally abolished extracellular polysaccharide production causing a biofilm defect. The single mutants did not phenocopy the kinase or modulator double mutants and were still able to produce exopolysaccharides. However, colony structure and pellicle formation was affected in the single mutants (Gerwig *et al*., 2014) suggesting that both kinase systems contribute in a distinct way to biofilm formation. The loss of the EpsB kinase reduced wrinkle formation and the production of extracellular polysaccharides, but did not destroy the rough colony surface, which is indicative of the formation of fruiting bodies for sporulation (Elsholz *et al*., 2014; Gerwig *et al*., 2014). Thus, EpsB does not seem to affect sporulation. In contrast, loss of the EpsB homolog PtkA did not affect extracellular polysaccharide production but instead drastically reduced sporulation in biofilm cells thus leading to a loss of the rough appearance of the outer region of the colonies (Kiley & Stanley-Wall, 2010; Gerwig *et al*., 2014). These observations indicate that the protein tyrosine kinases EpsB and PtkA influence cell differentiation of *B. subtilis* at different levels: EpsB acts downstream of the central regulator of cell differentiation, Spo0A, whereas PtkA is likely to act upstream of Spo0A (Fig. 5.2).

How do the tyrosine kinases PtkA and EpsB influence cell differentiation?

In order to influence sporulation efficiency as shown by Kiley & Stanley-Wall (2010), PtkA most likely has to affect the phosphorelay that governs the phosphorylation state of the Spo0A protein. Since PtkA is a tyrosine kinase it seems reasonable that this influence involves post-translational tyrosine phosphorylation rather than acting e.g. on transcriptional level. Unfortunately, the most difficult question has not yet been solved: what is the phosphorylation target of the PtkA kinase and how can we identify it?

In order to explain altered biofilm formation and the sporulation defect of the *ptkA* mutant, Kiley & Stanley-Wall (2010) conducted an intensive search for possible phosphorylation targets but failed to identify one. Deletion of the long-known PtkA targets (the UDP-glucose dehydrogenases Ugd and TuaD) did not exert an effect on biofilm formation. Moreover, several other targets proposed by large-scale phosphoproteomics and other studies (Macek *et al*., 2007; Jers *et al*., 2010) were not of relevance. Therefore, it remains unclear how PtkA affects biofilm formation and sporulation. Unfortunately, a recent phosphoproteome study did not reveal obvious targets related to the phosphorelay (Ravikumar *et al*., 2014), except the regulator of transition phase genes AbrB which was found to be phosphorylated on a tyrosine. However, the physiological relevance of this phosphorylation is unclear, and serine phosphorylation of AbrB was observed in another study (Kobir

et al., 2014). Clearly, more work is required to dissect the potential control of AbrB activity by phosphorylation.

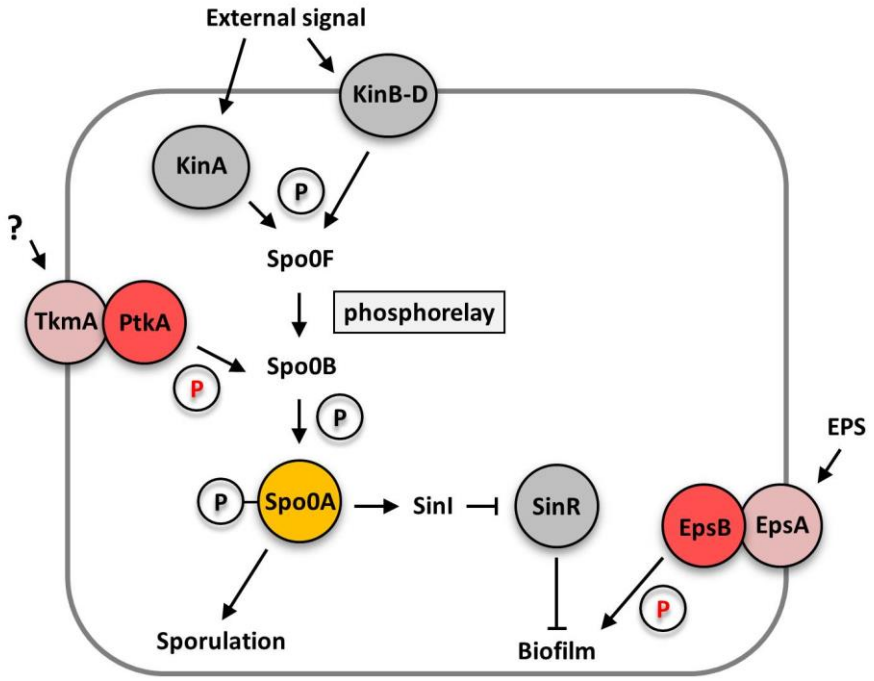

Figure 5.2. Schematic overview how the bacterial tyrosine kinases PtkA and EpsB control cell differentiation at different levels. The PtkA kinase controls sporulation and biofilm matrix expression by acting upstream of the central regulator of cell differentiation Spo0A by an unknown mechanism. In contrast, the EpsB kinase acts downstream of the Spo0A protein and controls exopolysaccharide production by phosphorylation of the glycosyltransferase EpsE. Arrows indicate activating effects, T-bars inhibitory effects. EPS = extracellular polysaccharides, P = phosphate group.

A more or less obvious problem for the identification of tyrosine phosphorylated proteins with the potential to be of regulatory relevance for control of biofilm formation and sporulation is that most of the experiments published so far were performed with cells from domesticated laboratory strains harvested from exponentially growing cultures and under non-biofilm inducing conditions. Thus, it seems reasonable that not all proteins relevant for biofilm formation and especially sporulation are expressed under the tested conditions. Furthermore, regulatory phosphorylations are considered as a fast way to adapt cellular processes to environmental changes. Thus, it is likely that not all phosphorylations are present permanently. Interestingly, all so far known tyrosine phosphorylations with functional relevance have been identified by attempts other than large-scale phosphoproteomics in the first run. Examples include the regulator of unsaturated fatty acid synthesis FatR (Derouiche *et al*., 2013), single stranded DNA-binding proteins (Mijakovic *et al*., 2006) and the glycosyltransferase EpsE, a target of the tyrosine kinase EpsB (Elsholz *et al*., 2014). All of these proteins, except the UDP-glucose dehydrogenase Ugd (by Macek *et al*., 2007), were not identified in the latest large-scale phosphoproteome experiments (Macek *et al*., 2007; Ravikumar *et*

al., 2014). An example for non-functional phosphorylation sites from *B. subtilis* is the FlgN (formerly YvyG) protein that was found to be phosphorylated on a tyrosine residue (Macek *et al*., 2007; Jers *et al*., 2010) and on an arginine residue (Elsholz *et al*., 2012). Furthermore, Jers *et al*. (2010) proposed that tyrosine phosphorylation regulated cellular localization of FlgN that is required for flagella assembly. Control of flagella assembly and motility by phosphorylation of FlgN was an attractive idea but mutational analysis of the phosphorylation sites rebutted a functional relevance (Cairns *et al*., 2014b). Thus, results from large-scale phosphoproteomic experiments have to be considered carefully.

In conclusion, identification of the PtkA phosphorylation target and explanation of the sporulation defect of the mutant remains elusive but it is tempting to speculate that the highly complex network for the control of Spo0A is affected by the PtkA kinase. Since cross-phosphorylation of kinases is an established concept in eukaryotes and hints supporting this idea in prokaryotes are emerging (Baer *et al*., 2014; Shi *et al*., 2014a, b) phosphorylation of phosphorelay proteins is a highly attractive hypothesis.

The second level of regulatory tyrosine phosphorylation is provided by the EpsB kinase that phosphorylates the glycosyltransferase EpsE (Elsholz *et al*., 2014). The kinase and the phosphorylation target are both encoded in the *eps* operon for exopolysaccharide production. Hence, the regulation of the two corresponding genes is very similar. The *eps* operon is only strongly expressed if the SinR anti-activator protein is inhibited by either of its antagonists SinI and SlrR under biofilm forming conditions (Winkelman *et al*., 2013; Kearns *et al*., 2005; Newman *et al*., 2013). This observation implies that EpsB-mediated phosphorylation might not have a global effect and that the phosphorylated target is among the proteins expressed under biofilm forming conditions that are also subject to repression by SinR. Indeed, deletion of the *epsB* gene only affects exopolysaccharide production but leaves sporulation unaffected (Gerwig *et al*., 2014). Strikingly, deletion of the gene for the EpsE glycosyltransferase leads to a complete loss of exopolysaccharide production and complex colony formation, whereas deletion of the gene for the EpsB kinase has a milder effect (Guttenplan *et al*., 2010). Therefore, it is tempting to speculate that PtkA can partially take over the function of EpsB. However, this needs to be demonstrated experimentally.

Functional cross-talk between tyrosine kinase/ modulator couples

Straight signal transduction is an important issue for many conserved multi-component signal transduction system families and has been extensively studied for two-component regulatory systems and phosphotransferase system-controlled RNA-binding antitermination proteins. These systems have evolved in a way to avoid non-cognate interactions either by restricting the interactions with non-cognate proteins partners, ligands, and target molecules. Moreover, differential gene expression of the non-cognate components has been observed to prevent non-

productive cross-talk (Schilling *et al*., 2006; Szurmant & Hoch, 2010; Hübner *et al*., 2011; Podgornaia & Laub, 2013). However, this might be different for regulatory tyrosine phosphorylation, as suggested for the interplay between EpsB and PtkA. In yeast (Shi *et al*., 2014b) and bacterial two-hybrid studies (our unpublished results) the TkmA modulator and the EpsB kinase interact with each other, whereas the EpsA modulator and the PtkA kinase do not interact. Additionally, a genetic analysis of a potential cross-talk in the background of the laboratory strain 168 revealed that simultaneous loss of PtkA and EpsA does not affect stable pellicle formation, whereas simultaneous deletion of the genes for EpsB and TkmA inhibited stable pellicle formation. These observations further support a functional connection between the two systems. However, confirmation of this result in the background of the NCIB3610 wild type strain was not successful (results not shown). Although the functional relevance of the TkmA/EpsB cross-talk remains unclear, similar observations come from *Staphylococcus aureus* that also contains two similar tyrosine kinase/ modulator couples. In this case, the Cap5A1 modulator protein of one couple and the Cap5B2 protein tyrosine kinase of the other couple show functional cross-talk suggesting that interplay between different tyrosine/ modulator couples might not be limited to *B. subtilis* (Soulat *et al*., 2007).

5.4. Outlook

Survival in frequently changing environments requires the ability to adapt to new conditions. This adaptation can be achieved on the genetic level by acquiring mutations or, without any mutations, on the level of gene expression and regulation. This work pointed out the relevance of tyrosine phosphorylation for the regulation of biofilm formation and addressed the function of the YmdB protein in the control of protein amounts of the SinR biofilm regulator.

The identification of elevated SinR protein amounts in the *ymdB* mutant was a surprising observation but further explained the biofilm defect of the mutant. In order to test if the SinR protein is subject to regulatory proteolysis in the wild type strain deletion of the most promising protease genes (e.g. ClpX and ClpP) need to be constructed. Then the mutants have to be checked for a biofilm phenotype and in case of differences to the wild type for SinR protein amounts.

In general, it remains to be further studied if elevated SinR protein amounts are really present under biofilm forming conditions or if they are induced in response to the cultivation conditions. For this purpose, protein extract from complex colony samples need to be isolated and tested for SinR protein amounts by Western blotting. In parallel, an elegant way to test if the biofilm defect of the *ymdB* mutant is solely due to increased SinR protein levels is the overexpression of SinR in the wild type background and assay of biofilm formation. Since SinR expression is considered to be constant, elevated SinR protein amounts in the *ymdB* mutant are an unusual event. However, Mandic-Mulec *et al*. (1995) found that overexpression of SinR inhibits induction of *spo0A* gene expression for the initiation of sporulation. *Vice versa* deletion of the *sinR* gene increased the induction of *spo0A* at the

initial state of sporulation. Decreased abundance of the Spo0A protein would explain decreased expression of the SinI antagonist and induced expression of the AbrB regulator leading to a biofilm defect.

To further elucidate the function of the YmdB phosphodiesterase the *in vivo* RNA co-purification experiments need to be repeated without any cross-linking agents. This way, it should be possible to enhance the specificity of the method. To get a global view of the YmdB "RNA interactome" RNA sequencing approaches of the co-purified RNA could reveal novel targets. Especially small regulatory RNAs and RNAs encoding proteins involved in proteolysis might be promising candidates for YmdB processing. One challenging aspect of this experiment will be to ensure that the amount of co-purified RNA is sufficient for RNA sequencing approaches. In this context it might be useful to perform *in vitro* RNase assays with the YmdB protein to show that the protein can in general degrade RNA. This way the interplay between YmdB and RNase Y could also be tested.

Finally, identification of unknown mutation that partially restored matrix gene expression in the *ymdB* background will, hopefully, shed some additional light on the role of *ymdB* in biofilm formation.

The detection of a regulatory interplay between protein tyrosine phosphorylation and classical sensing via the phosphorelay in the control of cell differentiation in *B. subtilis* is one of the most exciting results of recent studies. This is underlined by the observation of extensive links between the different signal transduction systems that involve post-translational modifications (Shi *et al*., 2014a, b; van Noort *et al*., 2012). One main task for future work is the identification of phosphorylation targets of the tyrosine kinase PtkA in order to get a better understanding of its implication in biofilm formation and sporulation. To demonstrate that PtkA affects cell differentiation upstream of the central regulator Spo0A, the phosphorylation state of Spo0A has to be analyzed in a *ptkA* deletion mutant. Furthermore, large-scale phosphoproteomics under biofilm-promoting conditions could help to identify potential tyrosine phosphorylated targets. Additional tasks are the identification of substances that can be sensed by the PtkA modulator protein TkmA and to further dissect the potential cross-talk between the two known tyrosine kinase/ modulator couples EpsB/ EpsA and PtkA/ TkmA in *B. subtilis*. One open question that arose from the publication of Elsholz *et al.* (2014) is how exactly autophosphorylation at the C-terminal tyrosine cluster of EpsB influences protein activity. The authors showed that mutations of the residues Tyr-225 and Tyr-227 to a phenylalanine induced complex colony structure, whereas mimicking a phosphorylation by exchanging the two residues by a glutamate reduced complex colony structure similar to the deletion mutant. This is controversy to the results obtained by Kiley & Stanley-Wall (2010) for the PtkA kinase and also for EpsB (personal communication Nicola Stanley-Wall). In their hands blocking the phosphorylation of the C-terminal tyrosine residues of EpsB and PtkA by exchanging them against alanine residues did not alter biofilm formation. Therefore, the stability of the mutated proteins needs to be tested to

assure that this is not affected. However, effects on protein instability are unlikely because this would lead to less structured colonies as shown for the deletion mutant.

6. References

Aguilar, C., Vlamakis, H., Guzman, A., Losick, R., and Kolter, R. (2010) KinD is a checkpoint protein linking spore formation to extracellular-matrix production in *Bacillus subtilis* biofilms. *MBio* **1**: e00035–10.

Andersson, D.I., and Hughes, D. (2009) Gene amplification and adaptive evolution in bacteria. *Annu Rev Genet* **43**: 167–195.

Babitzke, P., Baker, C.S., and Romeo, T. (2009) Regulation of translation initiation by RNA binding proteins. *Annu Rev Microbiol* **63**: 27–44.

Baer, C.E., Iavarone, A.T., Alber, T., and Sassetti, C.M. (2014) Biochemical and spatial coincidence in the provisional Ser/Thr protein kinase interaction network of *Mycobacterium tuberculosis*. *J Biol Chem* **289**: 20422–20433.

Bai, U., Mandic-Mulec, I., and Smith, I. (1993) SinI modulates the activity of SinR, a developmental switch protein of *Bacillus subtilis*, by protein-protein interaction. *Genes Dev* **7**: 139–148.

Barends, T.R.M., Hartmann, E., Griese, J.J., Beitlich, T., Kirienko, N. V, Ryjenkov, D.A., *et al.* (2009) Structure and mechanism of a bacterial light-regulated cyclic nucleotide phosphodiesterase. *Nature* **459**: 1015–1018.

Battesti, A., and Gottesman, S. (2013) Roles of adaptor proteins in regulation of bacterial proteolysis. *Curr Opin Microbiol* **16**: 140–147.

Beauregard, P.B., Chai, Y., Vlamakis, H., Losick, R., and Kolter, R. (2013*) Bacillus subtilis* biofilm induction by plant polysaccharides. *Proc Natl Acad Sci U S A* **110**: E1621–1630.

Bechet, E., Gruszczyk, J., Terreux, R., Gueguen-Chaignon, V., Vigouroux, A., Obadia, B., *et al.* (2010) Identification of structural and molecular determinants of the tyrosine-kinase Wzc and implications in capsular polysaccharide export. *Mol Microbiol* **77**: 1315–1325.

Bischofs, I.B., Hug, J.A., Liu, A.W., Wolf, D.M., and Arkin, A.P. (2009) Complexity in bacterial cell-cell communication: quorum signal integration and subpopulation signaling in the *Bacillus subtilis* phosphorelay. *Proc Natl Acad Sci U S A* **106**: 6459–6464.

Blair, K.M., Turner, L., Winkelman, J.T., Berg, H.C., and Kearns, D.B. (2008) A molecular clutch disables flagella in the *Bacillus subtilis* biofilm. *Science* **320**: 1636–1638.

Blötz, C. (2013) Der Einfluss von zyklischem di-Guanosinmonophosphat auf die Biofilmbildung von *Bacillus subtilis*. Bachelor thesis.

Boehm, A., Kaiser, M., Li, H., Spangler, C., Kasper, C.A., Ackermann, M., *et al.* (2010) Second messenger-mediated adjustment of bacterial swimming velocity. *Cell* **141**: 107–116.

Boyd, C.D., and O'Toole, G.A. (2012) Second messenger regulation of biofilm formation: breakthroughs in understanding c-di-GMP effector systems. *Annu Rev Cell Dev Biol* **28**: 439–462.

Bradford, M.M. (1976) A rapid and sensitive method for the quantitation of microgram quantities of protein utilizing the principle of protein-dye binding. *Anal Biochem* **72**: 248–254.

Branda, S.S., Chu, F., Kearns, D.B., Losick, R., and Kolter, R. (2006) A major protein component of the *Bacillus subtilis* biofilm matrix. *Mol Microbiol* **59**: 1229–1238.

Branda, S.S., González-Pastor, J.E., Ben-Yehuda, S., Losick, R., and Kolter, R. (2001) Fruiting body formation by *Bacillus subtilis*. *Proc Natl Acad Sci U S A* **98**: 11621–11626.

Burbulys, D., Trach, K.A., and Hoch, J.A. (1991) Initiation of sporulation in *B. subtilis* is controlled by a multicomponent phosphorelay. *Cell* **64**: 545–552.

Butcher, L.A., and Tomkins, J.K. (1985) A comparison of silver staining methods for detecting proteins in ultrathin polyacrylamide gels on support film after isoelectric focusing. *Anal Biochem* **148**: 384–388.

Cairns, J., and Foster, P.L. (1991) Adaptive reversion of a frameshift mutation in *Escherichia coli*. *Genetics* **128**: 695–701.

Cairns, J., Overbaugh, J., and Miller, S. (1988) The origin of mutants. *Nature* **335**: 142–145.

Cairns, L.S., Hobley, L., and Stanley-Wall, N.R. (2014a) Biofilm formation by *Bacillus subtilis*: new insights into regulatory strategies and assembly mechanisms. *Mol Microbiol* **93**: 587–598.

Cairns, L.S., Marlow, V.L., Kiley, T.B., Birchall, C., Ostrowski, A., Aldridge, P.D., and Stanley-Wall, N.R. (2014b) FlgN is required for flagellum-based motility by *Bacillus subtilis*. *J Bacteriol* **196**: 2216–2226.

Carabetta, V.J., Tanner, A.W., Greco, T.M., Defrancesco, M., Cristea, I.M., and Dubnau, D. (2013) A complex of YlbF, YmcA and YaaT regulates sporulation, competence and biofilm formation by accelerating the phosphorylation of Spo0A. *Mol Microbiol* **88**: 283–300.

Chai, Y., Beauregard, P.B., Vlamakis, H., Losick, R., and Kolter, R. (2012) Galactose metabolism plays a crucial role in biofilm formation by *Bacillus subtilis*. *MBio* **3**: e00184–12.

Chai, Y., Chu, F., Kolter, R., and Losick, R. (2008) Bistability and biofilm formation in *Bacillus subtilis*. *Mol Microbiol* **67**: 254–263.

Chai, Y., Kolter, R., and Losick, R. (2009) Paralogous antirepressors acting on the master regulator for biofilm formation in *Bacillus subtilis*. *Mol Microbiol* **74**: 876–887.

Chai, Y., Kolter, R., and Losick, R. (2010) Reversal of an epigenetic switch governing cell chaining in *Bacillus subtilis* by protein instability. *Mol Microbiol* **78**: 218–229.

Chai, Y., Norman, T., Kolter, R., and Losick, R. (2010b) An epigenetic switch governing daughter cell separation in *Bacillus subtilis*. *Genes Dev* **24**: 754–765.

Chao, J.D., Wong, D., and Av-Gay, Y. (2014) Microbial protein-tyrosine kinases. *J Biol Chem* **289**: 9463–9472.

Chen, L.-H., Köseoğlu, V.K., Güvener, Z.T., Myers-Morales, T., Reed, J.M., D'Orazio, S.E.F., *et al.* (2014) Cyclic di-GMP-dependent signaling pathways in the pathogenic Firmicute *Listeria monocytogenes*. *PLoS Pathog* **10**: e1004301.

Chen, Y., Chai, Y., Guo, J., and Losick, R. (2012) Evidence for cyclic Di-GMP-mediated signaling in *Bacillus subtilis*. *J Bacteriol* **194**: 5080–5090.

Chu, F., Kearns, D.B., Branda, S.S., Kolter, R., and Losick, R. (2006) Targets of the master regulator of biofilm formation in *Bacillus subtilis*. *Mol Microbiol* **59**: 1216–1228.

Chu, F., Kearns, D.B., McLoon, A., Chai, Y., Kolter, R., and Losick, R. (2008) A novel regulatory protein governing biofilm formation in *Bacillus subtilis*. *Mol Microbiol* **68**: 1117–1127.

Claessen, D., Emmins, R., Hamoen, L.W., Daniel, R.A., Errington, J., and Edwards, D.H. (2008) Control of the cell elongation-division cycle by shuttling of PBP1 protein in *Bacillus subtilis*. *Mol Microbiol* **68**: 1029–1046.

Colledge, V.L., Fogg, M.J., Levdikov, V.M., Leech, A., Dodson, E.J., and Wilkinson, A.J. (2011) Structure and organisation of SinR, the master regulator of biofilm formation in *Bacillus subtilis*. *J Mol Biol* **411**: 597–613.

Collins, R.F., Beis, K., Dong, C., Botting, C.H., McDonnell, C., Ford, R.C., *et al.* (2007) The 3D structure of a periplasm-spanning platform required for assembly of group 1 capsular polysaccharides in *Escherichia coli*. *Proc Natl Acad Sci U S A* **104**: 2390–2395.

Commichau, F.M., Rothe, F.M., Herzberg, C., Wagner, E., Hellwig, D., Lehnik-Habrink, M., *et al.* (2009) Novel activities of glycolytic enzymes in *Bacillus subtilis*: interactions with essential proteins involved in mRNA processing. *Mol Cell Proteomics* **8**: 1350–1360.

Costerton, J.W., Lewandowski, Z., Caldwell, D.E., Korber, D.R., and Lappin-Scott, H.M. (1995) Microbial biofilms. *Annu Rev Microbiol* **49**: 711–745.

Costerton, J.W., Stewart, P.S., and Greenberg, E.P. (1999) Bacterial biofilms: a common cause of persistent infections. *Science* **284**: 1318–1322.

Cousin, C., Derouiche, A., Shi, L., Pagot, Y., Poncet, S., and Mijakovic, I. (2013) Protein-serine/threonine/tyrosine kinases in bacterial signaling and regulation. *FEMS Microbiol Lett* **346**: 11–19.

Dasgupta, N., and Ramphal, R. (2001) Interaction of the antiactivator FleN with the transcriptional activator FleQ regulates flagellar number in *Pseudomonas aeruginosa*. *J Bacteriol* **183**: 6636–6644.

Denamur, E., and Matic, I. (2006) Evolution of mutation rates in bacteria. *Mol Microbiol* **60**: 820–827.

Derouiche, A., Bidnenko, V., Grenha, R., Pigonneau, N., Ventroux, M., Franz-Wachtel, M., *et al.* (2013) Interaction of bacterial fatty-acid-displaced regulators with DNA is interrupted by tyrosine phosphorylation in the helix-turn-helix domain. *Nucleic Acids Res* **41**: 9371–9381.

Diethmaier, C. (2011) Die Rolle von YmdB als Regulator der Zelldifferenzierung in *Bacillus subtilis*.

PhD thesis.

Diethmaier, C., Newman, J.A., Kovács, A.T., Kaever, V., Herzberg, C., Rodrigues, C., *et al.* (2014) The YmdB phosphodiesterase is a global regulator of late adaptive responses in *Bacillus subtilis*. *J Bacteriol* **196**: 265–275.

Diethmaier, C., Pietack, N., Gunka, K., Wrede, C., Lehnik-Habrink, M., Herzberg, C., *et al.* (2011) A novel factor controlling bistability in *Bacillus subtilis*: the YmdB protein affects flagellin expression and biofilm formation. *J Bacteriol* **193**: 5997–6007.

Dietrich, S., Wiegand, S., and Liesegang, H. (2014) TraV: a genome context sensitive transcriptome browser. *PLoS One* **9**: e93677.

Ditmarsch, D. van, Boyle, K.E., Sakhtah, H., Oyler, J.E., Nadell, C.D., Déziel, É., *et al.* (2013) Convergent evolution of hyperswarming leads to impaired biofilm formation in pathogenic bacteria. *Cell Rep* **4**: 697–708.

Dubnau, D., and Losick, R. (2006) Bistability in bacteria. *Mol Microbiol* **61**: 564–572.

Durand, S., Gilet, L., Bessières, P., Nicolas, P., and Condon, C. (2012a) Three essential ribonucleases-RNase Y, J1, and III-control the abundance of a majority of *Bacillus subtilis* mRNAs. *PLoS Genet* **8**: e1002520.

Durand, S., Richard, G., Bontems, F., and Uzan, M. (2012b) Bacteriophage T4 polynucleotide kinase triggers degradation of mRNAs. *Proc Natl Acad Sci U S A* **109**: 7073–7078.

El-Samad, H., and Khammash, M. (2006) Regulated degradation is a mechanism for suppressing stochastic fluctuations in gene regulatory networks. *Biophys J* **90**: 3749–3761.

Elsholz, A.K.W., Turgay, K., Michalik, S., Hessling, B., Gronau, K., Oertel, D., *et al.* (2012) Global impact of protein arginine phosphorylation on the physiology of *Bacillus subtilis*. *Proc Natl Acad Sci U S A* **109**: 7451–7456.

Eilers, H. (2010) Transcription in *Mycoplasma pneumonia*. PhD thesis.

Elsholz, A.K.W., Wacker, S.A., and Losick, R. (2014) Self-regulation of exopolysaccharide production in *Bacillus subtilis* by a tyrosine kinase. *Genes Dev* **28**: 1710–1720.

Fein, J.E. (1979) Possible involvement of bacterial autolytic enzymes in flagellar morphogenesis. *J Bacteriol* **137**: 933–946.

Ferrari, E., Canosi, U., Galizzi, A., and Mazza, G. (1978) Studies on transduction process by SPP1 phage. *J Gen Virol* **41**: 563–572.

Flemming, H.-C., and Wingender, J. (2010) The biofilm matrix. *Nat Rev Microbiol* **8**: 623–633.

Fujita, M., González-Pastor, J.E., and Losick, R. (2005) High- and low-threshold genes in the Spo0A regulon of *Bacillus subtilis*. *J Bacteriol* **187**: 1357–1368.

Fujita, M., and Losick, R. (2005) Evidence that entry into sporulation in *Bacillus subtilis* is governed by a gradual increase in the level and activity of the master regulator Spo0A. *Genes Dev* **19**: 2236–2244.

Gao, X., Mukherjee, S., Matthews, P.M., Hammad, L.A., Kearns, D.B., and Dann, C.E. (2013) Functional characterization of core components of the *Bacillus subtilis* cyclic-di-GMP signaling pathway. *J Bacteriol* **195**: 4782–4792.

Garfin, D.E. (2009) One-dimensional gel electrophoresis. *Methods Enzymol* **463**: 497–513.

Gaur, N.K., Cabane, K., and Smith, I. (1988) Structure and expression of the *Bacillus subtilis sin* operon. *J Bacteriol* **170**: 1046–53.

Gerwig, J. (2011) Novel factors involved in the Mfd-mediated decryptification of the *gudB* gene in *Bacillus subtilis*. Master thesis.

Gerwig, J., Kiley, T.B., Gunka, K., Stanley-Wall, N., and Stülke, J. (2014) The protein tyrosine kinases EpsB and PtkA differentially affect biofilm formation in *Bacillus subtilis*. *Microbiol (United Kingdom)* **160**: 682–691.

Gerwig, J., and Stülke, J. (2014a) Caught in the act: RNA-Seq provides novel insights into mRNA degradation. *Mol Microbiol* **94**: 5–8.

Gerwig, J., and Stülke, J. (2014b) Far from being well understood: Multiple protein phosphorylation events control cell differentiation in *Bacillus subtilis* at different levels. *Front Microbiol* **5**: 704.doi:10.3389/fmicb.2014.00704.

Göpel, Y., Papenfort, K., Reichenbach, B., Vogel, J., and Görke, B. (2013) Targeted decay of a regulatory small RNA by an adaptor protein for RNase E and counteraction by an anti-adaptor RNA. *Genes Dev* **27**: 552–564.

Görke, B., and Stülke, J. (2008) Carbon catabolite repression in bacteria: many ways to make the most out of nutrients. *Nat Rev Microbiol* **6**: 613–624.

González-Pastor, J.E. (2011) Cannibalism: a social behavior in sporulating *Bacillus subtilis*. *FEMS Microbiol Rev* **35**: 415–424.

Gottesman, S. (1999) Regulation by proteolysis: developmental switches. *Curr Opin Microbiol* **2**: 142–147.

Grangeasse, C., Cozzone, A.J., Deutscher, J., and Mijakovic, I. (2007) Tyrosine phosphorylation: an emerging regulatory device of bacterial physiology. *Trends Biochem Sci* **32**: 86–94.

Grangeasse, C., Nessler, S., and Mijakovic, I. (2012) Bacterial tyrosine kinases: evolution, biological function and structural insights. *Philos Trans R Soc Lond B Biol Sci* **367**: 2640–2655.

Grangeasse, C., Terreux, R., and Nessler, S. (2010) Bacterial tyrosine-kinases: structure-function analysis and therapeutic potential. *Biochim Biophys Acta* **1804**: 628–634.

Gundlach, J., Dickmanns, A., Schröder-Tittmann, K., Neumann, P., Kaesler, J., Kampf, J., *et al.* (2014) Identification, characterization and structure analysis of the c-di-AMP binding PII-like signal transduction protein DarA. *J Biol Chem* **290**: 3069-3080.

Guttenplan, S.B., Blair, K.M., and Kearns, D.B. (2010) The EpsE flagellar clutch is bifunctional and synergizes with EPS biosynthesis to promote *Bacillus subtilis* biofilm formation. *PLoS Genet* **6**: e1001243.

Hall-Stoodley, L., Costerton, J.W., and Stoodley, P. (2004) Bacterial biofilms: from the natural environment to infectious diseases. *Nat Rev Microbiol* **2**: 95–108.

Hämmerle, H., Amman, F., Večerek, B., Stülke, J., Hofacker, I., and Bläsi, U. (2014) Impact of Hfq on the *Bacillus subtilis* transcriptome. *PLoS One* **9**: e98661.

Hamoen, L.W., Venema, G., and Kuipers, O.P. (2003) Controlling competence in *Bacillus subtilis*: shared use of regulators. *Microbiology* **149**: 9–17.

Hamon, M.A., and Lazazzera, B.A. (2001) The sporulation transcription factor Spo0A is required for biofilm development in *Bacillus subtilis*. *Mol Microbiol* **42**: 1199–1209.

Hamon, M.A., Stanley, N.R., Britton, R.A., Grossman, A.D., and Lazazzera, B.A. (2004) Identification of AbrB-regulated genes involved in biofilm formation by *Bacillus subtilis*. *Mol Microbiol* **52**: 847–860.

Hengge, R. (2009) Principles of c-di-GMP signalling in bacteria. *Nat Rev Microbiol* **7**: 263–273.

Herzberg, C., Weidinger, L.A.F., Dörrbecker, B., Hübner, S., Stülke, J., and Commichau, F.M. (2007) SPINE: a method for the rapid detection and analysis of protein-protein interactions *in vivo*. *Proteomics* **7**: 4032–4035.

Hickman, J.W., and Harwood, C.S. (2008) Identification of FleQ from *Pseudomonas aeruginosa* as a c-di-GMP-responsive transcription factor. *Mol Microbiol* **69**: 376–389.

Hobley, L., Ostrowski, A., Rao, F. V, Bromley, K.M., Porter, M., Prescott, A.R., *et al.* (2013) BslA is a self-assembling bacterial hydrophobin that coats the *Bacillus subtilis* biofilm. *Proc Natl Acad Sci U S A* **110**: 13600–1365.

Hsieh, P., Richards, J., Liu, Q., and Belasco, J.G. (2013) Specificity of RppH-dependent RNA degradation in *Bacillus subtilis*. *Proc Natl Acad Sci U S A* **110**: 8864–8869.

Hübner, S., Declerck, N., Diethmaier, C., Coq, D. Le, Aymerich, S., and Stülke, J. (2011) Prevention of cross-talk in conserved regulatory systems: identification of specificity determinants in RNA-binding anti-termination proteins of the BglG family. *Nucleic Acids Res* **39**: 4360–4372.

Ilan, O., Bloch, Y., Frankel, G., Ullrich, H., Geider, K., and Rosenshine, I. (1999) Protein tyrosine kinases in bacterial pathogens are associated with virulence and production of exopolysaccharide. *EMBO J* **18**: 3241–3248.

Inoue, H., Nojima, H., and Okayama, H. (1990) High efficiency transformation of *Escherichia coli* with plasmids. *Gene* **96**: 23–28.

Irie, Y., Borlee, B.R., O'Connor, J.R., Hill, P.J., Harwood, C.S., Wozniak, D.J., and Parsek, M.R. (2012) Self-produced exopolysaccharide is a signal that stimulates biofilm formation in *Pseudomonas aeruginosa*. *Proc Natl Acad Sci U S A* **109**: 20632–20636.

Irnov, I., and Winkler, W.C. (2010) A regulatory RNA required for antitermination of biofilm and capsular polysaccharide operons in Bacillales. *Mol Microbiol* **76**: 559–575.

Jers, C., Pedersen, M.M., Paspaliari, D.K., Schütz, W., Johnsson, C., Soufi, B., *et al.* (2010) *Bacillus subtilis* BY-kinase PtkA controls enzyme activity and localization of its protein substrates. *Mol Microbiol* **77**: 287–299.

Karimova, G., Pidoux, J., Ullmann, A., and Ladant, D. (1998) A bacterial two-hybrid system based on a reconstituted signal transduction pathway. *Proc Natl Acad Sci U S A* **95**: 5752–5756.

Kearns, D.B. (2013) You get what you select for: better swarming through more flagella. *Trends Microbiol* **21**: 508–509.

Kearns, D.B., Chu, F., Branda, S.S., Kolter, R., and Losick, R. (2005) A master regulator for biofilm formation by *Bacillus subtilis*. *Mol Microbiol* **55**: 739–749.

Kennelly, P.J. (2014) Protein Ser/Thr/Tyr phosphorylation in the Archaea. *J Biol Chem* **289**: 9480–9487.

Kiley, T.B., and Stanley-Wall, N.R. (2010) Post-translational control of *Bacillus subtilis* biofilm formation mediated by tyrosine phosphorylation. *Mol Microbiol* **78**: 947–963.

Kirstein, J., Molière, N., Dougan, D.A., and Turgay, K. (2009) Adapting the machine: adaptor proteins for Hsp100/Clp and AAA+ proteases. *Nat Rev Microbiol* **7**: 589–599.

Kobayashi, K. (2008) SlrR/SlrA controls the initiation of biofilm formation in *Bacillus subtilis*. *Mol Microbiol* **69**: 1399–1410.

Kobayashi, K., and Iwano, M. (2012) BslA(YuaB) forms a hydrophobic layer on the surface of *Bacillus subtilis* biofilms. *Mol Microbiol* **85**: 51–66.

Kobir, A., Poncet, S., Bidnenko, V., Delumeau, O., Jers, C., Zouhir, S., *et al.* (2014) Phosphorylation of *Bacillus subtilis* gene regulator AbrB modulates its DNA-binding properties. *Mol Microbiol* **92**: 1129–1141.

Kolodkin-Gal, I., Elsholz, A.K.W., Muth, C., Girguis, P.R., Kolter, R., and Losick, R. (2013) Respiration control of multicellularity in *Bacillus subtilis* by a complex of the cytochrome chain with a membrane-embedded histidine kinase. *Genes Dev* **27**: 887–899.

Kommineni, S., Garg, S.K., Chan, C.M., and Zuber, P. (2011) YjbH-enhanced proteolysis of Spx by ClpXP in *Bacillus subtilis* is inhibited by the small protein YirB (YuzO). *J Bacteriol* **193**: 2133–2140.

Konijn, T.M., Meene, J.G. Van De, Bonner, J.T., and Barkley, D.S. (1967) The acrasin activity of adenosine-3’,5'-cyclic phosphate. *Proc Natl Acad Sci U S A* **58**: 1152–1154.

Konovalova, A., Søgaard-Andersen, L., and Kroos, L. (2014) Regulated proteolysis in bacterial development. *FEMS Microbiol Rev* **38**: 493–522.

Koonin, E. V, Makarova, K.S., and Aravind, L. (2001) Horizontal gene transfer in prokaryotes: quantification and classification. *Annu Rev Microbiol* **55**: 709–742.

Krispin, O., and Allmansberger, R. (1998) The *Bacillus subtilis galE* gene is essential in the presence of glucose and galactose. *J Bacteriol* **180**: 2265–2270.

Kruse, K. (2013) The link between the enzymatic activity of YmdB and its role in biofilm formation in *Bacillus subtilis*. Master thesis.

Kunst, F., and Rapoport, G. (1995) Salt stress is an environmental signal affecting degradative enzyme synthesis in *Bacillus subtilis*. *J Bacteriol* **177**: 2403–2407.

Laalami, S., Bessières, P., Rocca, A., Zig, L., Nicolas, P., and Putzer, H. (2013) *Bacillus subtilis* RNase Y activity *in vivo* analysed by tiling microarrays. *PLoS One* **8**: e54062.

Laemmli, U.K. (1970) Cleavage of structural proteins during the assembly of the head of bacteriophage T4. *Nature* **227**: 680–685.

Laney, J.D., and Hochstrasser, M. (2004) Ubiquitin-dependent control of development in *Saccharomyces cerevisiae*. *Curr Opin Microbiol* **7**: 647–654.

Lay, N. De, Schu, D.J., and Gottesman, S. (2013) Bacterial small RNA-based negative regulation: Hfq and its accomplices. *J Biol Chem* **288**: 7996–8003

Lazazzera, B.A., Solomon, J.M., and Grossman, A.D. (1997) An exported peptide functions intracellularly to contribute to cell density signaling in *B. subtilis*. *Cell* **89**: 917–925.

Le, A.T.T., and Schumann, W. (2009) The Spo0E phosphatase of *Bacillus subtilis* is a substrate of the FtsH metalloprotease. *Microbiology* **155**: 1122–1132.

Lederberg, E.M., and Cohen, S.N. (1974) Transformation of *Salmonella typhimurium* by plasmid deoxyribonucleic acid. *J Bacteriol* **119**: 1072–1074.

Lehnik-Habrink, M. (2011) An mRNA degradation complex in *Bacillus subtilis*. PhD thesis.

Lehnik-Habrink, M., Lewis, R.J., Mäder, U., and Stülke, J. (2012) RNA degradation in *Bacillus subtilis*: an interplay of essential endo- and exoribonucleases. *Mol Microbiol* **84**: 1005–1017.

Lehnik-Habrink, M., Newman, J., Rothe, F.M., Solovyova, A.S., Rodrigues, C., Herzberg, C., *et al.* (2011a) RNase Y in *Bacillus subtilis*: a natively disordered protein that is the functional equivalent of RNase E from *Escherichia coli*. *J Bacteriol* **193**: 5431–5441.

Lehnik-Habrink, M., Schaffer, M., Mäder, U., Diethmaier, C., Herzberg, C., and Stülke, J. (2011b) RNA processing in *Bacillus subtilis*: identification of targets of the essential RNase Y. *Mol Microbiol* **81**: 1459–1473.

Lewis, R.J., Brannigan, J.A., Offen, W.A., Smith, I., and Wilkinson, A.J. (1998) An evolutionary link between sporulation and prophage induction in the structure of a repressor:anti-repressor complex. *J Mol Biol* **283**: 907–912.

Leiman, S.A., Arboleda, L.C., Spina, J.S., and McLoon, A.L. (2014) SinR is a mutational target for fine-tuning biofilm formation in laboratory-evolved strains of *Bacillus subtilis*. *BMC Microbiol* **14**: 301.

Liu, J., Cosby, W.M., and Zuber, P. (1999) Role of lon and ClpX in the post-translational regulation of a sigma subunit of RNA polymerase required for cellular differentiation in *Bacillus subtilis*. *Mol Microbiol* **33**: 415–428.

Liu, B., Deikus, G., Bree, A., Durand, S., Kearns, D.B., and Bechhofer, D.H. (2014) Global analysis of mRNA decay intermediates in *Bacillus subtilis* wild-type and polynucleotide phosphorylase-deletion strains. *Mol Microbiol* **94**: 41–55.

Lockhorn, A. (2014) YmdB – ein RNA-bindenes Protein? Bachelor thesis.

Loomis, W.F. (2014) Cell signaling during development of *Dictyostelium*. *Dev Biol* **391**: 1–16.

López, D., Fischbach, M.A., Chu, F., Losick, R., and Kolter, R. (2009) Structurally diverse natural products that cause potassium leakage trigger multicellularity in *Bacillus subtilis*. *Proc Natl Acad Sci U S A* **106**: 280–285.

López, D., and Kolter, R. (2010) Extracellular signals that define distinct and coexisting cell fates in *Bacillus subtilis*. *FEMS Microbiol Rev* **34**: 134–149.

López, D., Vlamakis, H., and Kolter, R. (2010) Biofilms. *Cold Spring Harb Perspect Biol* **2**: a000398.

Ludwig, H., Homuth, G., Schmalisch, M., Dyka, F.M., Hecker, M., and Stülke, J. (2001) Transcription of glycolytic genes and operons in *Bacillus subtilis*: evidence for the presence of multiple levels of control of the *gapA* operon. *Mol Microbiol* **41**: 409–422.

Luria, S.E., and Delbrück, M. (1943) Mutations of Bacteria from Virus Sensitivity to Virus Resistance. *Genetics* **28**: 491–511.

Macek, B., Mijakovic, I., Olsen, J. V, Gnad, F., Kumar, C., Jensen, P.R., and Mann, M. (2007) The serine/threonine/tyrosine phosphoproteome of the model bacterium *Bacillus subtilis*. *Mol Cell Proteomics* **6**: 697–707.

Mackie, G.A. (1998) Ribonuclease E is a 5'-end-dependent endonuclease. *Nature* **395**: 720–723.

Magnuson, R., Solomon, J., and Grossman, A.D. (1994) Biochemical and genetic characterization of a competence pheromone from *B. subtilis*. *Cell* **77**: 207–216.

Mandic-Mulec, I., Doukhan, L., and Smith, I. (1995) The *Bacillus subtilis* SinR protein is a repressor of the key sporulation gene spo0A. *J Bacteriol* **177**: 4619–4627.

Martin-Verstraete, I., Débarbouillé, M., Klier, A., and Rapoport, G. (1994) Interactions of wild-type and truncated LevR of *Bacillus subtilis* with the upstream activating sequence of the levanase operon. *J Mol Biol* **241**: 178–192.

Marvasi, M., Visscher, P.T., and Casillas Martinez, L. (2010) Exopolymeric substances (EPS) from *Bacillus subtilis*: polymers and genes encoding their synthesis. *FEMS Microbiol Lett* **313**: 1–9.

Mathy, N., Bénard, L., Pellegrini, O., Daou, R., Wen, T., and Condon, C. (2007) 5'-to-3' exoribonuclease activity in bacteria: role of RNase J1 in rRNA maturation and 5' stability of mRNA. *Cell* **129**: 681–692.

McLoon, A.L., Guttenplan, S.B., Kearns, D.B., Kolter, R., and Losick, R. (2011) Tracing the domestication of a biofilm-forming bacterium. *J Bacteriol* **193**: 2027–2034.

Mehne, F.M.P., Gunka, K., Eilers, H., Herzberg, C., Kaever, V., and Stülke, J. (2013) Cyclic di-AMP homeostasis in *Bacillus subtilis*: both lack and high level accumulation of the nucleotide are detrimental for cell growth. *J Biol Chem* **288**: 2004–2017.

Meyer, F. M. (2009) Protein-Protein-Interaktionen im Cytratzyklus von *Bacillus subtilis*. Diploma thesis.

Mhatre, E., Monterrosa, R.G., and Kovács, A.T. (2014) From environmental signals to regulators: modulation of biofilm development in Gram-positive bacteria. *J Basic Microbiol* **54**: 616–632.

Mielich-Süss, B., and López, D. (2014) Molecular mechanisms involved in *Bacillus subtilis* biofilm formation. *Env Microbiol* **17**: 555-565.

Mielich-Süss, B., Schneider, J., and Lopez, D. (2013) Overproduction of flotillin influences cell differentiation and shape in *Bacillus subtilis*. *MBio* **4**: e00719–13.

Mijakovic, I., Petranovic, D., Macek, B., Cepo, T., Mann, M., Davies, J., *et al.* (2006) Bacterial single-stranded DNA-binding proteins are phosphorylated on tyrosine. *Nucleic Acids Res* **34**: 1588–1596.

Mijakovic, I., Poncet, S., Boël, G., Mazé, A., Gillet, S., Jamet, E., *et al.* (2003) Transmembrane modulator-dependent bacterial tyrosine kinase activates UDP-glucose dehydrogenases. *EMBO J* **22**: 4709–4718.

Monod, J. (1949) The Growth of Bacterial Cultures. *Annu Rev Microbiol* **3**: 371–394.

Morona, J.K., Morona, R., Miller, D.C., and Paton, J.C. (2003) Mutational analysis of the carboxy-terminal (YGX)4 repeat domain of CpsD, an autophosphorylating tyrosine kinase required for capsule biosynthesis in *Streptococcus pneumoniae*. *J Bacteriol* **185**: 3009–3019.

Morona, J.K., Paton, J.C., Miller, D.C., and Morona, R. (2000) Tyrosine phosphorylation of CpsD negatively regulates capsular polysaccharide biosynthesis in *Streptococcus pneumoniae*. *Mol Microbiol* **35**: 1431–1442.

Morona, R., Purins, L., Tocilj, A., Matte, A., and Cygler, M. (2009) Sequence-structure relationships in polysaccharide co-polymerase (PCP) proteins. *Trends Biochem Sci* **34**: 78–84.

Murray, E.J., Kiley, T.B., and Stanley-Wall, N.R. (2009) A pivotal role for the response regulator DegU in controlling multicellular behaviour. *Microbiology* **155**: 1–8.

Nakano, C., Ozawa, H., Akanuma, G., Funa, N., and Horinouchi, S. (2009) Biosynthesis of aliphatic polyketides by type III polyketide synthase and methyltransferase in *Bacillus subtilis*. *J Bacteriol* **191**: 4916–4923.

Nesterenko, M. V, Tilley, M., and Upton, S.J. (1994) A simple modification of Blum's silver stain method allows for 30 minute detection of proteins in polyacrylamide gels. *J Biochem Biophys Methods* **28**: 239–242.

Newman, J.A., and Lewis, R.J. (2013) Exploring the role of SlrR and SlrA in the SinR epigenetic switch. *Commun Integr Biol* **6**: e25658.

Newman, J.A., Rodrigues, C., and Lewis, R.J. (2013) Molecular basis of the activity of SinR protein, the master regulator of biofilm formation in *Bacillus subtilis*. *J Biol Chem* **288**: 10766–10778.

Nicolas, P., Mäder, U., Dervyn, E., Rochat, T., Leduc, A., Pigeonneau, N., *et al.* (2012) Condition-dependent transcriptome reveals high-level regulatory architecture in *Bacillus subtilis*. *Science* **335**: 1103–1106.

Noort, V. van, Seebacher, J., Bader, S., Mohammed, S., Vonkova, I., Betts, M.J., *et al.* (2012) Cross-talk between phosphorylation and lysine acetylation in a genome-reduced bacterium. *Mol Syst Biol* **8**: 571.

Norman, T.M., Lord, N.D., Paulsson, J., and Losick, R. (2013) Memory and modularity in cell-fate decision making. *Nature* **503**: 481–486.

Ohlsen, K.L., Grimsley, J.K., and Hoch, J.A. (1994) Deactivation of the sporulation transcription factor Spo0A by the Spo0E protein phosphatase. *Proc Natl Acad Sci U S A* **91**: 1756–1760.

Olivares-Illana, V., Meyer, P., Bechet, E., Gueguen-Chaignon, V., Soulat, D., Lazereg-Riquier, S., *et al.* (2008) Structural basis for the regulation mechanism of the tyrosine kinase CapB from *Staphylococcus aureus*. *PLoS Biol* **6**: e143.

Ostrowski, A., Mehert, A., Prescott, A., Kiley, T.B., and Stanley-Wall, N.R. (2011) YuaB functions synergistically with the exopolysaccharide and TasA amyloid fibers to allow biofilm formation by *Bacillus subtilis*. *J Bacteriol* **193**: 4821–4831.

Paul, K., Nieto, V., Carlquist, W.C., Blair, D.F., and Harshey, R.M. (2010) The c-di-GMP binding protein YcgR controls flagellar motor direction and speed to affect chemotaxis by a “backstop brake” mechanism. *Mol Cell* **38**: 128–139.

Pawson, T., and Scott, J.D. (2005) Protein phosphorylation in signaling – 50 years and counting. *Trends Biochem Sci* **30**: 286–290.

Pechter, K.B., Meyer, F.M., Serio, A.W., Stülke, J., and Sonenshein, A.L. (2013) Two roles for aconitase in the regulation of tricarboxylic acid branch gene expression in *Bacillus subtilis*. *J Bacteriol* **195**: 1525–1537.

Percival, S.L., Hill, K.E., Williams, D.W., Hooper, S.J., Thomas, D.W., and Costerton, J.W. (2012) marvasiA review of the scientific evidence for biofilms in wounds. *Wound Repair Regen* **20**: 647–657.

Perego, M., and Hoch, J.A. (1991) Negative regulation of *Bacillus subtilis* sporulation by the *spo0E* gene product. *J Bacteriol* **173**: 2514–2520.

Persuh, M., Mandic-Mulec, I., and Dubnau, D. (2002) A MecA paralog, YpbH, binds ClpC, affecting both competence and sporulation. *J Bacteriol* **184**: 2310–2313.

Petranovic, D., Grangeasse, C., Macek, B., Abdillatef, M., Gueguen-Chaignon, V., Nessler, S., *et al.* (2009) Activation of *Bacillus subtilis* Ugd by the BY-kinase PtkA proceeds via phosphorylation of its residue tyrosine 70. *J Mol Microbiol Biotechnol* **17**: 83–89.

Petranovic, D., Michelsen, O., Zahradka, K., Silva, C., Petranovic, M., Jensen, P.R., and Mijakovic, I. (2007) *Bacillus subtilis* strain deficient for the protein-tyrosine kinase PtkA exhibits impaired DNA replication. *Mol Microbiol* **63**: 1797–1805.

Piton, J., Larue, V., Thillier, Y., Dorléans, A., Pellegrini, O., Li de la Sierra-Gallay, I., *et al.* (2013) *Bacillus subtilis* RNA deprotection enzyme RppH recognizes guanosine in the second position of its substrates. *Proc Natl Acad Sci U S A* **110**: 8858–8863.

Podgornaia, A.I., and Laub, M.T. (2013) Determinants of specificity in two-component signal transduction. *Curr Opin Microbiol* **16**: 156–162.

Piggot, P.J., and Hilbert, D.W. (2004) Sporulation of *Bacillus subtilis*. *Curr Opin Microbiol* **7**: 579–586.

Pooley, H.M., and Karamata, D. (1984) Genetic analysis of autolysin-deficient and flagellaless mutants of *Bacillus subtilis*. *J Bacteriol* **160**: 1123–1129.

Pietack, N. (2010) Investigation of Glycolysis in *Bacillus subtilis*. PhD thesis.

Pottathil, M., and Lazazzera, B.A. (2003) The extracellular Phr peptide-Rap phosphatase signaling circuit of *Bacillus subtilis*. *Front Biosci* **8**: d32–d45.

Pozsgai, E.R., Blair, K.M., and Kearns, D.B. (2012) Modified mariner transposons for random inducible-expression insertions and transcriptional reporter fusion insertions in *Bacillus subtilis*. *Appl Environ Microbiol* **78**: 778–785.

Prajapati, R.S., Ogura, T., and Cutting, S.M. (2000) Structural and functional studies on an FtsH inhibitor from *Bacillus subtilis*. *Biochim Biophys Acta* **1475**: 353–359.

Prepiak, P., and Dubnau, D. (2007) A peptide signal for adapter protein-mediated degradation by the AAA+ protease ClpCP. *Mol Cell* **26**: 639–647.

Ravikumar, V., Shi, L., Krug, K., Derouiche, A., Jers, C., Cousin, C., *et al.* (2014) Quantitative phosphoproteome analysis of *Bacillus subtilis* reveals novel substrates of the kinase PrkC and phosphatase PrpC. *Mol Cell Proteomics* **13**: 1965–1978.

Richards, J., Liu, Q., Pellegrini, O., Celesnik, H., Yao, S., Bechhofer, D.H., *et al.* (2011) An RNA pyrophosphohydrolase triggers 5'-exonucleolytic degradation of mRNA in *Bacillus subtilis*. *Mol Cell* **43**: 940–949.

Romeo, T., Vakulskas, C.A., and Babitzke, P. (2013) Post-transcriptional regulation on a global scale: form and function of Csr/Rsm systems. *Environ Microbiol* **15**: 313–324.

Romero, D., Aguilar, C., Losick, R., and Kolter, R. (2010) Amyloid fibers provide structural integrity to *Bacillus subtilis* biofilms. *Proc Natl Acad Sci U S A* **107**: 2230–2234.

Romero, D., Vlamakis, H., Losick, R., and Kolter, R. (2011) An accessory protein required for anchoring and assembly of amyloid fibres in *B. subtilis* biofilms. *Mol Microbiol* **80**: 1155–1168.

Romero, D., Vlamakis, H., Losick, R., and Kolter, R. (2014) Functional analysis of the accessory protein TapA in *Bacillus subtilis* amyloid fiber assembly. *J Bacteriol* **196**: 1505–1513.

Römling, U., and Balsalobre, C. (2012) Biofilm infections, their resilience to therapy and innovative treatment strategies. *J Intern Med* **272**: 541–561.

Rothe, F. (2012) Regulation der Aktivität und Lokalisation von Antiterminatorproteinen der BglG-Familie. PhD thesis.

Ross, P., Weinhouse, H., Aloni, Y., Michaeli, D., Weinberger-Ohana, P., Mayer, R., *et al.* (1987) Regulation of cellulose synthesis in *Acetobacter xylinum* by cyclic diguanylic acid. *Nature* **325**: 279–281.

Roth, J.R., Kugelberg, E., Reams, A.B., Kofoid, E., and Andersson, D.I. (2006) Origin of mutations under selection: the adaptive mutation controversy. *Annu Rev Microbiol* **60**: 477–501.

Sale, J.E., Lehmann, A.R., and Woodgate, R. (2012) Y-family DNA polymerases and their role in tolerance of cellular DNA damage. *Nat Rev Mol Cell Biol* **13**: 141–152.

Sandegren, L., and Andersson, D.I. (2009) Bacterial gene amplification: implications for the evolution of antibiotic resistance. *Nat Rev Microbiol* **7**: 578–588.

Sambrook, J., E. F. Fritsch, and T. Maniatis (1989) Molecular cloning: a laboratory manual, 2nd ed. *Cold Spring Harbor Laboratory Press*, Cold Spring Harbor, NY.

Sanger, F., Nicklen, S., and Coulson, A.R. (1977) DNA sequencing with chain-terminating inhibitors. *Proc Natl Acad Sci U S A* **74**: 5463–5467.

Sanson, B., and Uzan, M. (1993) Dual role of the sequence-specific bacteriophage T4 endoribonuclease RegB. mRNA inactivation and mRNA destabilization. *J Mol Biol* **233**: 429–446.

Schlessinger, J. (2000) Cell signaling by receptor tyrosine kinases. *Cell* **103**: 211–225.

Schilling, O., Herzberg, C., Hertrich, T., Vörsmann, H., Jessen, D., Hübner, S., *et al.* (2006) Keeping signals straight in transcription regulation: specificity determinants for the interaction of a family of conserved bacterial RNA-protein couples. *Nucleic Acids Res* **34**: 6102–6115.

Schneider, C.A., Rasband, W.S., and Eliceiri, K.W. (2012) NIH Image to ImageJ: 25 years of image analysis. *Nat Methods* **9**: 671–675.

Sekiguchi, J., Ohsu, H., Kuroda, A., Moriyama, H., and Akamatsu, T. (1990) Nucleotide sequences of the *Bacillus subtilis flaD* locus and a *B. licheniformis* homologue affecting the autolysin level and flagellation. *J Gen Microbiol* **136**: 1223–1230.

Shahbabian, K., Jamalli, A., Zig, L., and Putzer, H. (2009) RNase Y, a novel endoribonuclease, initiates riboswitch turnover in *Bacillus subtilis*. *EMBO J* **28**: 3523–3533.

Shi, L., Pigeonneau, N., Ravikumar, V., Dobrinic, P., Macek, B., Franjevic, D., *et al.* (2014a) Cross-phosphorylation of bacterial serine/threonine and tyrosine protein kinases on key regulatory residues. *Front Microbiol* **5**: 495.

Shi, L., Pigeonneau, N., Ventroux, M., Derouiche, A., Bidnenko, V., Mijakovic, I., and Noirot-Gros, M.-F. (2014b) Protein-tyrosine phosphorylation interaction network in *Bacillus subtilis* reveals new substrates, kinase activators and kinase cross-talk. *Front Microbiol* **5**: 538.

Shin, D.H., Proudfoot, M., Lim, H.J., Choi, I.-K., Yokota, H., Yakunin, A.F., *et al.* (2008) Structural and enzymatic characterization of DR1281: A calcineurin-like phosphoesterase from *Deinococcus radiodurans*. *Proteins* **70**: 1000–1009.

Slechta, E.S., Harold, J., Andersson, D.I., and Roth, J.R. (2002) The effect of genomic position on reversion of a *lac* frameshift mutation (*lacIZ33*) during non-lethal selection (adaptive mutation). *Mol Microbiol* **44**: 1017–1032.

Sondermann, H., Shikuma, N.J., and Yildiz, F.H. (2012) You've come a long way: c-di-GMP signaling. *Curr Opin Microbiol* **15**: 140–146.

Solomon, J.M., Lazazzera, B.A., and Grossman, A.D. (1996) Purification and characterization of an extracellular peptide factor that affects two different developmental pathways in *Bacillus subtilis*. *Genes Dev* **10**: 2014–2024.

Soulat, D., Grangeasse, C., Vaganay, E., Cozzone, A.J., and Duclos, B. (2007) UDP-acetyl-mannosamine dehydrogenase is an endogenous protein substrate of *Staphylococcus aureus* protein-tyrosine kinase activity. *J Mol Microbiol Biotechnol* **13**: 45–54.

Soulat, D., Jault, J.-M., Duclos, B., Geourjon, C., Cozzone, A.J., and Grangeasse, C. (2006) *Staphylococcus aureus* operates protein-tyrosine phosphorylation through a specific mechanism. *J Biol Chem* **281**: 14048–14056.

Soper, T., Mandin, P., Majdalani, N., Gottesman, S., and Woodson, S.A. (2010) Positive regulation by small RNAs and the role of Hfq. *Proc Natl Acad Sci U S A* **107**: 9602–9607.

Spangler, C., Böhm, A., Jenal, U., Seifert, R., and Kaever, V. (2010) A liquid chromatography-coupled tandem mass spectrometry method for quantitation of cyclic di-guanosine monophosphate. *J Microbiol Methods* **81**: 226–231.

Stanley, N.R., and Lazazzera, B.A. (2005) Defining the genetic differences between wild and domestic strains of *Bacillus subtilis* that affect poly-gamma-DL-glutamic acid production and biofilm formation. *Mol Microbiol* **57**: 1143–1158.

Stöver, A.G., and Driks, A. (1999a) Secretion, localization, and antibacterial activity of TasA, a *Bacillus subtilis* spore-associated protein. *J Bacteriol* **181**: 1664–1672.

Stöver, A.G., and Driks, A. (1999b) Control of synthesis and secretion of the *Bacillus subtilis* protein YqxM. *J Bacteriol* **181**: 7065–7069.

Strauch, M., Webb, V., Spiegelman, G., and Hoch, J.A. (1990) The Spo0A protein of *Bacillus subtilis* is a repressor of the *abrB* gene. *Proc Natl Acad Sci U S A* **87**: 1801–1805.

Subramaniam, A.R., Deloughery, A., Bradshaw, N., Chen, Y., O'Shea, E., Losick, R., and Chai, Y. (2013) A serine sensor for multicellularity in a bacterium. *Elife* **2**: e01501.

Sudarsan, N., Lee, E.R., Weinberg, Z., Moy, R.H., Kim, J.N., Link, K.H., and Breaker, R.R. (2008) Riboswitches in eubacteria sense the second messenger cyclic di-GMP. *Science* **321**: 411–413.

Sureka, K., Choi, P.H., Precit, M., Delince, M., Pensinger, D.A., Huynh, T.N., *et al.* (2014) The Cyclic Dinucleotide c-di-AMP Is an Allosteric Regulator of Metabolic Enzyme Function. *Cell* **158**: 1389–1401.

Szurmant, H., and Hoch, J.A. (2010) Interaction fidelity in two-component signaling. *Curr Opin Microbiol* **13**: 190–197.

Terra, R., Stanley-Wall, N.R., Cao, G., and Lazazzera, B.A. (2012) Identification of *Bacillus subtilis* SipW as a bifunctional signal peptidase that controls surface-adhered biofilm formation. *J Bacteriol* **194**: 2781–2790.

Tholen, S. (2009) Charakterisierung des *gudB*-Gens aus *Bacillus subtilis*. Diploma thesis.

Tschowri, N., Schumacher, M.A., Schlimpert, S., Chinnam, N.B., Findlay, K.C., Brennan, R.G., and Buttner, M.J. (2014) Tetrameric c-di-GMP mediates effective transcription factor dimerization to control *Streptomyces* development. *Cell* **158**: 1136–1147.

Tuckerman, J.R., Gonzalez, G., Sousa, E.H.S., Wan, X., Saito, J.A., Alam, M., and Gilles-Gonzalez, M.-A. (2009) An oxygen-sensing diguanylate cyclase and phosphodiesterase couple for c-di-GMP control. *Biochemistry* **48**: 9764–9774.

Turgay, K., Hahn, J., Burghoorn, J., and Dubnau, D. (1998) Competence in *Bacillus subtilis* is controlled by regulated proteolysis of a transcription factor. *EMBO J* **17**: 6730–6738.

Uzan, M., Favre, R., and Brody, E. (1988) A nuclease that cuts specifically in the ribosome binding site of some T4 mRNAs. *Proc Natl Acad Sci U S A* **85**: 8895–8899.

Vlamakis, H., Chai, Y., Beauregard, P., Losick, R., and Kolter, R. (2013) Sticking together: building a biofilm the *Bacillus subtilis* way. *Nat Rev Microbiol* **11**: 157–168.

Wach, A. (1996) PCR-synthesis of marker cassettes with long flanking homology regions for gene disruptions in *S. cerevisiae*. *Yeast* **12**: 259–265.

Wang, P., Robert, L., Pelletier, J., Dang, W.L., Taddei, F., Wright, A., and Jun, S. (2010) Robust growth of *Escherichia coli*. *Curr Biol* **20**: 1099–1103.

Whitfield, C. (2006) Biosynthesis and assembly of capsular polysaccharides in *Escherichia coli*. *Annu Rev Biochem* **75**: 39–68.

Wiegert, T., and Schumann, W. (2001) SsrA-mediated tagging in *Bacillus subtilis*. *J Bacteriol* **183**: 3885–3889.

Wicht, S. (2010) Die Rolle von YmdB bei der Biofilmbildung in *Bacillus subtilis*.

Winkelman, J.T., Bree, A.C., Bate, A.R., Eichenberger, P., Gourse, R.L., and Kearns, D.B. (2013) RemA is a DNA-binding protein that activates biofilm matrix gene expression in *Bacillus subtilis*. *Mol Microbiol* **88**: 984–997.

Winkler, A., Udvarhelyi, A., Hartmann, E., Reinstein, J., Menzel, A., Shoeman, R.L., and Schlichting, I. (2014) Characterization of elements involved in allosteric light regulation of phosphodiesterase activity by comparison of different functional BlrP1 states. *J Mol Biol* **426**: 853–868.

Wugeditsch, T., Paiment, A., Hocking, J., Drummelsmith, J., Forrester, C., and Whitfield, C. (2001) Phosphorylation of Wzc, a tyrosine autokinase, is essential for assembly of group 1 capsular polysaccharides in *Escherichia coli*. *J Biol Chem* **276**: 2361–2371.

Yasbin, R.E., and Young, F.E. (1974) Transduction in *Bacillus subtilis* by bacteriophage SPP1. *J Virol* **14**: 1343–1348.

Yepes, A., Schneider, J., Mielich, B., Koch, G., García-Betancur, J.-C., Ramamurthi, K.S., *et al.* (2012) The biofilm formation defect of a *Bacillus subtilis* flotillin-defective mutant involves the protease FtsH. *Mol Microbiol* **86**: 457–471.

Zhang, Q., Lambert, G., Liao, D., Kim, H., Robin, K., Tung, C., *et al.* (2011) Acceleration of emergence of bacterial antibiotic resistance in connected microenvironments. *Science* **333**: 1764–1767.

Internet sources: http://www.lukemiller.org/ImageJ_gel_analysis.pdf (November 2014)

7. Appendix

7.1. Materials

7.1.1. Chemicals

Acrylamide	Carl Roth, Karlsruhe
Agar	Carl Roth, Karlsruhe
Agarose	Peqlab, Erlangen
Ammonium iron(III) citrate	Sigma-Aldrich, Taufkirchen
Ammonium persulfate	Sigma-Aldrich, Taufkirchen
Antibiotics	Carl Roth, Karlsruhe
	Sigma-Aldrich, Taufkirchen
Blocking reagent	Roche Diagnostics, Mannheim
β-mercaptoethanol	Sigma-Aldrich, Taufkirchen
Bromophenol blue	Serva, Heidelberg
Casein, acidic / hydrolysed	Sigma-Aldrich, Taufkirchen
CDP*	Roche Diagnostics, Mannheim
Coomassie Brillant Blue, R350	Amersham, Freiburg
D(+)-Glucose	Merck, Darmstadt
D-Desthiobiotin	IBA, Göttingen
dNTPs	Roche Diagnostics, Mannheim
Ethidium bromide	Sigma-Aldrich, Taufkirchen
Paraformaldehyde	Carl Roth, Karlsruhe
Yeast extract	Oxoid, Heidelberg
Skim milk powder, fat-free	Carl Roth, Karlsruhe
Sodium dodecyl sulfate	Serva, Heidelberg
Stains all dye	AppliChem, Darmstadt
Nutrient broth	Carl Roth, Karlsruhe
Strep-Tactin Sepharose™	IBA, Göttingen
Ni^{2+}-NTA Sepharose	IBA, Göttingen
TEMED	Carl Roth, Karlsruhe
Tryptone	Oxoid, Heidelberg
Tween 20	Sigma, München
X-Gal	Peqlab, Erlangen

Other chemicals were purchased from Merck, Serva, Sigma-Aldrich or Carl Roth.

7.1.2. Utilities

6-well plates	SPL Life Sciences, South Korea
24-well plates	TPP, Switzerland
Single-use syringes (5 ml, 10 ml)	Becton Dickinson Drogheda, Ireland
Reaction tubes	Greiner, Nürtingen
Falcon tubes	Sarstedt, Nürmbrecht
Gene Amp Reaction Tubes (PCR)	Perkin Elmer, Weiterstadt
Glas pipettes	Brand, Wertheim
Cuvettes (microlitre, plastic)	Greiner, Nürtingen
Petri dishes	Greiner, Nürtingen
Microlitre pipettes (2µl, 20µl, 200µl, 1000µl)	Eppendorf, Hamburg & Gilson, Düsseldorf
Nylon membrane, positively charged	Roche Applied Science
Pipette tips	Sarstedt, Nürmbrecht
Poly-Prep Chromatography Columns	Bio-Rad Laboratories GmbH, München
Polyvinylidene fluoride membrane (PVDF)	Bio-Rad Laboratories GmbH, München
Centrifuge cups	Beckmann, München

7.1.3. Equipment

Fluorescence microscope Axioskop 40 FL + camera AxioCam MRm	Carl Zeiss, Göttingen
SteREO Lumar.V12 stereo microscope	Carl Zeiss, Göttingen
Steam autoclave	Zirbus, Bad Grund
Biofuge fresco	Heraeus Christ, Osterode
Blotting device VacuGene™XI	Amersham, Freiburg
ChemoCam Imager	Intas, Göttingen
High accuracy scale	Sartorius, Göttingen
Gel electrophoresis device	Waasetec, Göttingen
Heating bloc Dri Block DB3	Waasetec, Göttingen
Horizontal shaker	GFL, Burgwedel
Refrigarated centrifuge PrimoR	Heraeus Christ, Osterode
Incubator shaker Innova 2300	New Brunswick, Neu-Isenburg
Magnetic stirrer	JAK Werk, Staufen
Mikro-Dismembrator S	Satorius, Göttingen
pH meter	Knick, Berlin

Nanodrop ND-1000	Thermo Scientific, Bonn
French pressure cell press	G. Heinemann, Schwäbisch Gmünd
Standard power pac	Bio-Rad Laboratories, California, USA
Spectral photometer Ultraspec 2000	Amersham, Freiburg
Thermocycler Tpersonal, LabCycler	SensorQuest, Göttingen
Ultracentrifuge Sorvall WX Ultra Pro 80	Thermoscientific, Bonn
Scale Sartorius universal	Sartorius, Göttingen
Water desalination plant	Millipore, Schwalbach

7.1.4. Commercial systems

Gene Ruler DNA ladder mix	Thermo Scientific, St. Leon-Rot
iScript One-Step RT-PCR kit with SYBR green	Bio-Rad Laboratories GmbH, München
Nucleospin Plasmid kit	Macherey-Nagel, Düren
QIAquick PCR-Purification kit	Qiagen, Hilden
DNeasy Blood&Tissue Kit (250)	Qiagen, Hilden
RNeasy Plus Mini Kit (50)	Qiagen, Hilden
Unstained Protein Marker	Thermo Scientific, St. Leon-Rot
Prestained Protein Marker	Thermo Scientific, St. Leon-Rot

7.1.5. Antibodies and enzymes

Rabbit anti-FLAG polyclonal antibodies	Sigma-Aldrich, Hamburg
Secondary antibody anti-rabbit IgG-AP coupled	Promega, Mannheim
RNase A	Roche Diagnostics, Mannheim
DNase I	Thermo Scientific, Lithuania
Lysozyme from chicken egg white	Carl Roth, Karlsruhe
Phusion™ DNA polymerase	Finnzymes, Espoo Finland
Restriction endonucleases	Thermo Scientific, Lithuania
FastAP alkaline phosphatase	Thermo Scientific, St. Leon-Rot
T4 DNA ligase	Thermo Scientific, Lithuania
Taq DNA polymerase	Roche Diagnostics, Mannheim

7.2. Bacterial strains

Table 7.1. *B. subtilis* strains constructed in this work

[1]arrows indicate construction by transformation, asteriks by SPP1 phage transduction

Name	Genotype	Construction[1]
GP1517	*trpC2* Δ*epsA*::*aphA3* (w/o terminator)	LFH → 168
GP1518	*trpC2* Δ*epsB*::*aphA3* (w/o terminator)	LFH → 168
GP1519	*trpC2* Δ*epsAB*::*aphA3* (w/o terminator)	LFH → 168
GP1520	*trpC2* Δ*ptkA*::*spc* (w/o terminator)	LFH → 168
GP1521	*trpC2* Δ*epsB*::*aphA3* Δ*ptkA*::*spc*	GP1520 → GP1518
GP1522	*trpC2* P*xyl-epsA-gfpmut1*::*amyE spc* Δ*epsA*::*aphA3*	pGP2112 → 168
GP1523	*trpC2* P*xyl-epsB-gfpmut1*::*amyE spc* Δ*epsB*::*aphA3*	pGP2113 → 168
GP1524	*trpC2* Δ*epsA*::*aphA3* Δ*ptkA*::*spc*	GP1517 → GP1520
GP1525	*trpC2* Δ*epsAB*::*aphA3* Δ*ptkA*::*spc*	GP1519 → GP1520
GP1526	*trpC2 epsA-FLAG* 3x *spc*	pGP2127 → 168
GP1527	*trpC2* Δ*epsB*::*aphA3* Δ*ptkA*::*spc amyE::(hag-yfp cat)*	BP496 → GP1521
GP1528	*trpC2 sfp*$^+$ *ermC epsC*$^+$ *swrA*$^+$ *degQ*$^+$ *amyE*::*P-rapP phrP cat* (*yvzG*/*yvyD* Ω*spc*) Δ*epsAB*::*aphA3*	GP1519 → AM373
GP1529	*trpC2* Δ*tkmA-ptkA*::*spc* (w/o terminator)	LFH → 168
GP1530	*trpC2* Δ*epsB* Δ*tkmA-ptkA*::*spc*	GP1529 → GP1518
GP1531	*trpC2* Δ*epsB*::*aphA3* Δ*ptkA*::*spc lacA:: p(tapA-yfp ermC)*	DL714 → GP1521
GP1532	*trpC2* Δ*epsB*::*aphA3* Δ*ptkA*::*spc xkdE*::P_{xyl}-*epsB ermC*	pGP2129 → GP1521
GP1533	*trpC2 amyE*::P_{epsA}-*epsA*-FLAG **2x (!)** *cat*	pGP2128 (*Sca*I) → 168
GP1534	Δ*epsA*::*aphA3 epsC*$^-$	GP1517 → NCIB3610*
GP1535	*trpC2 sfp*$^+$ *ermc epsC*$^+$ *swrA*$^+$ *degQ*$^+$ *amyE*::*P-rapP phrP cat* (*yvzG*/*yvyD* Ω*spc*) Δ*epsB*::*aphA3*	GP1518 → ALM373
GP1536	*trpC2* Δ*epsA*::*aphA3* Δ*tkmA-ptkA*::*spc*	GP1517 → GP1529
GP1537	*trpC2 lacA::p(tapA-yfp ermC)*	DL714 → 168
GP1538	*trpC2* Δ*epsB*::*aphA3 lacA::p(tapA-yfp ermC)*	DL714 → GP1518
GP1539	*trpC2* Δ*ptkA*::*spc lacA::p(tapA-yfp ermC)*	DL714 → GP1520
GP1540	*sfp*$^+$ *ermC epsC*$^+$ *swrA*$^+$ *degQ*$^+$ *amyE*::*P-rapP phrP cat* (*yvzG*/*yvyD* Ω*spc*) Δ*epsA*::*aphA3*	GP1517 → ALM373
GP1541	*trpC2 epsB*-FLAG *3x spc*	pGP2131 → 168

GP1542	*trpC2 xkdE*::(P_{xyl}-*epsB ermC*)	pGP2129 → 168
GP1543	*trpC2* Δ*epsB*::*aphA3* Δ*ptkA*::*spc xkdE*::(P_{xyl}-*empty ermC*)	pGP886 → GP1521
GP1544	*trpC2 ptkA*::*ermC* (w/o terminator)	LFH → 168
GP1545	*trpC2 lacA::(P_{xyl}- spo0F aphA3)*	pGP2120 → 168
GP1546	*trpC2* Δ*epsB*::*aphA3* Δ*ptkA*::*spc* Δ*sinR::tet*	GP736 → GP1521
GP1547	*trpC2 epsB*-FLAG *spc 3x* Δ*sinR::tet*	GP736 → GP1541
GP1548	*trpC2 abrB*::*ermC* (w/o terminator)	LFH → 168
GP1549	*trpC2 epsAB::aphA3 epsC*$^+$ *ptkA::ermC*	GP1528 → GP1544
GP1550	*trpC2 epsAB::aphA3 epsC*$^+$ *ptkA::ermC sinR::spc*	TMB079 → GP1549
GP1556	*trpC2 ymdB::cat abrB::ermC*	GP1548 → GP922
GP1557	*trpC2 ymdB::cat sinR::spc abrB::ermC*	GP1548 → GP923
GP1558	*trpC2 ymdB::aphA3* (w/o terminator)	LFH → 168
GP1559	*trpC2 ymdB::aphA3 amyE::tapA-lacZ cat*	GP1558 → GP993
GP1560	*trpC2 ymdB::spc lacA::(P_{xyl}- spo0F aphA3)*	pGP2120 → GP583
GP1561	*amyE::p(tapA-yfp spc) bglS::(hag-cfp aphA3)*	BP494 → DL382*
GP1562	*sinR::spc*	TMB079 → NCIB3610*
GP1563	*trpC2* Δ*sunA*::*aphA3*	Δ*sunA* → 168
GP1564	*trpC2* Δ*sunA*::*aphA3 sinR*::*spc*	Δ*sunA* → TMB079
GP1565	*trpC2* Δ*sunAI*::*aphA3*	Δ*sunA* Δ*sunI* → 168
GP1566	*trpC2* Δ*tkmA*::*spc*	LFH → 168
GP1567	*trpC2* Δ*epsA*::*aphA3* Δ*tkmA*::*spc*	GP1566 → GP1517
GP1568	*trpC2* Δ*epsA*::*aphA3* Δ*tkmA*::*spc xkdE*::P_{xyl}-*epsA ermC*	pGP2147 → GP1567
GP1569	*trpC2 epsA-gfp spc*	pGP2148 → 168
GP1570	*trpC2 epsA-gfp spc* Δ*sinR*::*tet*	GP736 → GP1569
GP1571	*trpC2* Δ*tasA*::*cat*	LFH → 168
GP1572	*trpC2* Δ*epsB*::*aphA3* Δ*tkmA*::*spc*	GP1566 → GP1518
GP1573	*trpC2 ymdB::aphA3*	LFH → 168
GP1574	*ΔymdB::cat amyE::p(tapA-yfp spc) bglS::(hag-cfp aphA3)*	BP494 → GP846*
GP1575	Δ*epsB*::*aphA3 epsC*$^+$	GP1535 → NCIB3610*
GP1576	*trpC2 ymdB::aphA3 amyE::tapA-lacZ cat*	GP1573 → GP993
GP1577	Δ*epsB*::*aphA3* Δ*ptkA*-markerless	GP1535 → NRS2544*
GP1578	*trpC2* Δ*ymdB*::*spc* Δ*ltaSA*::*ermC*	GP1397 Δ*ltaSA* (*yfnI*) → GP583
GP1579	*trpC2* Δ*ptkA*::*spc* Δ*epsB*::*aphA3 xkdE*::P_{xyl}-*ptkA ermC*	pGP2151 → GP1521

GP1580	*trpC2 lacA*::P_{xyl}-*spoVS aphA3*	pGP2152 → 168
GP1581	*trpC2* Δ*ymdB*::*spc lacA*::P_{xyl}-*spoVS aphA3*	pGP2152 → GP583
GP1582	*trpC2 xkdE*::P_{xyl}-*ykoW ermC*	pGP2153 → 168
GP1583	*trpC2 lacA*::P_{xyl}-*yuxH aphA3*	pGP2154 → 168
GP1584	*trpC2* Δ*sinR*::*spc amyE*::P_{epsA}-*epsA-FLAG* **2x (!)** *cat*	pGP2128 → TMB079
GP1585	*trpC2 lacA*::P_{xyl}-*yuxH aphA3 xkdE*::P_{xyl}-*ykoW ermC*	GP1582 → GP1583
GP1586	Δ*tasA*::*cat*	GP1571 → NCIB3610*
GP1587	*trpC2* Δ*ptkA*::*cat* (w/o terminator)	LFH → 168
GP1588	*trpC2* Δ*epsA::aphA3 epsB-FLAG 3x spc*	GP1517 → GP1541
GP1589	*trpC2 epsA-FLAG 3x spc* Δ*sinR::tet*	GP1526 → GP736
GP1590	*trpC2* Δ*yuxH::aphA3*	LHF → 168
GP1591	*trpC2* Δ*ytrP::tet*	LFH → 168
GP1592	*trpC2* Δ*ydaK::aphA3* (w/o terminator)	LFH → 168
GP1593	*trpC2* Δ*ymdB::spc* Δ*ykuI::tet* Δ*ykoW::cat*	GP1324 → GP714
GP1594	*trpC2* Δ*yybT::spc* Δ*yhcK::ermC* Δ*ykoW::cat*	GP998 → GP715
GP1595	*trpC2* Δ*ymdB::spc* Δ*yuxH::aphA3* Δ*ykuI::tet* Δ*ykoW::cat*	GP1590 → GP1593
GP1596	*trpC2* Δ*ytrP::tet* Δ*yybT::spc* Δ*yhcK::ermC* Δ*ykoW::cat*	GP1591 → GP1594
GP1597	*trpC2* Δ*yuxH::aphA3* Δ*ykuI::tet*	GP1324 → GP1590
GP1598	*trpC2* Δ*ydaK:: aphA3* Δ*ytrP::tet* Δ*yybT::spc* Δ*yhcK::ermC* Δ*ykoW::cat*	GP1592 → GP1596
GP1599	*trpC2* Δ*ykoW::cat* Δ*yuxH::aphA3* Δ*ykuI::tet*	GP850 → GP1597
GP1600	Δ*epsA*::*aphA3 epsC*$^{+}$	GP1540 → NCIB3610*
GP1601	*trpC2* Δ*spoVS*::*cat*	LFH → 168
GP1602	Δ*tkmA*::*spc*	GP1566 → NCIB3610*
GP1603	Δ*epsB*::*aphA3* Δ*sinR*::*spc*	GP1562 → GP1575
GP1604	Δ*ptkA* Δ*sinR*::*spc*	GP1562 → NRS2544
GP1605	Δ*epsB*::*aphA3* Δ*ptkA-markerless* Δ*sinR*::*spc*	GP1562 → GP1577
GP1606	Δ*epsA-O::tet* Δ*sinR*::*spc*	GP1562 → NRS2450
GP1607	Δ*epsB*::*aphA3* Δ*tkmA::spc*	GP1602 → GP1575
GP1608	Δ*ptkA* Δ*epsA*::*aphA3*	GP1600 → NRS2544
GP1609	*trpC2* Δ*ptpZ*::*spc*	LFH → 168
GP1610	*trpC2* Δ*ptkA-ptpZ*::*spc*	LFH → 168
GP1611	Δ*epsA*::*aphA3* Δ*tkmA::spc*	GP1602 → GP1600*
GP1612	*trpC2 amyE*::P_{lutA}-*lacZ*	pGP2149 → 168

GP1613	*trpC2* Δ*sinR*::*spc amyE*::P_{lutA}-*lacZ*	pGP2149 → TMB079
GP1614	*trpC2 amyE*::P_{ywbD}-*lacZ*	pGP2150 → 168
GP1615	*trpC2* Δ*sinR*::*spc amyE*::P_{ywbD}-*lacZ*	pGP2150 → TMB079
GP1616	Δ*ptpZ*::*spc*	GP1609 → NCIB3610*
GP1617	Δ*ptkA-ptpZ*::*spc*	GP1610 → NCIB3610*
GP1618	*(ymdB- cat)*	GP966 → NCIB3610*
GP1619	*ymdB*^{E39Q}*- cat*	GP969 → NCIB3610*
GP1620	*trpC2 tkmA*-FLAG	pGP2167 → 168
GP1621	*trpC2* Δ*epsA tkmA*-FLAG	pGP2167 → GP1517
GP1622	Δ*sinR-tasA*::*cat*	GP1672 → NCIB3610*
GP1623	Δ*epsB*::*aphA3* Δ*sinR-tasA*::*cat*	GP1672 → GP1575*
GP1624	Δ*ptkA*-markerless Δ*sinR-tasA*::*cat*	GP1672 → NRS2544*
GP1625	Δ*epsB*::*aphA3* Δ*ptkA*-markerless Δ*sinR-tasA*::*cat*	GP1672 → GP1577*
GP1626	Δ*epsA*::*aphA3* Δ*sinR-tasA*::*cat*	GP1672 → GP1600*
GP1627	Δ*tkmA*::*spc* Δ*sinR-tasA*::*cat*	GP1672 → GP1602*
GP1628	Δ*epsA*::*aphA3* Δ*tkmA*::*spc* Δ*sinR-tasA*::*cat*	GP1672 → GP1611*
GP1629	Δ*epsA-O*::*tet* Δ*sinR-tasA*::*cat*	GP1672 → NRS2450*
GP1630	*trpC2 amyE*::P_{epsA}-*epsB* DxD-His-*lacI cat* Δ*sinR*::*spc*	TMB079 → NRS3338
GP1631	*trpC2 amyE*::P_{epsA}-His-*epsB* DxD-*lacI cat* Δ*sinR*::*spc*	TMB079 → NRS3339
GP1632	*trpC2 amyE*::P_{epsA}-*epsB*-His-*lacI cat* Δ*sinR*::*spc*	TMB079 → NRS3589
GP1633	*trpC2 amyE*::P_{epsA}-His-*epsB-lacI cat* Δ*sinR*::*spc*	TMB079 → NRS3590
GP1634	Δ*epsB*::*aphA3* Δ*ptkA*-markerless *xkdE*::P_{xyl}-*epsB ermC*	GP1542 → GP1577*
GP1635	Δ*epsB*::*aphA3* Δ*ptkA*-markerless *amyE*::P_{epsA}-*epsB lacI cat*	NRS2543 → GP1577*
GP1636	Δ*epsA*::*aphA3* Δ*tkmA*::*spc xkdE*::P_{xyl}-*epsA ermC*	GP1568 → GP1611*
GP1637	Δ*epsAB*::*aphA3*	GP1528 → NCIB3610*
GP1638	*ΔymdB::cat amyE::p(tapA-yfp spc) bglS::(hag-cfp aphA3)*	GP1574 suppressor (SinR operator between the *epsA* and *slrR* genes)
GP1639	*ΔymdB::cat amyE::p(tapA-yfp spc) bglS::(hag-cfp aphA3)*	GP1574 suppressor BpsA (BcsA): Val257Leu (GTG → CTG)
GP1640	*trpC2* Δ*ymdB*::*spc* P_{comG}-*gfp cat*	IDJ046 → GP583
GP1641	*amyE*::$P_{sspE\text{-}2G}$-*gfp cat*	stJS01 → NCIB3610*
GP1642	Δ*ymdB*::*spc amyE*::$P_{sspE\text{-}2G}$-*gfp cat*	stJS01 → GP921*

GP1643	P_{comG}-*gfp cat*	IDJ046 → NCIB3610*
GP1644	Δ*ymdB*::*spc* P_{comG}-*gfp cat*	IDJ046 → GP921*
GP1645	Δ*ymdB*::*spc* P_{skf}-*gfp cat*	IDJ053→ GP921*
GP1646	*ΔymdB::cat amyE::p(tapA-yfp spc) bglS::(hag-cfp aphA3)*	GP1574 suppressor (location not known)
GP1647	*ΔymdB::cat amyE::p(tapA-yfp spc) bglS::(hag-cfp aphA3)*	GP1574 suppressor (unknown location)
GP1648	*ΔymdB::cat amyE::p(tapA-yfp spc) bglS::(hag-cfp aphA3)*	GP1574 suppressor (unknown location)
GP1649	*ΔymdB::cat amyE::p(tapA-yfp spc) bglS::(hag-cfp aphA3)*	GP1574 suppressor SinR: Trp104Arg (TGG → AGG)
GP1650	*ΔymdB::cat amyE::p(tapA-yfp spc) bglS::(hag-cfp aphA3)*	GP1574 suppressor SinR: Ala85Thr (GCG → ACG)
GP1801	*ΔymdB::cat amyE::p(tapA-yfp spc) bglS::(hag-cfp aphA3)*	GP1574 suppressor SinR: Ala85Thr (GCG → ACG)
GP1802	*ΔymdB::cat amyE::p(tapA-yfp spc) bglS::(hag-cfp aphA3)*	GP1574 suppressor SinR: Ala85Thr (GCG → ACG)
GP1803	*ΔymdB::cat amyE::p(tapA-yfp spc) bglS::(hag-cfp aphA3)*	GP1574 suppressor SinR: Ala85Thr (GCG → ACG)
GP1804	*ΔymdB::cat amyE::p(tapA-yfp spc) bglS::(hag-cfp aphA3)*	GP1574 suppressor SinR: Ala85Thr (GCG → ACG)
GP1805	*ΔymdB::cat amyE::p(tapA-yfp spc) bglS::(hag-cfp aphA3)*	GP1574 suppressor SinR: Leu99Ser (TTA → TCA)
GP1806	*ΔymdB::cat amyE::p(tapA-yfp spc) bglS::(hag-cfp aphA3)*	GP1574 suppressor SinR: Ala85Thr (GCG → ACG)
GP1807	*ΔymdB::cat amyE::p(tapA-yfp spc) bglS::(hag-cfp aphA3)*	GP1574 suppressor SinR: Ala85Thr (GCG → ACG)
GP1808	*ΔymdB::cat amyE::p(tapA-yfp spc) bglS::(hag-cfp aphA3)*	GP1574 suppressor SinR: Ala85Thr (GCG → ACG)
GP1809	*ΔymdB::cat amyE::p(tapA-yfp spc) bglS::(hag-cfp aphA3)*	GP1574 suppressor SinR: Leu99Ser (TTA → TCA)
GP1810	*trpC2 ΔymdB::spc ΔpnpA::aphA3*	GP584 → GP583
GP1811	*trpC2 epsAB::aphA3 epsC*$^{+}$ *ptkA::ermC ΔmcsB::spc*	BP69 → GP1549
GP1812	*ΔbslA::cat*	NRS2097 suppr. (unknown location)
GP1813	*ΔbslA::cat*	NRS2097 suppr. (unknown location)
GP1814	*ΔepsB::aphA3 ΔptkA::spc*	GP1577 suppr. (unknown location)
GP1815	*ΔepsA-O::tet*	NRS2450 suppr. (unknown location)
GP1816	*ΔtasA::cat*	GP1586 suppr. (unknown location)

GP1817	*ΔtasA::cat*	GP1586 suppr. (unknown location)
GP1818	*ΔymdB::cat amyE::p(tapA-yfp spc) bglS::(hag-cfp aphA3) ΔsinR::tet*	GP736 → GP1574*
GP1819	*trpC2 ΔtasA::aphA3*	LFH → 168

Table 7.2. Foreign strains used in this work

Name	Genotype	Paper/ received from
E. coli		
BTH101	*F-, cya-99, araD139, galE15, galK16, rspL1 (Strr), hsdR2, mcrA1, mcrB1*	Euromedex, BACTH-System (Karimova *et al.*, 1998)
BL21	*F⁻, lon ompT* $r_B m_B$ *hsdS gal(*cI_{ts}*857 indI Sam7 nin5 lacUV5-T7 gene1)*	(Sambrook et al., 1989)
DH5α	*80dlacZΔM15, recA1, endA1, gyrA96, thi-1, hsdR17(rK,mK+),supE44,relA1, deoR,ΔlacZYAargF)U169*	Woodcock *et al.*, 1989
XL1 Blue	*recA1 endA1 gyrA96 thi-1 hsdR17 supE44 relA1 lac (F' proAB lacI*^{q} *ZΔ (M15 Tn10 (Tet*^{R}*))*	Stratagene
B. subtilis		
AM373	*sfp*$^+$ *ermC epsC*$^+$ *swrA*$^+$ *degQ*$^+$ *amyE::P-rapP phrP cat* (*yvzG/yvyD* Ω*spc*)	McLoon *et al.* (2011)
BP69	*trpc2 ΔmcsB::spc*	K. Gunka, AG Commichau
BP494	*trpC2 bglS::(hag-cfp aphA3)*	Bisicchia *et al.,* 2010; lab collection
BP496	*trpC2 amyE::(hag-yfp cat)*	Bisicchia *et al.,* 2010; lab collection
CJ1	Δ*ptkA* (w/o a marker)	Carsten Jers/ Ivan Mijakovic; lab collection
DL382	*amyE::p(tapA-yfp spc)* in NCIB3610	Daniel Lopez, Würzburg; lab collection
DL714	*trpC2 lacA:: p(tapA-yfp ermC)* in CU1065	Daniel Lopez, Würzburg; lab collection
GP583	*trpc2 ΔymdB::spc*	Diethmaier *et al.* (2011)
GP584	*trpc2 ΔpnpA::spc*	Pietack (2010) PhD thesis
GP714	*trpC2 ΔykoW::cat ΔymdB::spc*	K. Gunka
GP715	*trpC2 ΔyhcK::ermC ΔykoW::cat*	K. Gunka
GP736	*trpC2 sinR::tet*	C. Herzberg
GP846	*amyE::p(tapA-yfp spc) ΔymdB::cat*	K. Gunka
GP850	*trpC2 ΔykoW::cat*	K. Gunka
GP922	*trpC2 ΔymdB::cat*	Diethmaier *et al.* (2011)
GP923	*trpC2 ΔymdB::cat ΔsinR::spc*	Diethmaier *et al.* (2011)
GP966	*trpC2 (ymdB-cat)*	Diethmaier *et al.* (2014)
GP969	*trpC2 ymdB*^{E39Q}*- cat*	Diethmaier *et al.* (2014)

GP993	*trpC2 amyE::(tapA-lacZ cat)*	Diethmaier *et al.* (2011)
GP994	*trpC2 amyE::(tapA-lacZ cat) ΔymdB::spc*	Diethmaier *et al.* (2011)
GP1324	*trpC2 ΔykuI::tet*	Mehne (2013) PhD thesis
GP1397	*trpC2 lacA::(p_{xyl}cdaS$_{L44F}$ aphA3) ΔgdpP::spc ΔyfnI::ermC*	Mehne (2013) PhD thesis
GP1661	Δ*ymdB*::*spc*, SinR Trp104Leu (G311T)	Kruse (2013)
GP1672	*trpC2* Δ*sinR-tasA*::*cat*	Kruse (2013)
IDJ046	*trpC2* P_{comG}*-gfp cat*	De Jong *et al*. (2012) Environ Microbiol. **14**:3110-21
IDJ053	*trpC2* P_{skf}*-gfp cat*	De Jong *et al*. (2012) Environ Microbiol. **14**:3110-21
NCIB3610	undomesticated wild type	Branda *et al.* (2001); lab collection
NRS2097	NCIB3610 *bslA::cat*	Verhamme *et al.* (2009) Journal Bacteriol. **191**:100–108
NRS2450	NCIB3610 *epsA-O::tet*	N. Stanley-Wall, Dundee; Branda *et al.* (2006)
NRS2543	*trpC2 amyE*::P_{epsA}*-epsB lacI cat*	N. Stanley-Wall, Dundee
NRS2544	NCIB3610 *ptkA*-markerless	Kiley & Stanley-Wall (2010)
NRS3338	*trpC2 amyE*::P_{epsA}*-epsB* DxD-His-*lacI cat*	N. Stanley-Wall, Dundee
NRS3339	*trpC2 amyE*::P_{epsA}-His-*epsB* DxD *lacI cat*	N. Stanley-Wall, Dundee
NRS3589	*trpC2 amyE*::P_{epsA}*-epsB*-His-*lacI cat*	N. Stanley-Wall, Dundee
NRS3590	*trpC2 amyE*::P_{epsA}-His-*epsB lacI cat*	N. Stanley-Wall, Dundee
stJS01	*trpC2 amyE::*$P_{sspE\text{-}2G}$*-gfp cat*	O. Kuipers, Groningen
TMB079	*trpC2 sinR::spc*	Torsten Mascher
Δ*sunA*-Δ*yolF*	*trpC2* Δ*sunI*-Δ*sunA*::*aphA3*	Dubois *et al*. (2009) Antimicrob Agents Chemother. **53**:651-61
Δ*sunA*	*trpC2* Δ*sunA*::*aphA3*	Dubois *et al.* (2009)

7.3. Oligonucleotids

The oligonucleotids were purchased from Sigma-Aldrich, Hamburg, Germany.

Table 7.3. Oligonucleotids

[1]restriction sites are underlined, promoters are in italics

Name	Sequence[a]	Gene / purpose	Characteristics
JG51	CGACAGGCGGCTTGGCATAGG	LFH for the deletion of *epsA*, upstream-forward	
JG52	CCTATCACCTCAAATGGTTCGCTGCCATA ATAAGGGTGACGCCGATTGTG	LFH for the deletion of *epsA*, upstream-reverse	
JG53	CGAGCGCCTACGAGGAATTTGTATCGGG CAGCTCAGCGAGAGAACCG	LFH for the deletion of *epsA*, downstream-forward	

JG54	CGGCAGCAGCTAAACCGACAATAC	LFH for the deletion of *epsA*, downstream-reverse	
JG55	GACATACAAGCAATCCTCGGACTGG	sequencing primer, detection of *epsA* deletion, forward	
JG56	GGTAAGCAGTAATGCTCCGGAGTC	sequencing primer, detection of *epsA* deletion, reverse	
JG57	GGGAAGTGCAGTAAATTAGAGGAAAATCATG	LFH for the deletion of *epsB*, upstream-forward	
JG58	CCTATCACCTCAAATGGTTCGCTGGTCCGAATGGTGCGATATTGTTCCG	LFH for the deletion of *epsB*, upstream-reverse	
JG59	CGAGCGCCTACGAGGAATTTGTATCGCCGATACCGTTCTGAAAGCAAAAGATGC	LFH for the deletion of *epsB*, downstream-forward	
JG60	GCTTACTCCGGTTCGCACACATTC	LFH for the deletion of *epsB*, downstream-reverse	
JG61	GACGGATTCGTGTGAACGCCTC	sequencing primer, detection of *epsB* deletion, forward	
JG62	CCTTTGATGCGGTTCGAAATTTCGCTAG	sequencing primer, detection of *epsB* deletion, reverse	
JG63	GAGAACGTGACTGCCCGAATAAGAG	LFH for the deletion of *ptkA*, upstream-forward	
JG64	CCTATCACCTCAAATGGTTCGCTGGCAAATTCTATATTCGTGCGAATCGTCCG	LFH for the deletion of *ptkA*, upstream-reverse	
JG65	CGAGCGCCTACGAGGAATTTGTATCGGAAAGAGGCGCTTGCAACGTGC	LFH for the deletion of *ptkA*, downstream-forward	
JG66	CGGGTACAGCCTGTACAGATTTCTG	LFH for the deletion of *ptkA*, downstream-reverse	
JG67	GATGCATGCACATGAAATTGGTGAGCAG	sequencing primer, detection of *ptkA* deletion, forward	
JG68	CACCTGTCACAAGACCGACATAGC	sequencing primer, detection of *ptkA* deletion, reverse	
JG69	CGATACAAATTCCTCGTAGGCGCTCGGTTTCCACCATTTTTTCAATTTTTTTATAATTTTTTAATCTG	Amplification of the *spc*^{R} cassette from pDG1726, reverse	without terminator spec rev o.T
JG70	CTTGGCGAGCTGATTGTC	qRT-PCR PCR primer *epsC*, forward	
JG71	AATACGGGTCCCTCCAATAG	qRT-PCR PCR primer *epsC*, reverse	
JG72	AAATCTAGAGATGAATGAGAATATGAGTTTCAAAGAATTATATGCG	Amplification of *epsA* for BACTH, forward	*Xba*I
JG73	TTTGGTACCCGCTCCCCGAAATGTTTTATCCCGCG	Amplification of *epsA* for BACTH, reverse	*Kpn*I, without stop codon
JG74	AAATCTAGAGGTGATCTTTAGAAAAAAGAAAGCAAGGCGAG	Amplification of *epsB* for BACTH, forward	*Xba*I
JG75	TTTGGTACCCGGTAGGAATAGTGTTCCGATTTTTTCATTTTCTTTTTG	Amplification of *epsB* for BACTH, reverse	*Kpn*I, without stop codon
JG76	AAAGGTACCATGAATGAGAATATGAGTTTCAAAGAATTATATGCG	Amplification of *epsA* for pSG1154, forward	*Kpn*I
JG77	TTTGAATTCCTCCCCGAAATGTTTTATCCCGCG	Amplification of *epsA* for pSG1154, reverse	*Eco*RI, without stop codon
JG78	AAAGGTACCGTGATCTTTAGAAAAAAGAAAGCAAGGCGAG	Amplification of *epsB* for pSG1154, forward	*Kpn*I

JG79	TTTGAATTCGTAGGAATAGTGTTCCGATTTTTTCATTTTCTTTTTG	Amplification of *epsB* for pSG1154, reverse	*Eco*RI, without stop codon
JG80	AAAGGATCCATGAATGAGAATATGAGTTTCAAAGAATTATATGCG	Amplification of *epsA* for pSG1729, forward	*Bam*HI
JG81	TTTGAATTCTCACTCCCCGAAATGTTTTATCCCGC	Amplification of *epsA* for pSG1729, reverse	*Eco*RI
JG82	AAAGGATCCGTGATCTTTAGAAAAAAGAAAGCAAGGCGAG	Amplification of *epsB* for pSG1729, forward	*Bam*HI
JG83	TTTGAATTCCTAGTAGGAATAGTGTTCCGATTTTTTCATTTTCTTTTTG	Amplification of *epsB* for pSG1729, reverse	*Eco*RI
JG84	AAAGGATCCGTGATCTTTAGAAAAAAGAAAGCAAGGCGAG	Amplification of *epsB* for pGP380, forward	*Bam*HI
JG85	TTTGTCGACCTAGTAGGAATAGTGTTCCGATTTTTTCATTTTCTTTTTG	Amplification of *epsB* for pGP380, reverse	*Sal*I
JG86	AAACAATTGAAAGGAGGAAACAATCATGGATTACAAGGATGACGATGACAAGGATTAC	Amplification of the FLAG-tag from pGP1331; cloning into pBP7; N-terminal fusion; forward	*Mfe*I, RBS, start codon
JG87	TTTAGATCTGAATTCCCGGGGATCCCTTGTCATCGTCATCCTTGTAATCCTTGTC	Amplification of the FLAG-tag from pGP1331; cloning into pBP7; N-terminal fusion; reverse	*Bgl*II, MCS with *Eco*RI, *Sma*I and *Bam*HI
JG88	AAACAATTGGAATTCCCGGGGATCCGATTACAAGGATGACGATGACAAGGATTAC	Amplification of the FLAG-tag from pGP1331; cloning into pBP7; C-terminal fusion; forward	*Mfe*I, MCS with *Eco*RI, *Sma*I and *Bam*HI
JG89	TTTAGATCTTTATCACTTGTCATCGTCATCCTTGTAATCC	Amplification of the FLAG-tag from pGP1331; cloning into pBP7; C-terminal fusion; reverse	*Bgl*II
JG90	AAAGAATTCATGAATGAGAATATGAGTTTCAAAGAATTATATGCG	Amplification of *epsA*, forward	*Eco*RI
JG91	TTTGGATCCTCACTCCCCGAAATGTTTTATCCCGC	Amplification of *epsA*, reverse	*Bam*HI
JG92	GTGATCTTTAGAAAAAAGAAAGCAAGGCGAG	Amplification of *epsB*, forward	
JG93	CTAAGCGGAAGCGTGTTCCGATTTTTTCATTTTCTTTTTG	Amplification of *epsB*, reverse	mutagenesis Y225→A, Y227→A
JG94	GAGCGGAACGAAAGAAAAAAGATTTCTAGTGTCGCTTCACTCCCCGAAATGTTTTATCC	LFH for the mutagenesis of the C-terminal Y-cluster of *epsB*, upstream-reverse	
JG95	CAAAAAGAAAATGAAAAAATCGGAACACGCTTCCGCTTAGTTTTTGTAAAGGTGATGTCTCCTGACCTG	LFH for the mutagenesis of the C-terminal Y-cluster of *epsB*, downstream-forward	
JG96	TGTAAGCTTGGGAAGTGCAGTAAATTAGAGGAAAATCATG	cloning of *epsB* +/- 1000 bp into pBlueScript SK$^-$ for MMR, forward	*Hind*III
JG97	ACAGAATTCGCTTACTCCGGTTCGCACACATTC	cloning of *epsB* +/- 1000 bp into pBlueScript SK$^-$ for MMR, reverse	*Eco*RI
JG98	GAAAGTACTGCTGGTGGCTGCCGCTTTAAGAAAGCCGACCATC	mutagenesis of the Walker A' motif of *epsB* by CCR, 5'-phosphoprimer	Tm=71°C, D81A and D83A
JG99	AAATCTAGACTCAACAGCCAGCTGATTAATAGAATAGCC	Amplification of *epsB* +/- 1000 bp CCR, forward	*Xba*I
JG100	TTTGGTACCCCGGCAGTTCGTGTGCCAA	Amplification of *epsB* +/- 1000 bp	*Kpn*I

	GC	CCR, reverse	
JG101	ACAGGATCCTCGCTTCACTCCCCGAAATGTTTTATCC	Amplification of *epsB* upstream flank for markerless deletion, reverse	*Bam*HI
JG102	TGTGGATCCTTTTTGTAAAGGTGATGTCTCCTGACCTG	Amplification of *epsB* downstream flank for markerless deletion, forward	*Bam*HI
JG103	CAGACGGCAGCGTGCTCGTC	Sequencing of *epsB* C-terminal Y-cluster, forward	
JG104	CCGAATGGTGCGATATTGTTCCGC	Sequencing of the *epsB* upstream region, reverse	
JG105	TTTGGTACCCGGGCGGAAGCGTGTTCCGATTTTTTCATTTTCTTTTTG	Amplification of *epsB* for BACTH, reverse	*Kpn*I, mutagenesis Y225A, Y227A, w/o stop codon
JG106	ACATCTAGAATGAATGAGAATATGAGTTTCAAAGAATTATATGCG	Amplification of the entire *epsA* gene for pGP1331, forward	*Xba*I (cuts vector!)
JG107	TGTCTGCAGCTCCCCGAAATGTTTTATCCCGCG	Amplification of the last 600 bp of the *epsA* gene for pGP1331, reverse	*Pst*I
JG108	ACAGAATTCGTCGTTATTTCGTTCATTATAAGGAATTTTTCGTTC	Amplification of *epsA* with its promoter for pAC5, forward	*Eco*RI
JG109	AAAGGATCCAAAGGAGGAAACAATCGTGATCTTTAGAAAAAAGAAAGCAAGGCGAG	Amplification of *epsB* for pGP382, forward	*Bam*HI, *gapA* RBS
JG110	TTTGTCGACGTAGGAATAGTGTTCCGATTTTTTCATTTTCTTTTTG	Amplification of *epsB* for pGP382, reverse	*Sal*I, without a stop codon
JG111	ACAGGATCCGGTCATTTCACCGACCTACCAGG	Amplification of the last 600 bp of *epsA* for pGP1331, forward	*Bam*HI
JG112	TTTGGTACCCGTCACTAGTAGGAATAGTGTTCCGATTTTTTCATTTTCTTTTTG	Amplification of *epsB* for pGP886, reverse	*Kpn*I, 2x stop codon
JG113	TCATTGCGACACCTCATCAT	qRT-PCR PCR primer *ptpZ*, forward	
JG114	CCTCGCCGTAGATTCTGATT	qRT-PCR PCR primer *ptpZ*, reverse	
JG115	CCCACTCGCTCGAACATTGCATATAC	LFH for the deletion of *tkmA*, upstream-forward	
JG116	CCTATCACCTCAAATGGTTCGCTGCTAATGAGTCCGCCGGCAGCAG	LFH for the deletion of *tkmA*, upstream-reverse	
JG117	CGAGCGCCTACGAGGAATTTGTATCGCAGTTTCCACCATTGCGAATGAGCAG	LFH for the deletion of *tkmA*, downstream-forward	
JG118	CACACCGTTGTTATGATGAGGTGTCG	LFH for the deletion of *tkmA*, downstream-reverse	
JG119	CTTCTGGCGTACGTGCCTGCC	Sequencing primer, detection of *tkmA* deletion, forward	
JG120	CAAGGTCTTGTTCCACCTCGCC	Sequencing primer, detection of *tkmA* deletion, reverse	
JG121	AAAGGATCCATGATTATTGCGCTGGATACTTACCTCGT	Amplification of *epsC* for pGP380, forward	*Bam*HI
JG122	TTTGTCGACCTAATGAACGCTGGCAGCCGTC	Amplification of *epsC* for pGP380, reverse	*Sal*I

JG123	GAAATGCCTTGCGTACAACA	qRT-PCR PCR primer *bslA*, forward	
JG124	TCTCCGCACGGAAAGTATATG	qRT-PCR PCR primer *bslA*, reverse	
JG125	ACAGGATCCCGCACCATTCGGACAAACATTGAGTTC	Amplification of the last 600 bp of *epsB* for pGP1331, forward	*Bam*HI
JG126	ACAGTCGACCTCAACAGCCAGCTGATTAATAGAATAGCC	markerless deletion of *epsB* with pMAD, upstream-forward	*Sal*I
JG127	TGTGAATTCCCGGCAGTTCGTGTGCCAAGC	markerless deletion of *epsB* with pMAD, downstream-reverse	*Eco*RI
JG128	CCGCTCAATATCAACGAGCTGAGTTTC	LFH for the deletion of *abrB*, upstream-forward	
JG129	CCTATCACCTCAAATGGTTCGCTGGATAGGAATAACTACACGTCCTAATTCATCAAC	LFH for the deletion of *abrB*, upstream-reverse	
JG130	CGAGCGCCTACGAGGAATTTGTATCGGAAGGCGCTGAGCAAATCATCAGCG	LFH for the deletion of *abrB*, downstream-forward	
JG131	GCGGAACAGCAAGGAGGCTGTATATG	LFH for the deletion of *abrB*, downstream-reverse	
JG132	CGCGTATTTCCCCATGCGGAAG	Sequencing primer, detection of *abrB* deletion, forward	
JG133	CAACAAAGCGGGAAGCTATGCAGG	Sequencing primer, detection of *abrB* deletion, reverse	
JG134	AAAGGATCCAAAGGAGGAAACAATCATGATTATTGCGCTGGATACTTACCTCGT	Amplification of *epsC* for pGP382, forward	*Bam*HI, Shine dalgarno sequence (*gapA*)
JG135	TTTGTCGACATGAACGCTGGCAGCCGTCATTTCTTC	Amplification of *epsC* for pGP382, reverse	*Sal*I, without a stop codon
JG136	AAATCTAGAGATGATTATTGCGCTGGATACTTACCTCGT	*epsC* for BACTH, forward	*Xba*I
JG137	TTTGGTACCCGATGAACGCTGGCAGCCGTCATTTCTTC	*epsC* for BACTH, reverse	*Kpn*I, without a stop codon
JG138	GCAACGCGGGCATCCCGATG	pMAD sequencing, forward	
JG139	CCCAATATAATCATTTATCAACTCTTTTACACTTAAATTTCC	pMAD sequencing, reverse	
JG140	AAAGGATCCAAAGGAGGAAACAATCATGTGGAGGGACCCGTATTTTATCCAGAG	Amplification of a truncated *epsC* for pGP382, forward	*BamH*I, *gapA* RBS
JG141	TTTGGTACCCGTCACTAGGCGGAAGCGTGTTCCGATTTTTTCATTTTCTTTTTG	Cloning of *epsB* into pGP886, reverse	*Kpn*I, with two stop codons, mutagenesis Y225A/ Y227A
JG142	AAATCTAGAGTTGGCGCTTAGAAAAAACAGAGGCTCG	*ptkA* for BACTH, forward	*Xba*I
JG143	TTTGGTACCCGTTTTTGCATGAAATTGTCCTTGGTTCCGTAATATC	*ptkA* for BACTH, reverse	*Kpn*I, no stop codon
JG144	AAATCTAGAGATGGGAGAATCTACAAGCTTAAAAGAGATATTATC	*tkmA* for BACTH, forward	*Xba*I
JG145	TTTGGTACCCGAGCGCCAAAATGTCCACTCCCC	*tkmA* for BACTH, reverse	*Kpn*I, no stop codon
JG146	TTTGGTACCCGTCACTACTCCCCGAAATG	Amplification of *epsA* for pGP886,	*Kpn*I, 2x stop

	TTTTATCCCGCG	reverse	codon
JG147	GTCTGCTCATCCTGGTCCGGC	Sequencing primer, detection of *sinR* deletion, forward	
JG148	CATATACTGGGCCGTCTCGATGG	Sequencing primer, detection of *sinR* deletion, reverse	
JG149	AAAGAATTCCATATACTGCACTCCTGGGAGATCG	Amplification of the *lutA* (*yvfV*) promoter for pAC5, forward	*Eco*RI
JG150	AAAGGATCCGGAACAAGACAAGTGACAAAAAGTGAGACTTTCAT	Amplification of the *lutA* (*yvfV*) promoter for pAC5, reverse	*Bam*HI
JG151	AAAGAATTCGTTCGTGTGAGTGATGCGATCCTTC	Amplification of the *ywbD* promoter for pAC5, forward	*Eco*RI
JG152	AAAGGATCCGGAGCGTGTGCTTTTTTTAGGGTGAGTAGCTTCAT	Amplification of the *ywbD* promoter for pAC5, reverse	*Bam*HI
JG153	CGGCGATTCACTTTATAAAATTGAGACCAAG	LFH for the deletion of *tasA*, upstream-forward	
JG154	CCTATCACCTCAAATGGTTCGCTGGCTAATCCTAGTGCTGCAGAAGCAAC	LFH for the deletion of *tasA*, upstream-reverse	
JG155	CGAGCGCCTACGAGGAATTTGTATCGCGGCTTGACAATCAAAAAGGACCATACTG	LFH for the deletion of *tasA*, downstream-forward	
JG156	CAGGCGCTGAAAACCTTGTATCAACC	LFH for the deletion of *tasA*, downstream-reverse	
JG157	GTGGAAGTGGGAGCTTCATAAGCTTG	Sequencing primer, detection of *tasA* deletion, forward	
JG158	GACTGGGCGGAACAGGCGGT	Sequencing primer, detection of *tasA* deletion, reverse	
JG159	AAAGGTACCTCATTAGCGAGGCTCCACGATTAATTTAATCG	Amplification of *spoVS* for pGP888, reverse	*Kpn*I, 2x stop codon
JG160	AAAGGTACCTCATTATTTTTGCATGAAATTGTCCTTGGTTCCGTAATATC	Amplification of *ptkA* for pGP886, reverse	*Kpn*I, 2x stop codon
JG161	AAAGGTACCTCATTATTTTTGCATGAAATTGTCCTTGGTTCCGGCAGCTCCGGCTTCAGAG	Amplification of *ptkA* for pGP886, reverse	*Kpn*I, 2x stop codon, mutagenesis $Y^{225}A$, $Y^{227}A$, $Y^{228}A$
JG162	AAAGGTACCTCATTATTTTTGCATGAAATTGTCCTTGGTTCCGAAAAATCCGAATTCAGAG	Amplification of *ptkA* for pGP886, mutagenesis of Y225→F/ Y227→F/ Y228→F, reverse	*Kpn*I, 2x stop codon
JG163	AAATCTAGAGATGAGGGTGTTTGTTGCAAGACAGCC	Amplification of *yuxH* for pGP888, forward	*Xba*I
JG164	TTTGGTACCTCATCATTTTGCGTCCATAAGATTATGACACCATTC	Amplification of *yuxH* for pGP888, reverse	*Kpn*I, 2x stop codon
JG165	CAGTAAGTCCTCATCTTGCGGATTTATTGCA	Sequencing primer *yuxH*, reverse	
JG166	GCCTTCTTACTTGTCGGAATCTCTC	LFH for the deletion of *ydaK*, upstream-forward	
JG167	CCTATCACCTCAAATGGTTCGCTGGAGCACCTTCTGATTGCTGGGCTG	LFH for the deletion of *ydaK*, upstream-reverse	
JG168	CGAGCGCCTACGAGGAATTTGTATCGGTGTCGCTTACGTTCCACGTTTGC	LFH for the deletion of *ydaK*, downstream-forward	
JG169	CAAATCCCTCTCCTGTTTCACTGTAGC	LFH for the deletion of *ydaK*, downstream-reverse	

JG170	CAGTCGGCGACAGAAGTGAATGCC	Sequencing primer, detection of *ydaK* deletion, forward
JG171	GGTTCAAGATAGCTGTGATAGGCTTGTTC	Sequencing primer, detection of *ydaK* deletion, reverse
JG172	CGTTCAGGCATGCCGAACGCG	LFH for the deletion of *yuxH*, upstream-forward
JG173	CCTATCACCTCAAATGGTTCGCTGGATCGCCGTCTTTAGCGCTATACAC	LFH for the deletion of *yuxH*, upstream-reverse
JG174	CGAGCGCCTACGAGGAATTTGTATCGGCAACAACTGGGACACTTGCTCAGA	LFH for the deletion of *yuxH*, downstream-forward
JG175	CGTTTCTTTAATATCAAGTTCGAGTCGGAATAAC	LFH for the deletion of *yuxH*, downstream-reverse
JG176	CGCATGCGCTTGTGCAGGCTTAC	Sequencing primer, detection of *yuxH* deletion, forward
JG177	CTTGTTTCCAAGTCTTTTTCACGAAATTTTCATTGC	Sequencing primer, detection of *yuxH* deletion, reverse
JG178	GCGCTTCGTTAATTTCCGGAGCAAGTT	LFH for the deletion of *ytrP*, upstream-forward
JG179	CCTATCACCTCAAATGGTTCGCTGCGAAGTCAGCCATATGAAAGAGTCGG	LFH for the deletion of *ytrP*, upstream-reverse
JG180	CGAGCGCCTACGAGGAATTTGTATCGCTGCGGTATCTCCTGCTGGACG	LFH for the deletion of *ytrP*, downstream-forward
JG181	GATATTGCTTGCCGCTGTTTCAAGCG	LFH for the deletion of *ytrP*, downstream-reverse
JG182	GGCCAGCAAGAGGCGAAAGCC	Sequencing primer, detection of *ytrP* deletion, forward
JG183	CGAGTTAATTGACGATGATTATGCTGATAGG	Sequencing primer, detection of *ytrP* deletion, reverse
JG184	TGGCGATGTATGCGGCTAAA	qRT-PCR *ykoW*, forward
JG185	GCGGCTGATAATGCAAGACAA	qRT-PCR *ykoW*, reverse
JG186	TTGAGAAGCTGACGGAAGGG	qRT-PCR *yuxH*, forward
JG187	TGCATCTAGAAATGAGGGCCG	qRT-PCR *yuxH*, reverse
JG188	GAGGAGCAGAAGGTTGTCGG	qRT-PCR *ykuI*, forward
JG189	GTCAAGAGCCTGGCGGATAA	qRT-PCR *ykuI*, reverse
JG190	CAGAAGAAATCAAGCGGGCG	qRT-PCR *ydaK*, forward
JG191	CGCTTGTCCTGATTTGCTGAC	qRT-PCR *ydaK*, reverse
JG192	GGTGAAGAATTTGCCGTGCTC	qRT-PCR *yhcK*, forward
JG193	ATGAGCGGCCCCTAGTGATA	qRT-PCR *yhcK*, reverse
JG194	AGTGTGCAGCGTTTGATTGG	qRT-PCR *gdpP*, forward
JG195	CCGTTCCTCCATGACGAGTG	qRT-PCR *gdpP*, reverse
JG196	GTGACATGGTCAAAGAATATGTACCAAAGC	LFH for the deletion of *spoVS*, upstream-forward
JG197	CCTATCACCTCAAATGGTTCGCTGCTGCAAGCGCACCTGCCACTG	LFH for the deletion of *spoVS*, upstream-reverse
JG198	CGAGCGCCTACGAGGAATTTGTATCGCGGCTTTTACAGATATTCAAATCGATGGGG	LFH for the deletion of *spoVS*, downstream-forward
JG199	GCAAGCCTCAGCCTGTATTCATTCTTATC	LFH for the deletion of *spoVS*, downstream-reverse
JG200	GAGAGACTCGAGCCGTAGAGTATGC	Sequencing primer, detection of *spoVS* deletion, forward
JG201	CCTTCTCCACTCGTTAAAGCGCTTAC	Sequencing primer, detection of

		spoVS deletion, reverse	
JG202	AAATCTAGAGATGACGAAAAAGATATTGTTTTGCGCGACTG	Amplification of *epsD* for BACTH, forward	*Xba*I
JG203	TTTGGTACCCGTACGCTTTTCTCCTTTGTATCCATATCCATG	Amplification of *epsD* for BACTH, reverse	*Kpn*I
JG204	AAATCTAGAGATGAACTCAGGACCGAAAGTTTCTGTCATTATG	Amplification of *epsE* for BACTH, forward	*Xba*I
JG205	TTTGGTACCCGTTCATGCTTGACAAGCCCTTCCTTTTGG	Amplification of *epsE* for BACTH, reverse	*Kpn*I
JG206	AAATCTAGAGATGAATAGCAGCCAAAAGCGCGTGC	Amplification of *epsF* for BACTH, forward	*Xba*I
JG207	TTTGGTACCCGTCGGTTATGGTCCTTTTCCGTGCTG	Amplification of *epsF* for BACTH, reverse	*Kpn*I
JG208	AAATCTAGAGATGATTGTATATGCCGTCAATATGGGGATTG	Amplification of *epsG* for BACTH, forward	*Xba*I
JG209	TTTGGTACCCGCCGGGAAAAAATCGTTCTGTAAGGCAG	Amplification of *epsG* for BACTH, reverse	*Kpn*I
JG210	AAATCTAGAGATGGAAACACCTGCGGTTAGTCTGTTAG	Amplification of *epsH* for BACTH, forward	*Xba*I
JG211	TTTGGTACCCGCCCTCTGTTTCTCATTTTGTACTCGATCAC	Amplification of *epsH* for BACTH, reverse	*Kpn*I
JG212	AAATCTAGAGATGTCGTTACAATCGTTGAAAATCAATTTTGCAGAATG	Amplification of *epsI* for BACTH, forward	*Xba*I
JG213	TTTGGTACCCGTTGCGCTTCACCGCTGATTTTGTCAC	Amplification of *epsI* for BACTH, reverse	*Kpn*I
JG214	AAATCTAGAGATGATCCCGCTCGTCAGCATTATTGTC	Amplification of *epsJ* for BACTH, forward	*Xba*I
JG215	TTTGGTACCCGTGCCTGCTTCGCACTGCCTTTCATTC	Amplification of *epsJ* for BACTH, reverse	*Kpn*I
JG216	AAATCTAGAGATGAAATTCACGATAAATTTCAGCGCGAATCTC	Amplification of *epsK* for BACTH, forward	*Xba*I
JG217	TTTGGTACCCGAAGATTCACAGCTCCTTTCGTTTTTCGAAACC	Amplification of *epsK* for BACTH, reverse	*Kpn*I
JG218	AAATCTAGAGTTGATCCTGAAACGACTTTTTGATCTGACGG	Amplification of *epsL* for BACTH, forward	*Xba*I
JG219	TTTGGTACCCGTGAGGACACATCTCCGCTTCCGG	Amplification of *epsL* for BACTH, reverse	*Kpn*I
JG220	AAATCTAGAGATGAAAAATGTGGCCATTGTGGGTGACG	Amplification of *epsM* for BACTH, forward	*Xba*I
JG221	TTTGGTACCCGTCCTTTGTTTGATGTTTGAATGGAAGAAATGATGC	Amplification of *epsM* for BACTH, reverse	*Kpn*I
JG222	AAATCTAGAGATGCATAAAAAAATCTACTTATCTCCCCCTCATATG	Amplification of *epsN* for BACTH, forward	*Xba*I
JG223	TTTGGTACCCGTCGAATGCTTGCTGTCCATTTCTTCACC	Amplification of *epsN* for BACTH, reverse	*Kpn*I
JG224	AAATCTAGAGATGGACAGCAAGCATTCGATGATCAGC	Amplification of *epsO* for BACTH, forward	*Xba*I
JG225	TTTGGTACCCGCATGTGAGCAGGAAGGTTTTCCTTCTTTG	Amplification of *epsO* for BACTH, reverse	*Kpn*I
JG226	GATTGGCGGGAAGCATCGGACTG	LFH for the deletion of *ptpZ*, upstream-forward	

JG227	CCTATCACCTCAAATGGTTCGCTGGCCATTTCTATGCTGTCGGCCGAATC	LFH for the deletion of *ptpZ*, upstream-reverse	
JG228	CGAGCGCCTACGAGGAATTTGTATCGGCTTCTCCTGCGGAATCAGACCATC	LFH for the deletion of *ptpZ*, downstream-forward	
JG229	CCGCTTATCCTGTCCCATCCCG	LFH for the deletion of *ptpZ*, downstream-reverse	
JG230	CAATGTCAGCATTCTGTCAAAAGCCGAG	Sequencing primer, detection of *ptpZ* deletion, forward	
JG231	GGCAATTTGCACGAGGGCGTTTGTG	Sequencing primer, detection of *ptpZ* deletion, reverse	
JG232	ACAGGATCCCAGATTCTGGTCAACCAATCGAAAAATGAACG	Amplification of the last 600 bp of *tkmA* for pGP1331, forward	*Bam*HI
JG233	TGTCTGCAGAGCGCCAAAATGTCCACTCCCC	Amplification of the last 600 bp of *tkmA* for pGP1331, reverse	*Pst*I, no stop codon
JG234	AAAGGATCCATGAACTCAGGACCGAAAGTTTCTGTCATTATG	Amplification of *epsE* for pGP380, forward	*Bam*HI
JG235	TTTGTCGACCTATTCATGCTTGACAAGCCCTTCCTTTTG	Amplification of *epsE* for pGP380, reverse	*Sal*I
JG236	AAAGGATCCAAAGGAGGAAACAATCATGAACTCAGGACCGAAAGTTTCTGTCATTATG	Amplification of *epsE* for pGP382, forward	*Bam*HI, *gapA* RBS
JG237	TTTGTCGACTTCATGCTTGACAAGCCCTTCCTTTTGG	Amplification of *epsE* for pGP382, reverse	*Sal*I, without a stop codon
JG238	ATATCTAGAGATGATGAATGAAAAAATTTTAATCGTTGATGATCAATACGGC	Amplification of *spo0F* for pGP888, forward	*Xba*I
JG239	ATAGGTACCCGTTATCAGTTAGACTTCAGGGGCAGATATTTTTTGAC	Amplification of *spo0F* for pGP888, reverse	*Kpn*I, 2x stop codon
JG240	GCGGCTCAACTTTTTCGTTGAGCC	Sequencing primer *artQ*, forward	
JG241	CCTCACCCTCAGCGATTGTTGTTG	Sequencing primer *artQ*, reverse	
JG242	CGGAATAACAAAAATGGAATGTTCCAATGATGAC	Sequencing primer *yddS*, forward	
JG243	CCTTACTATAATAAATAGAAAAAGGAGGTTCCGG	Sequencing primer *yddS*, reverse	
JG244	GGTGTAAAAGTCTGGATCTATCGTGGAG	Sequencing primer *rplP*, forward	
JG245	GCGAAGATTGAAAAGTTCTTCTTTAAG	Sequencing primer *rplP*, reverse	
JG246	GTGGAAGCTTATCAGGAGATTATGAGAATGC	Sequencing primer *fliF*, forward	
JG247	CTAACCCCAAGGAAATCATGAGAATGGC	Sequencing primer *fliF*, reverse	
JG248	CTAAAAAACACGGTTCCGATCCTAAAAGAACG	Sequencing primer *yozQ*, forward	
JG249	GGGGTTGGCTACTTTTACTGTGGTTG	Sequencing primer *yozQ*, reverse	
JG250	GATGGGAGATATCTTTGACATGCTTGAGG	Sequencing primer *srfAC*, forward	
JG251	CAGCCCGACCATATGTTCAACGCC	Sequencing primer *srfAC*, reverse	
JG252	AAAGGTACCCGCTCCTCTTTTTGGGATTTTCTCCGTTTTTG	Amplification of *sinR* Trp104Arg for BACTH, reverse	*Kpn*I
JG253	AAAGGTACCCGCTCCTCTTTTTGGGATTTTCTCAATTTTTG	Amplification of *sinR* Trp104Leu for BACTH, reverse	*Kpn*I
JG254	GTATTGCATAAAAATGAGAAACTGTTTAAAATACAAATTAACG	Sequencing of *artP*, forward	

JG255	AAATTCATAGCCTTTGTCTCCTTTTCTTACAGG	Sequencing of *artP*, reverse
JG256	GACTGCTTTAAAATAAGTAGTTAGAATAGGAGTCTATG	Sequencing of *yddK*, forward
JG257	GAAACTAAATCAAATATGTCTTCTAAGAATAGATTTATGGG	Sequencing of *yddK*, reverse
JG258	GATGAGCGGGAAATTACCTTTACTGCTG	Sequencing of *tsaB*, forward
JG259	CGATTTCGTATACGTGATCTATATCTTCAAGC	Sequencing of *tsaB*, reverse
JG260	GGAAAAAGTAAGGTATCCTAGTTCGTACAAAG	Sequencing of *ylmA*, forward
JG261	CAAACGGAGTCCGATGTACTCCGC	Sequencing of *ylmA*, reverse
JG262	GAAGACATCTCGATAAAAGAAATACAAAGGTTGTG	Sequencing of *yoaG*, forward
JG263	CTGCGCCTTTATCCGCGGAGGAT	Sequencing of *yoaG*, reverse
JG264	GCAGCCAGAAGTCATACCG	qRT-PCR primer *sinI-sinR* processing, forward
JG265	ACTTCGCTACCCCAGCTTTT	qRT-PCR primer *sinI-sinR* processing, reverse
JG266	AAATTGAAAATGGCGGATTG	qRT-PCR primer *yqhG-sinI* processing, forward
JG267	GTCATTTGCCATTAAATCACCA	qRT-PCR primer *yqhG-sinI* processing, reverse
JG268	TGCGGCAAGCGCTGATAATAGCAAATTTC	Sequencing of NCIB3610 *lutR* promoter region, forward
JG269	CCTTCAGATACGTGCCTTCTCCCTG	Sequencing of NCIB3610 *lutR* promoter region, reverse
JG270	CGGGGCGTTGTCATTGCTTATGATTC	Sequencing of NCIB3610 *pgcA* middle region, forward
JG271	GATGCCGAGGCGGTCAGCATC	Sequencing of NCIB3610 *pgcA* middle region, reverse
JG278	CTATGTAAGTTCTGATATCATGATAATAGTTTGATTGTTG	Sequencing of NCIB3610 *ycgE* bp 139662, forward
JG279	GTAACTTGTACAATTTATTCGGGAACGGGC	Sequencing of NCIB3610 *ycgE* bp 139662, reverse
JG280	GGCTACGATATTGCGGGAACAGGTAC	Sequencing of NCIB3610 *ylbL* bp 554650, forward
JG281	GTCTGTTCCGCTTGTCAGCAAACTGTC	Sequencing of NCIB3610 *ylbL* bp 554650, reverse
JG282	CGAAGTAGGCGGGGCTGTTACC	Sequencing of NCIB3610 *yrkH* bp 1692999, forward
JG283	CCCGACTTTTACCGGCTCTAAATGTTC	Sequencing of NCIB3610 *yrkH* bp 1692999, reverse
JG284	CTTTATTTGAGCGTTGCACTCATCGCAG	Sequencing of NCIB3610 *ytxG* bp 2028278, forward
JG285	GCTGTAGTGGCACCGATGATTCCC	Sequencing of NCIB3610 *ytxG* bp 2028278, reverse
JG286	GAA TAT GAG AAT GGT CCC GGT TGA AAC TG	Sequencing of NCIB3610 *cheA* bp 1713474, forward
JG287	CTGTCAATAACTGCTGTCTCAATGATTGAAG	Sequencing of NCIB3610 *cheA* bp 1713474, reverse

JG288	CGTCTTCATTTGTAAAGGCGTTCTTAATA AAGG	Sequencing of NCIB3610 *kinB* bp 3229205, forward	
JG289	GAATGGATAAGCTGTGAACGCAGGG	Sequencing of NCIB3610 *kinB* bp 3229205, reverse	
JG290	CATACGGTCATGCTCAGTGGCGTC	Sequencing of NCIB3610 *skfF* bp 218854, forward	
JG291	CTCACCTATCGCTTGAACAATTGTGATCT C	Sequencing of NCIB3610 *skfF* bp 218854, reverse	
JG292	CGGCTCACTTGGTTCCGATGACAA G	Sequencing of NCIB3610 *argC* bp 1195324, forward	
JG293	CGGAGCAGCCTGAAAGTGGCTTTG	Sequencing of NCIB3610 *argC* bp 1195324, reverse	
JG294	GGCGAATCAGAAGGTTATTCAGGCTTAC	Sequencing of NCIB3610 *flhP* bp 3745025, forward	
JG295	CTTGGACAACGCCAAGATTAAACCGC	Sequencing of NCIB3610 *flhP* bp 3745025, reverse	
JG296	GACAGAAACAGCGGCGATTGGCAG	Sequencing of NCIB3610 *phoA lytE* intergenic region bp 1018068, forward	
JG297	GTCGATCCTAAAACAACTGCTGTCGTAG	Sequencing of NCIB3610 *phoA lytE* intergenic region bp 1018068, reverse	
JG298	GATCCCTCTTCACTTCTCAGAATACATAC G	Sequencing of *spo0A*, forward	
JG299	CTTAATATTCTTCTCCCATACTACAAATG TCCC	Sequencing of *spo0A*, reverse	
JG300	AAACATATGATTGGCCAGCGTATTAAAC AATACCG	Amplification of *sinR* Trp104Leu (GP1661) for pET24a, forward	*Nde*I
JG301	AAAGAATTCCTACTCCTCTTTTTGGGATT TTCTCAATTTTTG	Amplification of *sinR* Trp104Leu (GP1661) for pET24a, reverse	*EcoR*I
JG302	ATATAT*CTAATACGACTCACTATAGGGA G*ATGGCCGGACTG GCTGAAATACATAAAC	*sinI* RNA, forward	T7 promotor + overhang
JG303	CTGGCTGCCGGACCAGGATG	*sinI* RNA, reverse	
JG304	ATATAT*CTAATACGACTCACTATAGGGA G*AAGGAAGGTGAT GACATTGAT TGGCCA	*sinR* RNA, forward	T7 promotor + overhang
JG305	CAAAGTATGAACCGAGACGTCCAGAAC	*sinR* RNA, reverse	
JG306	AAGGAAGGTGATGACATTGATTGGCCA	*sinR* RNA, forward	
JG307	ATATAT*CTAATACGACTCACTATAGGGA G*CAAAGTATGAACCGAGACGTCCAGAA C	*sinR* RNA, reverse	T7 promoter + overhang
JG308	ATGGCCGGACTGGCTGAAATACATAAAC	*sinI* RNA, forward	
JG309	ATATAT*CTAATACGACTCACTATAGGGA G*CTGGCTGCCGGACCAGGATG	*sinI* RNA reverse	T7 promoter + overhang
JG310	TCCGATATTAATGATGTAGCCGGG	*hag* RNA, forward	
JG311	ATATAT*CTAATACGACTCACTATAGGGA G*CTCCATGTTCTTTTGGCTCGC	*hag* RNA, reverse	T7 promoter + overhang
JG312	CAGAAAACGCCTGGGAAACTAGGCG	Sequencing of *bslA*, forward	
JG313	GTAACTGCAGATTCTGGAATCCATGCTC	*ptsH* RNA, forward	
JG314	ATATAT*CTAATACGACTCACTATAGGGA*	*ptsH* RNA, reverse	T7 promoter +

	*G*GTTAAGAGCATCGTTTTCGTCAGCTCC		overhang
JG315	TAGGCTTAAACTTAAATAAGCTTATAAA AATTTG	*citZ* RNA, forward	
JG316	ATATAT*CTAATACGACTCACTATAGGGA G*CATATATAACATCTCCTTTTCAATAAAT TTCC	*citZ* RNA, reverse	T7 promoter + overhang
JG317	TTTGGTACCCGTCACTAAAAGGAGAAGT GTTCCGATTTTTTCATTTTCTTTTTG	Amplification of *epsB* for pGP886, mutagenesis of Y225→F and Y227→F, reverse	*Kpn*I, 2x stop codon

Foreign oligonucleotides

cat fwd	CAGCGAACCATTTGAGGTGATAGGCGG CAATAGTTACCCTTATTATCAAG	Amplification of *cat* from pGEM-cat, forward	
cat rev	CGATACAAATTCCTCGTAGGCGCTCGGC CAGCGTGGACCGGCGAGGCTAGTTACC C	Amplification of *cat* from pGEM-cat, reverse	
CD76	CTGCAGATTCTGGAATCCATG	qRT-PCR *ptsH* fwd	
CD77	CGCCTTTAGCGATACCTAAAG	qRT-PCR *ptsH* rev	
CD90	AAATCTAGAAATGGAAATCTTAAAAGTT TCAGCAAAATCGAG	*spoVS* fwd for BACTH/ cloning into pGP886	*Xba*I
CD137	AAAGGATCCTTGATTGGCCAGCGTATTA AACAATACC	Amplification of *sinR* for pGP380, forward	*Bam*HI
CD138	AAAGTCGACTTACTACTCCTCTTTTTGGG ATTTTCTCC	Amplification of *sinR* for pGP380, reverse	*Sal*I
CD139	GGCATTGGCGCGAGAAGACAG	LFH upstream fwd, Δ*sinR & sinI*-3xFLAG	
CD153	AAATCTAGAGTTGATTGGCCAGCGTATT AAACAATACC	*sinR* fwd BACTH	*Xba*I
kan rev	5'CGATACAAATTCCTCGTAGGCGCTCGG	Amplification of *aphA3* from pDG780, reverse	
kan rev o. T.	TTACTAAAACAATTCATCCAGTAAAATAT	Amplification of *aphA3* from pDG780 without a terminator, reverse	
kan check fwd	5'CATCCGCAACTGTCCATACTCTG	LFH-PCR, sequencing of the down fragment	
kan check rev	5'CTGCCTCCTCATCCTCTTCATCC	LFH-PCR, sequencing of the up fragment	
KG43	GTGTTGGGTTCACAATGTCG	qRT-PCR primer *rpsJ*, reverse	
KG44	GCGTCGTATTGACCCAAGC	qRT-PCR primer *rpsE*, forward	
KG45	TACCAGTACCGAATCCTACG	qRT-PCR primer *rpsE*, reverse	
JS40	CGGATTGGCGGGAAGCATCGG	Sequencing of *ptkA*, forward	
JS41	CCGAATCACCTGCCCCGTCATC	Sequencing of *ptkA*, reverse	
JK68	GCTGGATGTCACTGAGATTCGAG	Sequencing of intergenic region *epsA-slrR*, forward	
JK69	TTTTTCATACATCATTGTTTCTGCGTC	Sequencing of intergenic region *epsA-slrR*, reverse	
JK74	TGTTCGTTTTGCCTGGCCA	Sequencing of *bcsA*, forward	
JK75	GAAGAAAAAAATCAAATATACATAGAA GAAACACT	Sequencing of *bcsA*, reverse	

ML85	CTCTATTCAGGAATTGTCAGATAG	LFH-PCR, sequencing of the down fragment	cat check fwd
ML84	CTAATGGGTGCTTTAGTTGAAGA	LFH-PCR, sequencing of the up fragment	cat check rev
ML82	CAGAAACAATGATGTATGAAAAAATCAGC	qRT-PCR *slrR*, forward	
ML83	GGTAAGAGGCAGTTTCAGG	qRT-PCR *slrR*, reverse	
ML86	TGCTTACAATTTTCCGATGATACAAG	qRT-PCR *tapA*, forward	
ML87	ATCTGATATGTGCAAATCACTTTGATC	qRT-PCR *tapA*, reverse	
ML103	CTCTTGCCAGTCACGTTAC	Sequencing of the up-fragment of a gene deletion, reverse	spc check rev
ML104	TCTTGGAGAGAATATTGAATGGAC	Sequencing of the down-fragment of a gene deletion, forward	spc check fwd
ML279	CAGGTGTTATATAAAGAATGTGTGCGAACC	sequencing of *epsC*, reverse (mutation at bp 827 in *B.s*. 168)	
ML280	GATTGTGTTCCATTAAAGGCACATGCTTA TG	sequencing of *epsC*, reverse (mutation at bp 827 in *B.s*. 168)	
spc fwd	CAGCGAACCATTTGAGGTGATAGGGACTGGCTCGCTAATAACGTAACGTGACTGGCAAGAG	Amplification of *spc* from pDG1726, forward	
spc rev	CGATACAAATTCCTCGTAGGCGCTCGGCGTAGCGAGGGCAAGGGTTTATTGTTTTCTAAAATCTG	Amplification of *spc* from pDG1726, reverse	
spc rev o. T.	CGATACAAATTCCTCGTAGGCGCTCGGTTTCCACCATTTTTTCAATTTTTTTATAATTTTTTAATCTG	Amplification of *spc* from pDG1726 without a terminator, reverse	
ermC fwd	CAGCGAACCATTTGAGGTGATAGGGATCCTTTAACTCTGGCAACCCTC	Amplification of *ermC* from pDG647, forward	
ermC rev	CGATACAAATTCCTCGTAGGCGCTCGGGCCGACTGCGCAAAAGACATAATCG	Amplification of *ermC* from pDG647, reverse	
ermC rev o.T.	CGATACAAATTCCTCGTAGGCGCTCG	Amplification of *ermC* from pDG647, reverse	CZ68, w/o terminator
ermC check fwd	CCTTAAAACATGCAGGAATTGACG	Sequencing of the up-fragment of a gene deletion, forward	
ermC check rev	GTTTTGGTCGTAGAGCACACGG	Sequencing of the up-fragment of a gene deletion, reverse	
NP56	GCGTTCATGGCCTCCACCCAGATCTCATC	LFH for the deletion of *ymdB*, upstream-forward	
NP57	CGATGACTATATTCGTGAGATGGGTGAGCAAACGACA	Sequencing primer, detection of *ymdB* deletion, forward	
NP58	CCTATCACCTCAAATGGTTCGCTGGCCCGGTGAACCGACAACATCTCCG	LFH for the deletion of *ymdB*, upstream-reverse	
NP59	CCGAGCGCCTACGAGGAATTTGTATCGGACATTGACGATCAAACGAAAAAAG	LFH for the deletion of *ymdB*, downstream-forward	
NP60	GCAGACACATACTCTCCCACTTTTACACTGCTGACAT	LFH for the deletion of *ymdB*, downstream-reverse	

NP61	AGTATTGGTACACACATGAGATTTTCCT GTTAG	Sequencing primer, detection of *ymdB* deletion, reverse
pac5F	5'GCGTAGCGAAAAATCCTTTTC	Sequencing of pac5 constructs

7.4. Plasmids

Table 7.4. Plasmids constructed in this work

Name	Vector	Insert
pGP2104	pUT18	*epsA* JG72/ JG73 *Xba*I + *Kpn*I
pGP2105	pUT18C	*epsA* JG72/ JG73 *Xba*I + *Kpn*I
pGP2106	pKT25	*epsA* JG72/ JG73 *Xba*I + *Kpn*I
pGP2107	p25-N	*epsA* JG72/ JG73 *Xba*I + *Kpn*I
pGP2108	pUT18	*epsB* JG74/ JG75 *Xba*I + *Kpn*I
pGP2109	pUT18C	*epsB* JG74/ JG75 *Xba*I + *Kpn*I
pGP2110	pKT25	*epsB* JG74/ JG75 *Xba*I + *Kpn*I
pGP2111	p25-N	*epsB* JG74/ JG75 *Xba*I + *Kpn*I
pGP2112	pSG1154	*epsA* JG76/ JG77 *Kpn*I + *EcoR*I
pGP2113	pSG1154	*epsB* JG78/ JG79 *Kpn*I + *EcoR*I
pGP2114	pET24a	*sinR* (Trp104Leu) JG300/ JG301 *Nde*I + *EcoR*I
pGP2115	pGP886	*epsB* (C-terminal Y-cluster mutated) JG74/ JG141 *Xba*I + *Kpn*I
pGP2116	pGP380	*epsB* JG84/ JG85 *BamH*I + *Sal*I, overexpression did not work
pGP2117	pKT25	*epsE* JG204/ JG205 *Xba*I + *Kpn*I
pGP2118	pKT25	*epsL* JG218/ JG219 *Xba*I + *Kpn*I
pGP2119	pUT18	*sinR* (Trp104Leu) CD153/ JG253 *Xba*I + *Kpn*I
pGP2120	pGP888	*spo0F* JG238/ JG239 *Xba*I + *Kpn*I
pGP2121	pUT18C	*sinR* (Trp104Leu) CD153/ JG253 *Xba*I + *Kpn*I
pGP2122	pUT18	*epsB* (C-terminal Y-cluster mutated) JG74/ JG105 *Xba*I + *Kpn*I
pGP2123	pUT18C	*epsB* (C-terminal Y-cluster mutated) JG74/ JG105 *Xba*I + *Kpn*I
pGP2124	pKT25	*epsB* (C-terminal Y-cluster mutated) JG74/ JG105 *Xba*I + *Kpn*I
pGP2125	p25-N	*epsB* (C-terminal Y-cluster mutated) JG74/ JG105 *Xba*I + *Kpn*I
pGP2126	pGP382	*epsB* JG109/ JG110 *BamH*I + *Sal*I
pGP2127	pGP1331	*epsA*-FLAG 3x JG111/ JG107 *BamH*I + *Pst*I
pGP2128	pAC5	P_{epsA}-*epsA*-FLAG 2x JG108/ JG89 *EcoR*I + *BamH*I
pGP2129	pGP886	*epsB* JG74/ JG112 *Xba*I + *Kpn*I
pGP2130	pGP380	*epsC* (AM373) JG121/ JG122 *BamH*I + *Sal*I
pGP2131	pGP1331	*epsB*-FLAG 3x JG125/ JG110 *BamH*I + *Sal*I
pGP2132	pKT25	*sinR* (Trp104Leu) CD153/ JG253 *Xba*I + *Kpn*I
pGP2133	pGP382	*epsC* (AM373) JG140/ JG135 *BamH*I + *Sal*I, point mutation, truncated *epsC* without putative transmembrane domains
pGP2134	pKT25	*epsM* JG220/ JG221 *Xba*I + *Kpn*I

pGP2135	pKT25	*epsN* JG222/ JG223 *Xba*I + *Kpn*I
pGP2136	pKT25	*epsO* JG224/ JG225 *Xba*I + *Kpn*I
pGP2137	p25-N	*epsC (*AM373*)* JG136/ JG137 *Xba*I + *Kpn*I
pGP2138	p25-N	*sinR* (Trp104Leu) CD153/ JG253 *Xba*I + *Kpn*I
pGP2139	pUT18	*tkmA* JG144/ JG145 *Xba*I + *Kpn*I
pGP2140	pUT18C	*tkmA* JG144/ JG145 *Xba*I + *Kpn*I
pGP2141	pKT25	*tkmA* JG144/ JG145 *Xba*I + *Kpn*I
pGP2142	p25-N	*tkmA* JG144/ JG145 *Xba*I + *Kpn*I
pGP2143	pUT18	*ptkA* JG142/ JG143 *Xba*I + *Kpn*I
pGP2144	pUT18C	*ptkA* JG142/ JG143 *Xba*I + *Kpn*I
pGP2145	pKT25	*ptkA* JG142/ JG143 *Xba*I + *Kpn*I
pGP2146	p25-N	*ptkA* JG142/ JG143 *Xba*I + *Kpn*I
		Silent mutation at bp 576 (AAA → AAG)
pGP2147	pGP886	*epsA* JG72/ JG146 *Xba*I + *Kpn*I
pGP2148	pGP1870	*epsA*-GFP JG111/ JG107 *BamH*I + *Pst*I
pGP2149	pAC5	*lutA* (*yvfV*) JG149/ JG150 *EcoR*I + *BamH*I
pGP2150	pAC5	*ywbD* JG151/ JG152 *EcoR*I + *BamH*I
pGP2151	pGP886	*ptkA* JG142/ JG160 *Xba*I + *Kpn*I
pGP2152	pGP888	*spoVS* CD90/ JG159 *Xba*I + *Kpn*I
pGP2153	pGP886	*ykoW* from pGP1867 *Xba*I + *Kpn*I
pGP2154	pGP888	*yuxH* JG163/ JG164 *Xba*I + *Kpn*I
pGP2155	pGP1331	*tkmA*-FLAG 3x JG232/ JG233 *BamH*I + *Pst*I

Table 7.5. Plasmids used in this work

Name	purpose	Reference/ received from
pAC5	vector for the construction of translational *lacZ* fusions, integrates into the *amyE* site	Martin-Verstraete *et al*. (1992) J Mol Biol. **226**:85-99.
pBQ200	constitutive overexpression of proteins in *B. subtilis*	Martin-Verstraete *et al*. (1994)
pDG647	template for erythromycin resistance cassette	Guérout-Fleury *et al*. (1995)
pDG780	amplification of the kanamycin resistance cassette	Guérout-Fleury *et al*. (1995)
pDG1514	amplification of the tetracyclin resistance cassette	Guérout-Fleury *et al*. (1995)
pDG1726	amplification of the spectinomycin resistance cassette	Guérout-Fleury *et al*. (1995)
pET24a	overexpression of proteins with an N-terminal T7-Tag or an optional C-terminal His-Tag in *E. coli*	Novagen, received from Rick Lewis (Newcastle)
pGEM-cat	amplification of the chloramphenicol resistance cassette	Torsten Mascher, laboratory collection
pGP380	fusion with a N-terminal *Strep*-tag II, constitutive	Herzberg *et al*. (2007)

	overexpression in *B. subtilis*	
pGP381	constitutive overexpression of CsrA-*Strep* in *B. subtilis*	Dörrbecker (2007) Diploma thesis
pGP382	fusion with a C-terminal *Strep*-tag II, constitutive overexpression in *B. subtilis*	Herzberg *et al*. (2007)
pGP819	overexpression of YwjH-*Strep* in *E. coli*	Pietack (2007) Diploma thesis
pGP886	allows overexpression of genes by the P_{xyl}-promoter, integrates into *xkdE* site	Gerwig *et al.* (2014)
pGP888	allows overexpression of genes by the P_{xyl}-promoter, integrates into *ganA* site	Diethmaier *et al*. (2011)
pGP1094	*sinI* in pUT18 (BACTH)	Diethmaier *et al*. (2011)
pGP1095	*sinI* in pUT18c (BACTH)	Diethmaier *et al*. (2011)
pGP1096	*sinI* in pKT25 (BACTH)	Diethmaier *et al*. (2011)
pGP1097	*sinI* in p25-N (BACTH)	Diethmaier *et al*. (2011)
pGP1098	*slrR* in pUT18 (BACTH)	Diethmaier *et al*. (2011)
pGP1099	*slrR* in pUT18c (BACTH)	Diethmaier *et al*. (2011)
pGP1201	constitutive overexpression of RNase Y in *B. subtilis*	Lehnik-Habrink *et al*. (2011b)
pGP1331	chromosomal integration of a C-terminal *Strep*-tag II at the native locus in *B. subtilis*	Lehnik-Habrink *et al.* (2010) Mol Microbiol. **77**: 958-977.
pGP1867	cloning of the *ykoW* gene	Lehnik-Habrink (2011) PhD thesis
pGP1870	integrative plasmid for *B. subtilis*, fusion of GFP tag to C-terminus of a proteins at the native locus	Rothe *et al.* (2013) J Bacteriol. **195**: 2146-2154
pGP1901	*slrR* in pKT25 (BACTH)	Diethmaier (2011) PhD thesis
pGP1902	*slrR* in p25-N (BACTH)	Diethmaier (2011) PhD thesis
pGP1903	*slrA* in pUT18 (BACTH)	Diethmaier (2011) PhD thesis
pGP1904	*slrA* in pUT18c (BACTH)	Diethmaier (2011) PhD thesis
pGP1904	*slrA* in pKT25 (BACTH)	Diethmaier (2011) PhD thesis
pGP1906	*slrA* in p25-N (BACTH)	Diethmaier (2011) PhD thesis
pGP1916	overexpression of YmdB(E39Q)-*Strep* in *E. coli*	Diethmaier (2011) PhD thesis
pGP1917	Overexpression of YmdB-*Strep* in *E. coli*	Diethmaier (2011) PhD thesis
pGP1920	Overexpression of YmdB(E39Q)-*Strep* in *B. subtilis*	Diethmaier (2011) PhD thesis
pGP2603	Overexpression of YaaQ-*Strep*	Kampf (2013) Master thesis
pKT25	BACTH vector, C-terminal fusion of T25 domain	Karimova *et al.* (1998)
pKT25zip	BACTH control plasmid with a leucine zipper fused to the T25 fragment of pKT25	Karimova *et al*. (1998)
pSG1154	Integration of a c-terminal *gfpmut1* fusion gene into the *amyE* locus, allows overexpression by P_{xyl}	Lewis & Marston (1999) Gene **227**: 101-110
pUT18	BACTH vector, N-terminal fusion of T18 domain	Karimova *et al*. (1998)
pUT18C	BACTH vector, C-terminal fusion of T18 domain	Karimova *et al*. (1998)

pUT18zip	BACTH control plasmid with a Leucine zipper fused to the T18 fragment of pUT18	Karimova *et al.* (1998)
p25-N	BACTH vector, N-terminal fusion of T25 domain	Claessen *et al*., 2008

7.5. Internet programs and software

Table 7.6. Used internet programs

URL	Provider	Usage
http://www.ncbi.nlm.nih.gov/	National Institutes of Health, Bethesda, USA	Literature research
http://www.subtiwiki.uni-goettingen.de/	University of Göttingen	Database for *B. subtilis*
http://subtiwiki.uni-goettingen.de/subtipathways.html	University of Göttingen	Database for metabolic pathways of *B. subtilis*
http://genolist.pasteur.fr/SubtiList/	Institute Pasteur, Paris	Sequence analysis *B. subtilis*
http://bioinfo.ut.ee/primer3/	Whitehead Institute	Primer design for qRT-PCR
http://tools.neb.com/NEBcutter2/	New England Biolabs	Restriction site analysis
http://www.basic.northwestern.edu/biotools/oligocalc.html	Northwestern University, USA	Calculation of oligonucleotide annealing temperatures
http://biocyc.org/	SRI International, USA	NCIB3610 genome browser

Table 7.7. Used software

Software	Producer	Usage
ChemoCam Imager software	Intas	Analysis of chemiluminescence signals
iCycler software	Bio-Rad	Data analysis qRT-PCR
Genius Pro™ 4.7.6–7.1.3	Biomatters Ltd.	Analysis of sequencing results, primer design
ImageJ	National Institutes of Health, Bethesda, USA	Densitometry and image processing
AxioVision Rel 4.8.2.	Carl Zeiss, Jena, Germany	Single cell fluorescence microscopy
ZEN lite blue edition 2012	Carl Zeiss, Jena, Germany	Image acquisition and processing
Mendeley Desktop 1.12.3	Mendeley Ltd.	Reference managment
TraV transcriptome browser	Dietrich *et. al.* (2014)	RNA sequencing data analysis
Microsoft Office 2007-2010	Microsoft Inc.	Text and data processing

7.6. Supplementary data

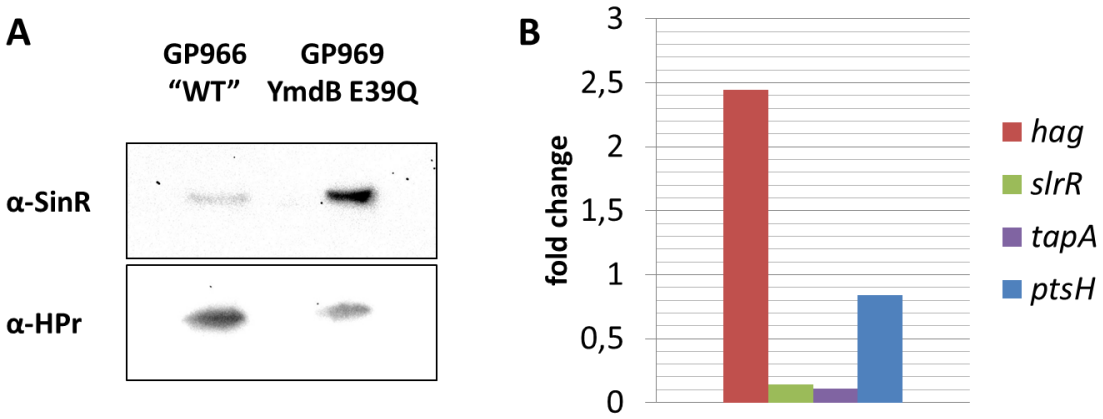

Figure 7.1. Western blot analysis (A) and qRT-PCR (B) to test the cultivations of cells for RNA sequencing. The strains were cultivated in LB medium at 37°C and 200 rpm until early stationary growth phase. From a single culture samples for RNA isolation and protein extraction were taken. Before sending the RNA of the strain GP966 and GP969 for RNA sequencing, overexpression of the *hag* motility gene and repression of the *slrR* gene and the *tapA* biofilm gene was tested by qRT-PCR. In parallel, elevated SinR protein amounts in the ymdB mutants strain GP969 was confirmed by Western blot analysis with a SinR-specific antibody. A specific antibody against the constitutively expressed HPr protein was used as a (loading) control.

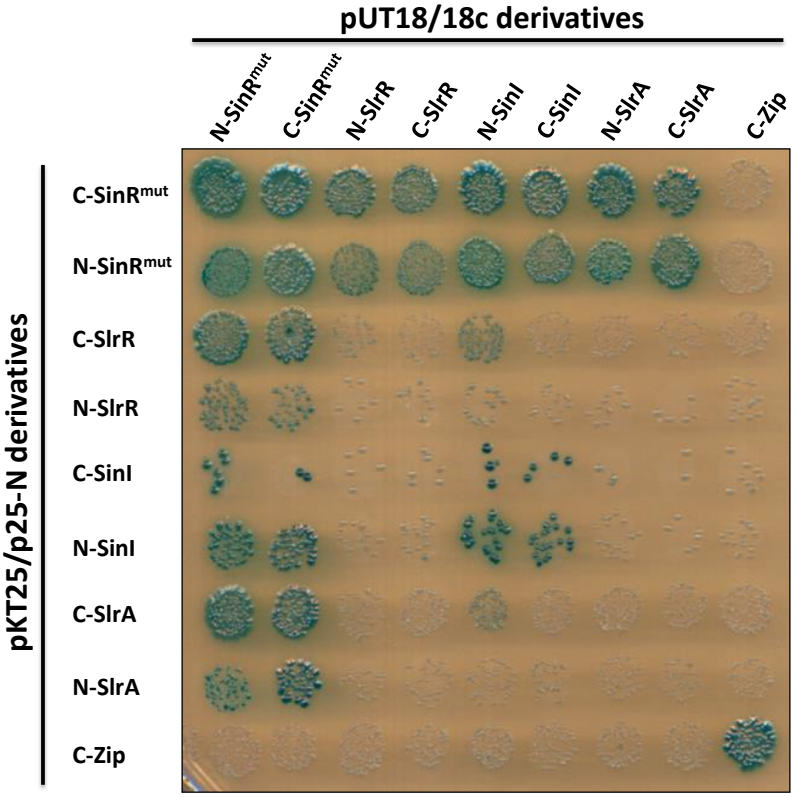

Figure 7.2. Bacterial two-hybrid assay of the SinR: Trp104Leu variant with its known interaction partners SinI, SlrR and SlrA. The mutated *sinR* variant was amplified with the primer pair CD153/ JG253. Strain GP1661 served as a PCR template.

Table 7.8. Abundance of transcripts encoding factors involved in proteolysis. [1]NPKM = nucleotide activity per kilobase of exon model per million mapped reads (compare Wiegand *et al.*, 2013 BMC Genomics **14**:667). The NPKM values represent the transcript level of a certain gene and were generated with the TraV transcriptome browser. The gene names were extracted from the SubtiWiki database (http://subtiwiki.uni-goettingen.de/wiki/index.php/Proteolysis).

Gene	BSU number	NPKMs[1] GP966 WT	NPKMs[1] GP969 YmdB^{E39Q}	Ratio (GP969/ GP966)
ctsR	BSU00830	61	133	2,18
clpC	BSU00860	220	630	2,86
clpP	BSU34540	742	1109	1,49
clpE	BSU13700	6	33	5,50
clpX	BSU28220	811	1166	1,44
immA	BSU04810	22	38	1,73
rasP	BSU16560	394	272	0,69
yraA	BSU27020	399	263	0,66
ctpB	BSU35240	2	1	0,50
spoIIGA	BSU15310	1	0	0,00
epr	BSU38400	67	522	7,79
mecA	BSU11520	525	781	1,49
yjbH	BSU11550	136	156	1,15
ypbH	BSU22970	66	149	2,26
ipi	BSU11130	114	265	2,32
ctpA	BSU19590	197	137	0,70
bpr	BSU15300	22	5	0,23
ypwA	BSU22080	104	99	0,95
mlpA	BSU16710	86	38	0,44
lonA	BSU28200	139	187	1,35
clpQ	BSU16150	422	383	0,91
clpY	BSU16160	632	588	0,93
ftsH	BSU00690	1492	1650	1,11
spoIVFB	BSU27970	6	3	0,50
ispA	BSU13190	3	10	3,33
lonB	BSU28210	1	2	2,00
htrA	BSU12900	102	110	1,08
htrB	BSU33000	105	98	0,93
prsW	BSU22940	164	199	1,21
wprA	BSU10770	3077	1193	0,39
mpr	BSU02240	98	182	1,86
nprB	BSU11100	5	5	1,00
vpr	BSU38090	16	93	5,81
yabG	BSU00430	0	1	
yirB	BSU33029	144	198	1,38
htpX	BSU13490	511	473	0,93
yqgP	BSU24870	16	18	1,13
yyxA	BSU40360	83	62	0,75